

به نام خدا



مرکز دانلود رایگان مهندسی متالورژی و مواد

www.Iran-mavad.com



POLYMERIC FOAMS SERIES *series editor S.T. Lee*

POLYMERIC FOAMS

Mechanisms and Materials

Edited by
S.T. Lee
N.S. Ramesh



CRC PRESS

Boca Raton London New York Washington, D.C.

www.iran-mavad.com

© 2004 by CRC Press LLC

مرجع دانشجویان و مهندسين مواد

Library of Congress Cataloging-in-Publication Data

Polymeric foams : mechanisms and materials / [edited by] S.T. Lee, N.S. Ramesh.

p. cm. — (polymeric foams series)

Includes bibliographical references and index.

ISBN 0-8493-1728-2 (alk. paper)

I. Plastic foams. I. Lee, S.-T. (Shau-Tarng), 1956- II. Ramesh, N. S. (Natarajan S.)
III. Title. IV. Series.

TP183 .F6P63 2004

668.4'93—dc22

2003068613

This book contains information obtained from authentic and highly regarded sources. Reprinted material is quoted with permission, and sources are indicated. A wide variety of references are listed. Reasonable efforts have been made to publish reliable data and information, but the author and the publisher cannot assume responsibility for the validity of all materials or for the consequences of their use.

Neither this book nor any part may be reproduced or transmitted in any form or by any means, electronic or mechanical, including photocopying, microfilming, and recording, or by any information storage or retrieval system, without prior permission in writing from the publisher.

All rights reserved. Authorization to photocopy items for internal or personal use, or the personal or internal use of specific clients, may be granted by CRC Press LLC, provided that \$1.50 per page photocopied is paid directly to Copyright Clearance Center, 222 Rosewood Drive, Danvers, MA 01923 USA. The fee code for users of the Transactional Reporting Service is ISBN 0-8493-1728-2/04/\$0.00+\$1.50. The fee is subject to change without notice. For organizations that have been granted a photocopy license by the CCC, a separate system of payment has been arranged.

The consent of CRC Press LLC does not extend to copying for general distribution, for promotion, for creating new works, or for resale. Specific permission must be obtained in writing from CRC Press LLC for such copying.

Direct all inquiries to CRC Press LLC, 2000 N.W. Corporate Blvd., Boca Raton, Florida 33431.

Trademark Notice: Product or corporate names may be trademarks or registered trademarks, and are used only for identification and explanation, without intent to infringe.

Visit the CRC Press Web site at www.crcpress

© 2004 by CRC Press LLC

No claim to original U.S. Government works

International Standard Book Number 0-8493-1728-2

Library of Congress Card Number 2003068613

Printed in the United States of America 1 2 3 4 5 6 7 8 9 0

Printed on acid-free paper

Dedication

To the Lord, whose breath brings forth wisdom.

Preface

Since World War II, polymeric foam has become a very important part of the polymer industry, influencing almost every aspect of our daily lives. The industry has grown rapidly due to the beneficial characteristics of polymeric foam, including its light weight, sound absorption properties, and positive role in material savings, and it is used widely in protective packaging, thermal insulation, and seat cushioning. Unique properties, processes, and technologies have been developed to satisfy and explore new application opportunities. As a result, the polymeric foam industry has become quite diversified.

Foaming itself is a dynamic and complex phenomenon that involves scientific principles and engineering parameters that govern the manufacturing process. One of the main objectives of this volume is to provide a clear understanding of the fundamental mechanisms and material characteristics of polymeric foam. [Chapter 1](#) offers an introduction to mechanisms and materials of polymeric foams. These fundamental mechanisms appear to be common to all foams, which are made through foaming phenomena consisting of basic mechanisms—cell nucleation, growth, and stability. [Chapters 3](#) and [5](#) are dedicated to these mechanisms.

Although foaming is an unstable separation process with dynamic complexity, material strength plays a key role in determining a foam's expansion boundary and cellular structure. [Chapter 2](#) is devoted solely to discussing material strength, which is crucial to thermoplastic foam extrusion. Foam processes are thoroughly discussed in [Chapters 4, 6, and 7](#), which cover thermoplastic foam and flexible and rigid thermoset polyurethane foams. It is our hope that this volume brings forth a clear comprehension of mechanisms and material features and their interactions with polymeric foams.

We acknowledge that as understanding expands, the number of unknowns also grows. We hope this book will help industrial and academic scientists, chemists, and engineers who are performing fundamental and applied research attain lucid understanding of foaming mechanisms and materials that will lead to great achievements. The volume can also be used as a textbook at the graduate level and a reference book for undergraduate courses on foams. We believe this book will generate a tremendous interest in developing new processes, technologies, and applications in the area of manufacturing foams.

S.T. Lee
N.S. Ramesh

Acknowledgments

The editors wish to thank all contributing authors and reviewers for their concentrated efforts in the process of preparing and revising the manuscripts. The team spirit developed through work on this volume is greatly valued. Nelson Malwitz, retired from Sealed Air Corporation in 2003, Richard Gendron of the Canadian Research Council, and Professor Masahiro Ohshima of Kyoto University offered prudent comments in review to make this book more professional. Input from Dr. Michael (Chien-Yuen) Huang of the New Jersey Institute of Technology is also appreciated. We also thank Sealed Air Corporation for its support, and Kevin Lee and Jenny Jun in particular for faithfully working extra long hours at their computers. Our gratitude to Mrs. Mjau-Lin Lee and Mrs. Malathi Ramesh for their invaluable support is beyond that which words can express. Finally, we thank God for the learning experience and for giving us the strength to continue during difficult times in the last three years.

Editors

S.T. Lee received his B.E. from the Chemical Engineering Department at National Tsing-Hua University, Taiwan, and his M.S. and Ph.D. from Stevens Institute of Technology. He has over 20 years experience working with foaming and polymeric foam.

Presently, Dr. Lee is with Sealed Air Corporation and resides with his wife, Mjau-Lin, and three children in New Jersey. To date, his publications exceed 80 and include 20 U.S. patents. Dr. Lee is the editor of *Foam Extrusion*, published by CRC Press. He is also a fellow of the Society of Plastics Engineers.

N.S. Ramesh is director of R&D in the Polyolefin Foam Division at Sealed Air Corporation. He received his BTech. in chemical engineering from the University of Madras and his M.S. and Ph.D. in chemical engineering from Clarkson University. He was awarded certificates for attending the summer rheology program at MIT and the executive management programs at the University of Michigan, Ann Arbor, and Southern Methodist University Cox business schools.

Dr. Ramesh has worked in the area of polymeric foams for 15 years and has received 2 best paper awards for his pioneering work on foams from the Society of Plastics Engineers. He has more than 50 publications, including 15 U.S. patents and 2 book chapters. Dr. Ramesh served as technical chair for the Foams 1998 and 2000 international conferences. In 2002, he was elected a fellow of the Society of Plastic Engineers.

Contributing Authors

P. Berthevas

The Dow Chemical Company
Midland, Michigan

J. Bicerano

Corporate R&D
The Dow Chemical Company
Midland, Michigan

R. van den Bosch

Polyurethanes R&D
Dow Benelux B.V.
Terneuzen, The Netherlands

M. Brown

The Dow Chemical Company
Midland, Michigan

F. Casati

The Dow Chemical Company
Midland, Michigan

C.P. Christenson

The Dow Chemical Company
Midland, Michigan

P. Clavel

Polyurethanes R&D
Dow Europe GmbH
Meyrin, Switzerland

R.D. Daussin

Polyurethanes R&D
Dow North America
Freeport, Texas

M.J. Elwell

Corporate R&D
The Dow Chemical Company
Midland, Michigan

W. Farrissey

The Dow Chemical Company
Midland, Michigan

J. Fosnaugh

The Dow Chemical Company
Midland, Michigan

R. de Genova

The Dow Chemical Company
Midland, Michigan

H.J.M. Grünbauer

Polyurethanes R&D
Dow Benelux B.V.
Terneuzen, The Netherlands

R. Herrington

The Dow Chemical Company
Midland, Michigan

J. Hicks

The Dow Chemical Company
Midland, Michigan

K. Hinze

The Dow Chemical Company
Midland, Michigan

K. Hock

The Dow Chemical Company
Midland, Michigan

D. Hunter

The Dow Chemical Company
Midland, Michigan

L. Jeng

The Dow Chemical Company
Midland, Michigan

H. Kawabata

Polyurethanes R&D
Dow Chemical Japan, Ltd.
Gotemba, Japan

H. Kramer

Polyurethanes R&D
Dow Benelux B.V.
Terneuzen, The Netherlands

D.D. Latham

Polyurethanes R&D
Dow North America
Freeport, Texas

D. Laycock

The Dow Chemical Company
Midland, Michigan

S.T. Lee

Sealed Air Corporation
Saddle Brook, New Jersey

W. Lidy

The Dow Chemical Company
Midland, Michigan

C.W. Macosko

Professor of Chemical Engineering
and Materials Science
Director of I PRIME, The Industrial
Partnership for Research in
Interfacial and Materials
Engineering
University of Minnesota
Minneapolis, Minnesota

C.A. Martin

Polyurethanes R&D
Dow North America
Freeport, Texas

H. Mispreuve

The Dow Chemical Company
Midland, Michigan

R. Moore

The Dow Chemical Company
Midland, Michigan

S.E. Moore

Polyurethanes R&D
Dow North America
Freeport, Texas

L. Nafziger

The Dow Chemical Company
Midland, Michigan

R.A. Neff

BASF Corporation
Wynadotte, Michigan

M. Norton

The Dow Chemical Company
Midland, Michigan

B.C. Obi

Polyurethanes R&D
Dow North America
Freeport, Texas

V. Parenti

Polyurethanes R&D
Dow Italia S.R.I.
Corregio, Italy

D. Parrish

The Dow Chemical Company
Midland, Michigan

R. Priestester

The Dow Chemical Company
Midland, Michigan

N.S. Ramesh

Director of R&D
North America Polyolefin Foam
Division
Sealed Air Corporation
Grand Prairie, Texas

A.K. Schrock

Polyurethanes R&D
Dow North America
Freeport, Texas

K. Skaggs

The Dow Chemical Company
Midland, Michigan

L. Stahler

The Dow Chemical Company
Midland, Michigan

F. Sweet

The Dow Chemical Company
Midland, Michigan

R. Thomas

The Dow Chemical Company
Midland, Michigan

R. Turner

The Dow Chemical Company
Midland, Michigan

H.A. de Vos

Polyurethanes R&D
Dow Benelux B.V.
Terneuzen, The Netherlands

H.R. van der Wal

The Dow Chemical Company
Midland, Michigan

G. Wiltz

The Dow Chemical Company
Midland, Michigan

T. Woods

The Dow Chemical Company
Midland, Michigan

M. Xanthos

Otto H. York Department of
Chemical Engineering and
Polymer Processing Institute
New Jersey Institute of Technology
Newark, New Jersey

M. Yamaguchi

TOSOH Corporation
Yokkaichi Research Laboratory
Yokkaichi, Japan

Q. Zhang

Center for Biomaterials &
Advanced Technologies—
Medical Devices Group
A division of Ethicon, Inc.
A Johnson & Johnson Company
Somerset, New Jersey

X.D. Zhang

Unilever Research
Edgewater, New Jersey

Contents

- 1 Introduction: Polymeric Foams, Mechanisms, and Materials**
S.T. Lee
- 2 Melt Elasticity of Polyolefins: Impact of Elastic Properties on Foam Processing**
M. Yamaguchi
- 3 Fundamentals of Bubble Nucleation and Growth in Polymers**
N.S. Ramesh
- 4 Material Properties Affecting Extrusion Foaming**
Q. Zhang and M. Xanthos
- 5 Foam Stability in Flexible Polyurethane Foam Systems**
X.D. Zhang, R.A. Neff, and C.W. Macosko
- 6 Flexible Polyurethane Foams**
J. Bicerano, R.D. Daussin, M.J.A. Elwell, H.R. van der Wal, P. Berthevas, M. Brown, F. Casati, W. Farrissey, J. Fosnaugh, R. de Genova, R. Herrington, J. Hicks, K. Hinze, K. Hock, D. Hunter, L. Jeng, D. Laycock, W. Lidy, H. Misprenue, R. Moore, L. Nafziger, M. Norton, D. Parrish, R. Priester, K. Skaggs, L. Stahler, F. Sweet, R. Thomas, R. Turner, G. Wiltz, T. Woods, C.P. Christenson, and A.K. Schrock
- 7 Rigid Polyurethane Foams**
H.J.M. Grünbauer, J. Bicerano, P. Clavel, R.D. Daussin, H.A. de Vos, M.J. Elwell, H. Kawabata, H. Kramer, D.D. Latham, C.A. Martin, S.E. Moore, B.C. Obi, V. Parenti, A.K. Schrock, and R. van den Bosch

1

Introduction: Polymeric Foams, Mechanisms, and Materials

S.T. Lee

CONTENTS

- 1.1 Introduction
- 1.2 Foaming Technology
- 1.3 Foaming Mechanisms
- 1.4 Materials
- References

1.1 Introduction

Foam is a material, and foaming is a phenomenon. Both involve the presence of a gas phase encapsulated by a spherical shell dense phase.

Gas exists throughout the universe and is a very interesting phase, especially on Earth. It is indispensable to organic life. Despite possessing a mass and sometimes a shape (e.g., fire), gas is basically formless. The light bonding of gas makes it almost omnipresent. There may be a large amount of gas molecules in a limited space, or a small amount in a large space. When gas is encapsulated in a dense medium, an interesting phenomenon or product is formed. In nature, cork, wood, and pumice are good examples of this type of product. In these materials, either there is a hollow space surrounded by solid, or gaseous voids are dispersed in the solid. The hollow space, as seen in bamboo and cork, is shaped like hollow sticks bundled together. But foam is often round in shape.¹

The tiny hollow space acts as an amazing transport vehicle for water, from the root to the top of a tree, a process known as the capillary effect. Foam impacts almost every aspect of human life. For example, when heated, water soaked into rice grain expands and renders the grain edible; and gas is

TABLE 1.1

General Foams in Our Daily Lives

Type	Function
Lungs	Exchanged gas
Rice and flour	Cellular for food
Popped corn, cereal	Cellular for food
Meringue	Blended air
Soda, beer	Froth
Seat cushions	Energy absorption
Walls, flooring	Insulation

generated in flour through yeast. Both rice and flour possess a cellular structure that has been compatible with our digestive tissue as food for thousands of years. Low surface tension surfactant-induced bubbles are another interesting function that removes dirt from textiles. Moreover, natural sponge, with its open cell structure, is a useful product in absorbing and desorbing liquids. Table 1.1 shows a brief summary of foams in our lives.²

In most synthesis, foaming is a necessary phenomenon to convert raw materials to foamed products. Our focus in this volume is on foam as a product and its processing mechanisms.

Foam contains porous structures perceived as gaseous voids surrounded by a dense phase or as a gas–solid composite. The drastic differences in nature between gases and solids make foams unique combinations that have special properties for applications. For instance, the presence of a cellular structure can regulate flow velocity, dissipate disturbance, and enlarge mass transfer area. Metal foam, polymeric foam, paper foam, and ceramic foam have been developed for unique applications to enrich our lives or to explore the mysterious universe.

Since the beginning of the twentieth century, synthetic polymers have become increasingly important materials in industry. As plastication technology advanced and allowed for more sophisticated operations, the addition of a blowing agent became a natural extension of polymer processing. Combining chemistry and engineering principles, foaming methodology continued to expand in Europe and North America during and after World War II. Japan joined the developmental list in the 1960s. Presently, foam extrusion, injection molding, molded bead, x-linked foam, reactive foaming, and gelation are well-known methods of making polymeric foams, and polymeric foams have become a well-developed branch in the polymer industry. A brief developmental history of polymeric foams is presented in [Table 1.2](#).^{3–10}

Polymers, especially thermoplastic polymers, are characterized by their viscoelastic nature, which possesses processing and material uniqueness. When fit into processing and foaming criteria, their expanded cellular structure shows interesting properties. However, not every polymer is a good candidate for foam. Considering compatibility with gas, processing window,

TABLE 1.2

A Brief Development History of Polymeric Foams

Year	Foam	Inventor/Author	Reference
1931	Polystyrene foam	Munters and Tandberg	3
1937	Polyurethane foam	Bayer	1
1941	Polyethylene foam	Johnson	4
1966	Polyisocyanurate foam	Ashida and Yagi	5
1967	ABS foam	Woollard	6
1967	PVC foam	Assigned to ICI	8
1968	X-PE foam	Asaaka et al.	7
1971	PET foam	Dijkstra et al.	9
1972	Polypropylene foam	Parrish	10

capability to hold dynamic foaming, and stability during gas replacement by air, few polymers are left on the list. Surprisingly, these polymeric foams developed solid and strong applications due to their unique properties.

The gaseous voids dispersed in the polymeric matrix evidently alter the polymer's structure, morphology, and properties. Its lighter density has lent itself to commercial flotation since the 1940s. Also, its cellular structure is a natural fit in insulation, which is currently a substantial business. Annual consumption of polymeric foams is forecast to rise to 7.8 billion lb in 2005, an amount valued at \$17.6 billion.¹¹ When a cell wall possesses enough elasticity, it can be used repeatedly in the athletic and furniture industries. Other industries, such as automotive, medical, and packaging, are also enhanced by the usage of polymeric foams. The growth in diversity of applications and intensity of usage continues. In essence, it is performance oriented. A simplified performance dependency summary chart is presented in [Figure 1.1](#). Materials and mechanisms are the primary variables that directly affect structure formation. When they are combined with residual gas, mechanical and thermal characteristics are determined.

Polymeric foam can be viewed from different practical perspectives, such as products, technology, and components. Products can be categorized by dimension, density, cell size, cell density, morphology, and property; for instance, block versus film, high density versus low density, microcellular versus cellular, open cell versus closed cell, and rigid versus soft. As for technology, it is basically classified as soluble foaming and reactive foaming, or physical foaming and chemical foaming. Foam can also be classified in accordance with polymer materials such as thermoplastic and thermoset foam. [Table 1.3](#) summarizes the perspectives, for which details can be found in References 12–14. Product variation has been addressed before, and new developments keep coming to the market, making updates necessary. However, this book focuses on technology and materials—more precisely, foaming mechanisms and materials. It is appropriate to highlight foaming technologies prior to discussing foaming and material issues.

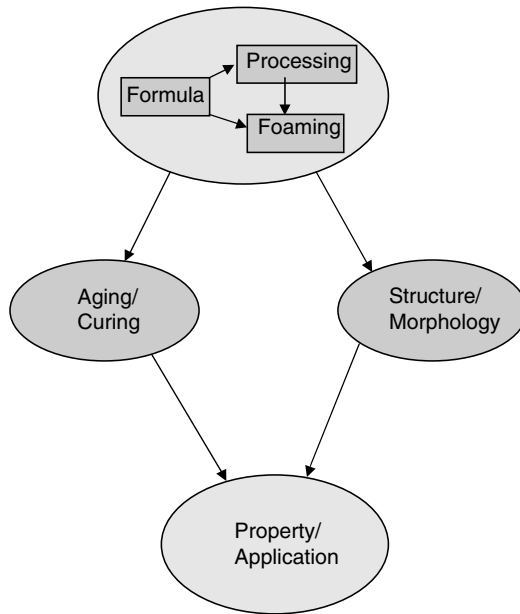


FIGURE 1.1
Polymeric foam performance dependency summary chart.

TABLE 1.3
Foaming Perspectives

Perspective	Terminology
Material	Thermoplastic and thermoset
Mechanism	Soluble foaming and reactive foaming
Nature	Flexible and rigid
Structure	Closed cell and open cell
Cell size	Microcellular and cellular
Density	High density and low density
Dimension	Board and thin sheet

1.2 Foaming Technology

The method for making foam is straightforward: generating bubbles and stabilizing them within a polymeric matrix. Bubble formation, in general, is a consequence of unstable phenomena or a way to dissipate a “disturbance”

to resume a stable state. Boiling is a good example that is often described as a transient phenomenon. When a system is excited into an unstable foaming state, a stabilization mechanism must be established in time to transform the foaming into a stable foamed product. Again, the fundamental concept sounds very simple, but there are a great variety of methods for making useful polymeric foams.

As pointed out, there are two major foaming methodologies in the polymeric foam industry: soluble foaming and reactive foaming, or physical foaming and chemical foaming. The former involves physical variation in polymer states, and the latter is solely dependent on chemical reaction. The two methodologies can also be described as follows: blowing an agent into the polymer by mixing within a chamber to take advantage of the vaporization of gas while reducing pressure; or blending reactants to reactive conditions for gas evolution within a dense medium. In both methods, the same three steps—gas implementation, gas expansion, and foam stabilization—are involved. It is reasonable to view foaming from the perspective of material strength. Figure 1.2 illustrates the different paths for common soluble foaming and reactive foaming. Many interesting techniques have been developed around each methodology in the last half century.

Plasticators, such as screw extrusion and injection molding, are very popular in making processing foamed polymers, owing to their capabilities in energy transfer to change the state of thermoplastic polymers to accommodate blowing agents in order to form a melting solution for subsequent bubbling while adequate reduction of pressure occurs. Temperature reduction is necessary to facilitate the stabilization process. Another common method is to saturate thermoplastic pellets with a blowing agent. When

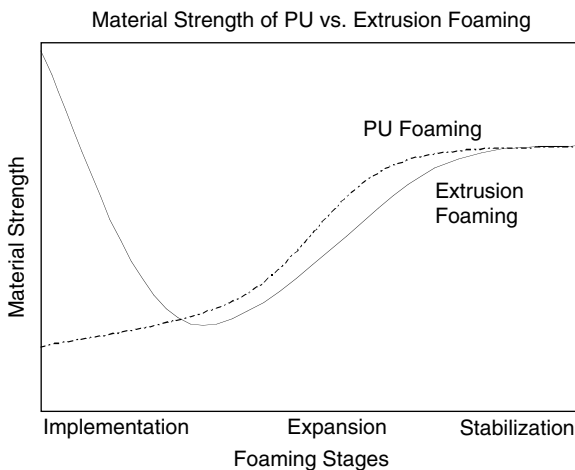


FIGURE 1.2

Material strength variation during PU reactive foaming and extrusion foaming.

TABLE 1.4

General Technologies Used to Make Polymeric Foams

Technology	Polymers	Applications
Reactive foaming	PU, Phenolics	Construction, automotive, sports, toy, furniture, packaging
Extrusion	PS, PVC, PE, PP, PET	Food, construction, decoration, packaging, medical
Injection Mold	PS, PP, PE	Automotive
Mold Bead	PS, PP, X-PE	Food, packaging, thermoforming
X-PE	PE	Sports, thermoforming

pressure reduction and temperature increase are applied for enough supersaturation, controlled foaming makes foamed products.

Reactive foaming generates foaming through chemical reaction. Gas can evolve out of simple reactions between reactants, or simply by thermally induced decomposition. Polyurethane, polyisocyanurate, and phenolics are good examples of foams made by reactive foaming. Basically, the amount of gas is governed by reactant quantity and ratio, reaction rate by catalyst and thermal condition, and foam stability by additives. Thermoset polymerization amid a gas reaction makes it very unique. The exothermic reaction enhances foaming by enthalpy. Also, changing formula and reaction conditions creates a great product spectrum for reactive foaming. Slightly over half of the foam market is designated for reactive foaming products.^{15,16}

Another common practice is to preblend chemicals, which is to decompose into gaseous components under a certain temperature with the thermoplastic to cause decomposition inside the processor for foaming. Normally, this type of reaction generates volatile gases, which makes stabilization of the polymer very critical. It is very popular for low expansion products. To increase expansion, polymer strength has to be improved. A good practice is to generate x-links among the polymer backbone prior to gas generation. Great success in polyolefin foam has been established. A summary on foaming technology is included in Table 1.4.¹⁷

1.3 Foaming Mechanisms

Production of foamed polymers includes three stages within the polymer: implementation of gas, expansion of gas, and stabilization of the polymer. Different mechanisms and parameters occur and sometimes overlap in different stages. When surrounding conditions change, competing mechanisms appear to make the kinetic process more complex. Sizable research and development efforts have been devoted to exploring the mechanisms, their individual roles, and their combined effects.^{18,19} Selected processing parameters and their effects are included in Table 1.5.

TABLE 1.5

Processing Parameters and Their Effects at Different Stages

	Implementation	Expansion	Stabilization
Temperature	Solubility ↑ Viscosity ↓ Reactivity ↑ Diffusivity ↑ Interaction parameter ↓	Volatility ↑ Surface tension ↓ Viscosity ↓	Solidification ↓ Permeability ↑
Pressure	Solubility ↑ Viscosity — Homogenization ↑	Shear heat ↑ Surface tension — Nucleation ↑	Solidification —
Shear	Solubility — Dissolution ↑ Dispersion ↑	Nucleation ↑ Growth ↑ Cell distribution ↑	Solidification ↓

The solubility limit is the overriding parameter in the implementation stage, which is strongly dependent on surrounding pressure, temperature, and interaction with the polymer. The amount of gas blending—or generated via reaction—into the polymer is a controllable processing parameter, which affects melt solution homogenization, foaming dynamics, and stabilization. The Flory–Huggins equation is a good guideline for determining how much gas can be implemented in the polymer; it is expressed as

$$\Delta F_m = kT(n_g \ln \phi_g + n_p \ln \phi_p + \chi n_g \phi_p) \quad (1.1)$$

where ΔF_m , k , T , and χ represent, in order, the free energy of mixing, the Boltzmann constant, the absolute temperature, and the interaction parameter. Respectively, n , ϕ , and the subscripts p and g denote the molar fraction, the volume fraction, the polymer, and the gas. The interaction parameter, χ , consists of two parts, entropy and enthalpy. For most polymer/gas systems, the former has a mean around 0.3, and the latter is determined by solubility parameters.²⁰ It is expressed as

$$\chi = 0.3 + V_g/RT (\delta_p - \delta_g)^2 \quad (1.2)$$

where V_g , R , and δ denote the molar volume of gas, the ideal gas constant, and the solubility parameter, respectively. Common polymer/gas interaction parameters are tabulated in Table 1.6.^{21,22}

Free energy of mixing for various polymer/gas systems can be prepared as illustrated in Figure 1.3, with polystyrene and butane at two different temperatures (processing and application temperatures). The lower the mixing energy, the more stable it is. The curve sometimes shows two dips (e.g., PS/butane at 30°C), which suggests stable gas/polymer coexistence. One is gas rich and the other polymer rich, corresponding to gas in the cell

TABLE 1.6

Solubility Parameter of Selected Common Polymers and Blowing Agents

B/A	δ (cal/cm) ^{1/2}	Polymer	δ (cal/cm) ^{1/2}
n-Pentane	7.0	Polyethylene	7.9
n-Butane	6.8	Polystyrene	8.6
Propane	6.4	Polypropylene	9.2
Ethane	6.0	Polyvinylchloride	9.4
CCl ₂ F ₂	11.3	Polyvinylacetate	8.9

and gas in the cell wall. Pressure-dependent parameters are included in the Sanchez–Lacombe model,²³ and additional temperature-dependent parameters in Simha–Somcynsky.²⁴ Since gas is so pressure sensitive, both models are better than Flory–Huggins for a gas-charged polymeric system.

The gas molecule is in the Angstrom (10⁻⁸ cm) domain, and the “holes” in the polymeric liquid are 10⁻⁶ to 10⁻⁷ cm.²⁵ Visible bubbles are of the same magnitude as cosmic dust, 10⁻⁵ cm. How free gas molecules transform into “clusters” to account for phase separation is an interesting subject. Due to the limits of analytical instrumentation, some theories have been developed to explain the transformation.

When the gas solubility limit is met, the gas phase tends to separate from the polymer phase. A typical phase diagram is illustrated in Figure 1.4, which suggests a stable single phase, then a metastable single phase, in the unstable two-phase region. It is believed that the dominant mechanism in the metastable state is nucleation (Nu), and that the dominant mechanism in the unstable state is spinodal decomposition (SD), or the domains of rearrangement and growth. Both are controlled by diffusion, although the directions

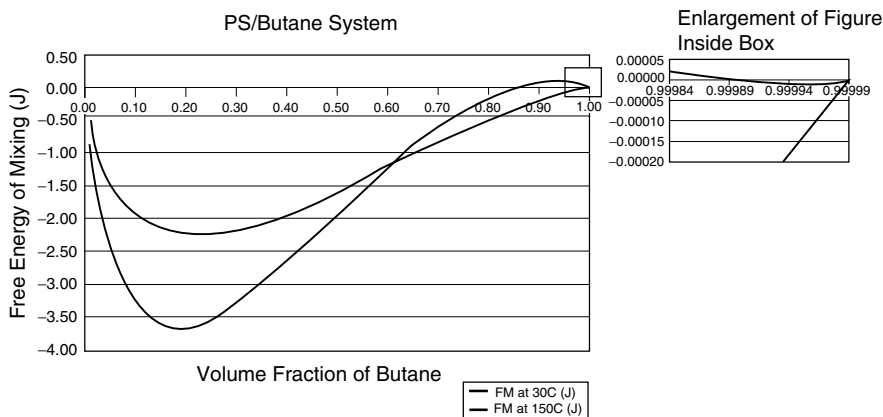


FIGURE 1.3

Free energy of mixing vs. volume fraction of butane at two different temperatures for PS/butane system.

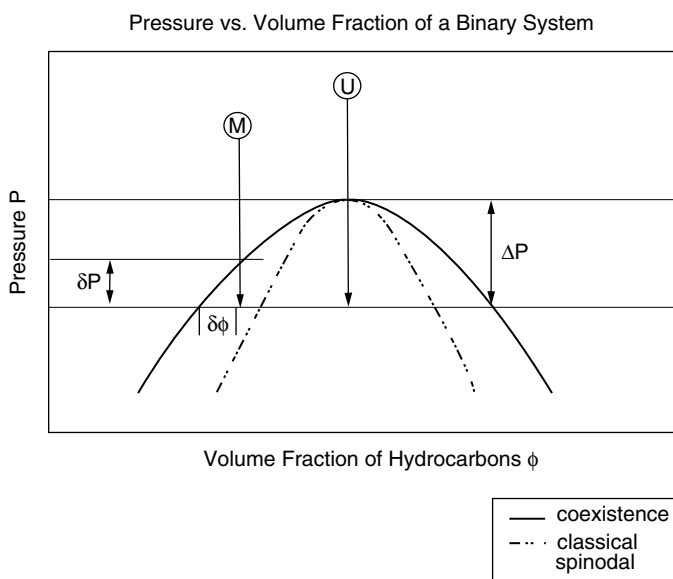


FIGURE 1.4

Bimodal and spinodal curves; M and U indicate metastable and unstable paths.

of diffusion are opposite, as presented in Figure 1.5.^{26,27} Figure 1.6 demonstrates the two different phase separation structures for polystyrene and partially brominated polystyrene at two different volume fractions.²⁸

SD, counterintuitively, exhibits negative diffusion; namely, diffusion moves from low concentration to high concentration. However, in the molecular domain, when driving force is high, a molecular cluster could grow above a certain concentration intensity (critical wavelength) to absorb the nearby molecules. Depending on the separation path, the metastable state could be dominant or negligible to cause SD or Nu separation. Table 1.7

TABLE 1.7

Phase Separation Mechanisms: Nucleation and Spinodal Decomposition

	Nucleation	Spinodal Decomposition
Initial state	Stable phase	Stable phase
$T \uparrow$ $P \downarrow$, or $T \downarrow$	Nucleating sites form	Composition fluctuation increases
Activation energy	Yes	No
Diffusion	Positive	Negative
Metastable state	Yes	Minimum
Growth	Separate growth	Interconnection
Late stage coarsening	No	Yes

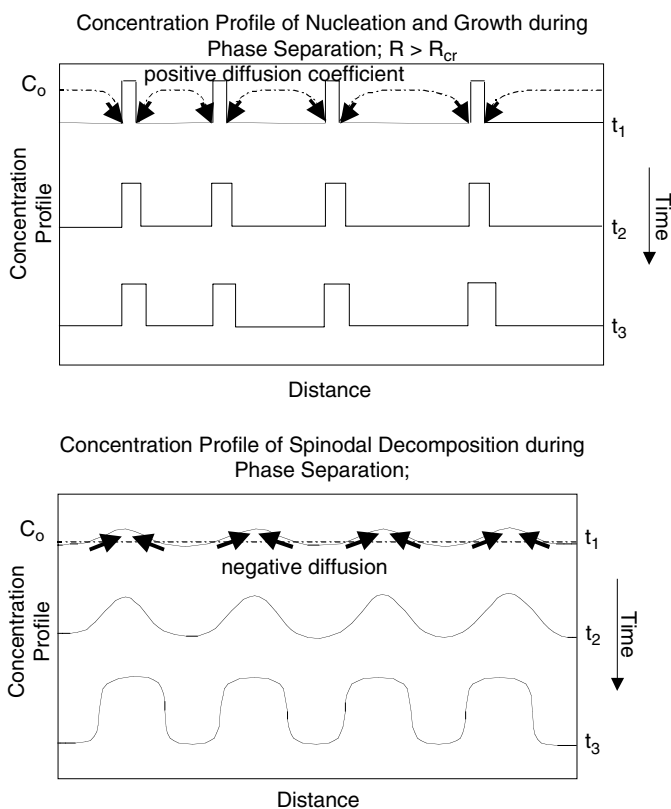


FIGURE 1.5

Phase separation comparison—nucleation [$R > R_{cr}$]; spinodal decomposition (SD) [$\lambda > \lambda_{cr}$]; R , λ , and subscript cr denote size, concentration wave length, and critical.

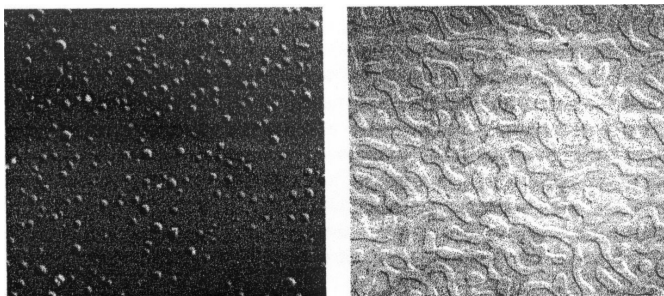


FIGURE 1.6

Structure patterns emerging during phase separation in PS/Br-PS blends. Left: nucleation with PS at 80 vol%. Right: spinodal decomposition (SD) with PS at 50 vol%.

tabulates the two different kinds of separation.²⁹ Clearly, the two different mechanisms, Nu and SD, are accountable for the separation in the early stage.

It is known that phase separation ranges from single phase (i.e., boiling and crystallization) to multiphase (i.e., polymer blend processing, foaming). Although SD has described certain separations in polymer blends, when we talk about foaming, it is extremely difficult to investigate the dynamic molecular movements to confirm its original mechanism: energy barrier into critical size (Nu) or energy fluctuation into growth mode (SD). When the gas phase exceeds the solubility limit, such as with gas evolution in PU foam, it tends to form a least-energy spherical shape to separate from the surrounding polymer. It dissipates energy by absorbing the upcoming gases to result in expansion to a stable state. The energy barrier does not exist. Another example is foam extrusion, in which a sharp change into a high degree of supersaturation occurs, with high temperature or low pressure. The volatile phase becomes too energetic to coexist with the surrounding polymer phase. Unstable separation occurs immediately.

Both Nu and SD are plausible mechanisms to account for phase separation in polymeric foaming, as illustrated in [Figure 1.7](#).³⁰ SD seems prone to develop more cell coalescence and the corresponding open cell and cell size distribution. Foaming induced by a sharp energy gradient tends to show more cell connections and ruptures. For a modest energy gradient, external aid, such as motion and deformation, is necessary to facilitate nucleation into existence; phase separation will not occur within process time. Diffusion to vapor phase above the polymeric melt may become the main mechanism to reduce the supersaturation and to re-establish the equilibrium.

Whether the process is Nu or SD, enough gas molecules need to gather together to be sustainable and to overcome surrounding confinement. Spherical shape contains the minimum surface area, or surface energy. According to the critical bubble radius:

$$R_{cr} = 2\sigma / (P_b - P) \quad (1.3)$$

where σ , P_b , and P represent gas surface tension, bubble pressure, and surrounding pressure, respectively. The critical bubble radius is unstable in nature, according to the mass balance equation.³¹ Any perturbation can cause it to move into unstable growth, during which size expansion lowers its concentration to encourage diffusion and to cause a reciprocal response until the driving force disappears.

When the surrounding pressure is greater than the gas pressure, gas molecules are suppressed into the polymer matrix to form a homogenized melt. In foam extrusion, high pressure is needed to keep phase separation from happening before the free expansion at the exit.³² Enough pressure reduction is necessary for gas molecules to gather together to overcome the curvature confinement. Experiments have determined that modest pressure reduction seems inadequate to drive the bubble phase into existence.³³ A laser beam

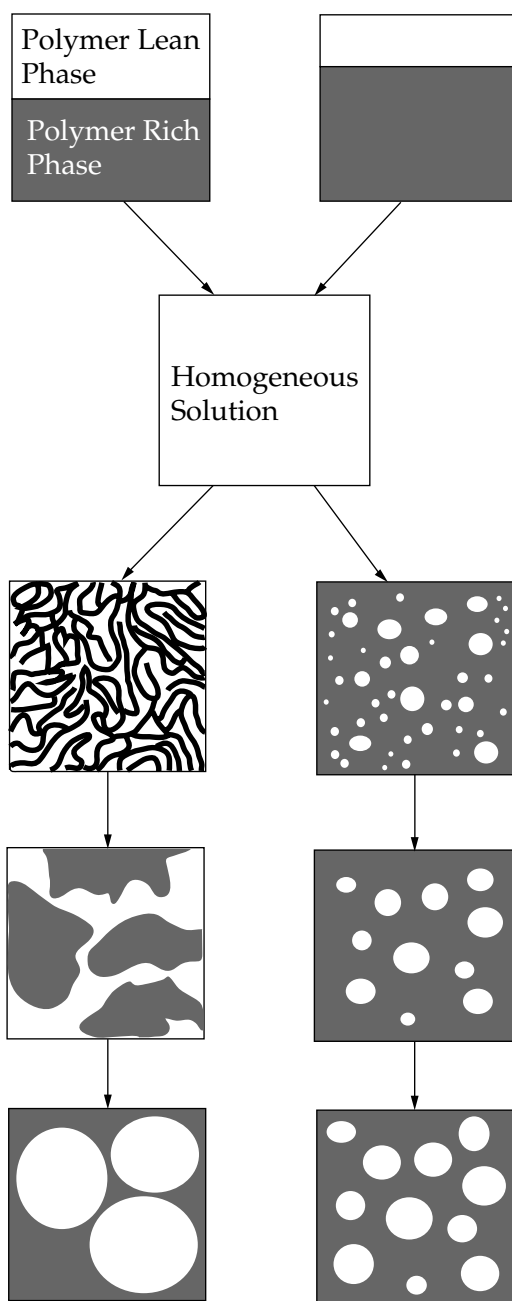


FIGURE 1.7

Phase separation illustration. Left: spinodal decomposition (SD). Right: nucleation (Nu).

was used to detect the nucleation site for foam extrusion, and extrapolation was applied to suggest the critical size.³⁴

Kinetics has been applied to the energy barrier nucleation phenomenon; this has led to the Arrhenius expression for nucleation rate:

$$J \propto \exp(-E_a/kT) \quad (1.4)$$

where E_a represents activation energy, which is determined by interfacial holding energy and degree of supersaturation. A detailed expression was presented by Blander and Katz:³⁵

$$J = N(2\sigma/(\pi m))^{1/2} \exp(-16\pi\sigma^3/(3kT\Delta P^2)) \quad (1.5)$$

where N , σ , m , and ΔP denote number of molecules per unit volume, surface tension, mass of a molecule, and pressure difference (or superheat), respectively.

More energy contribution, as with surface energy or flow energy, leads to further modification of Equation 1.5. Since nucleation is an unstable phenomenon, growth is in imminent convulsion, in which expansion and gas diffusion occur simultaneously.

Another interesting mechanism is cell opening, especially with high expansion or a weak cell wall. According to the packing theory, a spherical bubble begins to share a cell wall after expansion over four times. As a result of sharing a wall, thinning and rupture appear. Figure 1.8 shows five high-speed photographs of a polydimethylsiloxane membrane stretching to rupture under pressure-induced expansion. A black hole, weak spot, or low surface tension area forms on top before the membrane bursts out. It is common for a high degree of expansion to occur in low-density thermoplastic

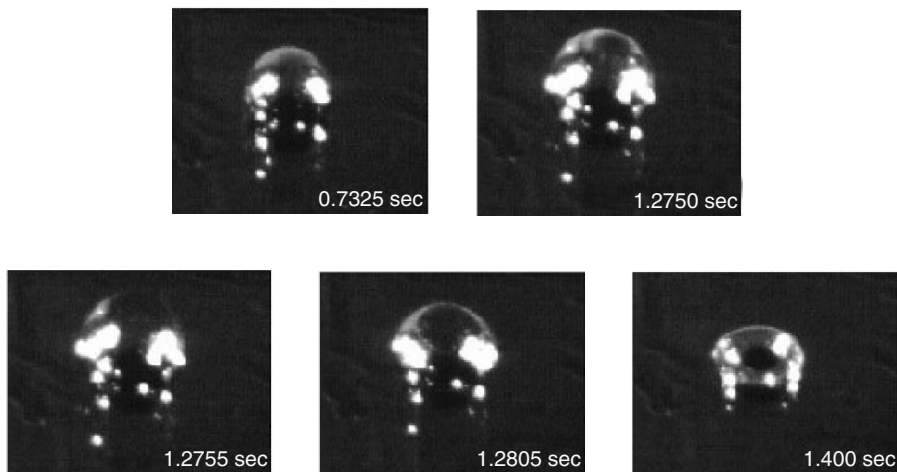


FIGURE 1.8

Polymethylsiloxane in a box with a hole to allow air to expand the membrane until it bursts; five high-speed camera photos showing black hole formation before rupture.

foam formation. As a result, an open cell is formed. This area needs further investigation to correlate it with other properties.

As for thermoset reactive foaming, cell stability involves drainage of the membrane. It tends to recede to a strut, forming an open cell skeleton. (A detailed description is presented in [Chapter 5](#).) In fact, when the strut retains enough strength, the open-cell structure presents unique performance characteristics and is especially good for sound and liquid absorption.

1.4 Materials

Polymeric foam is good for a wide variety of applications. Polymers and gases are the fundamental components. They are basically two different materials, both in nature and in general properties. The dissimilar materials stay together homogeneously under processing conditions, separate into a cellular structure, and stabilize within a reasonable time. There is no doubt that material and mechanism need to complement each other for a successful process. Polymers and gases have to satisfy every mechanism, such as the conditions of solubilization, homogenization, phase separation, and stabilization. Only certain polymeric foams survive these screening tests.

Different mechanisms involve different competing parameters. As a result, each step has a window, over or under which foaming efficiency is reduced. Moreover, the list of conditions is shortened when mass production and the economics of competition come into consideration.

For soluble foaming, gas solubility in the polymer under processing conditions is a top concern. Solubility is usually dictated by surrounding pressure; a pressure that is too high causes processor concerns, and a pressure that is too low may not generate enough superheat for proper foaming. Halogenated hydrocarbons demonstrate an excellent soluble nature in some thermoplastic melts, but they are too stable to decompose in the low atmosphere and become problematic in regard to ozone depletion and formation in the high atmosphere. Nowadays, a blowing agent has to comply with not only technical and economic requirements, but environmental and safety requirements as well. As for the polymer, it has to be processible with and without a blowing agent and must possess enough strength to maintain the dynamic expansion to create a unique cellular structure. The key system parameters for successful soluble foaming are shown in Table 1.8. Common

TABLE 1.8

Key Parameters for Soluble Foaming

Stage	Gas into polymer	Gas bubbles in polymer	Air bubbles in polymer
Mechanism	Dissolution/homogenization	Foaming	Curing
Parameters	Solubility, diffusivity	Volatility, surface tension	Permeability

TABLE 1.9

General Thermoplastic Foams

	Polystyrene	Polyvinylchloride	Polyolefin
Polymer	Amorphous		Semi-crystalline
Processing	Extrusion Injection molding Mold bead	Extrusion Injection molding	Extrusion Injection molding Mold bead X-linking
Product	Rigid Insulation	Flexible and rigid Fire retardancy Low temp stability	Soft to rigid Chemical resistance Low temp stability

foam materials that correspond to soluble foaming principles are polystyrene, polyvinylchloride, and polyolefin. Each has unique processing and product features, which are summarized in Table 1.9.

In reactive foaming, reaction kinetics characterizes materials. Reactions to generate gases and to form long chain polymers must occur at the right stage; transient bubbling or limited expansion may otherwise occur. Appropriate functional groups and their ratios with catalysts and surfactants should be controlled such that reaction time and desired foam property can be obtained. Reaction time dictates the reactor (or mixer) design. The exothermic nature can easily develop extra heat for additional expansion of formed gas to acquire a very high expansion, but it also makes stability hard to control. The right surfactant can certainly widen the favorable expansion window.³⁶

Polyurethane (PU) foam is a well-established foam technology that accounts for over half of overall polymeric foam production. It basically contains flexible and rigid PU foam. The two types of foam are based on a similar chemistry, and the type and degree of polymerization make the difference in product and property. A brief summary is presented in Table 1.10. [Chapters 6](#) and [7](#) are devoted to flexible and rigid PU foam, respectively.

TABLE 1.10

PU Foams

	Flexible PU Foam	Rigid PU Foam
Formula	Polyol + Isocyanate Long polyol with less -OH	Polyol + Isocyanate Short polyol with more -OH
Density, kg/m ³	5–200	15–800
Properties	Absorption Soft	Insulation Hard
Markets	Furniture	Construction Appliance

References

1. Lee, S.T. and Park, C.B., *Polymeric Foams: Understanding Foaming Technology*, CRC Press, Boca Raton, FL, in press, 2005.
2. Weaire, D. and Hutzler, S., *The Physics of Foams*, Oxford University Press, 2000.
3. Munters, G. and Tandberg, J.G., U.S. Patent 2,023,204, 1935.
4. Johnson, F.L., U.S. Patent 2,256,483, 1941.
5. Ashida, K. and Yagi, T., French Patent 1,511,865, 1966.
6. Woollard, D.C., *J. Cell. Plast.*, 4, 1, 16–21, 1968.
7. Assigned to ICI, French Patent 1,487,545, 1967.
8. Asaaka, M., Torii, K., and Yamanaka, E., *Jpn. Kokai Tokyo Koho*, 43–22 674, 1968.
9. Dijkstra, A.J., Goodman, I., and Reid, J.A.W., U.S. Patent 3,553,157, 1971.
10. Parrish, R.G., U.S. Patent 3,637,458, 1972.
11. Foamed Plastics, Freedonia Group, Inc., Cleveland, OH, 1997.
12. Klempner, D. and Frisch, K.C., eds., *Handbook of Polymeric Foams and Foam Technology*, Hanser, Munich, 1991.
13. Lee, S.T., ed., *Foam Extrusion: Principles and Practice*, CRC Press, Boca Raton, FL, 2000.
14. Frisch, K.C., Historical developments of polyurethanes, in *60 Years of Polyurethanes*, eds. J.E. Kresta and E.W. Eldred, Technomic, Lancaster, PA, 1998.
15. Herrington, R., *Dow Polyurethanes; Flexible Foams*, Dow Chemical, 1997.
16. Woods, G., *The ICI Polyurethanes Book*, ICI Polyurethanes, 1990.
17. Park, C.B. and Lee, S.T., Foam Seminar, sponsored by Society of Plastics Engineers, Nashville, TN, 2003.
18. Burt, J., The elements of expansion of thermoplastics. II. *J. Cell. Plast.*, Nov./Dec. 1978.
19. Naguib, H.E., Park, C.B., Yoon, E., and Reichelt, N., Fundamental foaming mechanisms governing volume expansion of extruded PP foams, Foams 2002, seminar sponsored by Society of Plastics Engineers, Nashville, TN, 2002.
20. Merrill, E.W., Thermodynamic aspects of devolatilization of polymers, in *Polymer Devolatilization*, ed. R.J. Albalak, Marcel Dekker Inc., New York, 1996, chap. 2.
21. Van Krevelen, D.W., *Properties of Polymers*, 3rd ed., Elsevier Science, Amsterdam, 1990.
22. Grulke, E.A., Solubility Parameter Values, VII/675, *Polymer Handbook*, 4th ed., eds. J. Brandrup, E.H. Immergut, and E.A. Grulke, John Wiley & Sons, New York, 1999.
23. Sanchez, I.C. and Lacombe, R.H., Statistical thermodynamics of polymer solutions, *Macromolecules*, 11, 6, 1145–1156, 1978.
24. Simha, R. and Moulinie, P., Statistical thermodynamics of gas solubility in polymers, in *Foam Extrusion*, ed. S.T. Lee, CRC Press, Boca Raton, FL, 2000, chap. 2.
25. Bueche, F., *Physical Properties of Polymers*, Interscience, New York, 1962.
26. Sperling, L.H., *Introduction to Physical Polymer Science*, John Wiley & Sons, New York, 2001.
27. Debenedetti, P.G., Phase separation by nucleation and by spinodal decomposition: fundamentals, in *Supercritical Fluids*, eds. E. Kiran, P.G. Debenedetti, and C.J. Peters, Kluwer, Dordrecht, the Netherlands, 2000.

28. Strobl, G.R., *The Physics of Polymers: Concepts for Understanding Their Structures and Behavior*, 2nd ed., Springer-Verlag, Heidelberg, 1997.
29. Kiran, E., Polymer miscibility and kinetics of pressure-induced phase separation in near-critical and supercritical fluids, in *Supercritical Fluids*, eds. E. Kiran, P.G. Debenedetti, and C.J. Peters, Kluwer, Dordrecht, the Netherlands, 2000.
30. Gunton, J.D., San Miguel, M., and Sahni, P.S., The dynamics of first-order phase transitions, in *Phase Transitions 8*, Academic Press, New York, 1983, chap. 3.
31. Amon, M. and Denson, C.D., A study of the dynamics of foam growth: analysis of the growth of closely spaced spherical bubbles, *Polym. Eng. Sci.*, 24, 13, 1026–1034, 1984.
32. Thiele, W.C., Foam extrusion machinery features, in *Foam Extrusion*, ed. S.T. Lee, CRC Press, Boca Raton, FL, 2000, chap. 8.
33. Biesenberger, J.A. and Lee, S.T., A fundamental study of polymer melt devolatilization part three: more experiments on foam-enhanced DV, *Polym. Eng. Sci.*, 27, 1987.
34. Han, J.H. and Han, C.D., Bubble nucleation in polymeric liquids. I. Bubble nucleation in concentrated polymer solutions, *J. Polym. Sci. B: Polym. Phys.*, 28, 711, 1990.
35. Blander, M. and Katz, J. L., Bubble nucleation in liquids, *AIChE J.*, 21, 833, 1975.
36. Hilyard, N.C. and Cunningham, A., *Low Density Cellular Plastics: Physical Basis of Behaviour*, Chapman & Hall, London, 1994.

Melt Elasticity of Polyolefins: Impact of Elastic Properties on Foam Processing

M. Yamaguchi

CONTENTS

- 2.1 Introduction
- 2.2 Melt Elasticity
 - 2.2.1 Elastic Properties
 - 2.2.2 Measurements of Elastic Response
 - 2.2.3 Role of Long-Chain Branches
 - 2.2.3.1 Model Polymer
 - 2.2.3.2 Low-Density Polyethylene
 - 2.2.4 Melt Elasticity of New Polyolefins
- 2.3 Modification of Melt Elasticity
 - 2.3.1 Effect of Processing History
 - 2.3.1.1 Origin of Shear Modification
 - 2.3.1.2 Processing History by Conventional Processing Machines
 - 2.3.2 Modification by Polymer Blends
 - 2.3.2.1 Background
 - 2.3.2.2 Blends with Weak Gel
 - 2.3.2.3 Processability of Foaming
- 2.4 Conclusion
- References

2.1 Introduction

It is generally accepted that low-density polyethylene (LDPE) produced by radical polymerization under high pressure is preferable to linear low-density polyethylene (LLDPE) for foaming. Similarly, high-density polyethylene (HDPE) with a chromium catalyst is often used for blow molding rather than that with a Ziegler–Natta catalyst. The reason in both cases is strong melt

elasticity due to long-chain branches. Therefore, a comprehensive knowledge of the primary elastic properties peculiar to polymer melts and their relation to foaming is required in order to decide the operating condition and the recipe for various foaming processes, such as extrusion gas-foaming, crosslinked foaming by a chemical blowing agent, and bead foaming.

It is, however, difficult to establish the precise relation between rheological properties, including melt elasticity, and processability. One of the reasons is that a foamable material in an extruder is not a simple polymer melt. The effect of solving gas on the rheological properties is dependent on the miscibility, which also affects the melting point.¹ Further, the concentration of the solving gas in a polymer melt decreases during expansion. Likewise, distribution of a chemical blowing agent in a polymer melt plays a decisive role on the cell morphology for crosslinked foaming. Another reason for the difficulty is that foaming is carried out under non-isothermal conditions. In particular, the processability of extrusion foaming for a crystalline polymer, such as LDPE, which is often performed near the crystallization temperature T_c , may be affected by the crystallization behavior, because even a small amount of crystallites can change the rheological properties drastically. Further, the crystallization temperature of LLDPE or LDPE rises rapidly when blended with a small amount of PE with a higher T_c because the PE with a higher T_c acts as a crystalline nuclei for the rest.² As a result, the blend shows marked melt elasticity around T_c since crystallites behave like crosslink points, in which molecular weight and polydispersity also play an important role. Hence, considerable attention has to be paid to the crystallization temperature for extrusion foaming of polyethylene blends. It should also be kept in mind that adding talc, as the nucleating agent of bubbles often enhances the crystallization temperature of polyolefins. As for crosslinked batch-foaming, temperature as well as pressure falls off sharply during foaming, since the gas in the cell is immediately cooled down by adiabatic expansion after ejection from a mold. Consequently, crystallization takes place rapidly, which prevents the expanded cells from shrinking.³

This chapter will not cover thoroughly the role that elastic properties play during the entire foaming process. Nor will it closely examine how this elasticity should be tailored for each of the different phases, such as nucleation, bubble growth, and stabilization. However, information about the basic rheological properties of simple polymer melts under isothermal conditions is still highly relevant for foam practitioners. In the following section, the relation between molecular structure and melt elasticity will be described, as that relation pertains to branched polymers and new polyolefins that are being developed by advanced polymerization technology. This follows a brief review of melt elasticity and experimental measuring methods. Further, the following recent experimental studies on the mechanical and material modifications of melt elasticity will be summarized in [Section 2.3](#): (1) the effect of applied processing history on the melt elasticity for a branched polymer, which should be controlled in various foaming processes for a better and more steady production; and (2) the polymer blend technique, used to enhance

melt elasticity, and its effect on foaming. Especially important in the polymer blend technique are the new types of blends with crosslinked polymers characterized as weak gels; these are explained in detail, since this blend technology may make various linear polymers with less melt elasticity available for foaming.

2.2 Melt Elasticity

2.2.1 Elastic Properties

A polymer melt, as a viscoelastic material, shows various elastic behaviors, such as strain recovery after cessation and the Weissenberg effect (produced by normal stress difference), as well as viscous features.⁴ Further, the Barus effect, also referred to as extrudate swell and generally ascribed to the Weissenberg effect, is quite familiar in actual processing. In general, these elastic properties are attributed to the recovery force from the low entropy state of polymer chains, such as anisotropy of molecular orientation and the stretching of a chain, which are given via entanglement couplings in a similar fashion to that of permanent, chemical crosslink points in a rubber molecule. Since entanglement couplings act as crosslink points only temporarily, the stress generated by deformation in the distant past is of less importance and fades significantly, as shown in [Figure 2.1](#).

The fading rate, represented by the inverse of relaxation time, dominates the viscoelastic characteristics of a polymer melt.⁴ When the relaxation time is longer than the characteristic time for flow, i.e., the inverse of the strain rate, the polymer melt responds like an elastic solid. On the other hand, the viscous properties overcome the elastic ones when the relaxation time is shorter than the flow characteristic time. Discussions on the mechanical response of a polymer melt are always carried out employing the dimensionless parameter known as the Deborah number, which is defined as the relaxation time divided by the inverse of the strain rate. Apparently, elastic properties are pronounced at a large Deborah number.

The molecular weight dependence of relaxation time is interpreted from the molecular point of view, which is known as the Doi-Edwards tube theory.⁵ Doi and Edwards proposed that large-scale motion of macromolecules is limited in a tube-like region composed of neighbor chains,⁵ as shown in [Figure 2.2A](#). Since lateral motion is restricted owing to the topological constraints of the temporary network, a polymer chain diffuses along the backbone chain by changing its conformation; i.e., it moves within the tube like a snake. This motion is called *reptation*. In a simple polymer melt, reptation is the terminal relaxation mechanism. Through reptation, molecular orientation (or the memory of the applied strain) decays with time. In the process of reptation, chain ends relax more quickly than the central part as the result of back-and-forth movement in the tube (Figures 2.2B, C, and D) in accordance with the

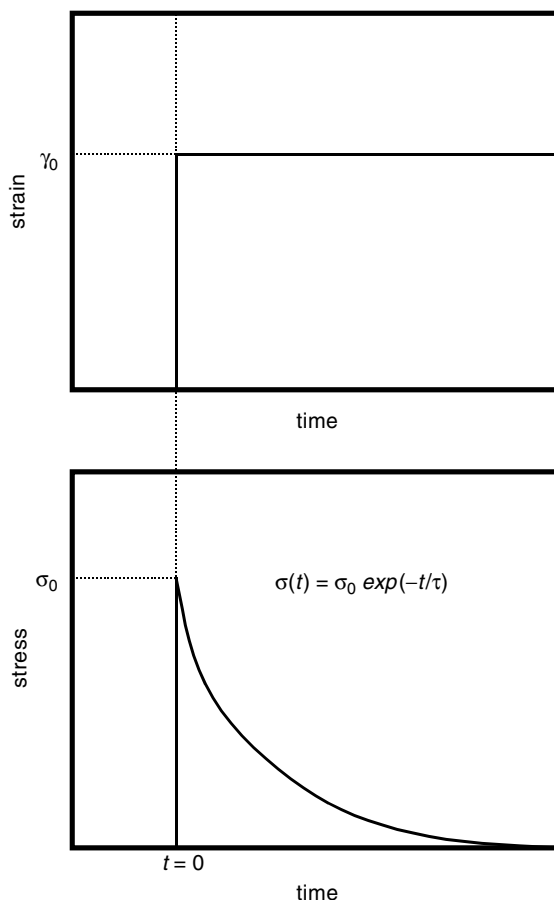


FIGURE 2.1

Schematic representation of stress relaxation process after a step strain γ_0 applied at $t = 0$ for a viscoelastic body having a characteristic relaxation time τ . The initial stress σ_0 at $t = 0$ decays with time following $\sigma(t) = \sigma_0 \exp(-t/\tau)$. In the case of a simple polymer melt, relaxation time in the terminal mode is determined by topological interaction between neighbor chains (entanglement couplings). Further, the molecular orientation also decays with time proportional to stress.

stress.⁵ (Doi and Edwards derive the relaxation modulus employing the concept of reptation.) Eventually, anisotropy of molecular orientation, one of the origins of melt elasticity, decreases with time. Apparently, a longer chain takes a longer time to relax. The diffusion time is given by the square of the contour length of the tube divided by the diffusion coefficient. Considering that the contour length is proportional to molecular weight M and the diffusion coefficient is proportional to M^{-1} , relaxation time of reptation τ_1 is proportional to M^3 , which is in close agreement with the experimental result $\tau_1 \propto M^{3.4}$.

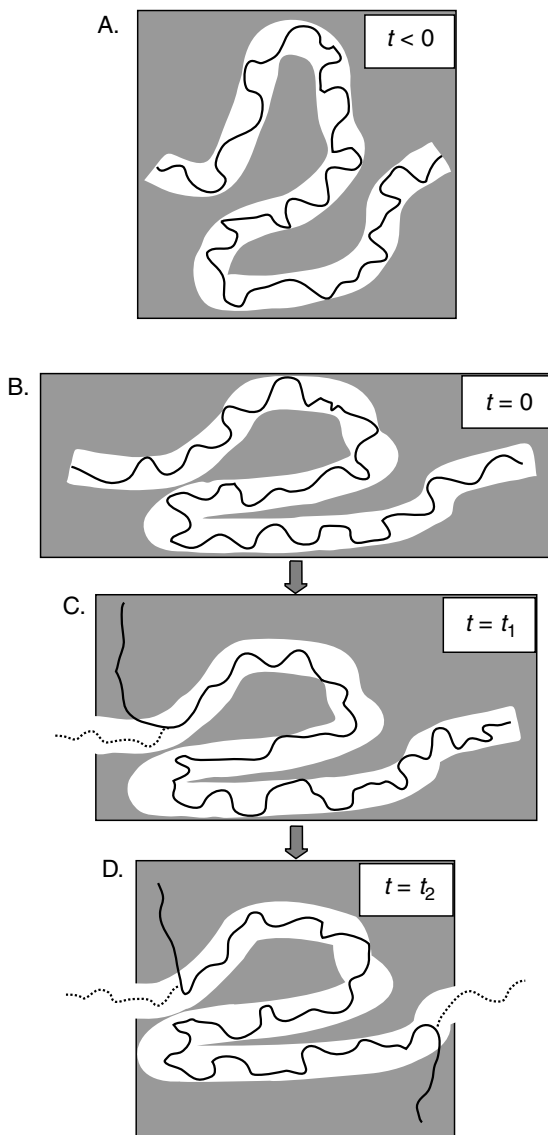


FIGURE 2.2

Schematic illustration following the tube model described in detail in Doi and Edwards. A polymer chain, a solid line, is confined within a tube, white region, generated by the topological constraints of neighbor chains. **(A)** At the equilibrium state, the orientation of chain segments is isotropic ($t < 0$). **(B)** Applied step strain deforms a chain and then orientation takes place ($t = 0$). **(C), (D)** The chain escapes from the tube by back-and-forth movement, or reptation. Consequently, the degree of orientation, or memory of the applied strain, decreases with time ($t = t_1, t_2$) in accordance with stress. Because of the back-and-forth movement, chain ends relax more quickly than the central part. In the figures, the dark rectangular regions represent the average orientation of the polymer chain.

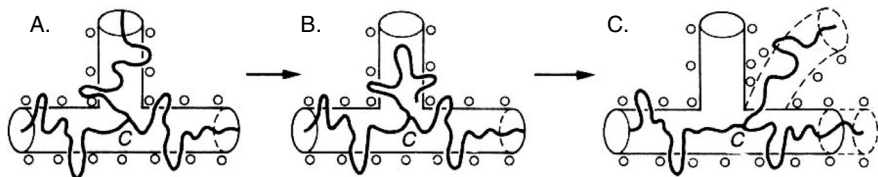


FIGURE 2.3

Relaxation process of a star-shaped polymer following the tube model. Since a branch prohibits simple reptation along the tube, the polymer changes its conformation by the contour length fluctuation. As shown in Figure 2.3B, this process needs the end segment of a branch down to the branch point, represented by the symbol C, which requires a low entropy state. (From Doi, M. and Edwards, S.F., *The Theory of Polymer Dynamics*, Clarendon Press, Oxford, 1986. With permission.)

Besides molecular weight and distribution, long-chain branches play a significant role in elastic properties. This is also explained by the Doi-Edwards theory.⁵ According to the theory, a branch point is assumed to be fixed, as shown in Figure 2.3, and thus simple reptation is prohibited. Consequently, conformation change of long-chain branches has to take place by utilizing contour length fluctuation, or retraction to the branch point within the tube. This retraction process requires exposing a polymer chain to a low enthalpy state, due to distorted conformation around the branch point. Hence, relaxation time increases exponentially with the length of branches.⁵

Since actual polymer melts have numerous relaxation times due to polydispersity and long-chain branches, the distribution as well as the strength of each relaxation mode is responsible for the viscoelastic properties. As a rule of thumb, elastic properties are strongly affected by terminal relaxation. For example, shear storage modulus G' representing elastic response to oscillatory deformation is more sensitive to the long tail of relaxation time τ than loss modulus G'' since G' is proportional to $\tau^2 / (1 + \omega^2 \tau^2)$, instead of $\tau / (1 + \omega^2 \tau^2)$ for G'' , as shown in Equations 2.1 and 2.2:

$$G' = \int_{-\infty}^{\infty} H(\tau) \frac{\omega^2 \tau^2}{1 + \omega^2 \tau^2} d \ln \tau \quad (2.1)$$

$$G'' = \int_{-\infty}^{\infty} H(\tau) \frac{\omega \tau}{1 + \omega^2 \tau^2} d \ln \tau \quad (2.2)$$

where ω is the angular frequency and $H(\tau)$ is the relaxation spectrum, which decides the linear viscoelastic properties.

Further, steady-state compliance J_e^0 , defined by Equation 2.3, is often discussed as an elastic parameter of the terminal zone in the linear viscoelastic

region, which represents average distortion of polymer coils during flow at $\omega \rightarrow 0$ or $\dot{\gamma} \rightarrow 0$.⁴

$$J_e^0 = \lim_{\omega \rightarrow 0} \frac{G'}{G''^2} = \frac{\int_{-\infty}^{\infty} H(\tau) \tau^2 d \ln \tau}{\left(\int_{-\infty}^{\infty} H(\tau) \tau d \ln \tau \right)^2} \quad (2.3)$$

The Rouse model predicted that steady-state compliance of a linear polymer relates to molecular weight distribution as follows:⁶

$$J_e^0 \propto \frac{M_z M_{z+1}}{M_w^2} \quad (2.4)$$

Similar to Equation 2.4, Milles has proposed the following relation, which is in good agreement with the data obtained for various polymers:⁷

$$J_e^0 \propto \left(\frac{M_z}{M_w} \right)^{3.4-3.7} \quad (2.5)$$

The equations demonstrate that polymers with broad molecular weight distribution exhibit pronounced melt elasticity, whereas zero-shear viscosity η_0 , the viscous parameter in the terminal zone, is proportional to $M_w^{3.4}$. Further, the product of J_e^0 and η_0 gives the weight-average terminal relaxation time τ_w , defined as follows:

$$\tau_w = \frac{\int_{-\infty}^{\infty} \tau^2 H(\tau) d \ln \tau}{\int_{-\infty}^{\infty} \tau H(\tau) d \ln \tau} = \eta_0 J_e^0 \quad (2.6)$$

Beyond the linear viscoelastic region—at a high strain rate or with a large strain—rheological properties are more complicated. However, some empirical rules have been proposed to relate steady-state nonlinear viscoelastic properties to the rheological parameters in the linear region, as follows:^{8,9}

$$\theta(\dot{\gamma}) \equiv \frac{N_1(\dot{\gamma})}{\dot{\gamma}^2} \cong 2 \frac{G'}{\omega} \left\{ 1 + \left(\frac{G'}{G''} \right)^2 \right\}^{0.7} \bigg|_{\omega \rightarrow \dot{\gamma}} \quad (2.7)$$

$$\eta(\dot{\gamma}) \equiv \frac{\sigma(\dot{\gamma})}{\dot{\gamma}} \equiv \frac{G''}{\omega} \left\{ 1 + \left(\frac{G'}{G''} \right)^2 \right\}^{0.5} \bigg|_{\omega \rightarrow \dot{\gamma}} \quad (2.8)$$

where $\theta(\dot{\gamma})$ is the primary normal stress coefficient, $N_1(\dot{\gamma})$ is the primary normal stress difference, $\eta(\dot{\gamma})$ is the shear viscosity, and $\sigma(\dot{\gamma})$ is the shear stress.

Equation 2.8 is the well-known Cox–Merz relation.⁹ Apparently, the primary normal stress difference, one of the elastic parameters, is affected by G' to a greater degree than by G'' , indicating that $\theta(\dot{\gamma})$ is more sensitive to terminal relaxation than $\eta(\dot{\gamma})$. In addition, the steady-state recoverable strain $\gamma_{rs}(\dot{\gamma})$, which relates directly to the degree of molecular orientation during flow in a simple polymer melt, is given by the following relation:⁸

$$\gamma_{rs}(\dot{\gamma}) \equiv \frac{G'}{G''} \left\{ 1 + \left(\frac{G'}{G''} \right)^2 \right\}^{1.5} \bigg|_{\omega \rightarrow \dot{\gamma}} \quad (2.9)$$

The steady-state recoverable strain is also an important elastic property for actual processing because it is responsible for the residual strain in products. Equations 2.7–2.9 are quite convenient for predicting nonlinear properties from linear viscoelastic properties, although they should not be employed for complex fluids such as polymer blends and composites. Further, they make it easier to comprehend the contribution of elastic and viscous properties to each steady-state property.

The elastic properties discussed above are ascribed mainly to the anisotropy of molecular orientation. The relation with stress is widely understood as the stress-optical rule. Furthermore, besides the molecular orientation, chain stretching within the tube, which also lowers the entropy of a molecular chain, can be the origin of melt elasticity when the strain rate is higher than the inverse of the characteristic time for chain contraction.¹⁰ This phenomenon is similar to the stress growth of rubber due to the extended chain effect.

Pearson et al. successfully explained the overshooting of the primary normal stress difference after startup of shear flow, considering chain stretching,¹⁰ whereas the overshooting of shear stress is predicted by molecular orientation.⁵ Since chain contraction from stretched state to equilibrium is a more rapid process than the relaxation of molecular orientation or reptation, the overshooting of the primary normal stress difference takes place at a higher shear rate than that of shear stress. The degree of chain contraction after sudden deformation is associated with the damping function, defined as the depression of the relaxation modulus at a large step strain from a linear one. Osaki demonstrated that the damping function of a comb-shape polymer and a random branched polymer like LDPE is larger than that of a linear polymer.¹¹ As for a branched polymer, especially a polymer having two or more

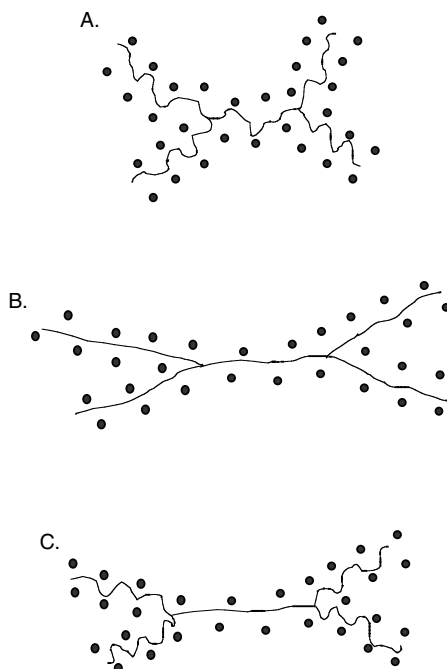


FIGURE 2.4

Schematic illustration of the recovery process from stretched condition for a branched polymer: (A) equilibrium state, (B) stretched state after sudden deformation, (C) prior to retraction process of branches ($t < \tau_a$; τ_a is the relaxation time for chain retraction). The chain segments between branch points are difficult to contract to the initial equilibrium condition because branches prohibit simple contraction along the tube, whereas the branch part can contract as shown in Figure 2.4C. Comparison of chain contraction among linear, branched, and fully crosslinked polymers has been discussed in detail by Laun.¹²

branch points in a chain, the segments between branch points cannot contract to the equilibrium state, owing to the topological interaction associated with long-chain branches as illustrated in Figure 2.4.¹² This leads to viscous enhancement in elongational flow. In order to contract the stretched segments, the retraction process of the branches must be completed. On the other hand, a linear polymer can contract within the tube to the equilibrium immediately.

Thus, once the strain rate is higher than the inverse of the characteristic time for a chain contraction, start-up curves of elongational viscosity at a constant strain rate exhibit nonlinear behavior, i.e., upturn departure from the low strain rate asymptote; this is often referred to as “strain hardening” or “viscous enhancement.” This elastic behavior affects the processability of various processes, including foaming. Because of the difficulty of chain contraction, strain hardening often takes place for a branched polymer. This feature was well described in recent advanced molecular theories based on the tube model, which can predict the nonlinear behavior under both shear

and elongational flow quantitatively.¹³⁻¹⁵ For example, the pom-pom model proposed by McLeish and Larson has been applied to various deformation modes and polymers.¹⁴ Moreover, the molecular stress function (MSF) theory developed by Wagner et al. has made it possible to predict the upturn behavior in elongational viscosity, considering the stress compression of branches.¹³ Further improvement of the MSF theory has recently provided accurate predictions for various branched polymers.¹⁵

Strain hardening plays an important role in foaming because of the reduction of localized deformation in a thinner part owing to stress increase, which depresses the coalescence of cells and results in uniform distribution of cell size. Therefore, rheological properties under elongational flow should be taken into consideration in order to predict the processability of foaming. Strictly speaking, discussions of the processability of foaming should be carried out based on equi-biaxial elongational flow, since biaxial rather than uniaxial deformation takes place during the growth of bubbles. Nevertheless, evaluation of uniaxial viscosity is still recommended because a measurement of the growth curve of biaxial viscosity is difficult, and the results will be less reliable. Moreover, some experimental results have clarified that material that shows marked strain hardening in uniaxial elongational viscosity also exhibits strain hardening in biaxial viscosity.¹⁶

In conclusion, the main origins of melt elasticity for a simple polymer melt are as follows: (1) anisotropy of molecular orientation, which is mostly responsible for the Weissenberg effect, the Barus effect, and strain recovery; and (2) chain stretching of contour length, leading to strain hardening in elongational viscosity and overshooting of normal stress difference in a steady-shear startup curve.

2.2.2 Measurements of Elastic Response

Experimental techniques for measuring melt elasticity are briefly summarized in this section. Details are well described by Macosko.¹⁷

Because of its accuracy, a cone-and-plate, drag-flow-type rheometer is preferable for the measurement of rheological properties under shear flow, such as oscillatory shear modulus, primary normal stress difference, recoverable strain, and so on. There are two systems for a cone-and-plate rheometer; one is strain control and the other is stress control. The former system, which is more widely available, is used to measure stress-relaxation and startup behavior under shear flow, whereas the latter gives recoverable strain after cessation of shearing. Further, steady-state properties and oscillatory shear modulus are evaluated by both systems.

In addition to measuring shear viscosity, a capillary, pressure-flow-type rheometer can also be used to examine extrudate swell, end-pressure drop, extensibility of a strand, and drawdown force. Further, this rheometer is also available to obtain the information on the occurrence of surface and/or gloss volumetric melt fracture because of a similarity to actual extrusion processing. The drawdown force, which is often employed as an elastic parameter

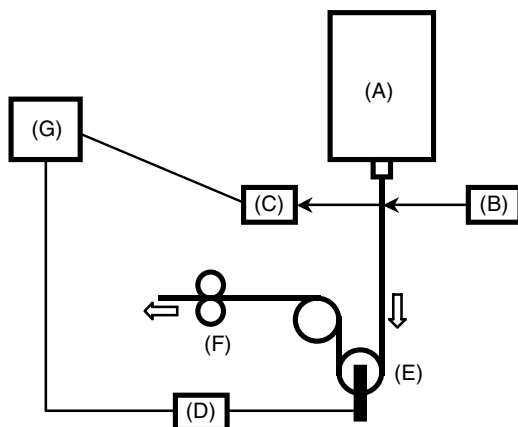


FIGURE 2.5

Typical experimental setup for drawdown force, extensibility, and extrudate swell ratio: (A) capillary rheometer; (B) laser beam emitter; (C) detector of laser beam; (D) transducer; (E) pulley; (F) rotating clamps; and (G) computer. (From Yamaguchi, M., *J. Polym. Sci. Polym. Phys. Ed.*, 39, 228, 2001. With permission.)

in industries, is defined as the force needed for stretching an extrudate strand at a certain draw ratio, and corresponds well to the elongational viscosity.^{16,18,19} Varying the draw ratio, the information on the elongational viscosity at various strain rates is collected. The drawdown force at the maximum stretching rate is called “melt strength.” A typical experimental setup for drawdown force, extensibility, and melt strength is shown in Figure 2.5.¹⁹

As denoted in the figure, drawdown force is measured by pulling the strand extruded vertically downward from the die set in a capillary rheometer (A) at a certain rate by two rotating clamps (F). Furthermore, this machine enables evaluation of extensibility—the ultimate draw ratio at the breaking point of the strand—by increasing the pulling rate constantly. Some capillary rheometers also have an attachment to measure the extrudate swell online. The diameter of the extrudates is measured using a laser beam emitted from (B) to (C). Then the extrudate swell ratio $B (= D/D_0)$, the ratio of the diameter of an extrudate strand D to that of the capillary die D_0 , is calculated. The strands are not pulled in case of extrudate swell measurements. Extrudate swell is affected by the length of a capillary die when $\tau_1 \gg t_{die}$, where τ_1 is the longest relaxation time and t_{die} is the duration in a capillary die, because the memory of molecular conformation prior to die entrance depends on the length; i.e., on t_{die} . When a die length is long enough to “forget” the memory, i.e., when $\tau_1 \ll t_{die}$, then B is described by the normal stress difference at steady-state as follows:²⁰

$$N_1^2 = 8\sigma^2(B^6 - 1) \quad (2.10)$$

TABLE 2.1

Experimental Methods for Elongational Viscosity

Mode	Method	Principle	Reference
Uniaxial Elongational Viscosity	Meissner-type	A rectangular or rod-shaped specimen, floating by buoyancy or air flow, is stretched by two rotating clamps.	21
	Fiber spinning	A strand extruded from a die is pulled downward.	23
	Converging flow	A melt flows from a wide cross-sectional area into a narrow one; i.e., converging.	24
	Tubeless siphon	A molten fiber appearing from the bath rises upward with free surface to nozzle; i.e., the opposite of fiber spinning.	25
Planar or Biaxial Elongational Viscosity	Meissner-type	A polymer sheet is stretched by multiple rotating clamps with scissors when needed. The deformation mode is determined by the ratio of rotating speed of each clamp.	26
	Lubricant squeezing	A short rod specimen with lubricant is compressed. Biaxial flow is attained by a simple one-axis compression and planar elongation is given by the compression of the specimen embedded in a rectangular channel.	27
	Stagnant flow	Elongational flow field, together with a stagnation point, is generated by impinging two steady-flows that flow the opposite direction in a line.	28
	Sheet inflation	A polymer sheet is inflated by air. Inflation of a sheet over a circular hole attains biaxial elongation and that from a polymer tube provides planar elongation.	29

In actual extrusion processing, however, the swell ratio is larger than the value predicted by the equation because molecular chains still “memorize” the conformation prior to entering the die.

The rheological properties under uniaxial extensional flow for a foamable material have often been measured by means of the well-known Meissner-type elongational rheometer,^{17,21,22} although other methods^{23–25} have been proposed, as listed in Table 2.1. Two types of machines are widely available for Meissner-type uniaxial extension. One of them is an air-supported system. A rectangular or rod-shaped sample is held by an upward air flow against gravity and gripped by two rotating clamps fixed in place. The clamps at both ends rotate at a constant rate, thereby pulling the sample at a constant strain rate.²¹ The actual strain rate is usually determined by

the time variation of the diameter or width of the sample, which is monitored by a video camera located over the sample. The other system is composed of the same attachment but uses an oil bath to float the sample by buoyancy. Both systems give reliable experimental results, with the exception of samples with low viscosity. In contrast to the development in uniaxial elongational measurements, the apparatus for equi-biaxial and planar elongational viscosities, especially their transient response, is less widely available. Therefore, only a few data have been published, although various methods have been proposed, as shown in Table 2.1.^{26–29}

2.2.3 Role of Long-Chain Branches

2.2.3.1 Model Polymer

Molecular structure, especially that of long-chain branches, predominantly affects melt elasticity. Therefore, linear viscoelastic properties and solution properties of a branched polymer have been well investigated employing model polymers such as star- and comb-shaped polymers.^{30–33} Steady-state compliance increases linearly with branch length for a star-shape polymer, irrespective of the number of branches, while compliance for a linear polymer is independent of molecular weight above a critical molecular weight.^{4,30,31} Broadening of the terminal relaxation mode due to chain retraction of branches is responsible for the enhancement of steady-state compliance.^{30,31} Since zero-shear viscosity increases exponentially with branch length, the relaxation time, i.e., $\tau = J_e^0 \eta_0$, also greatly increases. As for a comb-shape polymer, the terminal relaxation mode is the backbone relaxation that takes place after the chain retraction process for branches as discussed above. The characteristic time is proportional to $M_b^2 \tau_a$, where M_b is the molecular weight of the backbone chain, i.e., the chain segments between branch points, and τ_a is the relaxation time for chain retraction.^{30,32}

Raju et al. revealed that apparent flow activation energy increases linearly with the length of branches employing hydrogenated polybutadiene, the model polymer of polyethylene.³³ Since a larger shift factor is required only at the terminal zone—i.e., at a lower modulus—for the polymers with long-chain branches, time-temperature superposition is not applicable to them.³⁴ Thermo-rheological complexity is also connected with the chain retraction process, since a gauche-rich, compact conformation, which is dominant during the retraction of branches, has a higher energy state than a trans-rich, equilibrium conformation.³⁴ Consequently, the existence of long-chain branches can easily be detected by flow activation energy, at least for PE, although detailed characterization of branch structure should not be carried out only by flow activation energy for commercial LDPE with complicated structures.¹⁶ In the cases of polybutadiene, polystyrene, and polyisoprene, however, the effect of branch structure on the activation energy is obscure because the energy difference between both conformations is not large enough.³⁴

2.2.3.2 Low-Density Polyethylene

The branch structure of commercial LDPE has generally been studied according to dilute solution properties, based on the pioneering work performed by Zimm and Stockmeyer.³⁵ Recently, combination measurements of GPC and light scattering as well as intrinsic viscosity $[\eta]$ have become powerful tools for characterizing the branch structure of commercial LDPE in detail. The mean square radius of gyration $\langle Rg^2 \rangle$ of a branched polymer is lower than that of a linear polymer having the same molecular weight. Their ratio, defined by Equation 2.11, shows the number of branches:³⁵

$$g = \frac{\langle Rg^2 \rangle_{\text{branched}}}{\langle Rg^2 \rangle_{\text{linear}}} \quad (2.11)$$

Further, since the intrinsic viscosity $[\eta]$ of a branched polymer is also smaller than that of a linear polymer, their ratio g' is smaller than unity:³⁵

$$g' = \frac{[\eta]_{\text{branched}}}{[\eta]_{\text{linear}}} \quad (2.12)$$

Finally, the parameter β , given by Equation 2.13, gives information on the branch structure:

$$g' = g^\beta \quad (2.13)$$

Tackx and Tacx have investigated the branch structure of commercial LDPE and have found that LDPE produced by the autoclave process, having lower g and g' , has more long-chain branches than tubular LDPE. Moreover, they report that the parameter β decreases with an increase in molecular weight, demonstrating that the molecular shape is changing from star-like to comb-like with molecular weight for both tubular and autoclave LDPE.³⁶

In addition to dilute solution properties, rheological properties in a molten state have been studied for commercial LDPE. Yamaguchi and Takahashi compared various rheological properties for autoclave and tubular LDPE melts having similar linear viscoelastic properties.¹⁶ As seen in Table 2.2, the autoclave LDPE shows a higher level of drawdown force and a greater extrudate swell ratio, even though the melt flow ratio (MFR) is larger than that of tubular LDPE, demonstrating that autoclave LDPE exhibits higher melt elasticity. In particular, the drawdown force of autoclave LDPE is twice as high as that of tubular LDPE. This result can be attributed to the complicated, hierarchical branch structure of autoclave LDPE, which is in accordance with its dilute solution properties.¹⁶ Because of its high drawdown force, autoclave LDPE shows poor extensibility compared with tubular LDPE.

Further, the damping functions of autoclave and tubular LDPE are quite different. Autoclave LDPE shows larger values (less damping) than tubular

TABLE 2.2

Comparison of the Rheological Parameters Obtained by Capillary Rheometer for Autoclave LDPE and Tubular LDPE

	MFR (g/10 min) 190°C, 2.16 kg	Drawdown Force (mN) draw ratio = 5	Swell Ratio $\gamma = 10.8 \text{ s}^{-1}$	Extensibility
Autoclave LDPE	1.6	295	1.91	<15
Tubular LDPE	1.0	135	1.55	50–60

* Drawdown force, swell ratio, and extensibility were measured by the die with $L/D = 8/2.095$ at 160°C.

LDPE,¹⁶ suggesting that the branch structure of autoclave LDPE suppresses the chain contraction. Chain stretching due to multi-branch points causes autoclave LDPE to exhibit marked strain hardening in elongational viscosity. As shown in Figure 2.6, autoclave LDPE shows more pronounced upturn behavior at all strain rates.¹⁶ On the other hand, tubular LDPE shows less viscous enhancement. Further, the upturn behavior becomes weak at a lower strain rate, i.e., at a smaller Deborah number.

2.2.4 Melt Elasticity of New Polyolefins

Metallocene catalyst technology is a recent development in the field of polyolefins.³⁷ LLDPE (ethylene/ α -olefin copolymer) produced by a metallocene catalyst has excellent mechanical properties in the solid state, such as high tensile and impact strength, compared with conventional Ziegler–Natta LLDPE, since the number of short-chain branches is almost independent of the molecular weight. Because of narrow molecular weight distribution, however, poor processability due to less melt elasticity often becomes a serious problem. Therefore, blending with LDPE has been carried out extensively in order to improve the melt elasticity. Further, peroxide modification, which generates long-chain branches without microgel to enhance the melt elasticity, has also been investigated.³⁸ Irradiation by electron beam has also been found to generate long-chain branches in polyethylene. Horii et al. studied the branch structure of radiation-modified polyethylene and revealed that both Y-type and X-type branch points exist.³⁹

The processability of foaming for fully crosslinked metallocene LLDPE by peroxide modification has been investigated by Abe and Yamaguchi.³ According to their study, a foam with a high expansion ratio is obtained when the average molecular weight between neighbor crosslinked points is around 10^5 . Further, the rheological properties of the crosslinked LLDPE are found to be similar to those of a critical gel. Moreover, the expansion ratio of a crosslinked LLDPE foam is determined not only by the rheological properties in the molten state but also by the crystallization temperature,

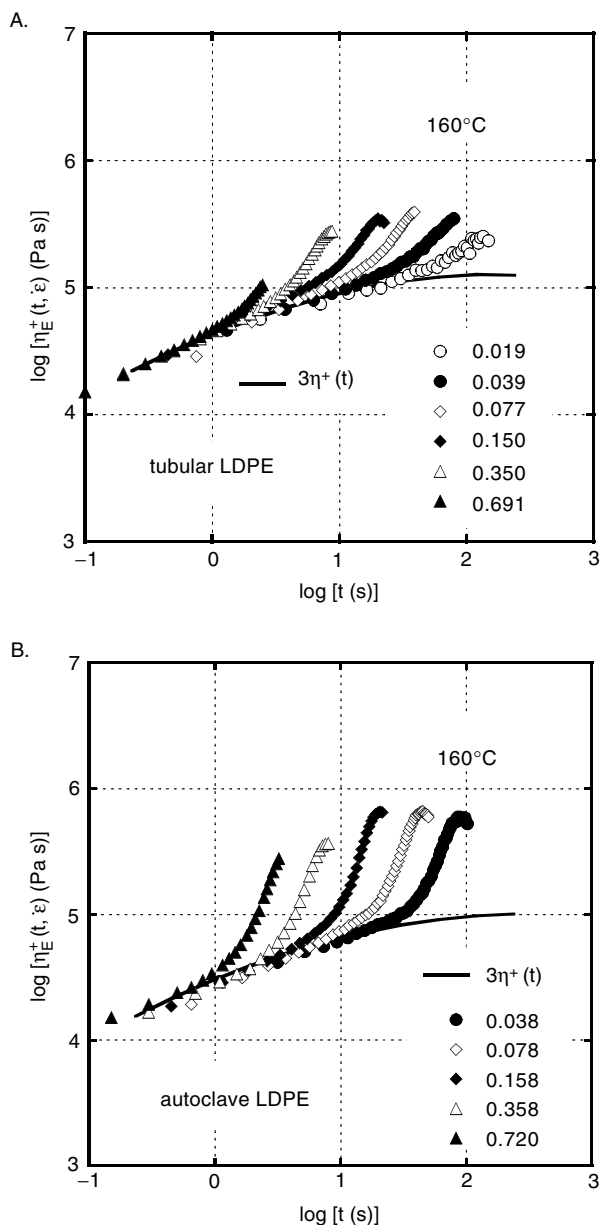


FIGURE 2.6

Growth curves of uniaxial elongational viscosity $\eta_E^+(t, \dot{\epsilon})$ at various strain rates $\dot{\epsilon}$ for (A) tubular LDPE and (B) autoclave LDPE at 160°C. The solid line represents $3\eta^+(t)$, where $\eta^+(t)$ is transient shear viscosity at the low strain rate asymptote calculated from linear viscoelastic properties. Numbers in the figure denote the strain rate. (From Yamaguchi, M. and Takahashi M., *Polymer*, 42, 8663, 2001. With permission of Elsevier Science.)

i.e., the number of short-chain branches. This result reveals that shrinkage after expansion is prominent for crosslinked PE in spite of rapid cooling due to adiabatic expansion of gas in cells. As a result, LLDPE with a low crystallization temperature is allowed to shrink more until crystallization prohibits large-scale molecular motion completely.³ Further, Abe clarified that the crosslinked foam obtained from LLDPE exhibits a homogeneous distribution of cell size, which is quite different from the distribution produced by conventional LDPE.⁴⁰ The homogeneous distribution of crosslink points in crosslinked LLDPE results in an excellent micro-cellular structure.

Further effort has been expended in metallocene technology on improving processability. A metallocene catalyst makes it possible to incorporate long-chain branches sparsely into a backbone chain,^{41,42} which enhances flow activation energy⁴¹ and strain hardening in elongational viscosity to some degree.⁴² Malmberg et al. obtained HDPE with long-chain branches by means of a metallocene catalyst, which shows higher flow activation energy than conventional HDPE.⁴³ There are many more long-chain branches in this version of HDPE than in HDPE produced by means of a chromium catalyst.⁴⁴ The level of melt elasticity of LLDPE and HDPE with long-chain branches produced by means of a metallocene catalyst is, however, still considerably lower than that of conventional LDPE, due to the presence of fewer and/or shorter long-chain branches.^{41,42} In the near future, the number and length of long-chain branches will be controlled by new technologies, such as the Brookhart catalyst,⁴⁵ or by copolymerization with a macromonomer obtained by a metallocene⁴⁶ or phenoxyimine-based catalyst.⁴⁷ These advanced technologies in the polyolefin industry may enable the synthesizing of a polymer with the appropriate melt elasticity for foaming. They also make it possible to produce a block or graft copolymer that can be employed for foaming because they may show unique mechanical properties in the solid state and widen the application of PE foam. Moreover, copolymers with a polar monomer, which may have attractive mechanical or environmental properties, will be available in the future. Currently, an ethylene/styrene copolymer⁴⁸ is available, and its foam properties have been studied.⁴⁹

The effort to incorporate long-chain branches has been made not only for polyethylene but also for isotactic polypropylene (PP), since the poor melt elasticity of conventional linear PP prohibits using it for foaming. In the past decade, PP with long-chain branches has been developed by radiation or peroxide modification and has become commercially available.^{1,50-53} One of the targets for the long-chain branch PP is, of course, a foam. Marked strain hardening in elongational viscosity, which has been described in detail by Hingmann and Marczinke and by Sugimoto et al.,⁵¹ results in less coalescence of cells and leads to a high expansion ratio with fine cells.^{50,52} Because of resistance to heat and organic solvents as well as excellent mechanical properties, PP foams are expected to replace some polystyrene foams. Its use in trays for oily foods is one proposed application.⁵³

Although extensive studies have already been carried out on the molecular architecture of polyolefins, further development bringing about new, tailor-made polyolefins is also expected in the next decade. This will widen the applications of polyolefin foams and improve their processability.

2.3 Modification of Melt Elasticity

2.3.1 Effect of Processing History

2.3.1.1 Origin of Shear Modification

Applied processing history has a significant effect on the rheological properties of a branched polymer, especially on the melt elasticity, including strain hardening in elongational viscosity, even though it has no effect on the primary molecular characteristics, such as molecular weight, polydispersity, and the number and length of long-chain branches.^{54–68} The phenomenon called “shear modification” or “shear working” is a reversible, mechanical modification of the rheological properties, since exposure to annealing or solvent treatment enables the rheological properties to recover to those of the original, unprocessed material. Further, the mechanical modification is barely observable for linear polymers,^{60,63} indicating that branch structure is primarily relevant to the phenomenon.

Table 2.3 shows normalized shear storage and loss moduli, i.e., the ratio of values for the sample processed by an internal batch mixer to those for the unprocessed sample at various frequencies. The processing history in an internal mixer noticeably depresses oscillatory shear moduli, especially G' rather than G'' , at lower frequencies, although there is no change in the molecular weight and the polydispersity.⁶⁶

The result suggests that applied processing history weakens the effect of the terminal relaxation mechanism, which is typical of mechanical modification. The elastic properties, such as primary normal stress difference, extrudate swell, recoverable strain, and strain-hardening in elongational viscosity, are thereby more susceptible to processing history than are the viscous proper-

TABLE 2.3

Normalized Oscillatory Shear Moduli for the Processed LDPE

	0.01 Hz	0.03 Hz	0.1 Hz	0.3 Hz	1 Hz
G'/G'_{eq}	0.394	0.593	0.696	0.790	0.899
G''/G''_{eq}	0.628	0.782	0.886	0.959	0.994

* G'_{eq} and G''_{eq} represent G' and G'' of the original, unprocessed sample, respectively.

* The sample, commercial LDPE produced by the autoclave process, was processed by a 60-cc internal batch mixer at 30 rpm for 120 min at 160°C.

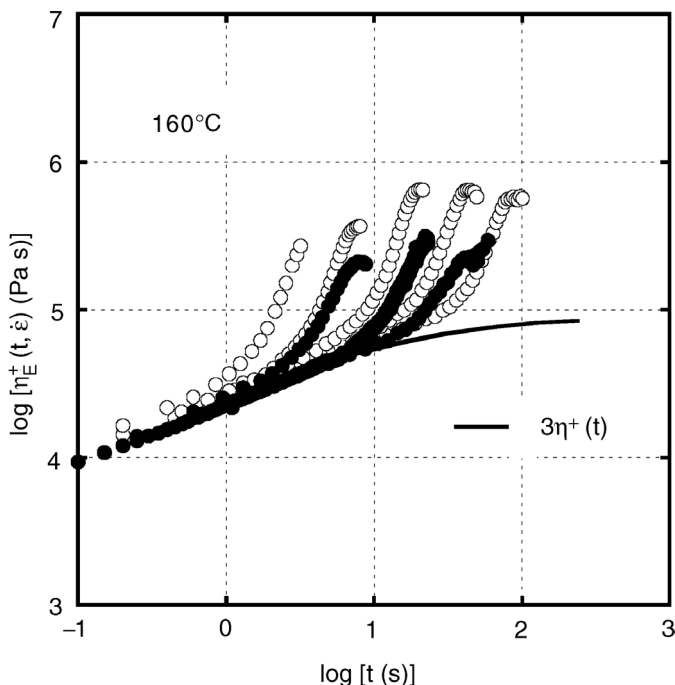


FIGURE 2.7

Growth curves of uniaxial elongational viscosity $\eta_E^+(t, \dot{\epsilon})$ at various strain rates $\dot{\epsilon}$ at 160°C for (o) unprocessed, original LDPE and (•) LDPE processed by a 60 cc internal batch mixer at 30 rpm for 15 min at 160°C. The solid line represents $3\eta^+(t)$ at the low strain rate asymptote calculated from linear viscoelastic properties of the unprocessed sample. (From Yamaguchi et al. Proceedings of the Annual Meeting of the Society of Polymer Processing, PPS-18. With permission of the Polymer Processing Society.)

ties.^{58–68} Figure 2.7 exemplifies the growth curves of uniaxial elongational viscosity at various strain rates for LDPE having different processing histories.⁶⁷

Unprocessed LDPE, represented in the figure by open symbols, deviates upward from $3\eta^+(t)$ (strain-hardening behavior) beyond a certain strain level, whereas the sample processed by an internal mixer shows less upturn. In contrast to this, the linear region of the transient elongational viscosity, in which $\eta_E^+(t)$ is independent of $\dot{\epsilon}$, is hardly changed by the applied processing history. The growth curves for the processed sample, however, may include some experimental error, because thermal history prior to and/or during extension has a strong influence on the transient elongational viscosity. Drawdown force is also found to be quite sensitive to applied processing history^{16,66–68} and is preferably employed in order to evaluate the magnitude of the mechanical modification, since the experimental error arising from applied thermal history after processing can be minimized, owing to the simplicity of the measuring method. In Figure 2.8, normalized drawdown force—i.e., the ratio of the drawdown force of the processed sample to that of the original measured at the same temperature—is plotted against the processing time in an internal mixer.

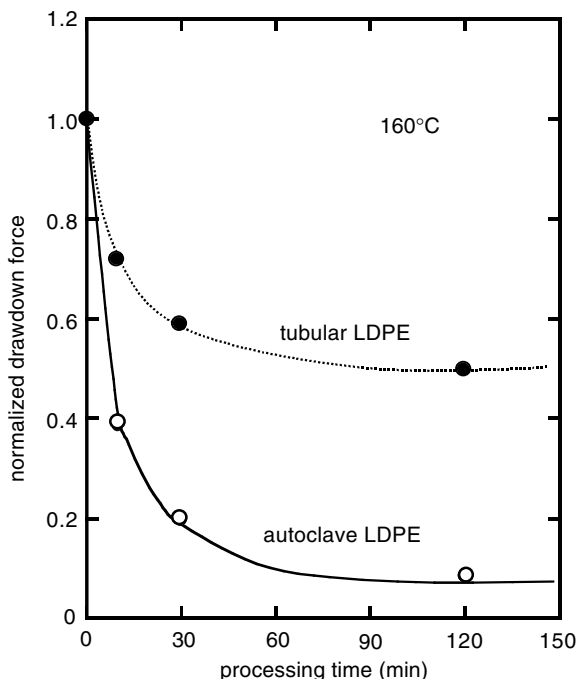


FIGURE 2.8

Normalized drawdown force at 160°C plotted against processing time in an internal mixer at 30 rpm at 160°C for (o) autoclave LDPE and (•) tubular LDPE. The drawdown force, measured at a draw ratio of 5, was collected without exposure to annealing in a capillary rheometer.

It has been generally accepted that intense processing history—high strain rate and/or long residence time in a processing machine—depresses the drawdown force notably,^{16,66} which corresponds to the result in Figure 2.8.

Furthermore, the mechanical modification of elastic properties is more apparent for a branched polymer with well-developed branch structure, as described below. Thus, LDPE produced by the autoclave process and having a more hierarchical and complicated branch structure is more susceptible to applied processing history than is tubular LDPE.¹⁶ Taking notice of the phenomenon, Rokudai proposed a characterization method of branch structure in LDPE,⁵⁷ which is quite useful because obtained characteristics directly relate to processability.

Exposure to annealing or solvent treatment makes the rheological properties recover to the original values. Figure 2.9 shows the recovery curves of oscillatory shear moduli, such as storage modulus G' and loss modulus G'' , as a function of annealing time in a rheometer for a sample processed in an internal mixer.⁶⁶

Oscillatory shear moduli, especially shear storage modulus G' at a lower frequency, increases more rapidly with annealing time. This is plausible because applied processing weakens, especially in terminal relaxation mode,

as shown in Table 2.3. Therefore, the increase in G' at low frequencies is prominent, owing to the recovery of terminal relaxation from the mechanical modification. Similar to G' , normalized drawdown force, the drawdown force divided by the plateau value at each temperature, also grows rapidly with annealing time and approaches the original value at the corresponding temperature, i.e., 1, as shown in Figure 2.10. The figure indicates that the normalized drawdown force at $t = 0$ (the value without exposure to annealing) is independent of the measurement temperature, suggesting that the same ratio of the drawdown force is lost at each temperature. This result implies that the normalized drawdown force without annealing, regardless of the measuring temperature, is the appropriate elastic parameter for discussing the magnitude of the applied processing history. The figure also demonstrates that quite a long time is required to recover, especially at a lower temperature; this becomes more obvious for the sample with a more intense processing history.^{16,66}

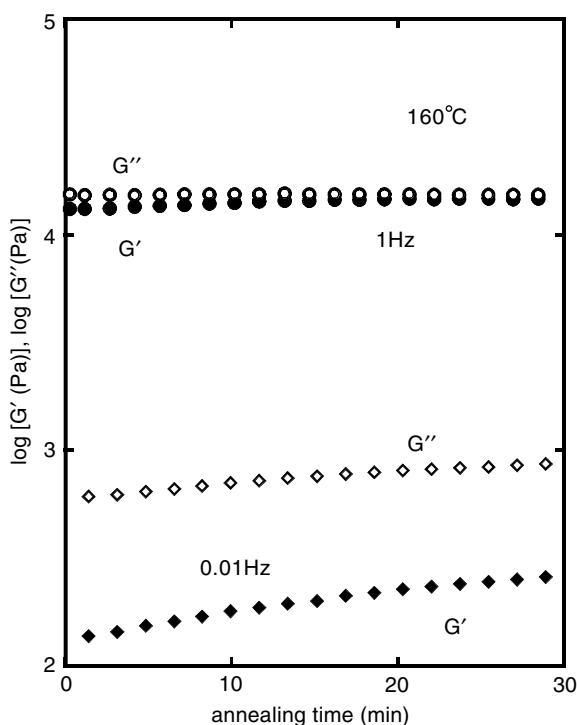


FIGURE 2.9

Growth curves of shear storage modulus G' (closed symbols) and loss modulus G'' (open symbols) at 1 Hz (circles) and 0.01 Hz (diamonds) at 160°C plotted against annealing time in a cone-and-plate rheometer at 160°C for LDPE processed in an internal mixer at 30 rpm at 160°C for 120 min. (From Yamaguchi, M. and Gogos, C.G., *Adv. Polym. Technol.*, 20, 261, 2001. With permission of John Wiley & Sons, Inc.)

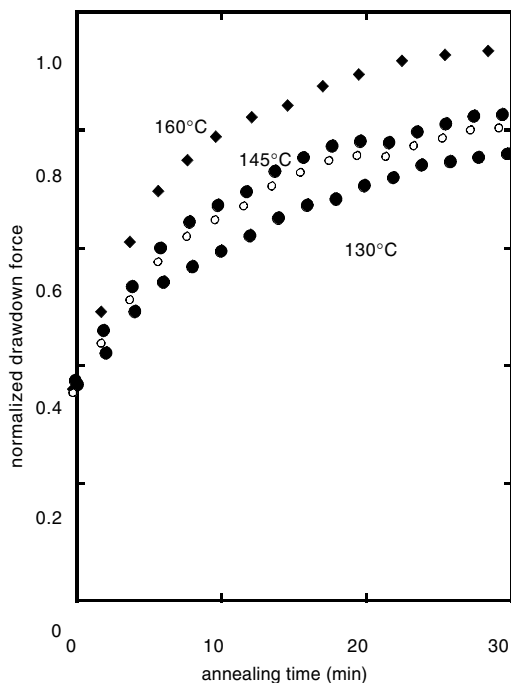


FIGURE 2.10

Growth curves of normalized drawdown force at a draw ratio of 5 with annealing time, i.e., residence time in the capillary rheometer at the measuring temperature, after processing history at various temperatures; (●) 130°C, (○) 145°C, and (◆) 160°C. The sample was processed three times by a 30-mm co-rotating twin-screw extruder having conventional conveying screws at 151°C at 50 rpm.

The quantitative relation between applied shear history and its resultant rheological properties has not been studied for a long time except by Hanson,⁵⁵ who concluded that the applied total strain determines the rheological properties. Nevertheless, recent studies employing a cone-and-plate rheometer as a processing machine made it clear that applied shear stress, not strain, determines the rheological properties of a processed sample.^{66,67} Figure 2.11 shows the recovery curves of the storage modulus plotted against the annealing time for a sample sheared by a cone-and-plate rheometer.^{67,68}

The figure demonstrates that the recovery curves are determined not by the total shear strain, i.e., the product of the applied shear rate and the duration of shearing as shown in Figure 2.11A, but by the product of the applied shear stress and the duration of shearing as shown in Figure 2.11B. Further, the result suggests that torque and residence time in an extruder or a batch mixer are fundamental parameters for controlling rheological properties, and thus processability. Figure 2.11 also indicates that processing at a lower temperature, i.e., at a higher stress because of high viscosity, depresses the melt elasticity more, as demonstrated by Maxwell.^{62,63} The

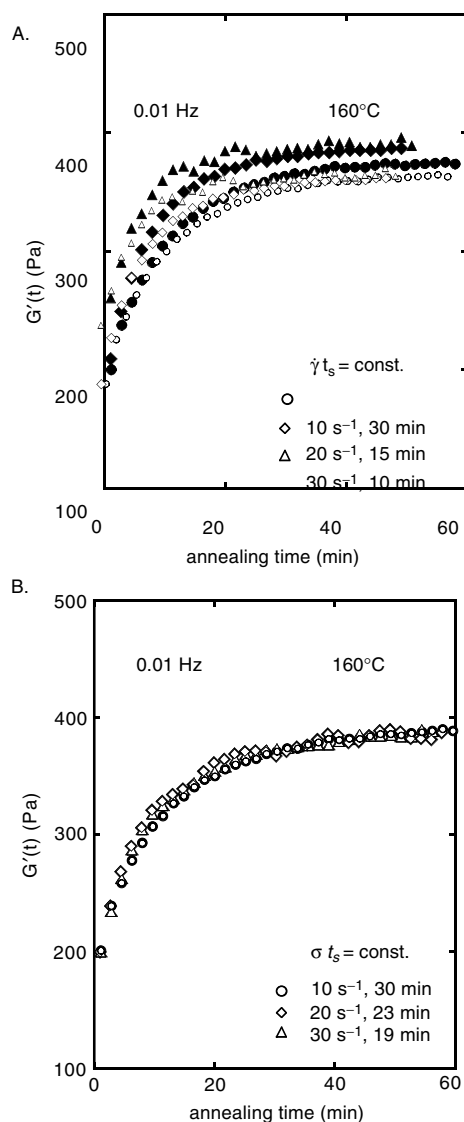


FIGURE 2.11

Growth curves of shear storage modulus G' at 0.01 Hz at 160°C for the samples sheared in a cone-and-plate rheometer at 160°C. **(A)** Applied total strain, i.e., the product of the shear rate $\dot{\gamma}$ and the duration of shearing t_s , is the same for all samples: (○) $\dot{\gamma} = 10 \text{ s}^{-1}$ for 30 min, (◇) $\dot{\gamma} = 20 \text{ s}^{-1}$ for 15 min, and (△) $\dot{\gamma} = 30 \text{ s}^{-1}$ for 10 min. (From Yamaguchi, M., and Gogos, C.G., *Adv. Polym. Technol.*, 20, 261, 2001. With permission of John Wiley & Sons, Inc.) **(B)** All samples have the same value of the product of the applied shear stress σ and the duration of shearing t_s : (○) $\dot{\gamma} = 10 \text{ s}^{-1}$ for 30 min, (◇) $\dot{\gamma} = 20 \text{ s}^{-1}$ for 23 min, and (△) $\dot{\gamma} = 30 \text{ s}^{-1}$ for 19 min. (From Yamaguchi, M. et al. Proceedings of the Annual Meeting of the Society of Polymer Processing, PPS-18, 2002. With permission of the Polymer Processing Society.)

results in Figure 2.11 will be explained as regards chain alignment to the flow direction. Molecular orientation, which is proportional to the stress, is responsible for disentanglement of temporary couplings associated with long-chain branches.^{60,65,66} Consequently, the polymer behaves like a linear polymer.⁶⁵ The schematic model of molecular conformation, based on the tube model, is illustrated in Figure 2.12, in which dots denote neighbor chains.

Exposure to flow and deformation in a processing machine drags the branches into the same tube of a backbone chain. Consequently, contraction of backbone chains between branch points takes place easily, as with a linear polymer, which results in less strain hardening in elongational viscosity, along with a low magnitude of the damping function. Moreover, the terminal relaxation mechanism, i.e., backbone relaxation after contour length fluctuation of branches, disappears, which allows the polymer chain to move along the tube by simple reptation, as with a linear polymer. The recovery of rheological properties by exposure to annealing can be ascribed to the relaxation of molecular conformation from a low entropy state, especially around branch points, to the equilibrium state by micro-Brownian motion. Therefore, higher temperature enables the rheological properties to recover more quickly, as shown in Figure 2.10. In contrast, keeping the processed sample below the crystallization temperature, or glass-rubber transition temperature in case of

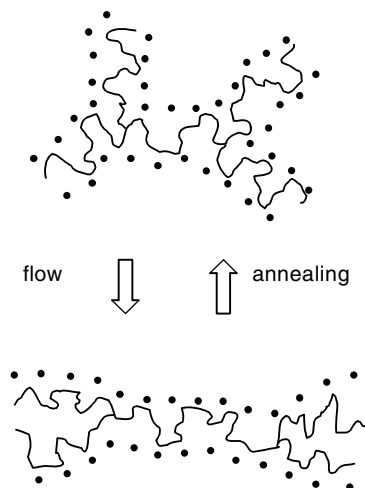


FIGURE 2.12

Schematic illustration of molecular conformation (top) before and (bottom) after mechanical modification, based on the tube model. Molecular motion of the polymer chain represented by a solid line is confined within the “tube” composed of neighbor chains, denoted by dots. Top: conformation at equilibrium state. Completion of retraction process of branches is required for terminal backbone relaxation. Further, chain contraction after sudden deformation is reduced by the topological constraint. Bottom: Conformation after processing. Because of molecular orientation resulting from applied flow, branches are aligned to the main chain, which makes it possible for the branched polymer to use simple reptation along the tube as well as chain contraction like a linear polymer.

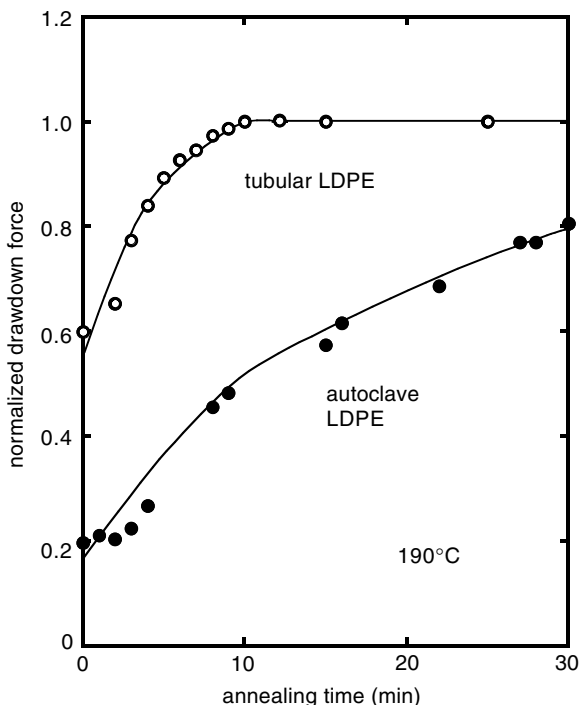


FIGURE 2.13

Growth curves of normalized drawdown force at a draw ratio of 5 at 190°C plotted against annealing time, i.e., residence time in the capillary rheometer at 190°C, for (o) tubular LDPE and (•) autoclave LDPE. The samples were processed by an internal mixer at 30 rpm for 30 min at 160°C.

amorphous polymers,⁵⁹ retains the rheological properties of the melt because molecular motion is frozen. Furthermore, it takes a longer time in the molten state to recover the rheological properties for a sample having a more intense applied shear history, indicating that intense flow and deformation cause longer branches to align to a greater degree.

Figure 2.13 compares the recovery curves of normalized drawdown force for tubular and autoclave LDPE having the same processing history. Autoclave LDPE shows a significantly lower value than tubular LDPE, indicating that applied flow and deformation efficiently lose the feature of the branched polymer having well-developed branch structure; this is due to the conformation change. Further, the figure demonstrates that autoclave LDPE needs a longer time to recover from mechanical modification.

In the recovery curve, the low value at $t = 0$ indicates that more long-chain branches exist in autoclave LDPE. Moreover, taking a longer time to recover indicates the existence of longer branches and/or a more hierarchical branch structure.

As we have observed, the rheological properties of a branched polymer are determined by mechanical and thermal histories. Under a low shear rate,

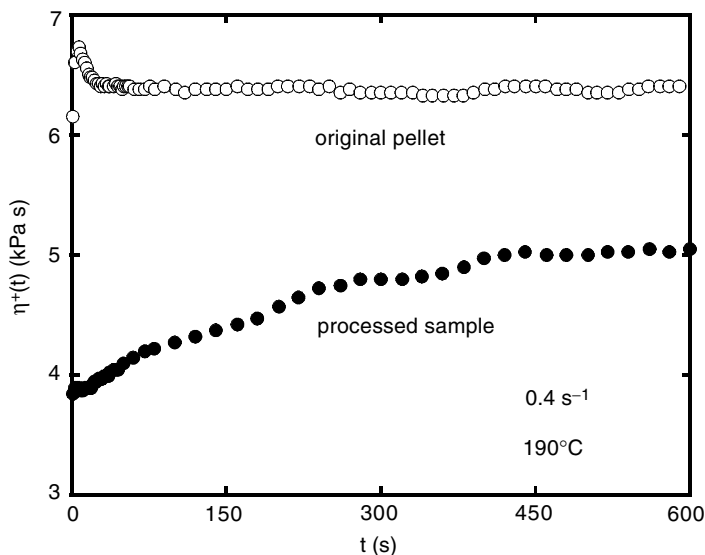


FIGURE 2.14

Growth curves of shear viscosity $\eta^*(t)$ at 0.4 s^{-1} at 190°C for (o) the original pellet and (•) the sample processed by an internal mixer at 30 rpm for 150 min at 150°C . (From Yamaguchi, M. et al. Proceedings of the Annual Meeting of the Society of Polymer Processing, PPS-18, 2002. With permission of the Polymer Processing Society.)

micro-Brownian motion may overcome the hydrodynamic force and then enhance the interaction due to entanglement couplings. Figure 2.14 shows the growth curve of shear viscosity at a constant shear rate for the sample processed by an internal mixer, as compared with the original, unprocessed sample.⁶⁷ The shear viscosity of the processed sample increases monotonically even under shear flow, indicating micro-Brownian force is dominant in this condition. Further, it is of great interest that stress overshoot, which is ascribed to overshooting of molecular orientation,⁵ disappears in the processed sample, whereas it is clearly detected in the growth curve of the original sample.

The recovery curve from mechanical modification, as described here, implies information on branch structure. Further research on the quantitative characterization of the recovery curve employing a model branched polymer will provide a better understanding of the unique rheological properties as well as the processability of a branched polymer.

2.3.1.2 Processing History by Conventional Processing Machines

It has been reported that inflation-blown film from a mechanically modified sample is more transparent than that from the original pellet, which is due to the low level of external haze, or smooth surface.^{55,58,60,64} The depression of surface roughness relates to the weak melt elasticity according to the processing history. Flow instability in extrusion is also improved by mechanical modification.^{54,56,67,68} Due to low melt elasticity, gross, volumet-

ric, and chaotic melt fractures, which are caused by long time relaxation (marked melt elasticity)⁶⁹ are reduced or take place at a higher shear rate by means of applied processing history. Moreover, mechanical modification enhances extensibility in a molten state^{60,64} because the depression of strain hardening in elongational viscosity reduces the stress needed for stretching. To the best of our knowledge, the direct relation between mechanical modification and the processability of foaming has unfortunately not been reported. However, it is expected that reduction of strain hardening for a processed sample presumably leads to coarse cell morphology, owing to the coalescence of cells.

The effect of processing history on rheological properties is, of course, dependent on the processing machine, as shown in Figure 2.15. Although it is difficult to comprehend quantitatively the difference among conventional processing machines because of the complicated flow pattern, Figure 2.15 demonstrates that two-roll mill processing has a different influence on the

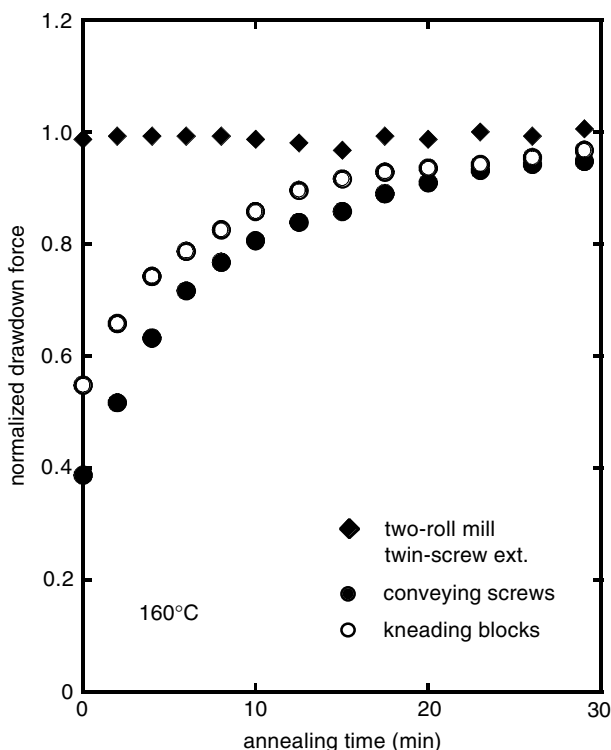


FIGURE 2.15

Growth curves of normalized drawdown force at a draw ratio of 5 at 160°C plotted against annealing time, i.e., residence time in the capillary rheometer at 160°C, for samples (♦) processed by two-roll mill, and processed three times by co-rotating twin-screw extruder with (●) conveying screw elements and (○) forward kneading blocks. (From Yamaguchi, M. et al. Proceedings of the Annual Meeting of the Society of Polymer Processing, PPS-18, 2002. With permission of the Polymer Processing Society.)

rheological properties than processing by other machines. The result suggests that understanding the processing history from the viewpoint of mechanical modification is required in order to choose a processing machine as well as to control processability. According to the flow simulation in a two-roll mill carried out according to Gaskell's model,⁷⁰ the magnitude of the product of the applied shear stress and the duration of shearing for each pass through the nip region is too low to depress the melt elasticity.⁶⁶⁻⁶⁸ Moreover, after passing through the nip region, molecular orientation can relax on the roll because no deformation takes place except in the nip region. This is why two-roll mill processing barely depresses melt elasticity.

Compared to the intermittent stress history in two-roll mill processing, an internal mixer, as shown in Figure 2.7, and extruders, which apply relentless stress history, depress the melt elasticity drastically. Furthermore, Figure 2.15 shows that screw configuration in a co-rotating twin-screw extruder affects the melt elasticity to different degrees. The samples in the figure were extruded three times by a twin-screw extruder with (a) 11.5 of 20-mm pitch forward conveying screw elements (the total length of the melt conveying region is 210 mm) or (b) 5 forward kneading blocks KB45/5/42 (each unit is 42-mm long with 5 discs staggered at 45°; total length of melt conveying and/or kneading region is 210 mm), followed by two reverse elements R20/10 (a unit 10-mm long with a pitch of 20 mm) at fully filled condition.⁶⁸ These two types of screw configuration provide the same level of extrusion torque, average residence time, and resin temperature at the same rotation rate. As seen in Figure 2.15, processing with the conveying screws depresses the melt elasticity more than with kneading blocks as long as the torque and the residence time are the same. Further, the appearance of extrudate strands is quite different, as shown in Figure 2.16.

The extrusion by conveying screw elements diminishes gross melt fracture, whereas it is still observed at the strand extruded three times by kneading blocks. Considering that gross melt fracture is ascribed to terminal relaxation,⁶⁹ the result also supports that conveying screws depress the melt elasticity more than kneading blocks. The flow direction in kneading blocks changes largely, abruptly, and frequently with time and location because of the compression–expansion deformation of a molten polymer.⁷¹ On the other hand, a polymer melt flows along a figure-eight pattern and thus gradually changes its flow direction along conveying screws.⁷² The large, abrupt, and frequent change of the flow direction prohibits a high degree of molecular orientation, which leads to a low level of melt elasticity. Further, more energy is consumed to change the flow direction in kneading blocks. Consequently, the degree of molecular orientation is less than that in the conveying screws at the same torque level. It is, however, interesting to note that the relentless change of flow direction, together with elongational deformation, leads to very effective mixing for polymer blends and composites.⁷¹⁻⁷⁴

From the experimental results shown in this section, the processing machine as well as the operating condition should be carefully chosen for foaming in view of the mechanical modification of rheological properties.

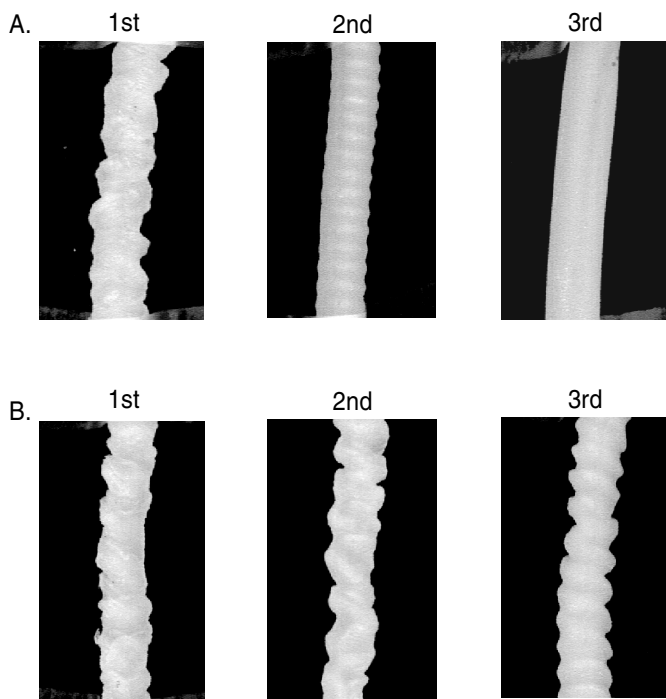


FIGURE 2.16

Appearance of the strands extruded by the co-rotating twin-screw extruder with (A) conveying screw elements and (B) forward kneading blocks. (From Yamaguchi M. et al. Proceedings of the Annual Meeting of the Society of Polymer Processing, PPS-18, 2002. With permission of the Polymer Processing Society.)

Since the bubble growth process in foaming requires relatively high melt elasticity, mechanical modification will not be preferable in many cases. When premixing with filler, such as a flame retardant, wooden powder, nucleating agent, or pigment, a foaming material must be composed of a branched polymer. The following should be kept in mind irrespective of the amount of the filler: Mixing at a high stress condition should be avoided, and employing a mixing screw is highly desirable for effective mixing without reduction of melt elasticity.

2.3.2 Modification by Polymer Blends

2.3.2.1 Background

Polymer blends and composite systems exhibit complicated rheological properties.²² As for immiscible polymer blends and polymer composites, there appears to be an additional relaxation mechanism, which is ascribed to phase separated morphology. Further, the characteristic time of the relaxation mechanism is, in general, longer than the reptation time of a matrix polymer.

www.iran-mavad.com

Nevertheless, the relaxation mechanism is of less importance at least for strain hardening in elongational viscosity, because it is not responsible for the chain stretching. In cases where the dispersed particles can be regarded as a rigid body or have a higher viscosity than the matrix, the system is in so-called suspension. Shikata and Pearson revealed that Brownian motion, the origin for restoring the equilibrium state from flow-distorted particle distribution, is responsible for melt elasticity in a suspension system, although it is weak.^{22,75} Furthermore, Mewis and Metzner have found that suspension with fiber particles having a large aspect ratio exhibits a high level of steady-state elongational viscosity because of the microscopic distortion of the flow field by rigid fibers.^{17,22,76,77} However, the system does not show strain hardening,^{77,78} whereas a marked overshoot of shear stress and primary normal stress difference is observed under shear flow, owing to the orientation of fibers.⁷⁶ According to Laun, elastic strain under elongational flow for a composite with long fibers decreases with increasing filler content, since rigid fibers impede the elongation of polymer melt.⁷⁷ Moreover, it has been generally accepted that extrudate swell is often depressed by blending fillers, regardless of the existence of long relaxation time in the system.⁷⁹ The result demonstrates that some elastic properties of polymer composites and polymer blends, especially the properties ascribed to the interaction due to entanglement couplings, are less than those of the unfilled polymer melt. Furthermore, the discontinuity of viscosity or modulus at the interface may cause localized deformations, which leads to poor extensibility.

When the viscosity of a matrix is higher than that of a dispersion, the interfacial tension contributes to the terminal relaxation because additional force is generated by deformation of the dispersion, owing to the increase in the interfacial area.^{17,22,80,81} Palierne focused on the phenomenon and proposed a constitutive equation, called the emulsion model, of linear viscoelastic properties for immiscible blend systems in which the matrix has higher viscosity.⁸¹ According to the model, a shoulder in the G' curve in a low frequency region for an immiscible blend is attributed to the relaxation from the deformed state of the dispersion to a sphere in order to minimize the interfacial tension.⁸¹ Further, Doi and Ohta studied the effect of interfacial tension on nonlinear viscoelastic properties and constructed a constitutive equation.⁸² Their theory agrees well with experimental results, demonstrating that primary normal stress difference as well as shear viscosity are enhanced by interfacial tension in a polymer blend. Strain hardening is, however, not significantly enhanced by blending an immiscible component. The most outstanding elastic property observed in this system is pronounced strain recovery after cessation of flow.⁸³ Although the exact relation with foaming has not been studied, shrinkage of the cells may take place after processing, especially in a foam produced from a polyolefin with a low degree of crystallinity.

Stated briefly, micro-heterogeneous morphology does not directly relate to strain hardening, one of the most important elastic properties for the bubble growth process in foaming, although it provides long time relaxation.

In the case of a miscible blend system, the terminal relaxation mechanisms are entanglement couplings, which bring about strain hardening. The rheological properties of a blend with a polymer with long-chain branches have been extensively studied, since long-chain branches are responsible for terminal relaxation as well as chain stretching. The blend enhances the melt elasticity, including the strain hardening, of a linear polymer to some degree. Further, it is quite easy to control processability because the rheological properties, or at least the linear viscoelastic properties, of the blends are between those of the individual components. Therefore, some blends, such as LLDPE/LDPE^{4,84,85} and LDPE/Ionomer,⁸⁶ are preferably employed for various kinds of processing, including foaming. Polyethylene blends are one of the most popular blends employed commercially. Although there is still controversy over this, most polyethylene blends, as far as the difference in the number of short-chain branches, are within 40 per 1000 backbone carbon atoms, and thus are considered miscible in the molten state from the rheological point of view.⁸⁷ As a result, strain hardening of LLDPE and HDPE is improved by blending LDPE, owing to the chain stretching of LDPE.^{63,84,88}

Another important miscible blend system is a blend with an ultrahigh molecular weight fraction of the same polymer species. It has been demonstrated by Münstedt⁸⁹ and Linster and Meissner⁹⁰ that broadening the molecular weight distribution, i.e., broadening the relaxation spectrum, is also responsible for strain hardening, at least when the Deborah number associated with terminal relaxation is beyond 0.5:

$$\tau_1 \dot{\epsilon} > \frac{1}{2} \quad (2.14)$$

Under this condition, coil-stretch transition takes place owing to the drag flow, and then the molecular chain is stretched. As shown by Dumoulin et al., however, mechanical mixing may not work for homogenizing the blend.⁹¹ This is reasonable because it takes a long time to dissolve each molecular chain, owing to the low diffusion constant of a high molecular weight fraction. Consequently, mixing has to be carried out intensively to obtain the thinner striation thickness, i.e., diffusion distance, of an ultrahigh molecular weight fraction. Nevertheless, the intense mixing often induces molecular scission due to high stress.

2.3.2.2 *Blends with Weak Gel*

Recently, Yamaguchi and Miyata found that blending a small amount of a crosslinked polymer characterized as a weak gel near the sol-gel transition point enhances melt elasticity of a linear polymer drastically, whereas it has less or no influence on steady-state shear viscosity.^{92,93} This is an interesting

and anomalous phenomenon since most polymer blends and composites, except for the system having a branched polymer as a matrix, do not exhibit strong melt elasticity.

Figure 2.17 shows the growth curves of uniaxial elongational viscosity at various strain rates for the blends of linear PP and gEHDM, the gel fraction of a crosslinked terpolymer composed of ethylene, 1-hexene, and ethylidene norbornene, produced by a metallocene catalyst system.^{19,92} The precursor of gEHDM, an uncrosslinked terpolymer (EHDM), is miscible with PP in a molten state⁹² because of its high hexene content, 67.5 mol%.⁸⁷

Strain hardening, which barely takes place for linear PP, is clearly detected in the curves for the blends at any strain rate in the experimental range, even though the amount of gEHDM is only 3000 ppm. Further, the upturn behavior becomes pronounced with gEHDM content, whereas the linear region prior to viscous enhancement is the same as that for pure linear PP. Moreover, deviation from the linear region is marked even at a low strain rate. The maximum value of the elongational viscosity for the blend with 3 wt% of gEHDM is almost 30 times as high as that for pure PP at a strain rate of 0.013–0.016. The upturn behavior is characterized in Figure 2.18, in which the abscissa axis represents the ratio of measured elongational viscosity to

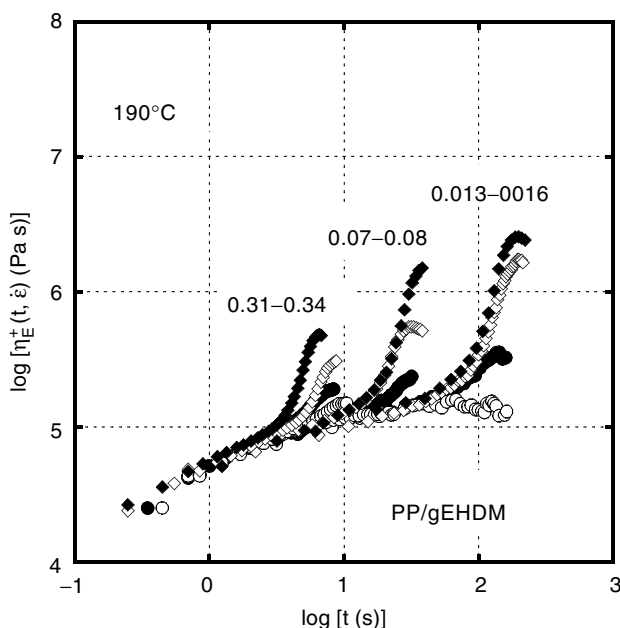


FIGURE 2.17

Growth curves of uniaxial elongational viscosity $\eta_E^+(t, \dot{\epsilon})$ at 190°C for PP and blends with gEHDM. (o) PP, (•) PP/gEHDM = 99.7/0.3, (◊) PP/gEHDM = 99/1, and (♦) PP/gEHDM = 97/3. Numerals in the figure represent strain rates $\dot{\epsilon}$. (From Yamaguchi, M. *J. Polym. Sci. Polym. Phys. Ed.*, 39, 228, 2001. With permission of John Wiley & Sons, Inc.)

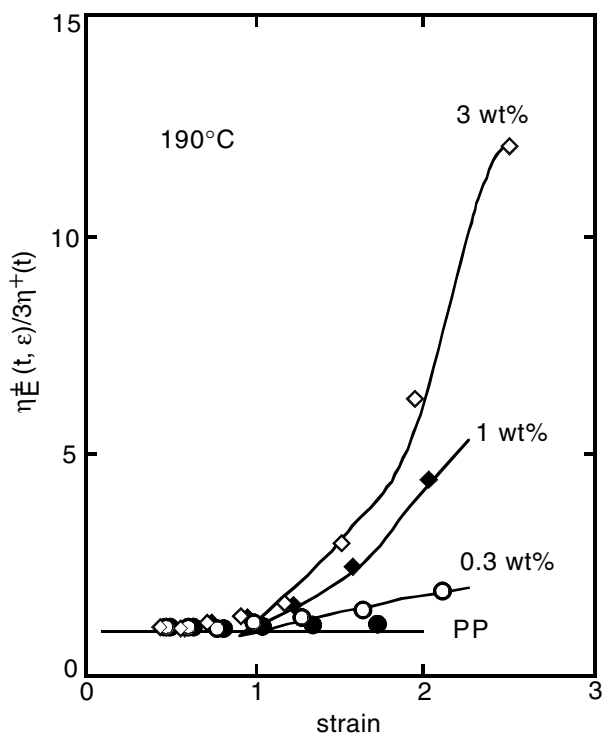


FIGURE 2.18

Nonlinear parameter, $\eta_E^+(t, \dot{\epsilon}) / 3\eta^+(t)$ where $\eta^+(t)$ is transient shear viscosity at the low strain rate asymptote calculated from linear viscoelastic properties, plotted against the elongational strain at 190°C for PP and blends with gEHDM. (From Yamaguchi, M., *SPE ANTEC*, 1149, 2001. With permission of the Society of Plastic Engineers.)

the ratio calculated from linear viscoelastic properties, i.e., the level of non-linearity, at a strain rate of 0.07–0.08.

All curves remain around unity until an elongational strain of 1, regardless of the blend ratio. Then the blends show rapid growth with the strain, which becomes evident with the gEHDM content.

The blend shows not only marked strain hardening but also a high level of extrudate swell ratio and drawdown force, as shown in Figure 2.19. The magnitude of extrudate swell ratio and drawdown force increases monotonically with the content of gEHDM, whereas extensibility is depressed because of the high level of extensional stress.¹⁹ The figure shows that the drawdown force of a blend with only 1% of gEHDM is about twice as high as that of pure PP. Further, the level of swell ratio and drawdown force of the blend with 3 wt% of gEHDM is higher than that of a branched PP produced by peroxide or radiation modification.⁵¹

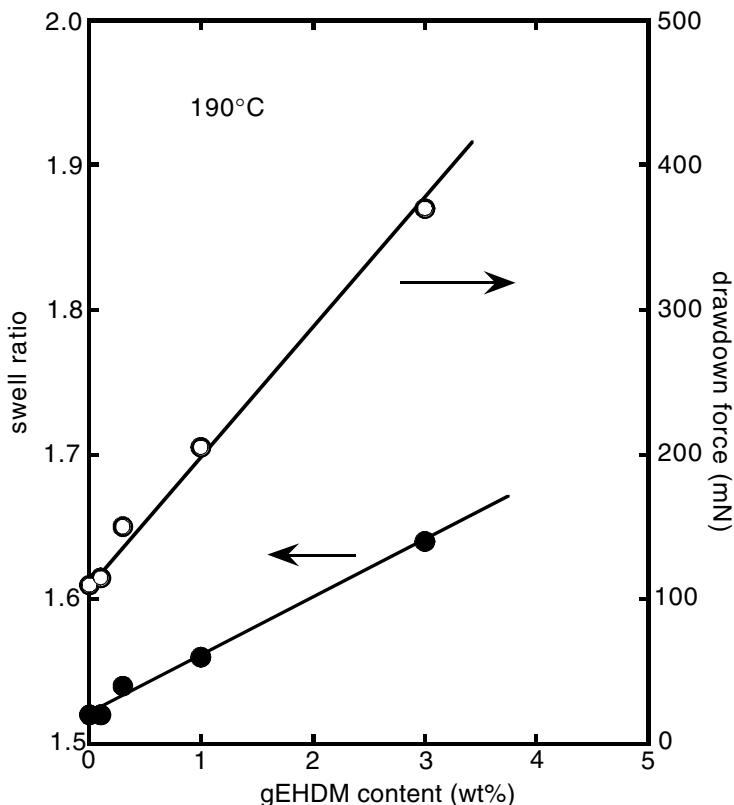


FIGURE 2.19

Relation between gEHDM content and (●) extrudate swell ratio at $\dot{\gamma} = 10.8 \text{ s}^{-1}$ and (○) draw-down force at a draw ratio of 5 at 190°C for PP/gEHDM blends. The dimension of the die employed was $L/D = 8/2.095$.

The steady-state shear viscosity of the blend is, on the other hand, similar to that of pure PP, as shown in Figure 2.20. Moreover, the blend shows a higher primary normal stress coefficient. The enhancement of primary normal stress difference is connected with the marked extrudate swell ratio.²⁰

These results prove that the gEHDM acts as a modifier of PP to enhance various kinds of elastic properties while retaining the viscous properties. Further, it has been found that gEHDM does not improve the melt elasticity of polystyrene, which is immiscible with EHDM,⁹² indicating that miscibility with network chains is required for the anomalous rheological properties. Besides miscibility, the molecular structure of a network has a great influence on the improvement of melt elasticity. The frequency dependence of oscillatory shear modulus of the gEHDM is shown in Figure 2.21.⁹²

Both G' and G'' increase with frequency, and there seems to be a plateau in the G' curve in the very low frequency region. Furthermore, $\tan \delta$

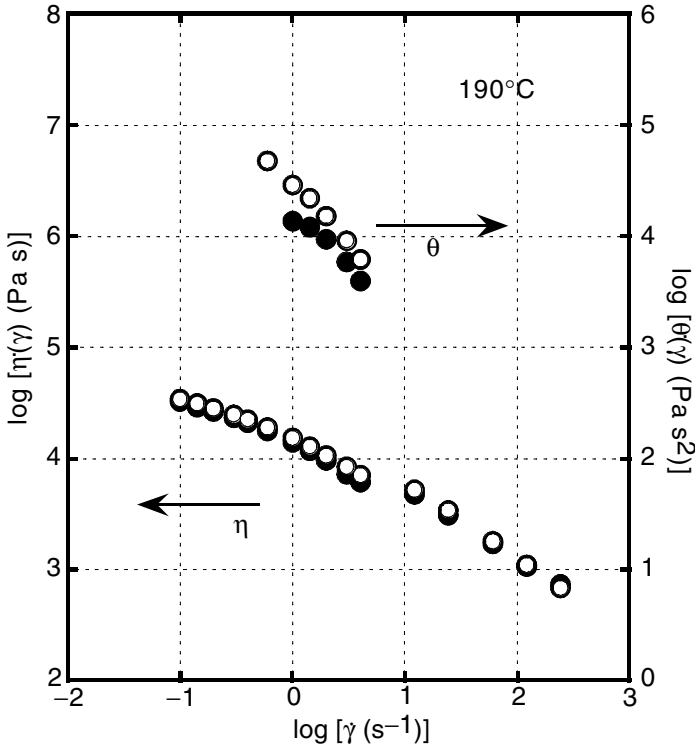


FIGURE 2.20

Steady-state shear viscosity $\eta(\dot{\gamma})$ and primary normal stress coefficient $\theta(\dot{\gamma})$ at 190°C as a function of shear rate $\dot{\gamma}$ for (•) PP and (o) PP/gEHDM (97/3) blend. The measurement was performed by means of a capillary rheometer ($\dot{\gamma} > 10 \text{ s}^{-1}$) and a cone-and-plate rheometer ($\dot{\gamma} < 10 \text{ s}^{-1}$).

remains almost a constant value irrespective of frequency. The curves demonstrate that gEHDM, having a strong ability to enhance melt elasticity, is characterized as a gel just beyond the sol-gel transition point at which the following scaling law governs linear viscoelastic properties:⁹⁴

$$G' \propto G'' \propto \omega^n \quad (0 < n < 1) \quad (2.15)$$

$$\tan \delta = \tan(n\pi / 2) \quad (2.16)$$

$$G(t) = St^{-n} \quad (2.17)$$

where S is gel strength.

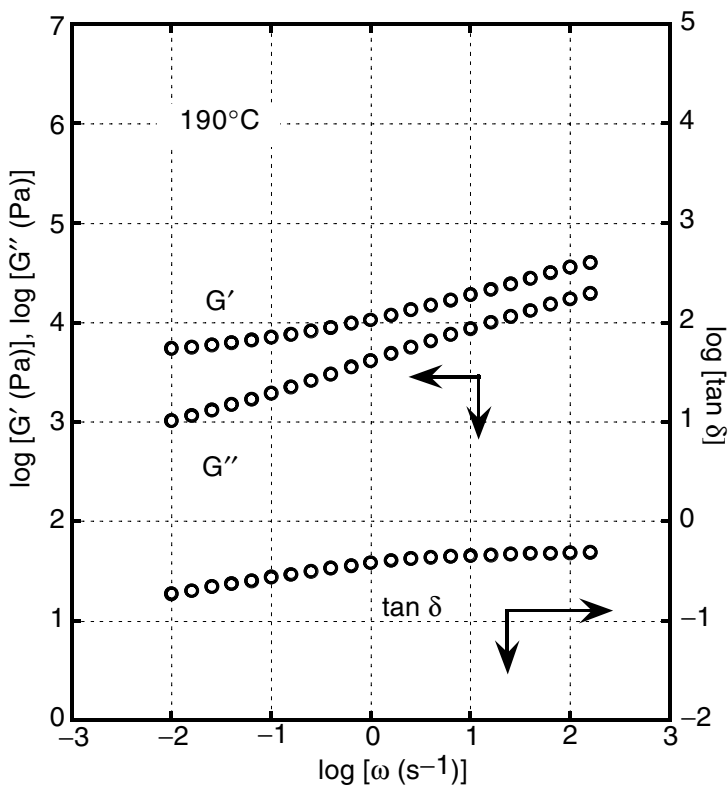


FIGURE 2.21

Frequency dependence of oscillatory shear moduli, such as shear storage modulus G' , loss modulus G'' , and loss tangent $\tan \delta$, for gEHDM at 190°C. (From Yamaguchi, M. and Miyata, H. *Polym. J.* 32, 164, 2000. With permission of the Society of Polymer Science, Japan.)

The average molecular weight between crosslink points of gEHDM is estimated to be 190,000, which is significantly larger than that between entanglement couplings of EHDM,⁹² suggesting that the crosslinked polymer has sparse crosslink points. According to our recent study,⁹⁵ homogeneous distribution of crosslink points is required for the crosslinked polymer to improve the melt elasticity of a linear polymer efficiently. Furthermore, the sol fraction does not play an important role in the improvement of melt elasticity, compared to that of the gel fraction.^{19,92} A blend with a sol fraction having many branches will have a similar influence to that with a branched polymer; e.g., a blend of LLDPE with LDPE. Moreover, a crosslinked polymer having many crosslink points also does not enhance melt elasticity, but acts as filler because of the high modulus. Consequently, the extrudate swell ratio of the PP/gEHDM blend is lower than that of pure PP.^{19,95} Further, such a crosslinked polymer with high modulus prohibits homogeneous

deformation of the blend due to the localized stress concentration, and thus results in poor extensibility.^{19,93,95}

The morphology of the blend also affects the rheological properties. Figure 2.22 shows transmission electron microscopy for the PP/gEHDM (90/10) blend stained by ruthenium tetroxide. The sample was cut out of the strand extruded from a capillary rheometer. Since gEHDM is an amorphous polymer (due to less ethylene sequence), the dark area in the picture represents a gEHDM-rich region, and the white lines with 10–20 nm thickness denote PP lamellae.

The picture provides evidence that PP lamellae exist even in gEHDM-rich dark regions, suggesting that mutual dissolution of PP and gEHDM takes place in the molten state. Further, most lamellae are extended in a horizontal direction, i.e., perpendicular to the flow direction. Considering that the PP chains orient perpendicular to the lamellae, the picture demonstrates that most PP chains orient to the flow direction. Dynamic mechanical properties in the solid state also support the interdiffusion of both polymer chains. As seen in Figure 2.23, the blend shows a single peak, ascribed to glass transition in the E'' curve of the blend, which is located between those of the individual pure components (represented by diamonds). The result proves that network chains of gEHDM are miscible with amorphous PP chains. Further, it also indicates that network chains are distributed in a wide spatial area of the blend in spite of the small amount of the gEHDM. Swelling of the network by PP molecules will be responsible for the wide distribution of network chains.

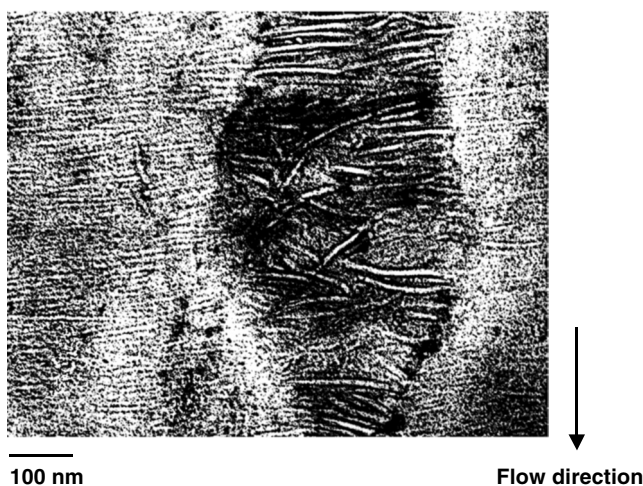


FIGURE 2.22

Transmission electron microscopy of PP/gEHDM (90/10) extruded from a capillary rheometer at 10.8 s^{-1} at 190°C . The sample was stained by ruthenium tetroxide. (From Yamaguchi, M. *SPE ANTEC*, 1149, 2001. With permission of the Society of Plastic Engineers.)

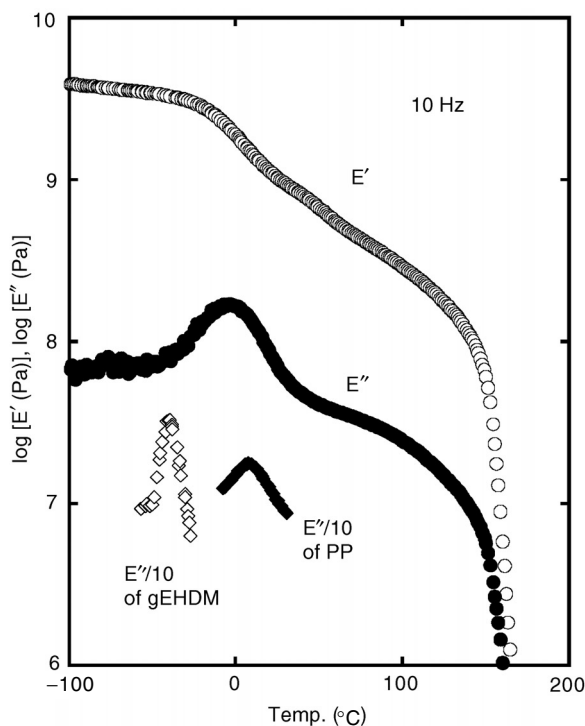


FIGURE 2.23

Temperature dependence of (o) tensile storage modulus E' and (•) loss modulus E'' for PP/gEHDM (90/10) at 10 Hz. In the figure, E'' peaks for (♦) pure PP and (◊) gEHDM, shifted vertically, are also shown. (From Yamaguchi, M. *SPE ANTEC*, 1149, 2001. With permission of the Society of Plastic Engineers.)

Although the mechanism of the anomalous rheological properties for this blend system has not been established precisely, the morphology indicates that entanglement couplings, especially trapped entanglements associated with the network, have a substantial effect on strain hardening.⁴ The trapped entanglements whose characteristic time is considerably long will lead to the chain stretching of the network.⁴ During extension, chain contraction of the network, maybe with some linear polymers, is prohibited by trapped entanglements. This is at least one of the origins of the strain hardening. Too many crosslink points in a crosslinked polymer inhibit swelling of the network, which results in less strain hardening. Further, sol will not play an important role in enhancing the melt elasticity because there is no network structure.^{19,95}

Trapped entanglement also leads to marked overshooting in the growth curves of shear stress and primary normal stress difference. Figure 2.24 shows the startup behavior of shear stress and primary normal stress difference for a blend with 10 wt% of gEHDM.

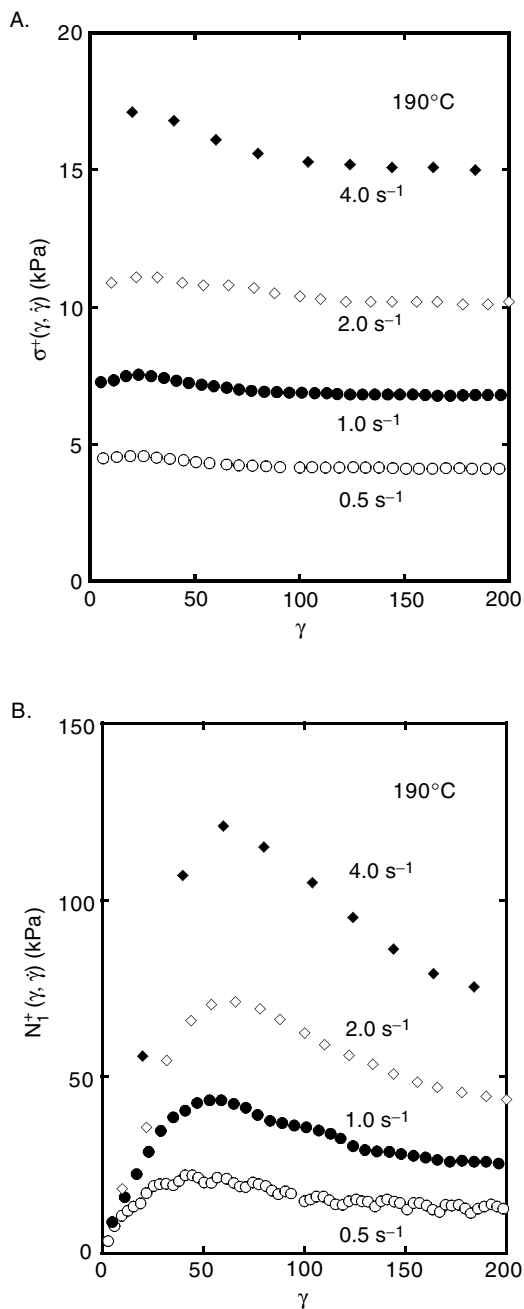


FIGURE 2.24

Startup behavior of (A) shear stress $\sigma^+(\gamma, \dot{\gamma})$ and (B) primary normal stress difference $N_1^+(\gamma, \dot{\gamma})$ plotted against shear strain γ at various shear rates 0.5–4.0 s⁻¹ at 190°C for PP/gEHDM (90/10).

The blend exhibits prominent overshooting in the curves of both shear stress and primary normal stress difference. Furthermore, the strain at the maximum point increases slightly with the strain rate, which is more obvious in the curve of primary normal stress difference. The level of the maximum stress rapidly increases with shear strain. It should be noted that the overshooting in Figure 2.24 appears at a much larger strain than that for a simple polymer melt, as shown in Figure 2.14. According to the Doi–Edwards theory, the strain at the maximum shear stress is around 2, irrespective of strain rate, which corresponds with numerous experimental results, including PP, with a minor departure.⁵ Moreover, it has been clarified by the theory that the maximum shear stress is ascribed to the overshooting of molecular orientation, whereas the stretching of contour length also contributes to the overshooting of primary normal stress difference. The large strain at the maximum of primary normal stress difference indicates that chain stretching keeps occurring to a larger strain via trapped entanglements, which will be connected with the upturn behavior in elongational viscosity. Beyond the maximum point, primary normal stress difference decreases with strain. Chain stretching will be reduced, presumably, by losing interaction due to trapped entanglements. In other words, prolonged shearing weakens the topological interaction generated between PP molecules and network chains of gEHDM.

Generally speaking, mismatching of viscosities, if present, will accelerate the rotation of the dispersion in shear flow, which gives rise to further disentanglement. On the other hand, under elongational flow, the disentanglement between PP molecules and network chains of gEHDM will be avoided for the following reasons. First, elongational flow is irrotational. Therefore, rotation of the crosslinked polymer, causing further disentanglement with the linear molecules, barely takes place. Second, deformation increases exponentially in elongational flow at a constant strain rate. Chain stretching occurs under the exponential growth of deformation, which has been confirmed also in shear flow for a branched polymer.⁶ As a result, the blend exhibits marked stress enhancement with strain only under extension. The mechanism of the overshooting discussed here suggests that applied shear flow changes the morphology in the melt and thus the rheological properties of the blend, as discussed below.

The mixing method is very important for the blend system because a crosslinked polymer is difficult to deform in the matrix of a linear polymer with lower viscosity. To begin, shear-dominant flow should be precluded as a possibility because it depresses melt elasticity due to the disentanglement associated with network chains. Further, the diffusion of linear polymers into the network is required in order to exhibit marked melt elasticity. Hence, chaotic mixing, in which strain increases exponentially with time, is preferably employed to decrease the striation thickness of a crosslinked polymer. Thinner striation enables linear polymers to penetrate into the network within a certain processing time. Therefore, a twin-screw extruder with kneading blocks, a rotor-type twin-screw extruder, and a two-roll mill should be employed for mixing the blend. A single-screw extruder with conven-

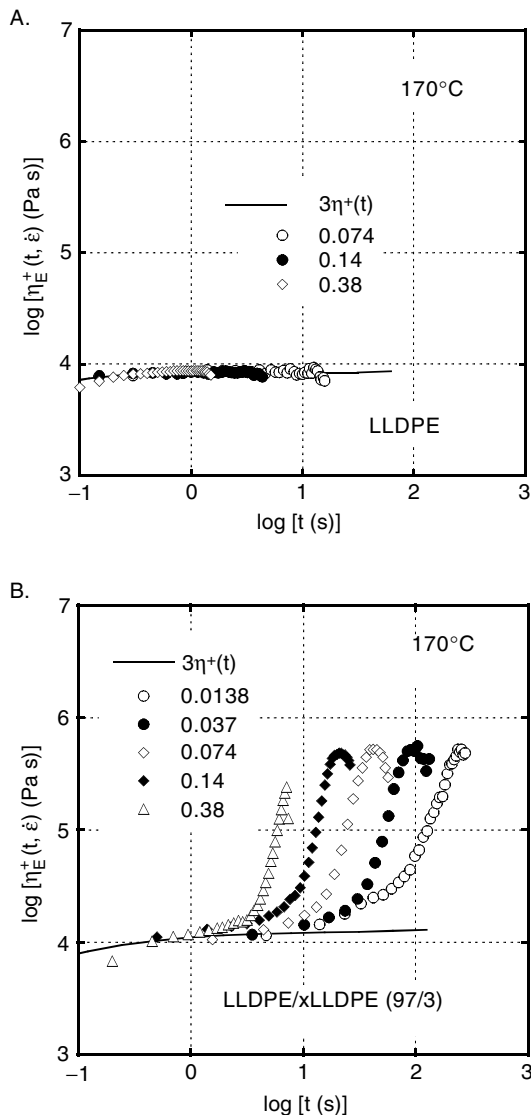


FIGURE 2.25

Growth curves of uniaxial elongational viscosity $\eta_E^+(t, \dot{\epsilon})$ at various strain rates at 170°C for (A) LLDPE and (B) LLDPE/xLLDPE (97/3) blend. The solid line represents $3\eta^+(t)$ at the low strain rate asymptote calculated from linear viscoelastic properties. (From Yamaguchi, M. and Suzuki, K., *J. Polym. Sci. Polym. Phys. Ed.*, 39, 2159, 2001. With permission of John Wiley & Sons, Inc.)

tional full-flight screws does not work for mixing, because shear flow dominates in the extruder.

This blend technique—improvement of melt elasticity by blending an appropriate crosslinked polymer—is available for various polymers. Figure 2.25 shows the growth curves of uniaxial elongational viscosity for LLDPE

produced by metallocene catalyst and the blend with 3 wt% of crosslinked LLDPE (xLLDPE), characterized as the gel just beyond the sol-gel transition point. The precursor of the crosslinked polymer is, of course, miscible with LLDPE, although it is difficult to detect the morphology of the blend. It has also been noted that the gel fraction of xLLDPE is 75 wt% and that the average molecular weight between crosslink points is 380,000 by swelling measurement.⁹⁷

Having no long-chain branch, pure LLDPE does not show upturn behavior at any strain rate. The viscosity coincides with that of the low strain rate asymptote calculated from linear viscoelastic properties. On the other hand, it is obvious that the blend exhibits stronger upturn behavior than conventional LDPE, as shown in Figure 2.6. At a high strain rate, the blend sample exhibits brittle behavior due to high stress. The maximum stress of the blend is almost 30 times as high as that of pure LLDPE. In contrast, the steady-state shear viscosity of the blend is similar to that of pure LLDPE. Further, blending xLLDPE has no effect on the onset of shark-skin failure,⁹⁷ which is often observed for linear polyethylenes. This is reasonable because shark-skin failure is generally dependent on the apparent shear stress. Figure 2.25B also indicates that strain hardening is observed even below a strain of 1. This may be due to the morphology of the blend; i.e., the conformation of the network chain and/or mutual dissolution between xLLDPE and LLDPE are not at an equilibrium state.

The experimental results shown here demonstrate that a crosslinked polymer having appropriate structure will be applicable as a modifier for processing. Since most linear polymers have less melt elasticity and less strain hardening in elongational viscosity, they will become available for various kinds of processing, including foaming, by means of the blend technique. Of course, the blend technique is also applicable to a branched polymer.

2.3.2.3 Processability of Foaming

The relation between strain hardening in elongational viscosity and the processability of various processes has been studied intensively, especially for fiber spinning, film processing, blow molding, and thermoforming, in which deformation with a free surface takes place most frequently.⁹⁷⁻¹⁰⁰ According to previous studies, enhanced strain hardening suppresses heat-sag and thus results in homogeneous thickness of the product. Also, for foaming, it is expected that elongational viscosity plays an important role during the bubble growth process in a similar manner.^{97,100} When the material does not show the strain-hardening behavior in elongational viscosity, the thinner part of a cell wall is liable to deform by an inner pressure. Consequently, the thinner part will become much thinner and the bubble may burst. In cases where the material has marked strain hardening, however, the deformation in the thinner part will be reduced because of the viscous enhancement with strain.⁹⁷⁻¹⁰⁰ As a result, the foam obtained will have uniform wall thickness, and thus a large expansion ratio is expected. This is the

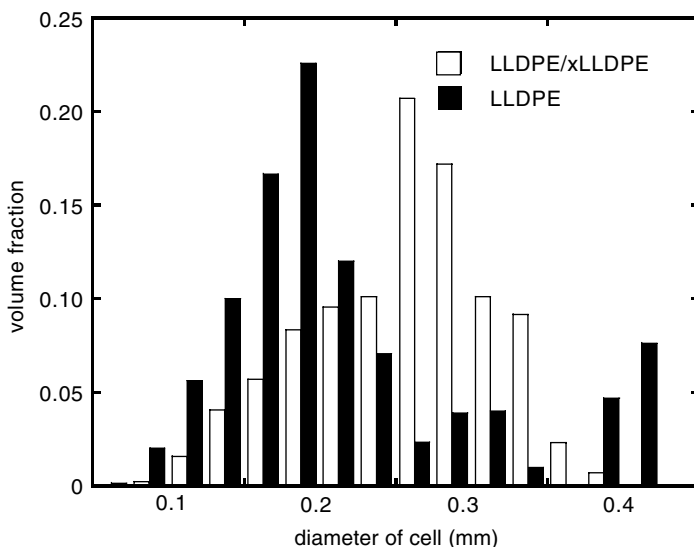


FIGURE 2.26

Cell size distribution of the foams from (■) original LLDPE and (□) LLDPE/xLLDPE (97/3) blend. (From Yamaguchi, M. and Suzuki, K., *J. Polym. Sci. Polym. Phys. Ed.* 39, 2159, 2001. With permission of John Wiley & Sons, Inc.)

primary reason why LDPE is preferably employed for foaming instead of LLDPE.

Yamaguchi and Suzuki have proved that the blends with a crosslinked polymer exhibit excellent processability for various processes, including foaming.^{97,99,100} According to their foaming experiments, conducted in a hot oven, for a compound containing a chemical blowing agent, the expansion ratio of the blend with 0.5–3% of the xLLDPE is larger than that of the original LLDPE.^{97,100} Further, cell-size distribution of the foams is significantly improved by blending the xLLDPE, as shown in Figure 2.26. In particular, the foam from the blend has no huge cell would lead to a rough surface.

The existence of huge cells in the foam from the original LLDPE indicates that some cells burst and coalesce. The results support that viscous enhancement under elongational flow dominates cell morphology as well as the expansion ratio. Although it should be based on biaxial elongational viscosity instead of uniaxial viscosity, as mentioned above, the conclusion will not change, because the sample showing marked strain hardening in uniaxial elongational viscosity is apt to exhibit larger strain hardening also in biaxial viscosity.¹⁶ Finally, it is found that the blend exhibits a much wider processing window (the temperature and the duration in an oven) than the original LLDPE and commercial LDPE,¹⁰⁰ because the melt elasticity of the blend is less sensitive to temperature than that of LLDPE and LDPE. Consequently, various blowing agents, such as ADCA and OBSH, are available for foaming, regardless of the decomposition temperature.¹⁰⁰ Similarly, blending gEHDM

enhances the processability of foaming for a linear PP. It should be emphasized that the blends that are not fully crosslinked exhibit excellent processability for foaming. Moreover, the foaming capability without a fully crosslinking process implies that the blend is available for gas extrusion foaming.

Processability of the blend is dependent not only on the mixing method but also on the processing machine, since the level of the mutual dissolution, i.e., the degree of swelling of the network, is affected by the applied processing history. Figure 2.27 shows the effect of processing history on the drawdown force.

Even though the initial mixing is carried out by a two-roll mill, the following extrusion history by a single-screw extruder with full-flight conveying screws, in which shear flow dominates, depresses the drawdown force to a great degree because of less strain hardening in elongational viscosity.⁹⁹ On the other hand, extrusion history by a counter-rotating twin-screw extruder with conveying screws has less of an effect on the drawdown force than does the single-screw extruder. This is a mechanical modification because reprocessing by a

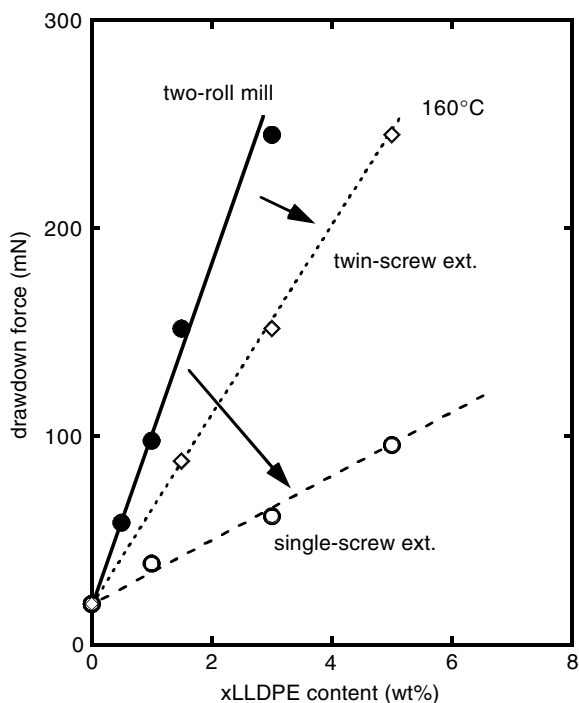


FIGURE 2.27

Drawdown force at 160°C at a draw ratio of 5 plotted against xLLDPE content for LLDPE/xLLDPE processed by (•) two-roll mill, (o) single-screw extruder with a conveying screw after mixing by two-roll mill, and (◊) counter-rotating twin-screw extruder with conveying screws after mixing by two-roll mill.

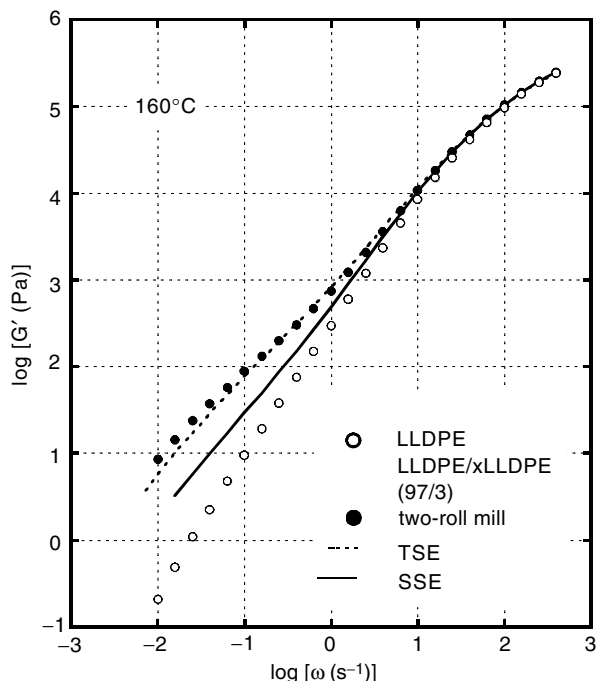


FIGURE 2.28

Frequency dependence of shear storage modulus G' at 160 °C for (o) LLDPE and (•) LLDPE/xLLDPE (97/3) blend processed by two-roll mill. Solid and dotted lines represent the blends reprocessed by single-screw extruder (SSE) and by counter-rotating twin-screw extruder (TSE) respectively, after mixing by a two-roll mill.

two-roll mill enhances the melt elasticity again, and molecular weight is unchanged by the processing.⁹⁹ The phenomenon—mechanical modification of the rheological properties of the blend system—is very similar to shear modification of a branched polymer, described in the previous section. It is interesting that shear dominant flow depresses melt elasticity also for the blend with a weak gel.

The linear viscoelastic properties for the samples with various processing histories for the LLDPE/xLLDPE blend are shown in Figure 2.28. It is clear that terminal relaxation, which may be ascribed to the entanglement couplings associated with network chains, appears in the blend processed by a two-roll mill because an apparent shoulder is observed in the G' curve in the low frequency region. Further, the magnitude of the shoulder is reduced by the processing history, especially that of a single-screw extruder processing with a conventional conveying screw, suggesting that the terminal relaxation mechanism—i.e., the interaction between LLDPE and xLLDPE—is weakened by the applied shear flow in the extruder. The magnitude of G' for the sample processed by a single-screw extruder is, however, still higher than that for pure LLDPE. The effect of the processing history

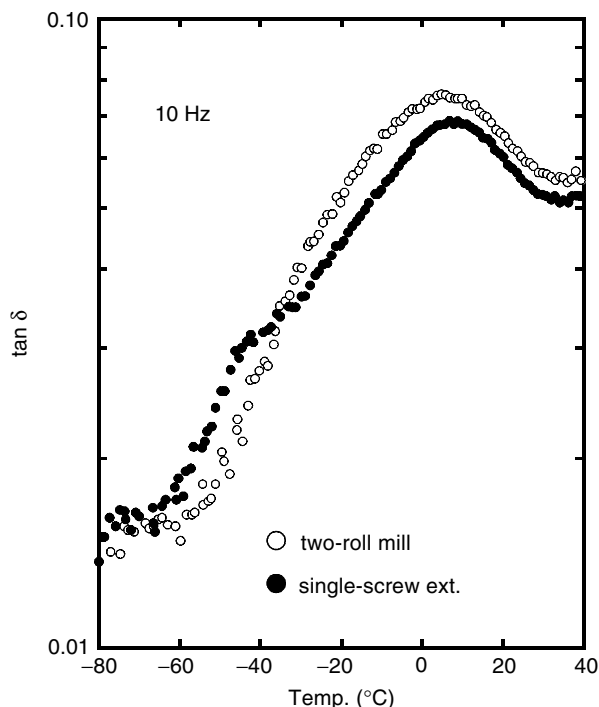


FIGURE 2.29

Temperature dependence of $\tan \delta$ at 10 Hz for PP/gEHDM (90/10) blends (o) processed by two-roll mill and (•) reprocessed by single-screw extruder with a conveying screw after mixing by a two-roll mill.

by a counter-rotating twin-screw extruder falls between that of the two-roll mill and that of the single-screw extruder, which is in accordance with the result of the drawdown force shown in Figure 2.27. The experimental result suggests that elongational flow, as in a two-roll mill, leads to mutual dissolution, whereas shear flow, which is dominant in a single-screw extruder, accelerates the disentanglements between them. The fact that the degree of mutual dissolution is affected by the applied processing history is also confirmed by the morphological study of the blend composed of linear PP and gEHDM. Figure 2.29 shows the temperature dependence of $\tan \delta$ for the blend in the solid state. The sample processed by a two-roll mill exhibits a single peak, suggesting that the amorphous chains dissolve each other. On the other hand, processing history by a single-screw extruder with a conveying screw leads to double peaks, ascribed to T_g of PP-rich and gEHDM-rich phases. This result indicates that the structure of the blend changes from a homogeneous to a heterogeneous morphology composed of PP-rich and gEHDM-rich phases by shear-dominant flow, although the level of melt elasticity of the blend having the shearing history is still considerably higher than that of pure PP.

Another example of the effect of applied processing history is exhibited in Figure 2.30. Processing history with a single-screw extruder having a conveying screw makes the magnitude of strain-hardening weaken for a blend of HDPE and xHDPE, i.e., crosslinked HDPE characterized as a weak gel, mixed by a two-roll mill.⁹⁹ It is, however, quite interesting that the blend having a single-screw extrusion history shows early upturn behavior.

The mechanical modification, i.e., the depression of melt elasticity by shear flow, is dependent on the molecular structure of both the crosslinked and the linear polymers. The crosslinked polymer having heterogeneous distribution of crosslink points and/or high density of crosslink points is liable to depress the melt elasticity by shear history. Further, shear flow has less effect on the depression of melt elasticity for the blend composed of the linear polymer with high molecular weight and narrow molecular weight distribution. Currently, the blend with a crosslinked polymer, which is not significantly affected by applied processing history, is being developed.¹⁰⁰

In conclusion, the blend with a crosslinked polymer, characterized as a weak gel just beyond the critical point, has great potential to make various polymers available for foaming. The processing method and mixing procedure, however, have to be taken into consideration.

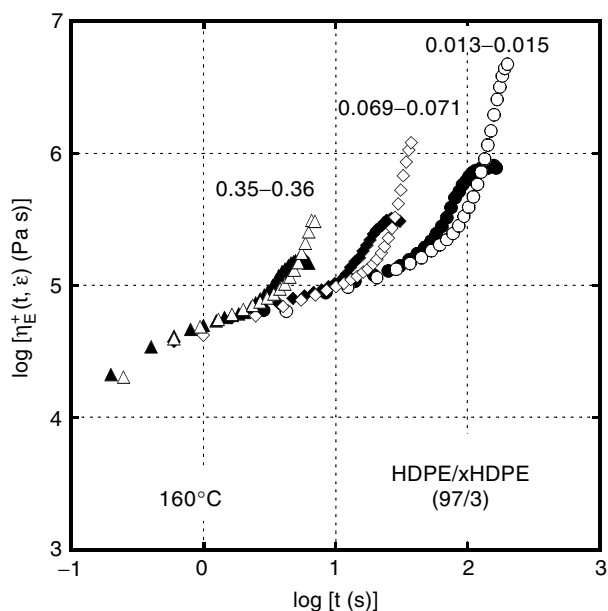


FIGURE 2.30

Growth curves of uniaxial elongational viscosity $\eta_E^+(t, \dot{\epsilon})$ at various strain rates at 160°C for HDPE/xHDPE (97/3) blend. Open symbols denote the sample mixed by two-roll mill, and closed symbols denote the sample reprocessed by single-screw extruder after mixing by a two-roll mill. Numbers in the figure represent the strain rate.

2.4 Conclusion

Melt elasticity and its effect on foaming for polyolefins have been described in this chapter. Since a linear polymer such as LLDPE and PP lacks the elasticity required for foaming, various approaches to enhance the melt elasticity have been studied. One of them is a blend technique with a crosslinked polymer having the appropriate network structure. Catalyst technology is also being developed extensively in order to incorporate the appropriate number and length of long-chain branches as well as to generate new types of polyolefins, such as block or graft copolymers and copolymers with a polar monomer. Further, applied processing history depresses the melt elasticity for a branched polymer to a great degree, which is owing to reduced interactions due to entanglement couplings associated with long chain branches. This phenomenon has to be considered seriously when a branched polymer is employed for foaming because the degree of mechanical modification is dependent on the processing temperature, screw configuration, screw rpm, and so on.

It has been shown that strain hardening in elongational viscosity has a strong effect on the bubble growth process of foaming. However, the quantitative relation between the degree of strain hardening and processability of foaming has not been established yet, since the reported experimental results are few and restricted. More time should be spent studying elongational flow, especially biaxial elongational flow, as well as the rheological features under non-isothermal conditions, in order to derive a more complete comprehension of foaming processability.

References

1. Gendron, R. and Daigneault, L.E., Rheology of thermoplastic foam extrusion process, in *Foam Extrusion*, ed. S.T. Lee, CRC Press, Boca Raton, FL, 2000, [chap 3](#).
2. Yamaguchi, M. and Abe, S., LLDPE/LDPE blends. I. Rheological, thermal, and mechanical properties, *J. Appl. Polym. Sci.*, 74, 3153, 1999.
3. Abe, S. and Yamaguchi, M., Study on the foaming of crosslinked polyethylene, *J. Appl. Polym. Sci.*, 79, 2146, 2001.
4. Ferry, J.D., *Viscoelastic Properties of Polymers*, 3rd ed., John Wiley & Sons, New York, 1980.
5. Doi, M. and Edwards, S.F., *The Theory of Polymer Dynamics*, Clarendon Press, Oxford, 1986.
6. Rouse, P.E., A theory of the linear viscoelastic properties of dilute solutions of coiling polymers, *J. Chem. Phys.*, 21, 1272, 1953.
7. Mills, N.J., The rheological properties and molecular weight distribution of polydimethylsiloxane, *Eur. Polym. J.*, 5, 675, 1969; Mills, N.J. and Nevin, A., Oscillatory shear measurements on polystyrene melts in the terminal region, *J. Polym. Sci.*, Part A-2, 9, 267, 1971.

8. Laun, H.M., Prediction of elastic strains of polymer melts in shear and elongation, *J. Rheol.*, 30, 459, 1986.
9. Cox, W.P. and Merz, E.H., Correlation of dynamic and steady flow viscosities, *J. Polym. Sci.*, 28, 619, 1958.
10. Pearson, D.S. et al., Flow-induced birefringence of concentrated polyisoprene solutions, *J. Rheol.*, 33, 517, 1989.
11. Osaki, K., On the damping function of shear relaxation modulus for entangled polymers, *Rheol. Acta*, 32, 429, 1993.
12. Larson, R.G., A constitutive equation for polymer melts based on partially extending strand convection, *J. Rheol.*, 28, 545, 1984.
13. Wagner, M.H. and Schaeffer, J., Nonlinear strain measures for general biaxial extension of polymer melts, *J. Rheol.*, 36, 1, 1992; Wagner, M.H., Bastian, H., Hachmann, P., Meissner, J., Kurzbeck, S., Münstedt, H., and Langouche, F. The strain-hardening behaviour of linear and long-chain-branched polyolefin melts in extensional flows, *Rheol. Acta*, 39, 97, 2000.
14. McLeish, T.C.B. and Larson, R.G., Molecular constitutive equations for a class of branched polymers; the pom-pom polymer, *J. Rheol.*, 42, 81, 1998; Inkson, N.J. and McLeish, T.C.B., Predicting low density polyethylene melt rheology in elongational and shear flows with "pom-pom" constitutive equations, *J. Rheol.*, 43, 873, 1999.
15. Wagner, M.H., Yamaguchi, M., and Takahashi, M., Quantitative assessment of MSF theory for LDPE, *J. Rheol.*, 47, 779, 2003.
16. Yamaguchi, M. and Takahashi, M., Rheological properties of low density polyethylenes produced by tubular and vessel processes, *Polymer*, 42, 8663, 2001.
17. Macosko, C.W., *Rheology: Principles, Measurements, and Applications*, Wiley, New York, 1994.
18. Wagner, W.H., Bernnat, A., and Schulze, V., The rheology of the rheotens test, *J. Rheol.*, 42, 917, 1998.
19. Yamaguchi, M., Rheological properties of linear and crosslinked polymer blends: Relation between crosslink density and enhancement of elongational viscosity, *J. Polym. Sci. Polym. Phys. Ed.*, 39, 228, 2001.
20. Tanner, R.I., *Engineering Rheology*, Oxford Science Publications, New York, 1985.
21. Meissner, J., Rheometer zur untersuchung der deformationsmechanischen eigenschaften von kunststoffe-schmelzen unter definierter zugbeanspruchung, *Rheol. Acta*, 8, 78, 1969; Meissner, J., Development of a uniaxial extension of polymer melts, *Trans. Soc. Rheol.*, 16, 405, 1972.
22. Larson, R.G., *The Structure and Rheology of Complex Fluids*, Oxford University Press, New York, 1999.
23. Ballman, R.I., Extensional flow of polystyrene melt, *Rheol. Acta*, 4, 137, 1965; Chang, J.C. and Denn, M.M., An experimental study of isothermal melt spinning of a Newtonian and a viscoelastic liquid, *J. Non-Newtonian Fluid Mech.*, 5, 39, 1979; Jones, D.M., Walters, K., and Williams, P.R., On the extensional viscosity of mobile polymer solutions, *Rheol. Acta*, 26, 20, 1987.
24. Metzner, A.B. and Metzner, A.P., Stress levels in rapid extensional flows of polymeric fluids, *Rheol. Acta*, 9, 174, 1970; Binding, D.M., An appropriate analysis for contraction and converging flows, *J. Non-Newtonian Fluid Mech.*, 27, 173, 1988; Tremblay, B., Estimation of the elongational viscosity of polyethylene blends at high deformation rates, *J. Non-Newtonian Fluid Mech.*, 33, 137, 1989.
25. Moan, M. and Maguer, A., Transient extensional viscosity of dilute flexible polymer solutions, *J. Non-Newtonian Fluid Mech.*, 30, 343, 1988.

26. Meissner, J., Stephenson, S.E., Demarmels, A., and Portman, P., Multiaxial elongational flows of polymer melts—classification and experimental realization, *J. Non-Newtonian Fluid Mech.*, 11, 221, 1982
27. Chatraei, S., Macosko, C.W., and Winter, H.H., Lubricated squeezing flow: A new biaxial extensional rheometer, *J. Rheol.*, 25, 433, 1981; Khan, S.H. and Larson, R.G., Step planar extension of polymer melts using a lubricated channel, *Rheol. Acta*, 30, 1, 1991.
28. Winter, H.H., Macosko, C.W., and Bennett, K.E., Orthogonal stagnation flow: A framework for steady extensional flow experiments, *Rheol. Acta*, 18, 323, 1979; Soskey, P.R. and Winter, H.H., Equibiaxial extension of two polymer melts: Polystyrene and low density polyethylene, *J. Rheol.*, 29, 493, 1985.
29. Denson, C.D. and Gallo, R.J., Measurements on the biaxial extensional viscosity of bulk polymers: The inflation of a thin polymer sheet, *Polym. Eng. Sci.*, 11, 174, 1971; Denson, C.D. and Crady, D.L., Measurements on planar extensional viscosity of bulk polymers: Inflation of a thin, rectangular polymer sheet, *J. Appl. Polym. Sci.*, 18, 1611, 1974; Denson, C.D. and Hylton, D.L., A rheometer for measuring the viscoelastic response of polymer melts in arbitrary planar and biaxial extensional flow fields, *Polym. Eng. Sci.*, 20, 535, 1980.
30. Watanabe, H., Viscoelasticity and dynamics of entangled polymers, *Prog. Polym. Sci.*, 24, 1253, 1999.
31. Pearson, D.S. and Helfand, E., Viscoelastic properties of star-shaped polymers, *Macromolecules*, 17, 888, 1984.
32. Roovers, J. and Toporowski, P.M., Relaxation by constraint release in combs and star-combs, *Macromolecules*, 20, 2300, 1987.
33. Raju, V.R., Rachapudy, H., and Graessley, W.W., Properties of amorphous and crystallizable hydrocarbon polymers. Part 4: Melt rheology of linear and star-branched hydrogenated polybutadiene, *J. Polym. Sci. Polym. Phys. Ed.*, 17, 1223, 1979.
34. Carella, J.M., Gotro, J.T., and Graessley, W.W., Thermorheological effects of long-chain branching in entangled polymer melts, *Macromolecules*, 19, 659, 1986.
35. Zimm, B.H. and Stockmayer, W.H., Dynamics of branched polymer molecules in dilute solution, *J. Chem. Phys.*, 17, 1301, 1949.
36. Tackx, P. and Tacx, J.C.J.F., Chain architecture of LDPE as a function of molar mass using size exclusion chromatography and multi-angle laser light scattering, *Polymer*, 39, 3109, 1998.
37. Scheirs, S. and Kaminsky, W., eds., *Metallocene-Based Polyolefins: Preparation, Properties, and Technology*, Wiley, New York, 2000.
38. Lachtermacher, M.G. and Rudin, A., Reactive processing of LLDPEs in co-rotating intermeshing twin-screw extruder. 1. Effect of peroxide treatment on polymer molecular structure, *J. Appl. Polym. Sci.*, 58, 2077, 1995.
39. Horii, F., Zhu, Q., and Kitamaru, R., Carbon-13 NMR study of radiation-induced crosslinking of linear polyethylene, *Macromolecules*, 23, 977, 1990.
40. Abe, S., personal communication, 2000.
41. Lai, S.Y., Wilson, J.R., Knight, G.W., Stevens, J.C., and Chum, P.W.S., Elastic substantially linear olefin polymers, U.S. Patent 5,272,236, 1993; Vega, J.F., Santamaria, A., Munoz-Escalona, A., and Lafuente, P., Small-amplitude oscillatory shear flow measurements as a tool to detect very low amounts of long chain branching in polyethylenes, *Macromolecules*, 31, 3639, 1998.
42. Wadud, S.E.B. and Baird, D.G., Shear and extensional rheology of sparsely branched metallocene-catalyzed polyethylenes, *J. Rheol.*, 44, 1151, 2000.

43. Malmberg, A., Kokko, E., Lehmus, P., Löfgren, B., and Seppälä, J. V., Long-chain branched polyethylene polymerized by metallocene catalysts $\text{Et}[\text{Ind}]_2\text{ZrCl}_2/\text{MAO}$ and $\text{Et}[\text{IndH}_4]_2\text{ZrCl}_2/\text{MAO}$, *Macromolecules*, 31, 8448, 1998.
44. Hogan, J.P., Levett, C.T., and Werkman, R.T., Melt elasticity in linear PE containing long branches, *SPE. J.*, 23, 87, 1967.
45. Johnson, L.K., Killian, R.M., and Brookhart, M., New Pd(II)- and Ni(II)-based catalysts for polymerization of ethylene and α -olefins, *J. Am. Chem. Soc.*, 117, 6414, 1995; Johnson, L.K., Mecking, S., and Brookhart, M., Copolymerization of ethylene and propylene with functionalized vinyl monomers by Paradium (II) catalysts, *J. Am. Chem. Soc.*, 118, 267, 1996.
46. Hauptman, E., Waymouth, R.M., and Ziller, J.W., Stereoblock polypropylene: Ligand effects on the stereospecificity of 2-arylidene Zirconocene catalysts, *J. Am. Chem. Soc.*, 117, 11586, 1995.
47. Kojoh, S., Matsugi, T., Saito, J., Mitani, M., Fujita, T., and Kashiwa, N., New monodisperse ethylene-propylene copolymers and a block copolymer created by a titanium complex having fluorine-containing phenoxy-imine chelate ligands, *Chem. Lett.*, 822, 2001.
48. Schmidt, G.F., Timmers, F.J., Knight, G.W., Lai, S., Nickias, P.N., Rosen, R.K., Stevens, J.C., and Wilson, D.R., Constrained geometry addition polymerization catalysts, processes for their preparation, precursors therefore, methods of use, and novel polymers formed therewith, Eur. Patent 0416815, 1991.
49. Yang, C.T. and Lee, S.T., Dimensional stability analysis of foams based on LDPE and ethylene-styrene interpolymer blends, *SPE ANTEC*, 1782, 2002; Ankrah, S., Verdejo, R., and Mills, N.J., The mechanical properties of ESI/LDPE foam blends and sport applications, *Cell. Polym.*, 21, 237, 2002.
50. Bradley, M.B. and Phillips, E.M., Novel polypropylenes for foaming on conventional equipment, *Plast. Eng.*, 82, 1991.
51. Hingmann, R. and Marcinke, B.L., Shear and elongational flow properties of polypropylene melts, *J. Rheol.*, 38, 573, 1994; Sugimoto, S., Tanaka, T., Masubuchi, Y., Takimoto, J., and Koyama, K., Effect of chain structure on the melt rheology of modified polypropylene. *J. Appl. Polym. Sci.*, 73, 1493, 1999.
52. Cheung, L.K., Park, C.B., and Behraves, A.H., Effect of branched structure on the cell morphology of extruded polypropylene foams, *SPE ANTEC*, 1941, 1996.
53. Lagendijk, R.P., Hogt, A.H., Buijtenhuijs, A., and Gotsis, A.D., Peroxydicarbonate modification of polypropylene and extensional flow properties, *Polymer*, 42, 10035, 2001.
54. Howells, E.R. and Benbow, J.J., Flow defects in polymer melts, *Trans. J. Plast. Inst.*, 30, 240, 1962.
55. Hanson, D.E., Shear modification of polythene, *Polym. Eng. Sci.*, 9, 405, 1969.
56. Fujiki, T., Concept of secondary heterogeneous structure of long-chain branched polyethylene, *J. Appl. Polym. Sci.*, 15, 47, 1971.
57. Rokudai, M., Influence of shearing history on the rheological properties and processability of branched polymers, part I, *J. Appl. Polym. Sci.*, 23, 463, 1979.
58. Rokudai, M., Mihara, S., and Fujiki, T., Influence of shearing history on the rheological properties and processability of branched polymers, part II, *J. Appl. Polym. Sci.*, 23, 3289, 1979.
59. Rokudai, M. and Fujiki, T., Influence of shearing history on the rheological properties and processability of branched polymers, part III, *J. Appl. Polym. Sci.*, 23, 3295, 1979.

60. Münstedt, H., The influence of various deformation histories on elongational properties of low density polyethylene, *Colloid Polym. Sci.*, 259, 966, 1981.
61. Stehling, F., Speed, C.S., and Westerman, L., Causes of haze of low-density polyethylene blown films, *Macromolecules*, 14, 698, 1981.
62. Maxwell, B. and Breckwoldt, A., Controlled shear modification of low-density polyethylene, *J. Rheol.*, 25, 55, 1981.
63. Maxwell, B., Dormier, E.J., Smith, F.P., and Tong, P.P., Processing properties of high- and low-density polyethylene and their blends, *Polym. Eng. Sci.*, 22, 280, 1982.
64. Ritzau, G., Shear modification of polyolefins and its integration in polymer processing, *Intern. Polym. Process.*, 1, 188, 1987.
65. Leblans, P.J.R. and Bastiaansen, C., Shear modification of low-density polyethylene: Its origin and its effect on the basic rheological functions of the melt, *Macromolecules*, 22, 3312, 1989.
66. Yamaguchi, M. and Gogos, C.G., Quantitative relation between shear history and rheological properties of LDPE, *Adv. Polym. Technol.*, 20, 261, 2001.
67. Yamaguchi, M., Todd, D.B., and Gogos, C.G., Effect of processing history on rheological properties and processability of LDPE, Proceedings of the Annual Meeting of the Society of Polymer Processing, PPS-18, Guimaraes, Portugal, June 2002.
68. Yamaguchi, M., Todd, D.B., and Gogos, C.G., Rheological properties of LDPE processed by conventional processing machines, *Adv. Polym. Technol.*, 22, 179, 2003.
69. White, J.L., Critique on flow patterns in polymer fluids at the entrance of a die and instabilities leading to extrudate distortion, *Appl. Polym. Symp.*, 20, 155, 1973; Yamaguchi, M., Flow instability in capillary extrusion of plasticized poly (vinyl chloride), *J. Appl. Polym. Sci.*, 82, 1277, 2001.
70. Gaskell, R.E., The calendering of plastic materials, *J. Appl. Mech.*, 17, 334, 1950.
71. Todd, D.B., Introduction to compounding, and APV systems, *Plastics Compounding, Equipment and Processing*, ed. D.B. Todd, Hanser, New York, 1998, [chaps. 1 and 6](#).
72. Sakai, T., Intermeshing twin-screw extruders, *Mixing and Compounding of Polymers*, ed. I. Manas-Zloczower and Z. Tadmor, Hanser, New York, 1994, chap. 21.
73. Andersen, P.G., Mixing practices in corotating twin-screw extruders, *Mixing and Compounding of Polymers*, ed. I. Manas-Zloczower and Z. Tadmor, Hanser, New York, 1994, chap. 20; Anderson, P.G., The Warner and Pfeleiderer twin-screw corotating extruder system, *Plastics Compounding, Equipment and Processing*, ed. D.B. Todd, Hanser, New York, 1998, [chap. 4](#).
74. Cheng, H. and Manas-Zloczower, I., Chaotic features of flow in polymer processing equipment, relevance to distributive mixing, *Intern. Polym. Process.*, 12, 83, 1997.
75. Shikata, T. and Pearson, D.S., Viscoelastic behavior of concentrated spherical suspension, *J. Rheol.*, 38, 601, 1994.
76. Mewis, J. and Metzner, A.B., The rheological properties of suspensions of fibres in Newtonian fluids subjected to extensional deformations, *J. Fluid Mech.*, 62, 249, 1974.
77. Laun, H.M., Orientation effects and rheology of short glass fiber-reinforced thermoplastics, *Colloid Polym. Sci.*, 262, 257, 1984.
78. Chan, Y., White, J.L., and Oyanagi, Y., A fundamental study of the rheological properties of glass-fiber-reinforced polyethylene and polystyrene melts, *J. Rheol.*, 22, 507, 1978.

79. Lin, L., Viscoelastic properties of particle-filled polymers in the molten state, Ph.D. thesis, Kyoto University, Kyoto, 1989.
80. Taylor, G.I., The formation of emulsions in definable fields of flow, *Proc. R. Soc. A*, 146, 501, 1934.
81. Palierne, J.F., Linear rheology of viscoelastic emulsions with interfacial tension, *Rheol. Acta*, 29, 204, 1990.
82. Doi, M. and Ohta, T., Dynamics and rheology of complex interfaces I, *J. Chem. Phys.*, 95, 1242, 1991.
83. Santamaria, A. and White, J.L., Rheological properties, shrinkage and melt spinning instability of blends of linear polyolefins with low density polyethylene, *J. Appl. Polym. Sci.*, 31, 209, 1986.
84. Micic, P., Bhattacharya, S.N., and Field, G., Rheological behavior of LLDPE/LDPE blends under elongational deformation, *Intern. Polym. Processing*, 12, 110, 1997; Transient elongational viscosity of LLDPE/LDPE blends and its relevance to bubble stability in the film blowing process, *Polym. Eng. Sci.*, 38, 1685, 1998.
85. Lee, S.T. and Baker, J.J., Foam comprising polyolefin blend and method for producing same, U.S. Patent 6,096,793, 1998.
86. O'Brain, J.C. and Ehrenfreund, H.A., Synthetic cork-like material and method of making same, U.S. Patent 4,091,136, 1976; Lee, S.T., Polyolefin/ionomer blend for improved properties in extruded foam products, U.S. Patent 6066393, 1998.
87. Lohse, D.J. and Graessley, W.W., Thermodynamics of polyolefin blends, *Polymer Blends*, ed. D.R. Paul and C.B. Bucknall, Wiley, New York, 1999, chap. 8.
88. Valenza, A., La Mantia, F.P., and Acierno, D., The rheological behavior of HDPE/LDPE blends. V. Isothermal elongation at constant stretching rate, *J. Rheol.*, 30, 1085, 1986; La Mantia, F.P., Valenza, A., and Acierno, D., Elongational behavior of low density/linear low density polyethylenes, *Polym. Eng. Sci.*, 28, 90, 1988.
89. Münstedt, H., Dependence of the elongational behavior of melts on molecular weight and molecular weight distribution, *J. Rheol.*, 24, 847, 1980.
90. Linster, J.J. and Meissner, J., Melt elongation and structure of linear polyethylene, *Polym. Bull.*, 16, 187, 1986.
91. Dumoulin, M.M., Utracki, L.A., and Lara, J., Rheological and mechanical behavior of the UHMWPE/MDPE mixtures, *Polym. Eng. Sci.*, 24, 117, 1984.
92. Yamaguchi, M. and Miyata, H., Strain hardening behavior in elongational viscosity for binary blends of linear polymer and crosslinked polymer, *Polym. J.*, 32, 164, 2000.
93. Yamaguchi, M., Anomalous strain hardening behavior in elongational viscosity for blends of linear polymer and crosslinked polymer, *SPE ANTEC*, 1149, 2001.
94. Winter, H.H. and Chambon, F., Analysis of linear viscoelasticity of a crosslinking polymer at the gel point, *J. Rheol.*, 30, 367, 1986.
95. Yamaguchi, M., Suzuki, K., and Maeda, S., Enhanced strain-hardening in elongational viscosity for HDPE/crosslinked HDPE blend: 1. Characteristics of crosslinked HDPE, *J. Appl. Polym. Sci.*, 86, 73, 2002.
96. Zülle, B., Linster, J.J., Meissner, J., and Hürliman, H.P., Deformation hardening and thinning in both elongational and shear of a low density polyethylene melt, *J. Rheol.*, 31, 583, 1987; Graham, R.S., McLeish, T.C.B., and Harlen, O.G., Using the pom-pom equations to analyze polymer melt in exponential shear, *J. Rheol.*, 45, 275, 2001.

97. Yamaguchi, M. and Suzuki, K., Rheological properties and foam processability for blends of linear and crosslinked polyethylenes, *J. Polym. Sci. Polym. Phys. Ed.*, 39, 2159, 2001.
98. Sebastian, D.H. and Dearborn, J.R., Elongation rheology of polyolefins and its relation to processability, *Polym. Eng. Sci.*, 23, 572, 1983; Fleissner, M., Elongational flow of HDPE samples and bubble instability in film blowing, *Intern. Polym. Proc.*, 2, 229, 1988; Shinohara, M., Uniaxial elongational viscosity of high molecular weight high density polyethylene melts, *J. Soc. Rheol. Jpn.*, 19, 118, 1991; Kanai, T., Dynamics, heat transfer, and structure development, *Film Processing*, ed. T. Kanai and G.A. Campbell, Hanser, New York, 1999, **chap. 3**.
99. Yamaguchi, M. and Suzuki, K., Enhanced strain-hardening in elongational viscosity for HDPE/crosslinked HDPE blend: 2. Processability of thermoforming, *J. Appl. Polym. Sci.*, 86, 79, 2002.
100. Yamaguchi, M., Foaming of novel linear polyethylene with enhanced melt elasticity, *Proceedings of the Annual Meeting of the Society of Polymer Processing, PPS-19*, Melbourne, Australia, July 2003.

3

Fundamentals of Bubble Nucleation and Growth in Polymers

N.S. Ramesh

CONTENTS

- 3.1 Introduction
- 3.2 Foaming Process
- 3.3 Bubble Nucleation Studies
- 3.4 Nucleation Models and Experiments
 - 3.4.1 Classical Nucleation Principles
- 3.5 Homogeneous Foam Nucleation
- 3.6 Heterogeneous Foam Nucleation
- 3.7 Shear Effects on Heterogeneous Nucleation
- 3.8 Microvoid Nucleation
 - 3.8.1 Nucleation Mechanism
 - 3.8.2 Nucleation Model
 - 3.8.3 Results and Discussion
- 3.9 Effect of Concentration of Particles on Nucleation
- 3.10 Effect of Rubber Particle Size on Nucleation
- 3.11 Nucleation in Polyurethane Foams
 - 3.11.1 Bubble Nucleation
 - 3.11.2 Bubble Growth Model for Polyurethane Foam
- 3.12 Foam Growth in Polymers
 - 3.12.1 Bubble Growth Models
 - 3.12.1.1 Single Bubble Growth Models (1917–1984)
 - 3.12.1.2 Cell Model (1984–1998)
- 3.13 Foam Extrusion Modeling
 - 3.13.1 Foam Growth Equations
 - 3.13.2 Boundary Conditions
 - 3.13.3 Comparison of Theory with Experiment
- 3.14 Conclusion
- Acknowledgment
- Nomenclature
- References

3.1 Introduction

Interest in cellular plastics is growing for a number of reasons. The principal reason has to do with the favorable economics of manufacturing innovative products at a lower weight. The banning of chlorofluorocarbons (CFCs) in the early 1980s, along with strong health, safety, and environmental considerations in the foam industry, have increased interest in developing better methods of controlling foaming operations. In order to control the foaming process effectively, two key events must be controlled: bubble nucleation and bubble growth during foam expansion. In this chapter, these two topics will be discussed from the basics of thermodynamics and other physical principles. The use of nucleating systems to produce light density foams also has a potential impact on the disposable household, electronics packaging, and recreational sports markets.

Various nucleation mechanisms, such as homogeneous, heterogeneous, mixed-mode, shear-induced, and void nucleation theories, will be discussed. Suitable data are presented to support theoretical results. Extrusion of foam involves dissolving the foaming agent in the polymer under high pressure and then lowering the pressure suddenly by exiting through a die at a foaming temperature. The sudden instability instantaneously nucleates a myriad of bubbles with a subsequent uniform distribution. After cell nucleation, they grow due to the diffusion of excess gas. The viscosity of the polymer, the gas concentration, the foaming temperature, and the amount of nucleating agent and its nature are some of the variables that control the foam growth process. Foam dynamics are very complicated. Useful models and experimental data are presented to explain the basics of foam growth mechanisms in polymers.

3.2 Foaming Process

A typical foaming process involves the following four steps:

1. Dissolution of foaming agent
2. Bubble nucleation
3. Bubble growth
4. Stabilization

This chapter focuses primarily on the second and third steps. Thermoplastic polymeric foams are made with nucleating agents to aid in cell formation. The use of nucleating systems to produce various density foams also has a potential impact on the packaging and nonpackaging markets. Packaging foams are used everyday for protecting furniture and other objects during transportation. Polyurethane foams are used in packaging, carpet backing, sports, leisure, automobiles, and home applications such as seat cushions, sound, and thermal insulation. Foams are used everywhere from household items to industrial cushions. Thermosetting foams such as polyurethane foams are made by generating bubbles within a liquid through a simple chemical reaction. Foam nucleation is different for different systems. Foaming mechanisms are quite complex, since it is difficult to monitor cell formation in polymers and liquids at its birth. The size of potential nuclei is very small, on the order of nanometers or angstroms in scale. Nucleation occurs in a fraction of a second, and therefore it is difficult for foam scientists to capture in real life. The following section describes bubble nucleation studies.

3.3 Bubble Nucleation Studies

The birth of tiny bubbles in a polymer system is called nucleation of bubbles and is part of the process used to make polymeric foams. If the bubbles are generated from a single homogeneous phase containing no impurity or dirt, then the process is called homogeneous nucleation. This process is rare, since most resins are made with additives for various reasons. If tiny particles are present in the liquid, and if they assist in the formation of cells, then the process is called heterogeneous nucleation, since the nucleation took place at a solid and liquid interface. [Table 3.1](#) shows various nucleation studies. Because the subject of bubble nucleation is so vast, it is impossible to give a detailed explanation of each category and only key points are mentioned to explain the basic principles. Refer to the provided references for further reading about other mechanisms.

It is interesting to note that the physics of various nucleation mechanisms depend on energy levels involved in the systems. In other words, the birth of bubbles in a liquid or solid requires an increase in the free energy of the system. That increase is used to create new surfaces through the formation of tiny bubbles. The birth of a gas bubble in a polymer through a reversible thermodynamic process has an excess free energy associated with it. Mathematically, that can be expressed as

$$\Delta G = -V_b \Delta G_v + A \sigma \quad (3.1)$$

TABLE 3.1

Nucleation Types and Mechanisms

Nucleation Type	Nucleation Mechanism	Influencing Factors	Nucleating Systems	Reference/Discussion
Homogeneous	Bubbles formed due to superheat and pressure reduction	Temperature and pressure	Boiling water and organic liquids	1–5 (3.4)
Heterogeneous	Bubbles formed with assistance from tiny particles	Geometry and nature of particle	Bubble nucleation using fillers such as talc in polymers	6 (3.5)
Mixed-mode	Supersaturation of gas in polymers containing solid particles	Gas concentration in polymer and its solubility limit	Polystyrene with zinc stearate, stearic acid, and carbon black	7 (combination of the above 2 modes)
Cavity	Poor wetting of gas/liquid acts as a potential nucleating site	Geometry of cavity and pressure drop in the system	Boiling of water and organic liquids in a rough-surfaced vessel having microcavities.	8
Shear induced	Shear force induces birth of cells	Shear rate in foam extrusion	Polymeric foam extrusion	9 (3.6)
Microvoid	Presence of microvoids due to rapid polymer cooling and interface cavitations in polymer blends	Cooling rate of polymer melt	Bubble nucleation in High Impact Polystyrene or its blends with polystyrene	10 (3.8, 3.9, and 3.9)
Devolatalization	Volatile diffusion of solvent within polymer melt	Vacuum level and diffusion rate	Devolatilization of styrene monomer from polystyrene	11
Chemical reaction	Liquid reaction and generation of gas assisted by mixing causes bubble formation	Temperature, reactant ratio and degree of mixing	Reaction of polyol and isocyanate to form polyurethane	12 (3.10)
Mechanical energy (mixing and ultrasonic)	Pressure change generated by ultrasonic wave propagation and mixing of chemicals in polyurethane making	Ultrasonic frequency, agitator speed, shear rate, temperature	LPPE/PE Wax blend and high speed mixing of polyol and isocyanate	13–14

where

V_b = Volume of the bubble nucleus

ΔG_v = Difference between the gas and polymer phases of the standard
Gibbs free energy per unit volume

σ = Surface tension of the liquid or polymer

A = Interfacial area

V = Volume of the bubble

subscript b = Bubble

Thus, lowering the surface tension by using surfactants will assist in the formation of bubbles. Nucleating agents such as talc, diatomaceous earth, and silica are more effective because they offer voids at the interface.

Before we go into details, it will be useful to review the history of nucleation of bubbles in liquids and polymers. Several investigations involving the theoretical and experimental analyses of bubble nucleation in fluids and polymers have been available in the literature since 1900. The historical development of important models and data is reported in [Table 3.2](#). These models are applied every day to predict the nucleation rate in liquids, solids, and molten polymeric systems. The references are given at the end of the chapter.

3.4 Nucleation Models and Experiments

3.4.1 Classical Nucleation Principles

Classical nucleation theory is based on the following three basic principles outlined by Kumar:²⁶

- The probability of nucleation is directly proportional to an exponential function, $\exp(-W^*/kT)$, where W^* is the minimum work required to make the system unstable and to generate a large number of bubbles in a continuous phase. Einstein first proposed this relationship in 1930.¹⁵
- Fluctuations that create a stable nucleus form and decay by the same path.
- In 1931, Onsagar developed an idea that applies macroscopic laws to microscopic entities such as bubble embryos containing clusters of gas molecules.¹⁷

Based on these principles, the steady and transient rates of nucleation are given as

TABLE 3.2**Historical Development of Bubble Nucleation Studies**

Author(s)/Reference(s)	Year	Type of Work for Nucleation Theory; Related Work
Einstein (15)	1910	Exponential function on fluctuation probability
Volmer and Weber (16)	1926	Kinetic approach to homogeneous nucleation
Onsager (17)	1931	Principles that allow the application of macroscopic laws to microscopic entities such as embryos
Becker and Doring (18)	1935	Kinetic approach to homogeneous nucleation
Turnbull and Fisher (19)	1949	Rate of nucleation in condensed systems
Reiss (20); Lothe and Pound (21)	1950; 1962	Statistical mechanical concepts
Gibbs (22)	1961	Phase changes to generate bubbles; Embryo formation due to concentration changes
Zettlemoyer (23)	1969	Nucleation studies
Blander et al. (24)	1971	Bubble nucleation in hydrocarbons and water
Blander and Katz (2)	1975	Homogeneous nucleation theory
Martini (25)	1981	Homogeneous nucleation model for microcellular foams in high-impact polystyrene
Colton and Suh (7)	1985	Mixed-mode nucleation for polystyrene-zinc stearate system
Kumar (26)	1988	Experiments show the gap between homogeneous theory and data of polystyrene-nitrogen system
Han and Han (11)	1988	Modified free energy approach to study bubble nucleation in polystyrene/toluene solutions
Ramesh et al. (10, 27)	1992, 1994	Microvoid nucleation in high impact polystyrene
Ruengphrathuengsuka (28)	1992	Nucleation model with hydrodynamic, heat and mass transfer effects
Lee (9)	1993	Shear-induced nucleation in LDPE/CFC-12
Park et al. (29)	1998	Thermal effects on polystyrene/carbon dioxide system
Ohshima (30)	2002	Experimental studies in bubble nucleation and growth rates in batch and continuous foaming

$$J_s = Z\beta^* N \exp\left(\frac{-\Delta G^*}{kT}\right) \quad (3.2)$$

$$J(t) = J_s \exp\left(-\frac{t}{\tau}\right) \quad (3.3)$$

where

J = Nucleation rate (nuclei/cm³-s)

s = Steady state

t = Transient state

Z = Zeldovich non-equilibrium factor ($\cong 10^{-2}$)

β^* = Rate at which gas molecules are added to the critical nucleus

N = Number of nucleation sites per unit volume

ΔG^* = Gibb's free energy of forming a critical nucleus

kT = Boltzman's constant times absolute temperature

τ = Induction period for establishing steady-state nucleation conditions

All of these variables change based on the type of nucleating systems and process conditions. They must be carefully evaluated on an individual basis to fit real-life applications.

3.5 Homogeneous Foam Nucleation

Homogeneous nucleation represents the formation of a second phase (e.g., a gas bubble) in the primary phase (e.g., molten polymer). Homogeneous nucleation occurs when a sufficient number of dissolved gas molecules form clusters for a long enough time to make a critical bubble radius to cross over the resistance path, as shown in Figure 3.1.

Figure 3.2A shows a single phase containing molten polymer saturated with gas at a certain pressure. Figure 3.2B shows the formation of a second gas phase when the pressure is reduced from P_o to P_s . Thermodynamic instability is the reason for nucleation of tiny bubbles. Formation of bubbles involves creation of new surfaces with certain volumes. Usually the embryos are spherical in size and therefore easier mathematical expressions can be derived based on thermodynamic principles.

For homogeneous nucleation, Equation 3.1 can be rewritten to express Gibbs free energy as ⁷

$$\Delta G = -\frac{4}{3}\pi r^3 \cdot \Delta P + 4\pi r^2 \sigma \quad (3.4)$$

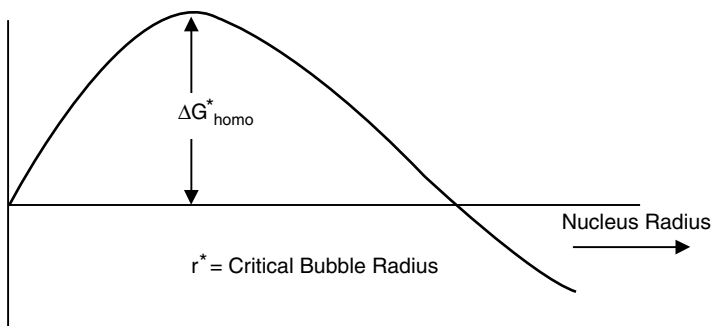


FIGURE 3.1
Homogeneous bubble nucleation.

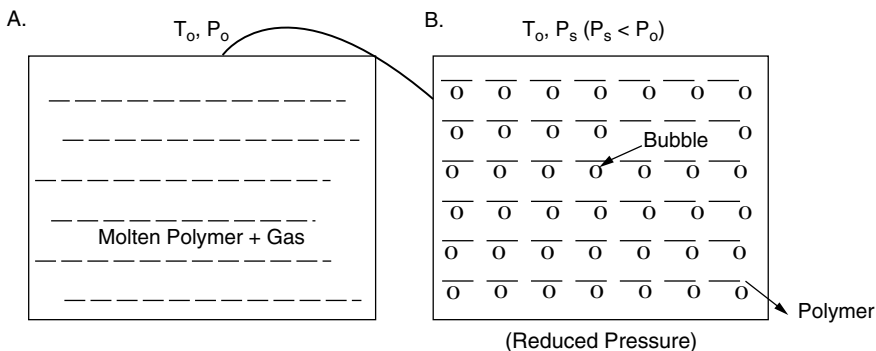


FIGURE 3.2
Typical nucleation process. T_o = temperature; P_o = initial pressure (higher than surrounding pressure); P_s = final pressure or surrounding atmosphere pressure.

where r is the bubble radius; ΔP is the pressure drop (e.g., die pressure drop in extrusion foaming); and σ is the surface tension of the polymer matrix. The maximum value of ΔG , denoted as ΔG^* , occurs at a critical size r^* , or when there is a critical number of gas molecules in the embryo, and represents the free energy of formation of the critical nucleus. If we differentiate the free energy term with respect to radius and set it equal to zero, the result becomes

$$\frac{\partial \Delta G}{\partial r} = 0 \quad (3.5)$$

which gives an expression for critical radius, r^* :

$$r^* = \frac{2\sigma}{\Delta P} \quad (3.6)$$

The spherical shape of the nucleus is assumed to represent minimum resistance for nucleation for a given volume. In general, such an assumption is reasonable. But in polymeric systems nonspherical geometries might be encountered. The activation free energy for homogeneous nucleation of a critical nucleus is derived as

$$\Delta G^*_{\text{homo}} = \frac{16\pi\sigma^3}{3\Delta P^2} \quad (3.7)$$

where σ is the surface tension of the polymer, and $\Delta P = P_{\text{sat}} - P_s$ is the supersaturated pressure. For a batch microcellular process system, P_{sat} is the gas saturation pressure and P_s is the surrounding pressure at which nucleation is to occur. Usually, P_s is equal to atmospheric pressure.

It should be cautioned that gaseous foaming agents often soften the polymer, and therefore surface tension of the polymer may decrease or increase based on the foaming agent dissolved in it. Hence, such effects must be taken into account when predicting real-life examples. Since the activation energy term has been calculated, the nucleation rate expression can be calculated based on the classical nucleation theory equation. According to Colton and Suh,⁷ the homogeneous nucleation in a gas–polymer system is given by

$$N_{\text{homo}} = f_o C_o \exp\left(\frac{-\Delta G^*_{\text{homo}}}{kT}\right) \quad (3.8)$$

where f_o is a frequency factor for the rate at which gas molecules join a critical nucleus; and C_o is the concentration of gas molecules. We can see from Equations 3.7 and 3.8 that when the degree of supersaturation is increased, both critical radius and critical free energy decrease. Physically this means that a greater amount of gas in the polymer makes it easier for bubbles to form. Similarly, the higher the pressure drop, the higher the nucleation rate of bubbles.

3.6 Heterogeneous Foam Nucleation

This is the most common type of nucleation found in polymer systems containing additives. The efficiency of producing bubbles depends on several factors, such as the type and shape of nucleating particles and interfacial tensions of solid and solid–gas interface. Blander and Katz proposed a simple heterogeneous nucleation model for liquids in 1975.² The primary benefit comes from the interface, which acts like a catalyst for nucleation. The presence of tiny particles and cavities reduces the activation energy required to

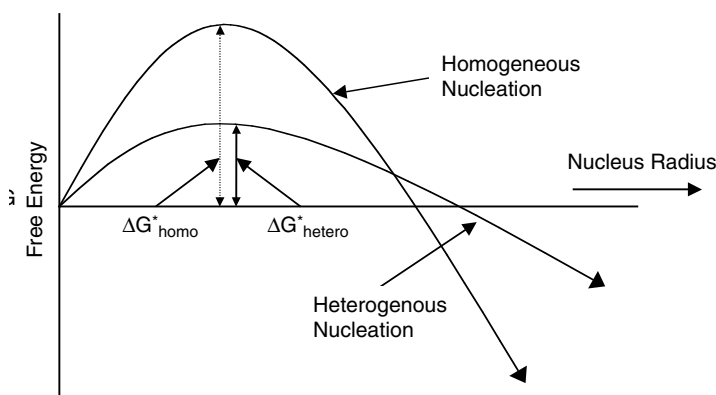


FIGURE 3.3

Heterogenous bubble nucleation. $\Delta G^*_{\text{hetero}} < \Delta G^*_{\text{homo}}$.

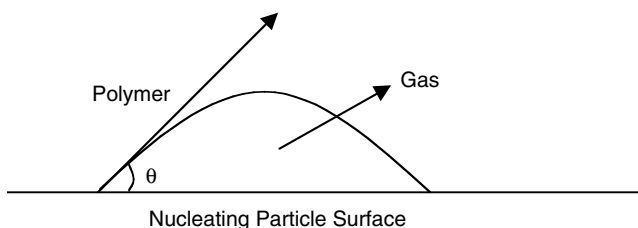


FIGURE 3.4

Schematic of nucleating particle interaction with gas and polymer.

achieve a stable nucleus. Figure 3.3 shows the reduction of Gibbs free energy associated with the heterogeneous nucleation process.

The thermodynamics of heterogeneous nucleation and its mathematical analysis are given in Uhlmann and Chalmers.⁴ The heterogeneity factor can be used to correct the activation energy term derived for homogenous nucleation, as shown in the following:

$$\Delta G^*_{\text{hetero}} = \Delta G^*_{\text{homo}} f(\theta) \quad (3.9)$$

For the configuration shown in Figure 3.4, Uhlman and Chalmers derived an expression for $f(\theta)$ as

$$f(\theta) = \frac{(2 + \cos \theta)(1 - \cos \theta)^2}{4} \quad (3.10)$$

$$\Delta G^*_{\text{hetero}} = \frac{16\pi\sigma^3}{3\Delta P^2} f(\theta) \quad (3.11)$$

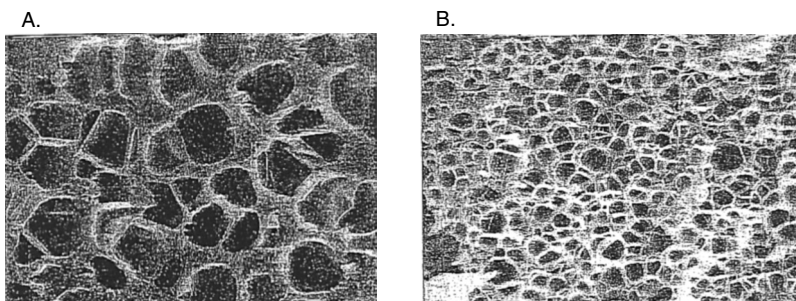


FIGURE 3.5

Heterogeneous nucleation assisted by rubber particles. **(A)** Polystyrene with no rubber particles. **(B)** Polystyrene with rubber particles. (Reproduced with permission from Ramesh et al., *Polym. Eng. Sci.*, 34, 1685–1706, 1994.)

where θ is the wetting angle, $f(\theta)$ is the heterogeneity factor, and σ represents the interfacial tensions of a polymer–gas bubble.

According to Colton and Suh, for a typical wetting angle of 20° , $f(\theta)$ is on the order of 10^{-3} , which means it is easy to produce several orders of magnitude of more bubbles using nucleating sites.⁷ This explains why polystyrene produces more bubbles when rubber particles are added, as shown in Figure 3.5A and Figure 3.5B. These examples show nucleation of bubbles when the polymer is not sheared. The next section shows the effect of shear force on the polymer and how it influences the nucleation process. There are several useful chemical nucleating agents available commercially. They are as follows:

- Citric acid/sodium bicarbonate (endothermic)
- Azodicarbonate (exothermic)
- p-Toluene sulfonyl hydrazide (exothermic)
- Sodium borohydride (endothermic)

These agents are often added to nucleate cells.

3.7 Shear Effects on Heterogeneous Nucleation

Often, nucleation of cells happens in a shear field. In a typical foam extrusion, the melt is sheared before exiting the die and shear rate plays an important role. Lee studied the effect of shear rate on foam nucleation for an LDPE/CFC-12 system.⁹ Talc was used to serve as a nucleating site. The key result of Lee's experiments is that the nucleation rate increases with an increase in shear rate. To show the effect of shear rate, the capillary number was expressed as

$$Ca = \frac{r^* \eta \dot{\gamma}}{4\sigma} \quad (3.12)$$

where r^* = critical bubble radius, η = polymer melt viscosity, $\dot{\gamma}$ = average shear rate, and σ = interfacial tension between polymer bubbles.

From Equation 3.12 it is clear that when the shear rate is increased, the capillary number also increases. It was found that the rate of nucleation of bubbles grew significantly with an increase in capillary number.⁹ For example, for an LDPE/CFC-12 system at 0.039% talc level concentration, the nucleation rate rose almost 300% when the capillary number increased from 1 to 2. Possible reasons for increased nucleation can be (a) the breaking up of agglomerated clumps or (b) the faster release of stable nuclei from cavities. The basic model describes shear force as a way to reduce the activation energy barrier so that the bubbles can form more easily through a shorter traveling path during the nucleation process. A thorough discussion can be seen in the literature.⁹

3.8 Microvoid Nucleation

The classical nucleation models in the literature predict a negligible nucleation rate up to a gas saturation pressure of about 34.475 MPa. Kumar has concluded that the cell nucleation phenomenon in thermoplastics is not well described by the classical homogeneous nucleation theory.²⁶ In this section, a new model for nucleation will be presented, based on the heterogeneity of rubber particles introduced into the polymer where stress-induced microvoids on the rubber provide the nucleation sites. The undiluted HPS contains 30% by volume of rubber particles with an average rubber domain size of 2 μm . This polymer was added to polystyrene to a final concentration of 0.3% of rubber gel by volume. At this concentration, the blended polymer has approximately 10^9 rubber particles per cm^3 of the polymer. The polystyrene diluted with HIPS or compounded HIPS/PS blend at 1% HIPS concentration can also be called nucleated PS or 1% HIPS for convenience.

3.8.1 Nucleation Mechanism

Nucleated polystyrene (PS) contains polybutadiene (PB) rubber particles dispersed in the continuous PS matrix. Composite rubber particles consist of a collection of occluded stiff PS inclusions in a topologically continuous minority phase of compliant PB, generally produced by grafted copolymerization as shown in Figure 3.6.

These rubber particles are assumed to have a perfect bond between themselves and the surrounding PS matrix transmitting all tractions. The polymer is in the form of cylindrical pellets. The diameter and the height of the pellets

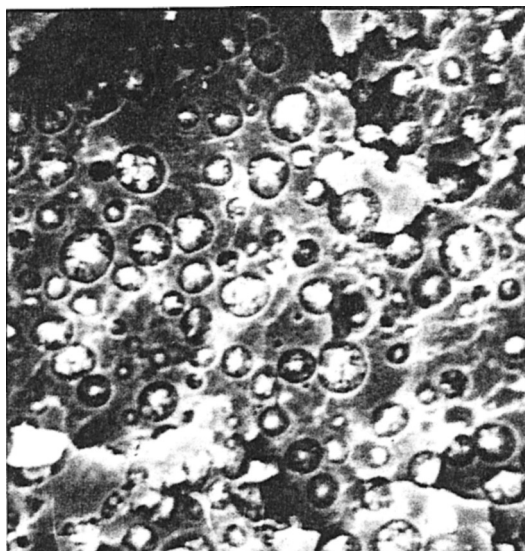


FIGURE 3.6

Scanning electron micrograph of plasma etched surface of HIPS polymer. (Original magnification $\times 3000$.) (Reproduced with permission from Ramesh et al., *Polym. Eng. Sci.*, 34, 1685–1706, 1994.)

are 2.5 mm and 3 mm approximately. The pellets are extruded at high temperature (438 K) and then cooled to room temperature. Since the glass transition temperatures of PS and PB rubber are 373 K and 181 K, respectively, the PS phase first “freezes” at approximately 373 K. The PB rubber phase continues to shrink at a faster rate until it reaches room temperature, 298 K. It is well known that cavitation may occur when cooling this polymer, due to a threefold difference in the coefficients of thermal expansion of the rubber particle and the matrix resulting in a triaxial tension.

When the polymer is cooled from 373 K to 298 K, PB has a higher coefficient of thermal expansion than PS. The cooling of a nucleated PS polymer from the melt, which can be considered stress free, produces stresses in the rubber particle and in the surrounding matrix. The magnitude of the thermal stresses can be calculated for an isolated particle from the theory of elasticity as described in Timoshenko and Goodier.³¹ Within the particle, thermal shrinkage produces a triaxial tensile stress given by this formula:^{32,33}

$$\Sigma_{rr} = \Sigma_{\theta\theta} = \Sigma_{\phi\phi} = \left(\frac{4(\beta_{pb} - \beta_{ps})(1 + \nu_{pb})G_{pb}G_{ps}\Delta T}{6(1 - 2\nu_{pb})G_{ps} + 3(1 + \nu_{pb})G_{pb}} \right) \quad (3.13)$$

And within the matrix:^{10,15}

$$\Sigma_{rr} = \left(\frac{R_p}{r} \right)^3 \left(\frac{4(\beta_{pb} - \beta_{ps})(1 + \nu_{pb})G_{pb}G_{ps}\Delta T}{6(1 - 2\nu_{pb})G_{ps} + 3(1 + \nu_{pb})G_{pb}} \right) \quad (3.14)$$

where

β = Thermal expansion coefficient

ν = Poisson ratio

ΔT = Temperature drop

G = Modulus

R_p = Particle radius

r = Radial distance from center of inclusion

subscript ps = PS phase

subscript pb = PB phase

The physical properties needed for Equations 3.13 and 3.14 are given in the literature.^{2,7} The calculated value of thermal shrinkage stress within the particle is 2.63×10^6 Pa. Schmitt suggested that these thermally induced stresses built up inside the rubber particle might cause the rubber to cavitate and microvoids to nucleate inside the rubber particle near the PS inclusions.³⁴ This hypothesis was confirmed later by Keskkula et al.³⁵ by studying the internal morphology of rubber particles using a transmission electron microscope (TEM). Figure 3.7 shows the presence of microvoids in the rubber membranes inside the rubber particle.¹⁰

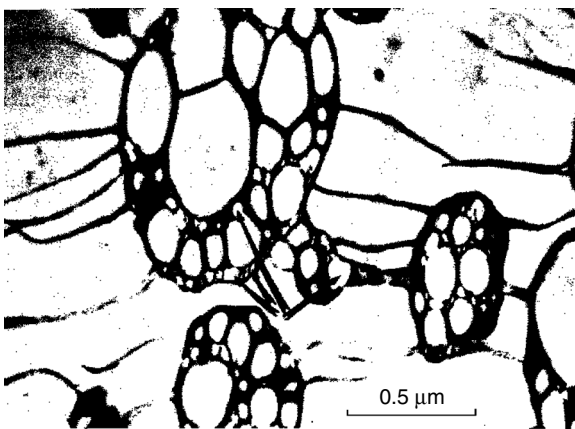


FIGURE 3.7

Transmission electron micrograph (TEM) of internal structure of HIPS rubber particles showing the presence of microvoids in the rubber membranes inside the particle. (Reproduced with permission from Ramesh et al., *Polym. Eng. Sci.*, 34, 1685–1706, 1994.)

It is important to note that the radial thermal stress within the matrix (Equation 3.14) depends strongly on the particle radius and thus on the particle size. This means that large particles should induce very high stresses and that they tend to nucleate microvoids with large radii. Thus, microvoid distribution is proposed to be analogous to rubber particle size distribution. Also, the microvoids are formed without penetration into the PS phase of the matrix. Similar results showing microdamage within rubber membranes was also reported by Donald and Kramer.³⁶ Recently, Adams et al. reported similar results for the influence of thermal and pressure history on microvoid formation in polycarbonate.³⁷ They concluded that samples that cooled quickly under low pressure resulted in more microscopic flaws and voids in homopolymers. Their analysis indicates that the polymer is self-constrained due to the temperature effects on modules and the thermal coefficient of expansion. Hence, it is clear that a population of microvoids exists inside the nucleated PS composite material and that the preexisting microvoids are present both in the matrix and inside the rubber particles. To obtain cell density, the population of viable microvoids with a sufficiently large radius to survive and overcome surface and elastic energy forces has been modeled. Here the assumption is that the voids in the rubber will dominate during the process in a heterogeneous system. The features of the mathematical model based on this hypothesis are presented in the following section.

3.8.2 Nucleation Model

The schematic of the nucleation model is shown in Figure 3.8. This diagram shows the presence of a single microvoid surrounded by a finite amount of polymer. The pressure inside the microvoid tends to grow into a cell while the opposing surface and elastic forces tend to collapse the microvoid. The scanning electron microscope (SEM) picture of microcellular foams obtained by foaming the nucleated PS at 388 K is also shown in Figure 3.9. These micrographs (Figures 3.6 and 3.9) indicate that both particles and cells vary in their diameters significantly over the cross section of the micrograph. The SEM micrographs were digitized and the resulting rubber particle size and cell size distributions were plotted against the cumulative number of particles, as shown in Figure 3.10 and Figure 3.11.

Two observations can be made from the data. First, the linearity in the data indicates that both rubber particles and cells exhibit log-normal distributions. Second, the nature of the rubber particles' distribution seems to influence the cell size distribution because the slopes of the distribution are nearly the same. This is not surprising because Equation 3.14 shows the role of particle size on the thermally induced stresses in the matrix, as already discussed. Since particle size distribution is one of the variables, in addition to the temperature difference and thermal expansion coefficients, that distribution controls the thermal stresses in the matrix, and it influences the size distribution of microvoids formed during the cooling of the polymer from its

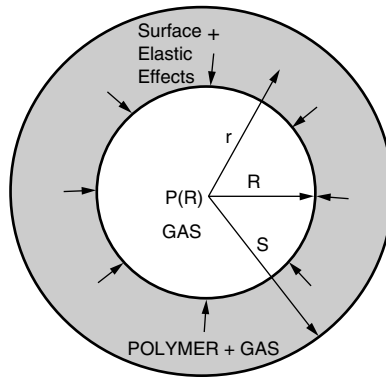
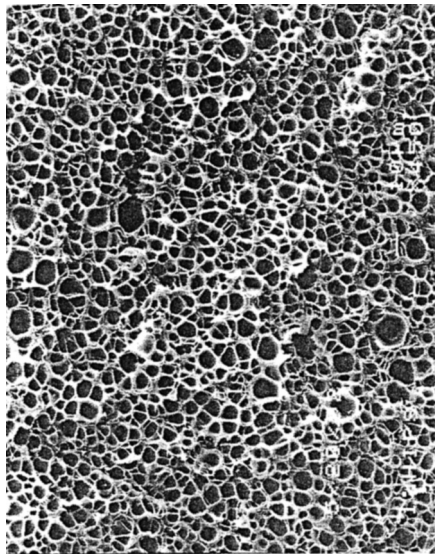


FIGURE 3.8

Schematic diagram of a single microvoid surrounded by a finite amount of polymer. (Reproduced with permission from Ramesh et al., *Polym. Eng. Sci.*, 34, 1685–1706, 1994.)



— 10 μm

Saturation Pressure = 13.8 MPa (2000 psig)

Foaming Temperature = 388 K

Gas: Nitrogen

Heating Medium: Ethylene Glycol Bath

FIGURE 3.9

Microcellular foams produced from nucleated PS. (Reproduced with permission from Ramesh et al., *Polym. Eng. Sci.*, 34, 1685–1706, 1994.)

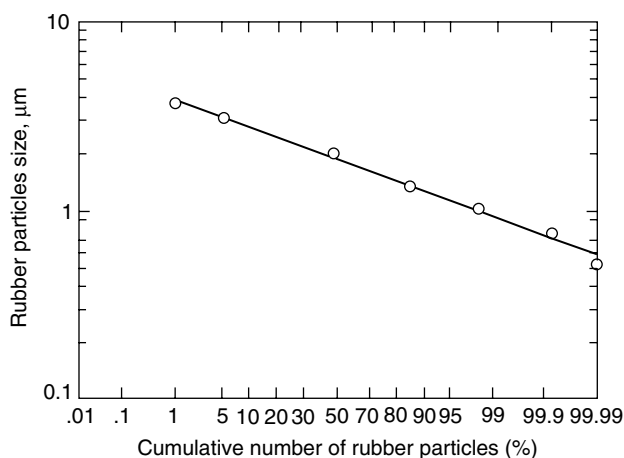


FIGURE 3.10

Particle size in the nucleated PS polymer as determined by the plasma etching process. (Reproduced with permission from Ramesh et al., *Polym. Eng. Sci.*, 34, 1685–1706, 1994.)

molten state to room temperature. Based on the aforementioned reasons, it was concluded that the log-normal distribution is appropriate to model the distribution of microvoids and that the microvoids in this heterogeneous process depend on the rubber particle size distribution. Though each particle may contain multiple voids, only the largest void among them will survive owing to its high radius, and all other smaller microvoids both inside the

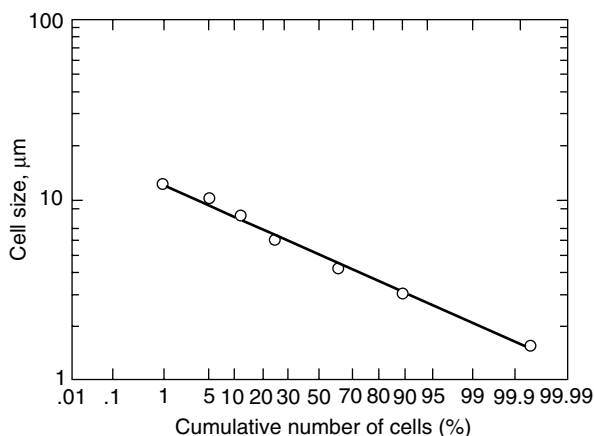


FIGURE 3.11

The cell size distribution after the microcellular foaming process. (Reproduced with permission from Ramesh et al., *Polym. Eng. Sci.*, 34, 1685–1706, 1994.)

particles and in the matrix will disappear. Therefore, it is reasonable to assume that each particle potentially contributes a single microvoid, whose radius is influenced by its own particle size. Mass transfer during the nucleation process was neglected because the time scale for nucleation is negligible in comparison with that of the foam growth process (0.0004 s vs. 120 s). In addition, the following assumptions were made to derive the nucleation model:

- The nucleation process is assumed to be governed by the mechanics and thermodynamics of the system.
- A Neo-Hookean model is considered here for modeling the elastic energy that opposes the growth of a preexisting microvoid. This is widely used for rubberlike solids since the foaming temperature is close to the glass transition temperature of the experimental observations. These models have been shown to be very useful in predicting the nucleation of bubbles in natural and PB rubber.¹⁰
- Spherical symmetry is assumed for simplicity.
- The loss of gas to the surrounding vapor during nucleation is neglected because it is limited to the skin of the polymer pellet.²⁶
- Solubility of the gas to the polymer is a function of both saturation pressure and temperature. The solubility of nitrogen in PS and PB is nearly the same.³⁸

With these assumptions, Ramesh et al.¹⁰ derived the following expression for the nucleation rate:

$$N = \frac{N_0}{2} \operatorname{erfc} \frac{\log(R / \xi)}{\sigma \sqrt{2}} \quad (3.15)$$

where N_0 = total number of potential microvoids (which can be estimated by the number of particles present in the continuous phase); R = instantaneous bubble radius; ξ = mean of the distribution of the void size; and σ = standard deviation of the distribution. More details are given elsewhere.²⁷

3.8.3 Results and Discussion

Ramesh²⁷ investigated the effect of gas saturation pressure on cell size for the HIPS/PS blend (1% HIPS), which has approximately 10^9 rubber particles per cm^3 . The average cell size obtained from this experiment for PS and 1% HIPS (containing 2 μm size particles) has been plotted (Figure 3.12) as a function of saturation pressure. The average cell size decreases with an increase in the saturation pressure of PS. On the other hand, it remains nearly the same for 1% HIPS.

It is interesting to note that particle size distribution plays a role in dictating the slope of cell size distribution data. It appears that there is a strong

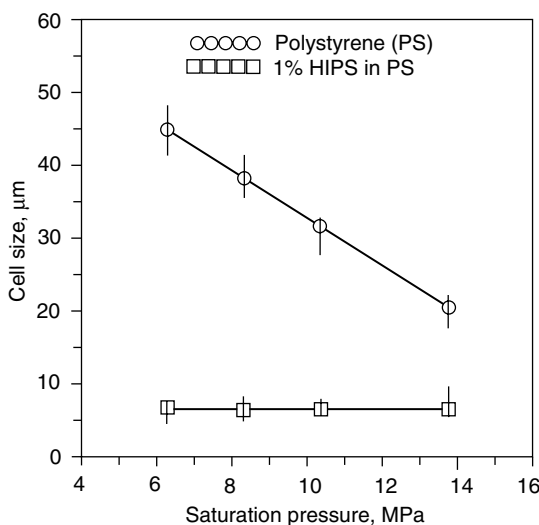


FIGURE 3.12

Cell size as a function of saturated pressure for polystyrene and 1% HIPS foamed at 388 K. (Reproduced with permission from Ramesh et al., *Polym. Eng. Sci.*, 34, 1685–1706, 1994.)

correlation between particle size and cell size prior to nucleation. This clearly indicates the ability of the rubber particles to control cell size during nucleation. In general, there is good agreement between theoretical predictions and the experimental data, as can be seen from Figure 3.13.

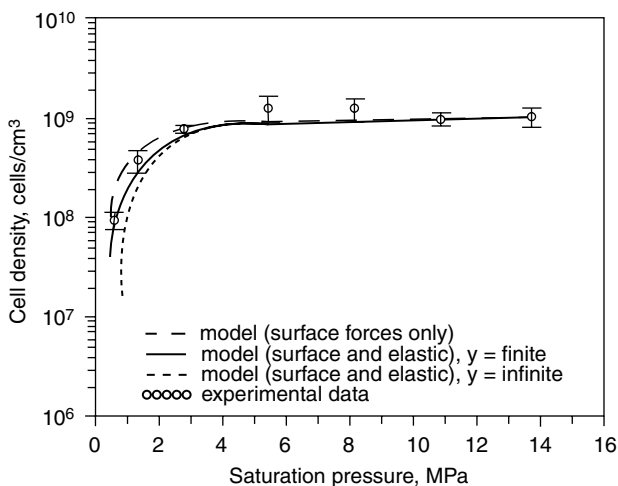


FIGURE 3.13

Comparison of theory with experiment for the influence of saturation pressure on cell density for 1% HIPS. (Reproduced with permission from Ramesh et al., *Polym. Eng. Sci.*, 34, 1685–1706, 1994.)

3.9 Effect of Concentration of Particles on Nucleation

To investigate the effect of particle concentration on cell density, HIPS/PS blends, 0.1% HIPS, 1% HIPS, and 10% HIPS were saturated with nitrogen at 13.78 MPa (2000 psi) and allowed to foam in an ethylene glycol bath at 388 K for sufficient time (5 min) to develop a limiting bubble size. The results were plotted on a log-log scale. The plot revealed that the foamability of the polymer was directly related to the number of rubber particles present in the sample, as illustrated in Figure 3.14. The theory (solid line) predicts a one-to-one increase in the number of cells with increases in concentration for the same level of supersaturation of the polymer. Comparison with experimental data shows that the predictions are reasonable, although some deviations are observed.

3.10 Effect of Rubber Particle Size on Nucleation

To study the effect of rubber particle size on cell density, a series of nucleated PS samples containing rubber with average particle size of 0.3, 0.5, 2.1, 4.2,

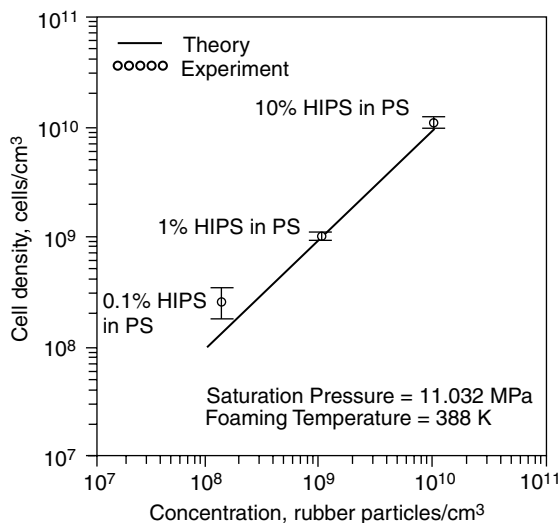


FIGURE 3.14

Comparison of theory with experiment for the influence of particle concentration on cell density for 1% HIPS foamed at 388 K. (Reproduced with permission from Ramesh et al., *Polym. Eng. Sci.*, 34, 1685–1706, 1994.)

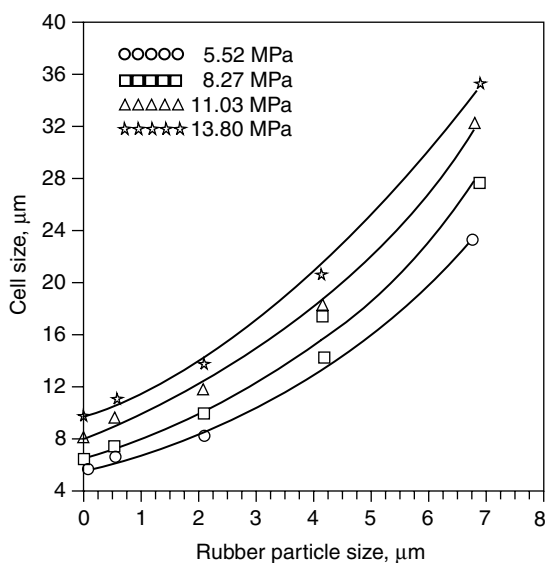


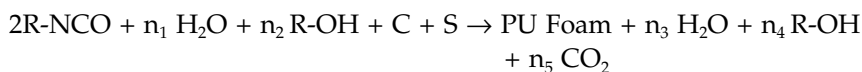
FIGURE 3.15

Influence of rubber particle size on cell size of the nucleated PS cells foamed at 388 K for various nitrogen saturation pressures. (Reproduced with permission from Ramesh et al., *Polym. Eng. Sci.*, 34, 1685–1706, 1994.)

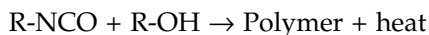
and 6.8 μm were selected. Figure 3.15 shows the trend. The cell size appears to increase with the rubber particle size in a batch foaming process. Its impact on the extrusion process still needs to be explored.

3.11 Nucleation in Polyurethane Foams

Polyurethane (PU) foam is well known for its wide range of commercial applications. PU foams are used in packaging, nonpackaging, carpet backing, sports and leisure applications, seat cushions, and insulation. PU foam is a thermosetting foam, whereas PS and polyethylene foams are thermoplastic foams that are easy to recycle. The typical reaction steps are shown below:



where n_1 to n_5 are the number of moles of reactant and product species. R-NCO, R-OH, C, and S are polyisocyanate, polyol, catalyst, and surfactants respectively, and



Nucleation of bubbles in PU systems can happen due to the following:

- Evolution of gases like carbon dioxide due to chemical reaction
- Additional gases dissolved in polyol component, including air
- Evaporation of water vapor to participate in the expansion of the foam

PU is formed because of a reaction between isocyanate and polyol. PU foam is produced when the PU polymer is expanded by the formation of carbon dioxide that is produced when reaction isocyanate and water react. The reaction is exothermic in nature, and the heat generated is used to change water into steam to help expand the foam.

Both carbon dioxide and steam act as blowing agents. While making very low density foams, below 2 lb per cubic ft (or 32 kg/m³), the water vapor is the dominant blowing agent.

Kanner and Decker demonstrated the impossibility of self-nucleating carbon dioxide from a mixture of polyol and toluene diisocyanate.^{39,40} They also showed that bubble formation was aided by physically mixing air into the above mixture with an appropriate amount of surfactant for proper stabilization. The addition of air bubbles having diameters in the range of 10–100 μm was found effective in forming cells. Elevated temperature due to pre-heating raw materials under pressure and the heat of reaction releases dissolved air. Thus, the nucleation of cells in PUs can be attributed, in part, to chemical mixing and agitation with the accompanying dissolution of inert gases.

Several other gases were considered besides air. These include carbon dioxide, hydrocarbons, and halogenated blowing agents. While carbon dioxide can be dissolved in a polyol side of a PU formulation, it is detrimental to foam formation as it works to neutralize the amine catalysts, preventing the reaction from occurring. Due to the detrimental effects of halogenated blowing agents on the earth's ozone layer, they are not used in the formation of PU foams. In some cases, hydrocarbons are used to assist in foam nucleation and growth. The largest commercial occurrence of hydrocarbons is the use of cyclopentane for appliance insulation foams in Europe.

As foam reaction is initiated, the viscosity of the polymer increases significantly due to urethane linkages between polyols and polyisocyanates, and this stabilizes cell formation and growth. The key difference between other thermoplastic systems and PU foam nucleation is a chemical reaction followed by viscosity increase for foam stabilization. The thermosetting nature of PU foams offer superior thermal stability over polyolefin foams.

3.11.1 Bubble Nucleation

Equation 3.16 applies to bubble nucleation.⁴¹ In order for the bubbles to nucleate, the Gibbs free energy of the system must exceed the mechanical work needed. Mathematically, this can be written as:

$$\Delta G > \frac{3 \cdot \sigma}{\rho \cdot r} \quad (3.16)$$

where σ is the surface tension, r is the nucleation bubble radius, and ρ is the gas density.

Surface tension is regulated with the use of silicone surfactants. The type of surfactant used varies with the formulation application. This area of formulation art is outside the scope of this chapter. However, silicone surfactants are almost always used to regulate cell count or cell size. In the cases of low density foams, below 30 kg/m³, surfactants play key roles in producing open cells to maintain dimensional stability upon cooling to ambient temperature.

3.11.2 Bubble Growth Model for Polyurethane Foam

Ramesh and Malwitz⁴² proposed a material and energy balance model based on the work by Wang, Frisch, and Malwitz.⁴³ It predicts accurately the foam expansion characteristics. The polyurethane foam process includes isocyanate, polyol, water, catalysts, and surfactants as reactants. The products are PU foam, unreacted reactants, carbon dioxide, and steam. The foam expands due to gas evolution and heat of reaction between isocyanate, polyol, and water. The heat vaporizes water and does the expansion work. The heat of reaction between isocyanate and polyol can be described as:

$$\text{Heat of reaction (Kcal/mol)} = \frac{312.6}{T} - 20.47 \quad (3.17)$$

The heat of reaction between isocyanate and water can be described as:

$$\text{Heat of reaction (Kcal/mol)} = \frac{543.9}{T} - 20.65 \quad (3.18)$$

where T is the temperature in Kelvin. The following equation applies to bubble growth:

$$\Delta P > \frac{2 \cdot \sigma}{r} \quad (3.19)$$

TABLE 3.3

Model Prediction vs. Experiment for Different Formulations

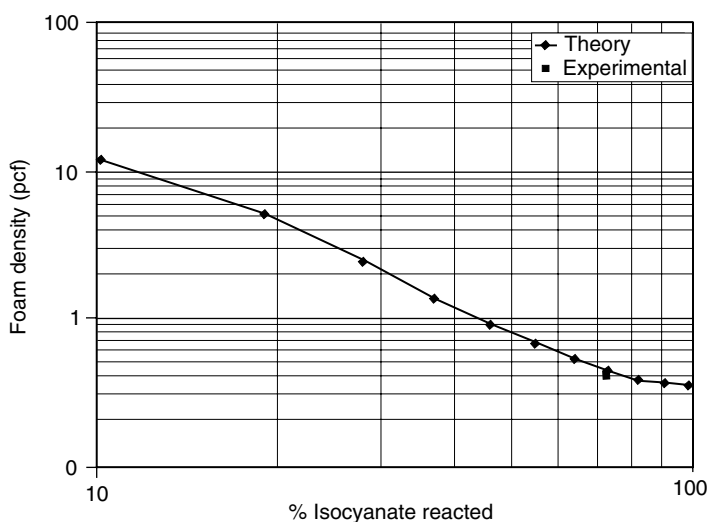
Foam	Model Prediction Density (pcf)	Experimental Density (pcf)
PU Formulation 1	2.037	2.0
PU Formulation 2	0.754	0.75
PU Formulation 3	0.43	0.4

where ΔP is the pressure from blowing agent generated by CO_2 and steam due to exothermic reaction.

Table 3.3 shows the theoretical prediction against experimental data. Based on the data, it seems possible to predict the PU foam expansion and density from simply knowing the chemical formulations, using the mathematical model.⁴²

Foam expansion with respect to percentage of isocyanate reacted for one formulation is shown in Figure 3.16.

It is important to recognize the difference between thermoplastic and thermosetting foams. Table 3.4 shows the differences in bubble nucleation, growth, and properties between thermoplastic and thermosetting foams. The differences in the table show that nucleation and bubble growth processes vary significantly.

**FIGURE 3.16**

Predictions of foam density—theoretical vs. experimental.

TABLE 3.4

Differences between Thermoplastic and Thermosetting Foams

Bubble Nucleation, Growth, and Properties	Thermoplastic Foam	Thermosetting Foam
System	Non-crosslinked PS and polyolefin foam	Polyurethane foam
Easy to recycle	Yes; melting and repelletizing is often used	More difficult; regrind, chemical hydrolysis, glycolysis, and pyrolysis options are available
Bubble nucleation reason	Thermodynamic instability of molten polymer-gas system	Thermodynamic instability with gas evolution due to chemical reaction
Bubble growth	Inertial and diffusion-controlled	Diffusion-controlled
Cell structure	Mostly closed cells are desired	Closed and open cells; open-cell foam is desired to have a balance of properties; cell opening and gelling due to crosslinking reaction
Gel point	No	Yes
Cell-opening process	No	Yes; influenced by kinetics of bubble growth, catalysts, surfactants, and surrounding conditions
Morphology	Amorphous and semi-crystalline	Urea hard domains distributed in polyether soft phase

3.12 Foam Growth in Polymers

After cell nucleation, the bubbles grow due to the diffusion of excess gas in the polymer. The viscosity of the polymer, the gas concentration, the foaming temperature, and the amount of nucleating agent and its nature are some of the variables that control the foam growth process. The expansion dynamic of polymeric foam is very complicated. It has been increasingly scrutinized by investigators for the past 90 years. Key milestones in the development of foam growth models are summarized in the following.

3.12.1 Bubble Growth Models

Several investigations addressing the theoretical and experimental analysis of bubble growth and collapse in fluids and polymers have been available in the literature since 1917. The historical development of important models is listed in [Table 3.5](#). Most of the models can be classified into three groups:

TABLE 3.5

History of Important Models

Author	Year	Momentum Transfer	Heat Transfer	Rheological Model	Bubble Count Study	Ref. No.
Rayleigh	1917	Inertial	Isothermal	—	Single	44
Epstein, Plesset	1950	—	Isothermal	—	Single	45
Scriven	1959	Yes	Nonisothermal	Newtonian	Single	46
Street, Fricke, Reiss	1971	Viscous	Conduction	Power Law	Single	47
Han, Yoo	1981	Yes	Isothermal	Viscoelastic	Single	48
Upadhyay	1985	Viscoelastic	Nonisothermal	Viscoelastic	Single	49
Amon, Denson	1984, 1986	Viscous	Conduction	Newtonian	Swarm	50, 51
Arefmanesh, Advani	1991	Viscoelastic	Conduction	Viscoelastic (Maxwell)	Swarm	52
Ramesh	1991, 1992	Viscoelastic	Conduction	Maxwell, Power Law	Swarm	27, 53
Lee, Ramesh, Campbell	1993	Viscoelastic	Conduction	Convected Maxwell	Swarm	54
Ramesh, Malwitz	1998	Viscoelastic	Nonisothermal	Maxwell	Swarm	55
Shafi, Joshi, Flumerfelt	1997	Viscous	—	Newtonian	Single	56
Ohshima	2000	Viscous	—	Newtonian	Swarm	57

(1) the single bubble growth model; (2) the cell model (a swarm of bubbles growing without interaction); and (3) the combined nucleation and bubble growth model.

3.12.1.1 Single Bubble Growth Models (1917–1984)

Between 1917 and 1984,^{44–51} the published models focused on the growth or collapse of a single bubble surrounded by an infinite sea of fluid with an infinite amount of gas available for growth. Although these models gave several insights into bubble growth phenomena, their practical application in industry was severely limited because the foaming process involves the growth of numerous bubbles expanding in close proximity to one another with a limited supply of gas. This led to the development of a new model called the “cell model,” which will be discussed in the next section.

3.12.1.2 Cell Model (1984–1998)

The cell model has been widely used to describe devolatilization, batch microcellular, and foam extrusion processes. Gross motion, no bubble motion, and motion without shear have different implications in the cell model.

The concept of a cell model was first introduced by Amon and Denson in 1984.⁵⁰ Their study involved the growth of a group of gas bubbles separated by a thin film of polymer and dissolved gas during the injection molding process. The foam was divided into spherical microscopic unit cells of equal and constant mass, each consisting of a liquid envelope surrounding a single bubble; the gas available for growth was thus limited. Because it relied on a more realistic assumption of gas availability, the cell model yielded a final radius while single bubble growth models showed the growth of bubble radius was infinite. This fundamental improvement caused more interest in this area of research, and several studies have emerged since then. However, the Newtonian viscosity equation was used to describe the rheology of the polymer due to the complexity of the problem. Later it was modified to account for the non-Newtonian viscoelastic effects to make it more suitable for polymeric systems.⁵¹

Cell models^{27,50–55,59} can be broadly classified into two groups: (a) the cell model for a closed system with no blowing agent and gas loss effects; and (b) the modified cell model for foam extrusion with a blowing agent and gas loss effects. These groups are described in the next section. Recently, Shafi et al. have worked on combining nucleation and foam growth processes.⁵⁶ They considered bubble size distributions in freely expanded polymer foams. The final bubble size distribution depended upon nucleation rate and bubble growth dynamics. However, their work focused only on the initial stages of bubble growth and the model does not predict an equilibrium radius, which is important when considering real industrial processes.

3.12.1.2.1 Viscoelastic Cell Model for Injection Molding Process (VCM-IM)

The validity of the cell model was initially tested in experimental work by Amon and Denson,⁵⁰ Arefmanesh and Advani,⁵² Ramesh and Malwitz,⁵⁸ and Ramesh et al.⁵⁴ The first two research groups concentrated on experiments to verify prediction of the cell model during the injection molding process, where the bubble growth occurs in a closed system. Amon and Denson⁵⁰ used low-density polyethylene with a chemical blowing agent whereas Arefmanesh and Advani⁵² used polycarbonate with a chemical blowing agent. The assumption of no gas loss from the mold was adequate because the foam growth occurred in a closed mold. These studies showed a qualitative agreement between experimental data and theoretical results and have led to a better understanding of the processing of polymeric foam materials.

Ramesh et al. tested the validity of the cell model by conducting a cell growth experiment during the microcellular foaming process.^{27,53} PS was used with physical blowing agents such as nitrogen and carbon dioxide. In

all the above cases, the blowing agent loss was considered to be negligible, and therefore the no-gas-loss boundary condition was adequate to predict the foam growth kinetics reasonably well. However, in the polymeric foam extrusion process of interest here, the foam sheet or rod is allowed to expand freely under atmospheric conditions. The assumption of no gas lost to surroundings no longer applies for the actual processing. Therefore, such gas escape must be accounted for, especially with thin foam shapes. Furthermore, the previous models do not include further complicating effects such as the influence of the blowing agent on polymer viscosity and the concentration dependence of the blowing agent on diffusion during the bubble growth process.

3.12.1.2.2 Modified Viscoelastic Cell Model for Foam Extrusion Process

Recently, Lee and Ramesh studied the effects of foam sheet thickness and nucleation cell density on thermoplastic foam sheet extrusion.⁵⁹ Low-density polyethylene was used with HCFC-22 and HCFC-142b to produce foam sheets of various thickness and nucleation characteristics. It was concluded that solubility, rheology, and gas loss transport mechanisms play an important role in determining the foaming efficiency during foam sheet extrusion. While predicting the foam density as a function of final cell density (or number of cells/unit volume) and foam sheet thickness, Lee and Ramesh used mathematical equations from packing theory to calculate the ratio of bubbles present closer to the surface to the bubbles present in the core portion of the foam sheet where there is no gas loss. The value of this ratio, of course, strongly depends on the nucleation density (which is defined as the number of bubbles nucleated per unit volume of the polymer) and the thickness of the foam sheet. With this theoretical background, they attempted to check the validity of the modified model by comparing with the experimental data. Although the improved cell model predicted the experimental data very well, between 919 kg/m³ and 60 kg/m³, it was observed that the agreement decreases for increased expansion ratios and volatility of blowing agent, where the nonspherical nature of the bubble, and bubble–bubble interaction phenomena, become pronounced. Higher nucleation rates and extrusion of thicker foam sheets seem to enhance foam efficiency. Correlation with cell geometry, nonspherical bubble dynamics, and consideration of interaction between bubbles during the growth process would greatly benefit understanding of the low-density foam process and assist in product design.

3.13 Foam Extrusion Modeling

A typical foam extrusion process is used here to demonstrate the carefulness of bubble growth modeling and its ability to predict experimental data. For

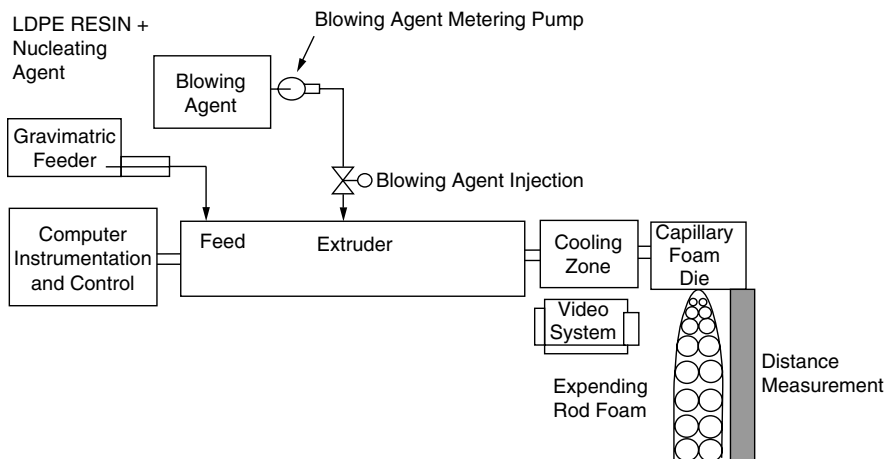


FIGURE 3.17
Rod extrusion from a die.

example, in a foam rod extrusion from a die shown in Figure 3.17, one-dimensional heat transfer is assumed.

Heat conduction becomes the dominant heat transfer mechanism. The heat loss effects on foam growth are less important when the diameter of the foam rod exceeds 10 mm. The average temperature of the thin foam as it is exposed to ambient conditions can be found from the standard heat transfer equation in the literature.⁶⁰

The schematic diagram of the cell model is shown in Figure 3.18. The appropriate bubble growth modeling equations are listed there.

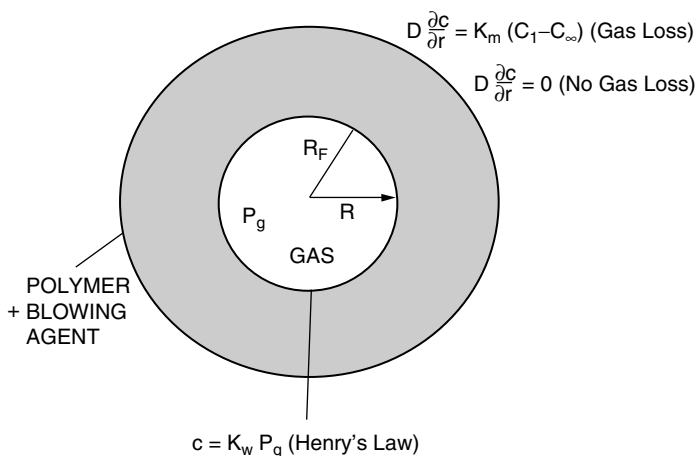


FIGURE 3.18
Gas loss boundary condition in the cell model.

3.13.1 Foam Growth Equations

To define gas pressure inside the bubble, the integrated momentum equation reduces to:

$$P_g - P_s - \frac{2\sigma}{R} + \int_R^{R_f} (\tau_{rr} - \tau_{\theta\theta}) \frac{dr}{r} = 0 \quad (3.20)$$

The rheological equations are

$$\tau + \frac{\eta_o^*}{G} \tau_{(1)} = -\eta_o^* \dot{\gamma} \quad (3.21)$$

$$\eta_o^* = \eta_o \exp \left[\frac{E_v}{R_g} \left(\frac{1}{T} - \frac{1}{T_o} \right) \right]^* f(C) \quad (3.22)$$

where

$$\begin{aligned} f(C) &= \text{viscosity reduction factor} \\ &= \frac{\text{Polymer viscosity with blowing agent}}{\text{Viscosity of polymer at same temperature}} \end{aligned} \quad (3.23)$$

The growth of radius is

$$\frac{d}{dt} (\rho_g R^3) = 3\rho D R^2 \left[\frac{\partial C}{\partial r} \right]_{r=R} \quad (3.24)$$

and the concentration-dependent diffusion equation is as follows:

$$\frac{\partial C}{\partial t} + V_r \frac{\partial C}{\partial r} = \frac{1}{r^2} \frac{\partial}{\partial r} \left(D r^2 \frac{\partial C}{\partial r} \right) \quad (3.25)$$

where diffusivity is a function of blowing agent concentration and it changes within the polymer envelope during the gas-diffusion process. The diffusivity also depends strongly on the temperature. Mathematically,

$$D(C, T) = [1 + aC] 10^{-7} e^{(b - \frac{c}{T})} \quad (3.26)$$

where a , b , and c are constants fitted to the experimental data that depend on the nature of the blowing agent. The values of a , b , and c need to be obtained experimentally. For this work, the values used based on our experimental data and the data provided by the resin supplier are listed in [Table 3.6](#).

TABLE 3.6

Experimental Parameters for Bubble Growth Calculations

Process Variables	Values
Surface tension of low-density polyethylene (LDPE)	$30 \frac{\text{mN}}{\text{m}}$
Molecular weight of butane (blowing agent)	58 kg/kg mol
Initial blowing agent concentration	6.0% by weight
Foaming temperature, T_o	383 K
Henry's law constant, K_w	$2.235 \times 10^8 \text{ Pa}$
Density of LDPE	920 kg/m^3
No. of bubbles per 1 cm^3 of foam (from experiment)	136
No. of bubbles across strand diameter	5
Diffusion empirical constant, a	0.5334
Diffusion empirical constant, b	21.93
Diffusion empirical constant, c	7090 K

3.13.2 Boundary Conditions

The initial and boundary conditions are

$$C(r, 0) = C_o = K_w P_g \quad (3.27)$$

$$C(R, t) = K_w P_g \quad (3.28)$$

For bubbles situated in the core of thick sheet expansion:

$$\frac{\partial C}{\partial r} = 0 \quad (3.29)$$

For bubbles on the surface of foam sheet that undergo gas loss:

$$D \frac{\partial C}{\partial r} = k_m (C_{surf} - C_s) \quad (3.30)$$

where

$$k_m = 2 \sqrt{\frac{D}{\pi t}} \quad (3.31)$$

and where k_m is defined as the mass transfer coefficient derived from penetration theory⁶⁰ and t is the foam growth time. The surface evaporation or gas loss condition is mathematically expressed in Equation 3.32:

$$R(t = 0) = R_o \quad (3.32)$$

The boundary condition, Equation 3.29, represents a closed cell system where there is no gas loss or escape to its surroundings. This is true in the injection molding process because the foam expansion occurs inside the mold.

But, in the practice of producing foams with unrestricted rise, gas loss is encountered from the bubbles that are adjacent to the top and bottom surfaces of the foam. The influence of gas loss on foaming efficiency is especially profound when the extruded shape is thin. Some of the gas close to the surface, instead of diffusing into the cell, diffuses to the surface and transpires into the atmosphere. As a result, the final surface cell size is smaller than that of the core cell. As the final foam density is lower, or the shape is thinner, more gas escape is anticipated. In other words, high concentrations of blowing agents or high surface-to-volume foam sheets accelerate gas loss from a sheet surface, thereby lowering the blowing agent effectiveness. This phenomenon is compounded at lower atmospheric temperatures that decrease the foam growth rate. A similar situation is encountered when a small diameter foam rod is extruded.

The above system of equations was solved numerically by an iterative numerical scheme. To facilitate the numerical simulation, a definite value of initial radius R_o is required. Bubble growth originates from thermodynamic and mechanical instability in the system with perturbed initial radius.^{50,56,61} Hence, the selection of initial radius is important to achieve accuracy in the predicted results. Great care is needed to model successfully. This principle has not been clearly emphasized in the literature so far. The bubble growth seems to be a strong function of the value of the perturbed initial radius during the induction period, which is less than 8% of the total expansion time. Beyond this initial growth time, i.e., greater than 8% of the total growth time, the foam growth rate is found to be independent of the growth radius, according to Amon and Denson,⁵⁰ Upadhyay,⁴⁹ Ramesh et al.,⁵³ and Arefmanesh and Advani.⁵² For all practical reasons, it is better to calculate the initial radius from fundamental mechanical equilibrium principles, which involve the calculation of a critical bubble radius. The value of the critical bubble radius r^* can be easily calculated from the force balance at the bubble wall, which can be written as:

$$r^* = \frac{2\sigma}{\Delta P} \quad (3.33)$$

where σ is the surface tension and ΔP is the pressure difference between the liquid polymer phase and the dissolved gas phase.

The simulation parameters used for all cases in this study are listed in Table 3.6. The model yields the result in terms of bubble radius as a function of time. The growing bubble reaches an equilibrium bubble radius once the gas is depleted. Finally, the bubble diameter is multiplied by the number of cells that are simultaneously growing across the diameter of the expanding rod to calculate the rod diameter. The simulated results are plotted in Figure 3.19.

3.13.3 Comparison of Theory with Experiment

Figure 3.19 shows the comparison model predictions with the viscoelastic model^{52,62} and experimental data. The solid line denotes the current model, and the dashed line denotes the previous model. The prediction of the foam strand diameter by the new model seems to agree well with the experimental data when the concentration and surface gas loss effects are included. The previous model predicts longer growth time due to neglecting concentration effects. Furthermore, the predicted induction time is longer and the shape of the curve does not seem to match with the characteristics exhibited by the experimental data. The previous model also predicts a higher strand diameter than is experimentally observed because it assumes no gas loss from the bubbles that are close to the surface. A significant difference in

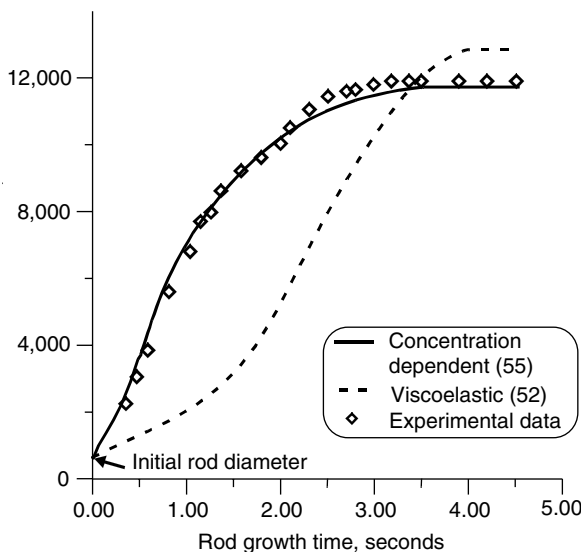


FIGURE 3.19

Comparison of experiment vs. theory for PE foam. (From Ramesh, N.S. and Lee, S.T., *Foams*, 99, 91, 1999.)

strand diameter leads to serious discrepancies in predicting the final foam density as it depends on the square of the rod diameter. Therefore, analysis including blowing agent concentration and surface escape effects into the thermoplastic foam expansion model is essential to accurately predict foam growth rate and density.

3.14 Conclusion

This chapter gives an overview of nucleation and bubble growth models and experiments since 1917. A large volume of literature exists for scientists to read and understand the complicated foaming process. The more we think we know about the foaming process, the more we realize how little we know, due to the complex variables involved in gas dissolution, bubble nucleation, bubble growth, and foam stabilization. Recent experimental studies by Ohshima³⁰ have opened up new opportunities to capture a nucleation and foam growth event. Similarly, the concentration-dependent bubble growth model⁵⁵ can be easily applied to describe the foam extrusion process. These are important steps in understanding foaming polymers to generate new products to serve automotive, packaging, and nonpackaging markets. Although 80 years of research has been done, much more work is needed to describe foaming mechanisms.

Acknowledgment

The author wishes to thank Kevin Lee for his assistance in preparing this manuscript.

Nomenclature

a	Experimental constant as per Equation 3.26
A	Interfacial area
b	Experimental constant as per Equation 3.26
c	Experimental constant as per Equation 3.26
C	Concentration of gas molecules
D	Diffusion coefficient (cm^2/s)
E_v	Activation energy for viscosity equation
$f(C)$	Viscosity reduction factor
f_o	Frequency factor for the rate at which gas molecules join a critical nucleus
$f(\theta)$	Heterogeneity factor

G	Modulus
ΔG^*	Gibbs free energy of forming a critical nucleus
k	Boltzman's constant
k_m	Mass transfer coefficient
K_w	Henry's Law constant
n	Number of moles
N	Number of nucleation sites per unit volume
N_o	Total number of potential microvoids
P	Pressure
ΔP	Pressure drop
r	Radial distance from the center
r^*	Critical bubble radius
R	Instantaneous bubble radius
R_f	Cell outer radius
R_g	Gas constant
S	Outer radius of cell as shown in Figure 3.8
T	Foam growth time
T	Absolute temperature
ΔT	Temperature drop
V_r	Radial component of velocity
y	Variable that signifies volume of polymer surrounding microvoid = $S^3 - R^3$
Z	Zeldovich non-equilibrium factor
β	Thermal expansion coefficient
β^*	Rate at which gas molecules are added to the critical nucleus
γ	Rate of strain tensor
$\dot{\gamma}$	Average shear rate
η	Polymer melt viscosity
η_o^*	Modified zero shear viscosity
ν	Poisson ratio
θ	Wetting angle
σ	Surface tension of the liquid or polymer
τ	Induction period for establishing steady-state nucleation conditions
τ_{rr}	Stress in radial direction
$\tau_{\theta\theta}$	Stress in circumferential direction
$\tau_{(1)}$	Convective time derive of stress tensor
ξ	Mean of the distribution of the void size

Superscript

* Critical point

Subscripts

g	Gas
hetero	Heterogeneous
homo	Homogeneous
o	Initial
p	Particle
pb	Polybutadiene
ps	Polystyrene
s	Final or surrounding
sat	Saturation
surf	Surface

References

1. Cole, R., Boiling nucleation, *Advances in Heat Transfer*, vol. 10, Academic Press, New York, 1974.
2. Blander, M. and Katz, J.L., *AIChE J.*, 21, 833–848, 1975.
3. Springer, G.S., Homogeneous nucleation, *Advances in Heat Transfer*, vol. 14, Academic Press, New York, 1978.
4. Uhlmann, D.R. and Chalmers, B., Nucleation phenomena, ACS Symposium, June 21–22, 1–12, 1965.
5. Becker, R., *Ann. Physik*, 32, 128, 1938.
6. Han, C.D. and Yang, H., *J. Appl. Polym. Sci.*, 29, 4465–4470, 1984.
7. Colton, J. and Suh, N., *Polym. Eng. Sci.*, 27, 485–492, 1987.
8. Cole, R., Bubble nucleation, growth and departure in boiling heat transfer, *Handbook of Heat and Mass Transfer*, Gulf Publishing, Houston, TX, 1986.
9. Lee, S.T., *Foam Extrusion: Principles and Practice*, CRC Press, Boca Raton, FL, 108–109, 2000, chap. 4.
10. Ramesh, N.S., Campbell, G.A., and Rasmussen, D.H., *Polym. Eng. Sci.*, 34, 1685–1706, 1994.
11. Han, C.D. and Han, J.H., *J. Polym. Sci., Polym. Phys. Ed.*, 28, 743, 1990.
12. Boureau, R.J., *Mod. Plast.*, 44, 133, 1967.
13. Bailey, F.E., *Polymeric Foams*, Hanser, New York, 1991.
14. Youn, J.R. and Byon, S.K., *Polym. Eng. Sci.*, 30, 147, 1990.
15. Einstein, A., *Ann. Physik*, 38, 1275, 1910.
16. Volmer, M. and Weber, A., *Z. Phys. Chem.*, 119, 277, 1926.
17. Onsager, L., *Phys. Rev.*, 37, 405, 1931.
18. Becker, R. and Doring, W., *Ann. Physik*, 24, 719, 1935.
19. Turnbull, D. and Fisher, J.C., *J. Chem. Phys.*, 17, 71–73, 1949.
20. Reiss, H., *J. Chem. Phys.*, 18, 840, 1950.
21. Lothe, J. and Pound, G.M., *J. Chem. Phys.*, 36, 2080–2085, 1962.
22. Gibbs, W., *The Scientific Papers*, vol. 1, Dover, New York, 1961.
23. Zettlemoyer, A.C., *Nucleation*, Marcel Dekker, New York, 1969.
24. Blander, M., Hengstenberg, D., and Katz, J.L., *J. Phys. Chem.*, 75, 3613, 1971.

25. Martini, J.E., The production and analysis of microcellular foam, S.M. thesis, MIT, 1981.
26. Kumar, V., Process synthesis for manufacturing microcellular thermoplastic parts: a case study in axiomatic design, Ph.D. thesis, MIT, 1988.
27. Ramesh, N.S., Investigation of the foaming characteristics of nucleation and growth of microcellular foams in polystyrene containing low glass transition particles, Ph.D. thesis, Clarkson University, 1992.
28. Ruengphrathuengsuka, W., Ph.D. thesis, Texas A&M University, 1992.
29. Park, C.B., Behraves, A.H., and Venter, R.D., *SPE ANTEC*, 2, 1958, 1998.
30. Ohshima, M. et al., Visual observations of batch and continuous foaming processes, *Foams*, 141–151, 2002.
31. Timoshenko, S. and Goddier, J.N., *Theory of Elasticity*, McGraw-Hill, New York, 1970.
32. Beck, R.H. Gratch, S., Neuman, S., and Rusch, K.C., *Polymer Melt*, 6, 1998.
33. Bucknell, C.B., *Toughened Plastics*, Applied Science Publishers, London, 1977.
34. Schmitt, J.A., *J. Appl. Polym. Sci.*, 12, 533, 1968.
35. Keskkula, H., Schwara, M., and Paul, D.R., *Polymer*, 27, 210, 1986.
36. Donald, A.M. and Kramer, E.J., *Phil. Mag. A*, 43, 873, 1981.
37. Adams, M.G., Cohen, A., and Campbell, G.A., *Polym. Eng. Sci.*, 31, 1036, 1991.
38. Van Krevelen, D.W., *Properties of Polymer*, Elsevier, Amsterdam, 1976.
39. Kanner, B. and Decker, T.G., *J. Cell. Plast.*, 5, 32, 1969.
40. Klemper, D. and Prisch, K.C., *Polymeric Foams*, Hanser, New York, 1991.
41. Harrington, R. and Hock, K., Flexible PU Foams, Dow Chemical, 1991.
42. Ramesh, N.S. and Malwitz, N., *SPE ANTEC*, 1941–1945, 1994.
43. Wang, S.L., Frisch, K.C., and Malwitz, N., 30th Annual Polyurethane Technical Conference, 363–368, 1986.
44. Lord Rayleigh, *Phil. Mag.*, 6th series, 34, 94, 1917.
45. Epstein, P.S. and Plesset, M.S., *J. Chem. Phys.*, 18, 1505, 1950.
46. Scriven, L.E., *Chem. Eng. Sci.*, 10, 1, 1959.
47. Street, J.R., Fricke, A.L., and Reiss, L.P., *Ind. Eng. Chem. Fundam.*, 10, 54, 1971.
48. Han, C.D. and Yoo, J.J., *Polym. Eng. Sci.*, 21, 518, 1981.
49. Upadhyay, R.K., *Adv. Polym. Tech.*, 5, 1, 55, 1985.
50. Amon, M. and Denson, C.D., *Polym. Eng. Sci.*, 24, 1026, 1984.
51. Amon, M. and Denson, C.D., *Polym. Eng. Sci.*, 26, 255, 1986.
52. Arefmanesh, A. and Advani, S., *Rheo. Acta*, 30, 274, 1991.
53. Ramesh, N.S., Campbell, G.A., and Rasmussen, D.H., *Polym. Eng. Sci.*, 31, 1657, 1991.
54. Ramesh, N.S., Lee, S.T., and Campbell, G.A., *SPE ANTEC*, 3033, 1993.
55. Ramesh, N.S. and Malwitz, N., *SPE ANTEC*, 1907, 1998.
56. Shafi, M.A., Joshi, K., and Flumerfelt, R.W., *Chem. Eng. Sci.*, 52, 635, 1997.
57. Ohshima, M., *Foam Extrusion: Principles and Practice*, ed. S.T. Lee, CRC Press, Boca Raton, FL, 2000, chap. 6.
58. Ramesh, N.S. and Malwitz, N., *SPE ANTEC*, 2171, 1995.
59. Lee, S.T. and Ramesh, N.S., Cellular and microcellular materials, ASME '96, 71–80, 1996.
60. Welty, J.R., Wicks, C.E., and Wilson, R.E., *Fundamentals of Heat and Mass Transfer*, John Wiley & Sons, New York, 1969, 556–557.
61. Lee, S.T., Study of foam-enhanced devolatilization: experiments and theories, Ph.D. thesis, Stevens Institute of Technology, 1986.

62. Arefmanesh, A., Numerical and experimental study of bubble growth in highly viscous fluids, Ph.D. thesis, University of Delaware, 1991.
63. Ramesh, N.S. and Lee, S.T., *Foams*, 99, 91, 1999.

4

Material Properties Affecting Extrusion Foaming

Q. Zhang and M. Xanthos

CONTENTS

- 4.1 Introduction
- 4.2 Importance of Material Properties in Extrusion Foaming
- 4.3 Physical Blowing Agents
 - 4.3.1 Types and Properties
 - 4.3.2 Blowing Agent Solubility
 - 4.3.2.1 Main Factors Affecting Blowing Agent Solubility
 - 4.3.2.2 Measurement of Blowing Agent Solubility
 - 4.3.2.3 Gas Dissolution Inside Foaming Extruders
- 4.4 Resin Properties
 - 4.4.1 Importance of Viscoelasticity
 - 4.4.2 Modification of Resins to Enhance Foamability
- 4.5 Concluding Remarks
- Acknowledgments
- References

4.1 Introduction

Extrusion foaming for the production of medium- and low-density thermoplastic foams has been carried out successfully for some time with physical blowing agents (PBAs). PBAs are atmospheric gases, volatile hydrocarbons, or hydrochlorofluorocarbons (HCFCs) that are metered and dissolved in the polymer melt during processing. The extrusion foaming process can use a single extruder or two extruders operating in tandem. The basic steps in the process involve (a) melting of the solid polymer; (b) injection and dissolution of the blowing agent into the polymer melt, which is a diffusion controlled

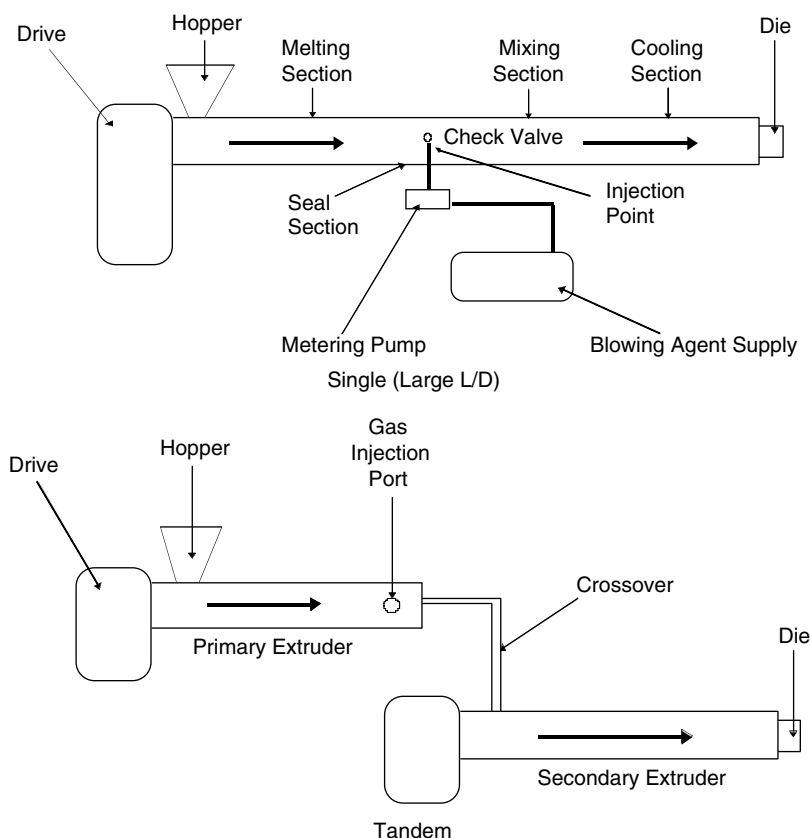


FIGURE 4.1

Schematics of single barrel and tandem foam extruders.

process; (c) cooling of the blowing agent laden melt; (d) expansion through the nucleation (often in the presence of nucleating agents) and growth of bubbles due to super-saturation and diffusion of gas into the nucleated bubbles (this is, generally, achieved by suddenly releasing the system pressure); and (e) stabilization of the resultant cellular structure, which is accomplished by subsequent cooling and solidification of the cell walls.

The schematics of single barrel and tandem foam extruders are given in Figure 4.1. In the single extruder case, high length to diameter ratio (L/D) equipment is normally required to provide sufficient elements for polymer melting, gas dissolution, cooling and pressurization, and foaming through the die. In such a process, typically a two-stage screw is used. The polymer composition fed in the extruder feed section is melted and mixed in the transition section of the screw and then the blowing agent is injected. The blowing agent is dispersed and dissolved in the melt; this process depends on several factors including the type of resin and blowing agent, temperature, pressure, and

conditions such as screw configuration, screw speed, and so on. The gas-laden melt is then pressurized and extruded through the die. The temperature profile on the extruder is set in such a way that for the zones prior to the gas injection, the temperature is high enough to ensure proper melting; for the zones past the injection section, temperature is gradually lowered substantially so as to allow for adequate cooling of the gas-laden melt prior to exiting the die, a necessary condition for cell expansion without coalescence. It is believed that bubble nucleation is heterogeneous and begins at the shaping die as the gas-laden melt emerging from the die experiences a sudden pressure drop; this thermodynamic instability causes phase separation. The escaping gas leads to expansion within the fluid matrix in such a manner that individual minute bubbles merge into cells and, through subsequent solidification, stable expanded structures are produced.

In the tandem process, the polymer and additives are melted and mixed in a primary extruder, which is typically equipped with a high shear mixing screw. The blowing agent is injected near the end of this primary extruder. The melt containing the blowing agent is then transferred to the feed section of the secondary extruder through the so-called crossover section. The main purpose of the secondary extruder is to cool the gas-laden melt to an optimum temperature and pressure for foam formation without cell coalescence. The tandem extruder setup normally allows for excellent control of process variables and is used in industry to produce very low-density foams.

The overall basic requirements for polymers, blowing agents, nucleators, equipment, and processing parameters for making extruded polymeric foams are shown schematically in Figure 4.2 (adapted from Khemani¹). The processes to be discussed in this chapter involve macrocellular foams (typically 100 μm or larger in cell size); we will not cover so-called microcellular

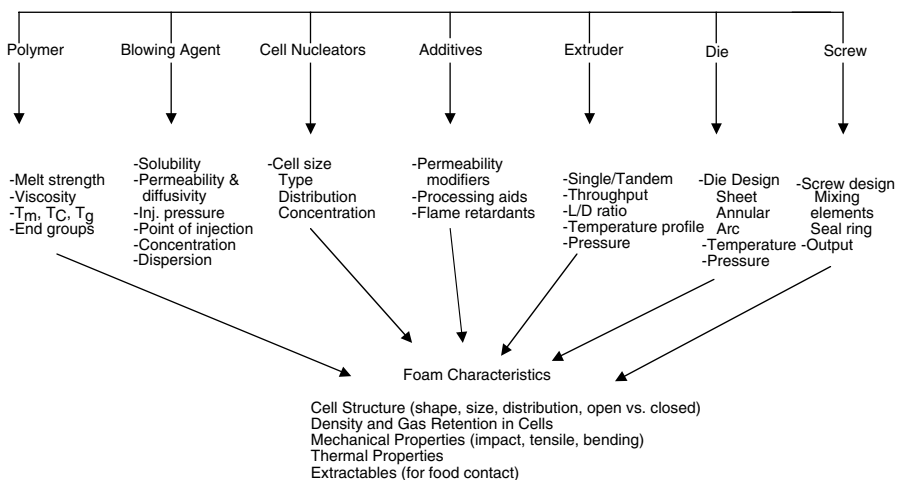


FIGURE 4.2

Parameters affecting the thermoplastics foam extrusion process.

foaming where resins, presaturated with blowing agents such as CO_2 , are heated at or above T_g and cooled rapidly to stabilize the cellular fine morphology and prevent excessive cell growth. Such morphology is characterized by closed cells up to $25\text{ }\mu\text{m}$ in size and a cell density of 10^8 cell/cm^3 and above.² Continuous microcellular processes involving extrusion equipment as described in various patents³ are under development,⁴ and some are already commercially available.

4.2 Importance of Material Properties in Extrusion Foaming

The solubility and diffusivity of the gas in the melt and the viscoelastic properties of the molten polymer are among the material parameters playing an important role during the various stages of low-density extrusion foaming. Material properties that influence these processes include melt shear and elongational viscosity, melt strength, and, if the polymer is crystallizable, the rate of crystallization. Gas/polymer interfacial properties also play a significant role in all these stages of operation. To summarize pertinent information from Throne:⁵

- PBAs need to be highly soluble (to alleviate the need for high extrusion and die pressures) and uniformly distributed in the polymer, since undissolved microbubbles may promote premature nucleation before the die. In addition, PBAs must diffuse at a high but controlled rate to allow rapid cell inflation.
- Melts with high viscosity, particularly extensional viscosity, are needed in the presence of dissolved gas which may act as a plasticizer, reducing the overall viscosity.
- Melts with high elasticity and high normal stress differences are needed during the extensional portion of bubble inflation, in addition to high resistance to stretching for stabilization of the growing bubbles.
- At the end of bubble growth during the final biaxial stretching, high melt elasticity to resist blow-out and moderately high elongational viscosity (the latter increased by cooling) and rapid crystallization are needed.

The first requirement for successful foaming is to form a uniform gas-laden melt. This means that all gas molecules are dispersed on a molecular level throughout the melt. The key here is the solubility of the gas in the polymer at the melt temperature. If inert gases of low solubility such as nitrogen and

argon are used as blowing agents to produce low-density foams of many commercial polymers, then very high extrusion and die pressures would be normally required.

The rheological properties of the gas-laden melt become very important; for example, the viscosity of the mixture has to be high enough to achieve the pressure required. The viscosity of the gas-laden melt is a strong function of the gas concentration. It has been shown that at a given temperature, the gas-laden polymer melt viscosity decreases exponentially with gas content throughout the practical range of gas concentration for many polymer–gas systems.⁶ The required high pressure is normally achieved by cooling the polymer–gas mixture substantially before reaching the extrusion die. Temperatures can be set to below the normal polymer melting point and near the crystallization temperatures, in cases of semi-crystalline polymers, and near T_g for amorphous polymers. This is possible because the inclusion of the gas causes depression of the glass transition temperature (T_g) of an amorphous polymer or the crystallization temperature (T_c) of a semicrystalline polymer. Depression of T_g , or T_c (the latter to a lesser extent) is a well-known phenomenon and experimental results are available for a number of polymer–gas systems.^{7–11}

A variety of materials can be used during extrusion foaming, mostly to control nucleation of bubbles and produce uniform cells of the desired density and dimensions. Fine inorganic minerals such as talc are commonly used, although polymers immiscible in the foamable matrix may play the same role. Glycerol stearate esters have also been used as additives in certain polyolefin foams to control gas diffusion through the cells and to control the “aging” time of the foams.

4.3 Physical Blowing Agents

4.3.1 Types and Properties

The optimal blowing agent must be environmentally acceptable and economically viable, or readily available at low cost. It must also meet safety regulations as required in storage, usage, and handling of both the blowing agent and the foams made from it. The ideal blowing agent should be non-toxic, non-flammable, and chemically and thermally stable. Other requirements include appropriate solubility in polymer melt, low vapor pressure at room temperature, low boiling point, and slow diffusion through the polymer compared to air.

Continuous extrusion foaming processes primarily used chlorofluorocarbons (CFCs) as blowing agents prior to their ban in mid-1990s. The release of CFCs and other ozone-depleting substances (ODSs) had been identified to be the main cause for rapid erosion of the stratospheric ozone layer, and

the foam industry was one of the main industries that used and released ozone-depleting chemicals. According to the U.S. Environmental Protection Agency's estimation,¹² in the U.S., foam plastics accounted for approximately 18% of all U.S. consumption of ozone-depleting chemicals in 1990.

Following the ban on the use of CFCs for foam production in 1996, the foam industry began to use other groups of chemicals. Currently, HCFCs, hydrofluorocarbons (HFCs), and volatile organic compounds (VOCs), mostly hydrocarbons, are the major chemicals being used as blowing agents. HCFCs are also ozone-depleting chemicals and are used only as transitional alternatives to CFCs facing staged phase-out. HFCs are being used as chlorine-free substitutes of HCFCs, and currently a number of HFC blowing agents are commercially available. Examples include HFC-134a (CH_2FCF_3), HFC-143a (CH_3CF_3), and HFC-152a (CHF_2CH_3). Hydrocarbons (such as butane and pentane) are still very popular but highly flammable and can produce explosive mixtures with oxygen despite sophisticated equipment and safety measures.

In response to increasing regulation of halocarbons and increasing safety and environmental concerns over the use of flammable, volatile hydrocarbons, recent research has focused towards replacing the traditional foaming agents with various inert blowing agents, including atmospheric gases such as CO_2 , N_2 , and Ar, but also water. Currently, CO_2 is being commercially used as a blowing agent in polyurethane foaming, along with CFC alternatives such as HCFC and HFC. Some thermoplastic foaming processes using CO_2 ¹³ and other atmospheric gases as blowing agents have also been developed, while most thermoplastic foams are still being manufactured using HCFCs, HFCs, and hydrocarbons as blowing agents. The use of inert gases in foam extrusion has been shown to demand a very narrow window of processing conditions as opposed to the use of halocarbons.¹⁴ Inert gases are much less soluble in the polymer melt and have much higher vapor pressures than CFCs or hydrocarbons.

A comparison of some of the properties of different blowing agents is given in Table 4.1. Comparison of solubility data of R-22 CFC and 142-B HCFC versus CO_2 in polystyrene shows higher values at a magnitude of four times or more.¹⁵ The effects of the lower CO_2 solubility coupled with its much higher vapor pressure and permeability versus conventional blowing agents are reflected in almost all stages of the foaming process, including gas dis-

TABLE 4.1

Comparison of PBA Properties in Polystyrene¹⁵

Blowing Agent	Vapor Pressure (psia)	Solubility at 24°C (pph/atm)	Permeability (Dow units)
CFC (R-22)	151	1.60	19
HCFC 142-B	49	6.25	0.21
CO_2	930	0.40	1430

solution, bubble nucleation and growth, and cell structure stabilization. In efforts to produce zero ozone-depleting-potential (ODP) polystyrene formulations, the issues in replacing HCFCs with CO₂ on an industrial scale have been addressed through rheological modification of the resin, the use of processing aids, the use of PBA mixtures, and modification of machine and process conditions.¹⁵

4.3.2 Blowing Agent Solubility

A very important parameter in the production of these multicomponent, multiphase systems is the solubility of physical blowing agents in the pressurized polymer melt, as affected by concentration, pressure, and temperature. Knowledge of the solubility characteristics of the gas in polymer melts is highly desirable in order to estimate the pressure requirements to keep it in the melt throughout the extruder all the way to the die, thus avoiding the formation of premature bubbles which would result in uneven cell growth.

For molten polymers, the solubility of a blowing agent dictates the conditions under which bubbles will start to nucleate and grow. After the foaming process, the long-term characteristics of the foam are still influenced by the solubility and diffusivity of the blowing agents. Diffusion of the blowing agent out of the cells and the polymer matrix will change the thermal and mechanical properties of the foam. This is especially the case when the blowing agent plasticizes the polymer and the material stiffens as the blowing agent diffuses out.¹⁶

4.3.2.1 Main Factors Affecting Blowing Agent Solubility

It is generally accepted that solubility is dependent on the free volume available to the gas molecules in the polymer, and therefore dependent on temperature and pressure. Free volume increases with temperature; therefore, solubility should increase with temperature. For many cases, however, interactions between gases and polymers cause solubility to decrease with increasing temperatures. For most gases, it turns out that more easily condensed gases have higher solubility.

Solubility is usually expressed through Henry's law¹⁷ as:

$$X = K_p P_g \quad (4.1)$$

where X is the concentration of gas in the melt (cm³ (STP)/g), P_g is partial pressure of dissolved gas (kPa), and K_p is the Henry's law constant (cm³ (STP)/g•kPa). For a number of gases, the logarithm of the experimental Henry's law constant has been shown to correlate linearly with $(T_c/T)^2$, where T_c is the critical temperature of the gas.^{18,19}

Features in the molecular structure of polymers which disrupt chain packing increase their free volumes. Therefore, polymers with branched

structures or bulky pendant groups in their repeat unit have increased solubility, relative to polymers with more linear structures. Specific interactions such as hydrogen bonds between the gas molecules and the polymer repeat structure can also promote solubility.

Experimental data reported by Durrill and Griskey^{20,21} indicate that Henry's law constants rank as $N_2 < CO_2 < ClF_3C$ for each polymer from the group of polyethylene (PE), polypropylene (PP), polyisobutylene (PIB), polystyrene (PS), and polymethyl methacrylate (PMMA). Thus, for these systems comprising nonpolar or low polarity polymers, solubility was primarily dependent on the type of gas rather than the type of polymer, with CFC showing much higher solubility than atmospheric gases. From the above data, other researchers²² working on microcellular foaming estimated very similar solubilities of CO_2 at 200°C and 27.6 MPa in various polymers, such as PP and PS (12%) and PMMA (15%). The heat of the solution was found to be positive for nitrogen in PE but negative for CO_2 in PE, PP, and PS.^{18,20} For the PS/ CO_2 system, recent data indicate good agreement between theory and experiment with correct prediction of decreasing solubility with increasing temperature.²³

For amorphous polymers without strong polar groups, the linear relation between log-solubility and critical temperature or boiling point of gas¹⁸ may be used as a first approximation. For polybutadiene (PB), for example, solubility of gases decreases with decreasing critical temperature in the order $CO_2 > CH_4 > Ar > N_2$,¹⁹ with a positive temperature dependence for N_2 and a negative dependence for CO_2 , CH_4 , and Ar. However, for amorphous polymers with strong polar groups, significant effects of the polymer polarity on gas solubility have been observed.^{24,25} For example, the solubility of CO_2 at 25°C in butadiene/acrylonitrile rubber increases with an increasing content of acrylonitrile polar groups in the polymer, whereas that of nitrogen, hydrogen, and oxygen (being already much lower than CO_2 by an order of magnitude) decreases.²⁴ Equilibrium uptakes of CO_2 at room temperature range from 3% in PE to 27% in PMMA to over 50% in PVAc. Equilibrium sorption of CO_2 in styrene/acrylonitrile copolymers increases with AN content and in ethylene/vinyl acetate with increasing vinyl acetate monomer. For a variety of polar polymers, solubility of CO_2 ranks as $EVA > PMMA > PC > PVC$.²⁵ The relatively high sorption values of CO_2 in polar polymers may result from enhanced specific interactions of CO_2 with carbonyl or nitrile groups; these could be related to its quadrupole moment or its H-bonding basicity.²⁵ Recent work^{26–29} on melt mixed PS/PMMA blends demonstrated that the solubility of CO_2 in the PMMA phase is, indeed, significantly higher than that in PS. Higher affinity with the carbonyl group of the PMMA polymer implies also higher plasticization capacity, which is manifested in lower T_g ⁸ and lower viscosity.

4.3.2.2 Measurement of Blowing Agent Solubility

Given the importance of blowing agent solubility, recent experimental efforts have focused on the measurement of solubility of gases in molten polymers

at high temperatures and pressures. Efforts have also been made to model gas solubility using, for example, equations of state (EOS). The Simha-Somcynsky theory has been used to model gas solubility in polymer melts and has found success in predicting gas solubility characteristics for a number of polymer-gas systems.³⁰

Experimental data on gas solubility in polymer melts have been reported by many investigators.^{19,20,31-34} These investigators used either the pressure decay method or a high-pressure vessel batch process to determine thermodynamic equilibrium data. More recently, a gravimetric method employing an electrobalance was also used.^{35,36}

On-line/in-line methods have drawn attention in recent years, since they allow measurements under dynamic conditions. Dual transmission infrared sensors have been used for on-line monitoring of foaming processes, the sensors being linked with fiber-optic cables to a Fourier Transform Infrared (FTIR) spectrophotometer which records spectra of the melt in the near-infrared region. Infrared probes were mounted on a slit die to monitor the polymer-gas mixtures during the extrusion of foams.^{16,37} This technique was also used to detect degassing in the melt. Ultrasonic sensors were also used in the same slit die for measuring the phase behavior of molten polymers.³⁸ Tsujimura et al.³⁹ studied the dynamic behavior of bubble nucleation in a slit die with quartz glass windows using a long-distance microscope and a high-speed video system. The effect of nucleating agents on bubble nucleation dynamics for a PP-butane system was also studied using this method. An in-line method has been developed in the laboratory of the authors which is capable of measuring PBA solubility in polymer melts under extrusion conditions. This method combines an optical flow cell with a foaming extruder (single or twin-screw) and generates apparent solubility data by observing the onset of bubble formation and dissolution in the melt, via a microscope-CCD (charged coupling device) camera-monitor-recorder system. The schematic of the experimental setup is shown in Figure 4.3. The onset of gas bubble presence or absence in the cell was monitored and recorded using an optical system consisting of a microscope, a CCD camera, a monitor (TV), and a recorder (VCR) (Figure 4.4). The important parameters, such as melt pressure and temperature at the die and the window, gas injection pressure, and flow rate, were digitized and recorded in a computer for real-time monitoring and off-line analysis.

At the beginning of each experiment, the window pressure is low, and the gas laden melt passing through the window is a two-phase system with many large bubbles dispersed in the continuous melt phase, as shown in Figure 4.5A. The window pressure is then slowly increased by adjusting (closing) the restricting valve. The number and size of the bubbles decrease with increasing melt pressure as indicated in Figure 4.5B. When the pressure is high enough, all bubbles will disappear and the system will appear as a single-phase system. Figure 4.5C shows this tendency; this pressure is considered to be the lowest pressure required to keep the gas in solution under the specified conditions. This method generates apparent solubility data that could be used directly to characterize and control a foaming process and

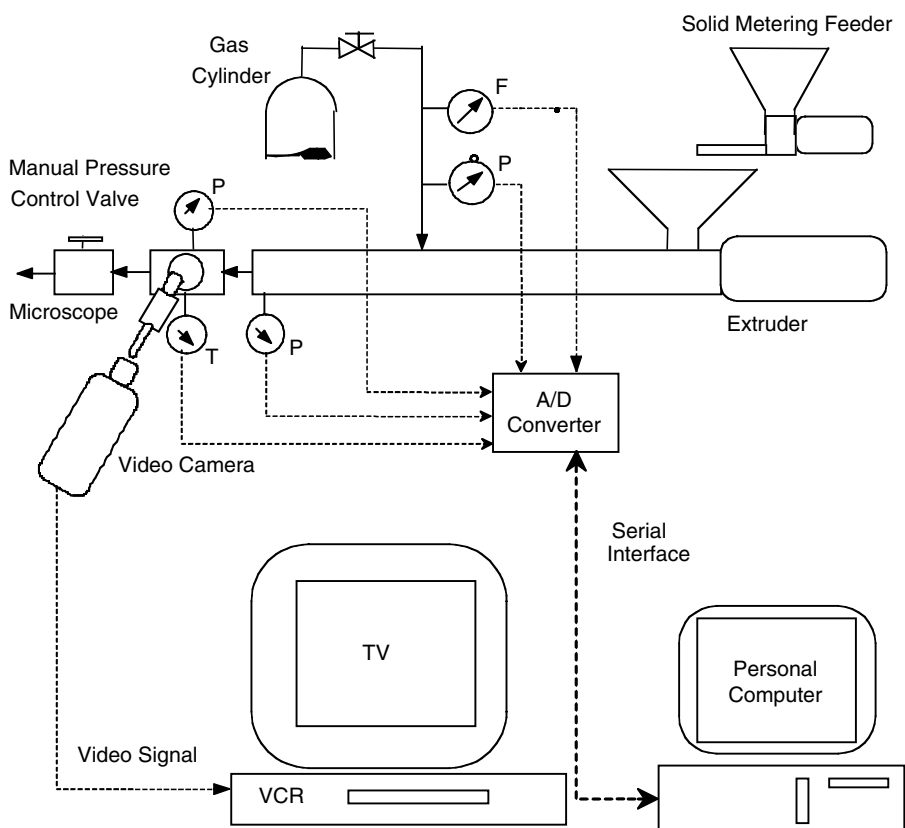


FIGURE 4.3
Schematic of the experimental setup to measure the dynamic solubility of blowing agents.

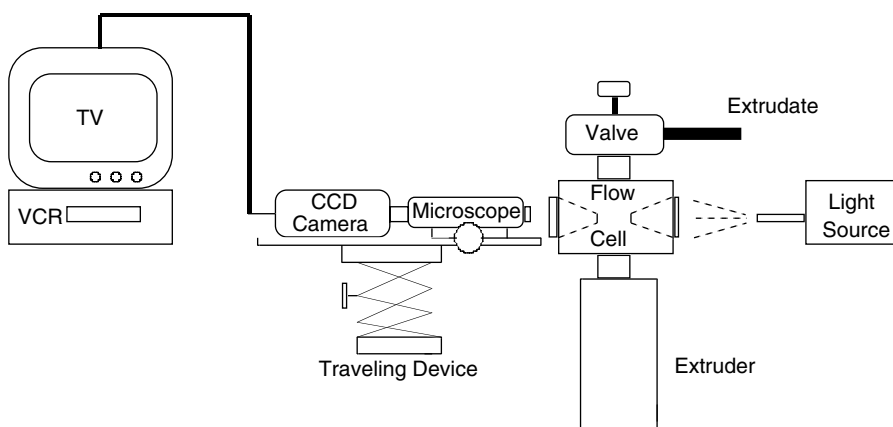


FIGURE 4.4
Schematic of the flow cell—monitoring/recording system used to measure the dynamic solubility of blowing agents.

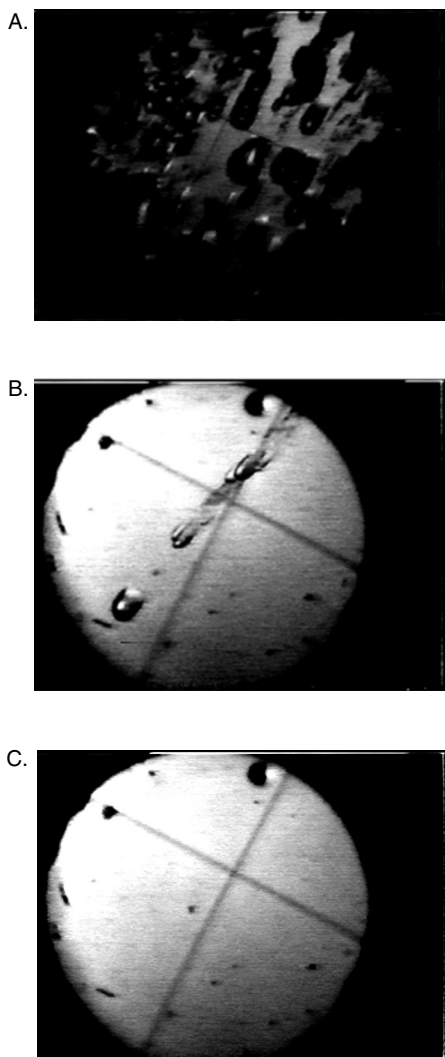


FIGURE 4.5

Monitoring of CO₂ bubbles in PS melt at 215°C. (Original magnification $\times 60$.) (A) Low pressure. (B) Pressure close to the targeted pressure. (C) High pressure.

serve as guidance in blowing agent selection and process design and optimization. Unlike traditional methods that generally require long hours for equilibrium, the apparent solubility measurements are carried out within the single or tandem extruder residence times (typically 5–20 min); thus, they are very useful in solubility measurements for temperature-sensitive polymers. They can be used to study effects of processing conditions on gas solubility characteristics and can also be potentially useful for studying the effects of polymer modification on solubility if used with a reactive extruder.

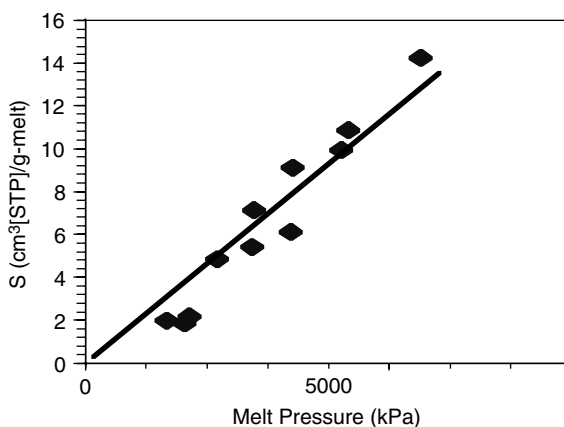


FIGURE 4.6
Solubility vs. melt pressure of CO₂ in PS melt at 215°C.

TABLE 4.2

Comparison of Experimental Results with Literature Data

	Temperature (°C)	H/Slope cm ³ [STP]/g•kPa	Pressure Range (kPa)
In-line data	190	0.0037	Up to 5575
Sorption experiment results (20)	188	0.0022	Up to 2030
Data from low temperature experiments (19)	180	0.0020	Up to 17000

Solubility data generated for CO₂ in polystyrene at 190°C are presented in Figure 4.6. These results are compared with literature values obtained from sorption experiments as shown in Table 4.2.

Temperature dependence of gas solubility in PS was also studied. Some results of CO₂ and nitrogen are presented in Figure 4.7 and Figure 4.8. These results show that for carbon dioxide, the solubility decreases with increasing temperature. This tendency has been generally observed in many gas–polymer and solute–solvent systems.^{17,19,20} For nitrogen, however, the solubility increases with increasing temperature. This tendency called reverse solubility has been observed for gases of low critical temperatures such as helium, hydrogen, nitrogen, and oxygen.¹⁹

Solubilities of three different atmospheric gases (CO₂, nitrogen, and argon) in polyethylene terephthalate (PET) were also obtained. The results given in Figure 4.9 indicate that carbon dioxide has the highest solubility in PET, nitrogen has the lowest, and Ar is somewhere in between. This trend is consistent with literature results obtained for the same systems under temperatures below the polymer T_g.³²

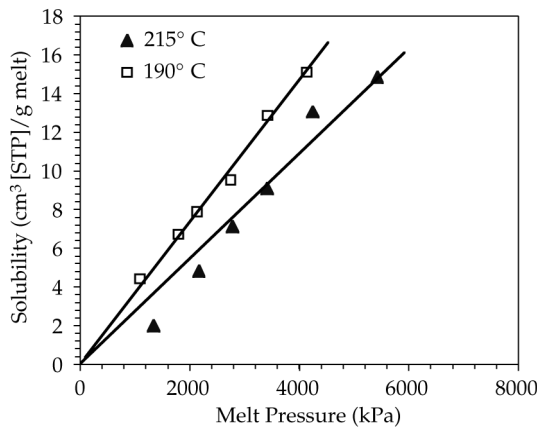


FIGURE 4.7

Solubility vs. melt pressure of CO₂ in PS melt at two different temperatures.

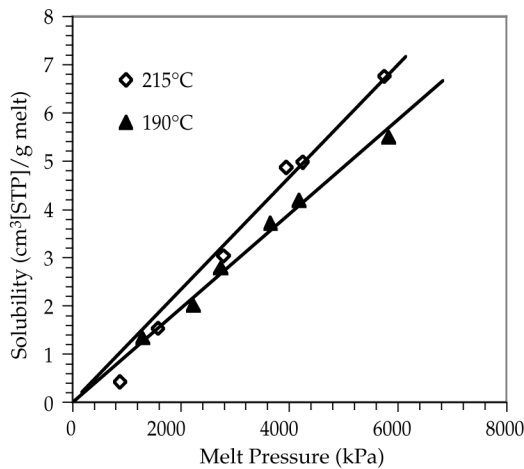


FIGURE 4.8

Solubility vs. melt pressure of N₂ in PS melt at two different temperatures.

4.3.2.3 Gas Dissolution Inside Foaming Extruders

Dissolution of physical blowing agents is affected by solubility, diffusivity, pressure, mixing, and residence time. Shear forces and interfacial tension may also play a significant role in affecting the gas dissolution process. Considerable research has been conducted on processes that involve the formation and growth of gas bubbles in polymer solutions or melts during foam formation or devolatilization of polymer solutions. Studies on gas dissolution processes in foaming extruders have been largely ignored, likely due to the fact that when traditional blowing agents (CFCs, HCFCs, and

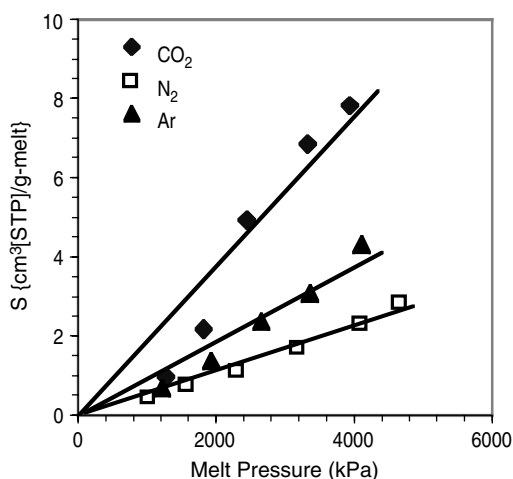


FIGURE 4.9

Solubility vs. melt pressure of inert gases in PET at 290°C.

hydrocarbons) are used, gas dissolution has never been a major concern thanks to the high solubility of those agents. However, when inert gases such as CO₂ and N₂, which have limited solubility in polymer melts, are used as blowing agents, solubility and dissolution become major factors in determining the process efficiency, feasibility, and product quality, since in these cases the system needs to operate at much higher pressures.

Solubility results obtained from the in-line method for a PS-CO₂ system along with gas injection conditions were used to study the gas dissolution behavior over the gas injection section of the foaming extruder, in an effort to elucidate the mechanisms involved in this complex process. In this case, the extruder used was a 34-mm intermeshing, corotating twin-screw extruder (Leistritz LSM34) having a L/D of 36.

Generally speaking, gas dissolution in the injection zone is dictated by solubility and diffusivity of the PBA and polymer/gas flow dynamics. The main mechanism for gas-melt mass transfer in a partially filled extruder is diffusion through the surface areas provided by the rotating melt pool and the barrel melt film⁴⁰ as shown schematically in Figure 4.10. In extruders the pool rotates in the partially filled channel under the influence of the cross channel component of the screw velocity, while being conveyed through the extruder in drag flow by the down channel component. A stationary melt film is deposited on the barrel wall due to the clearance between screw and barrel. The screw rotation causes continuous generation of the free surface of the rolling pool, significantly enhancing gas diffusion. Other possible mechanisms have also been speculated for some time. Some researchers⁴¹ believe that some degree of foaming or frothing happens inside the injection zone, which would increase the mass transfer area and, hence, enhance the rate of gas dissolution.

The actual amount of gas dissolved in the melt as measured downstream at the window in the twin-screw extruder is compared with the maximum possible amount that could be dissolved in the gas injection zone under a particular injection pressure. The latter is calculated using the gas injection pressure and assuming equilibrium is reached in the short gas injection zone. Comparative data for CO₂ in the PS melt under three different injection pressures are given in Figure 4.11. The results show that the actual total amount of gas in the polymer melt is more than that calculated from equilibrium under the corresponding injection pressure. Given the short residence time and the relatively low diffusivity values of CO₂, on the order of 10⁻⁶ cm²/sec,⁴² it is much less likely that the diffusion process could reach equilibrium in the short gas injection section of the screw. Calculations based on mechanism shown in Figure 4.10 and using typical solubility and diffusivity values have shown that under the applied experimental conditions, the system can only reach about 40–60% of the equilibrium values.⁴³ This indicates that the gas is carried downstream, possibly in the form of foam, and gets dissolved somewhere downstream under increased pressure over a longer residence time. Todd observed the formation of bubbles in twin-screw extruders when small amounts of air or water were injected into the melt.⁴¹ Some amount of gas may be trapped into the melt by the circular flow of the rotating melt pool, and this amount cannot readily dissolve into the melt due to limitations of mass transfer rates, limited solubility and diffusivity, and short contacting time. Thus, it can be envisioned that this trapped gas serves as the source for bubble nucleation and growth in the gas injection zone inside the extruder, and the extent of foaming continues to grow as the melt advances downstream. Data from Figure 4.11 show that the “carryover” or entrainment is quite significant and may play an important role during the foaming process.

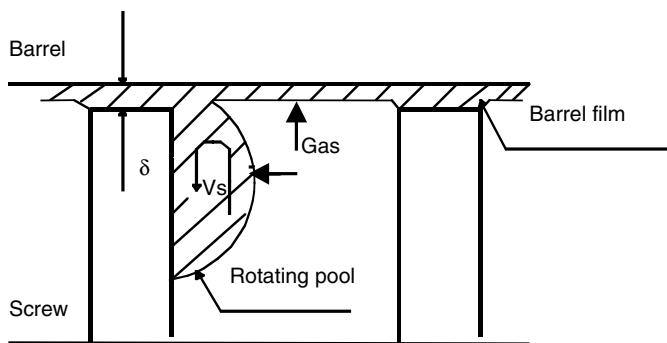


FIGURE 4.10

Schematic of the mass transfer areas in a particular filled screw channel (δ = flight clearance, V_s = melt circular flow velocity).

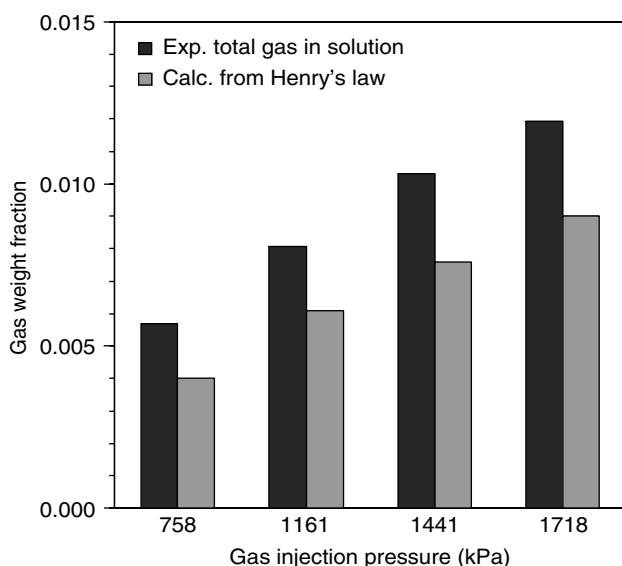


FIGURE 4.11

The amount of CO₂ dissolved in PS (at 215°C in twin-screw extruder) vs. that calculated from equilibrium.

The effects of the extrusion process parameters on solubility characteristics were also studied using the same in-line method. Detailed results can be found in Zhang et al.⁴⁴

4.4 Resin Properties

4.4.1 Importance of Viscoelasticity

During the cell growth phase of extrusion foaming, the polymeric melt undergoes intense elongational deformations. Rheologically inadequate resins cannot sustain these deformations and their foaming process is characterized by unstable cell growth, nonuniform cell size, and membrane tearing (blowout) leading to cell collapse and open cells. Many commercially available low molecular weight (MW) resins including PP, PET, and high-density polyethylene (HDPE), usually having narrow molecular weight distribution (MWD), exhibit inadequate rheology for low density foaming and a very narrow process foaming window. Such resins are characterized rheologically by low values of melt viscosity, particularly elongational viscosity that is not

dependent on increasing stress or time; poor shear sensitivity in viscosity curves; and low “melt elasticity” expressed with criteria such as melt strength and extrudate swell.⁴⁵

Effects related to melt rheology and melt elasticity of thermoplastics can, in general, be controlled through additives or through changes in MW and MWD during reactor or post-reactor processing by chain extension, grafting and branching, cross-linking, or controlled degradation. “Melt elasticity” changes can be related to changes in the values of viscoelastic functions such as normal stress difference, storage modulus, extensional viscosity, or recoverable shear strain; and also to changes in parameters of practical importance such as extrudate swell and melt strength.⁴⁶

For example, foamable polypropylene has higher “melt elasticity,” melt strength, and extensional viscosity with strain hardening behavior than conventional resins of the same melt flow index (MFI) (Figures 4.12 and 4.13); foamable PPs may also have higher M_z and high M_z/M_w , and possibly bimodal MW distribution with the higher MW component highly branched.⁴⁷ Strain hardening behavior, defined as the rapid increase of the elongational viscosity with time or strain under a constant strain rate, is also required for other processes such as thermoforming or blow molding. Particularly, high melt strength or elasticity is an important parameter usually associated with increases in the average relaxation time and broadening of relaxation time distribution as a result of long chain branching. Most polymers with long chain branches exhibit marked strain hardening.^{48,49} Such behavior was found in bimodal resins or resins of high polydispersity also having higher melt strength and higher extrudate swell. Improved melt elasticity may also be correlated with improved foamability of PET resins.⁵⁰ Long chain branching has also been

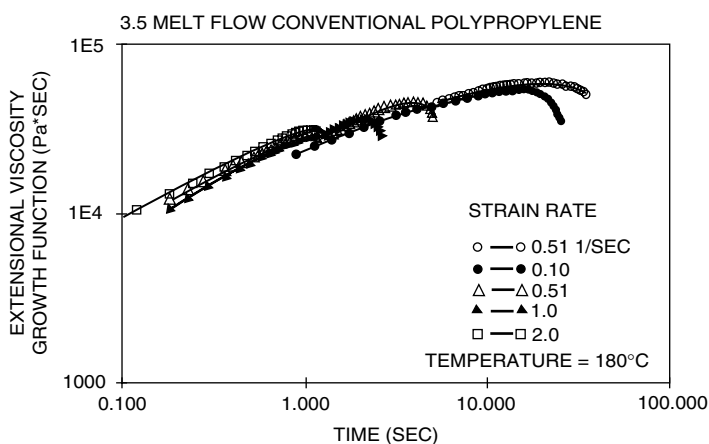


FIGURE 4.12

Extensional viscosity of linear PP.⁴⁷

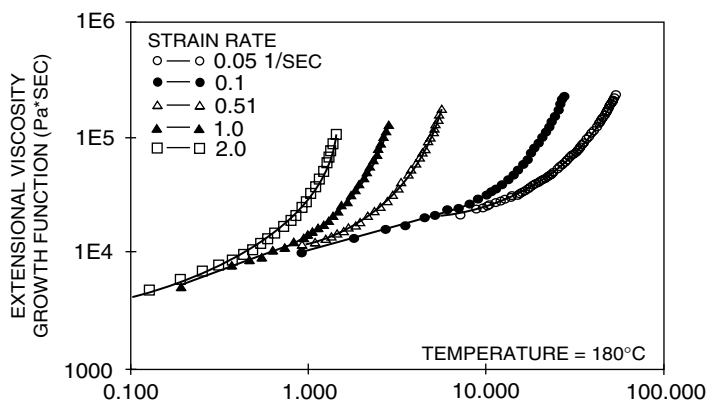


FIGURE 4.13
Extensional viscosity of high melt strength PP.⁴⁷

suggested to enhance the strain hardening behavior of the elongational viscosity because of the depression of chain contraction, which has been well recognized by theoretical approaches based on the Doi–Edwards “tube” model.^{51–53}

Yilmazer et al. studied the chain extension and branching of PET and reported that modified PET was characterized by low MFI, high extrudate or die swell, high viscosity, high shear sensitivity, high storage modulus, and pronounced non-Newtonian behavior⁵⁴ (Figure 4.14). The modified resins were suggested to have higher mean relaxation times and relaxation strength values than the unmodified ones.

Yamaguchi and Suzuki⁵⁵ studied the rheological properties and foam processability of blends of linear and crosslinked polyethylenes. They found

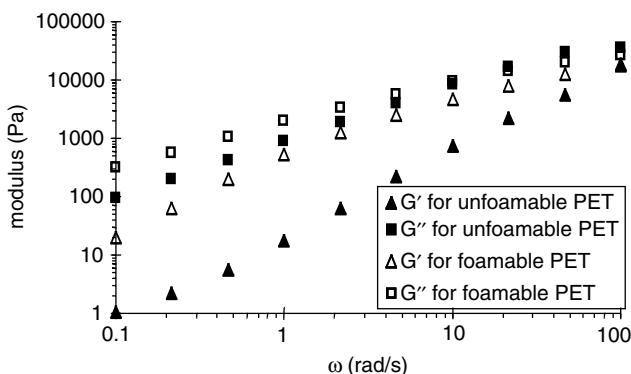


FIGURE 4.14
Comparison of G' and G'' at 290°C of unmodified (unfoamable) and modified (foamable) PET resins.

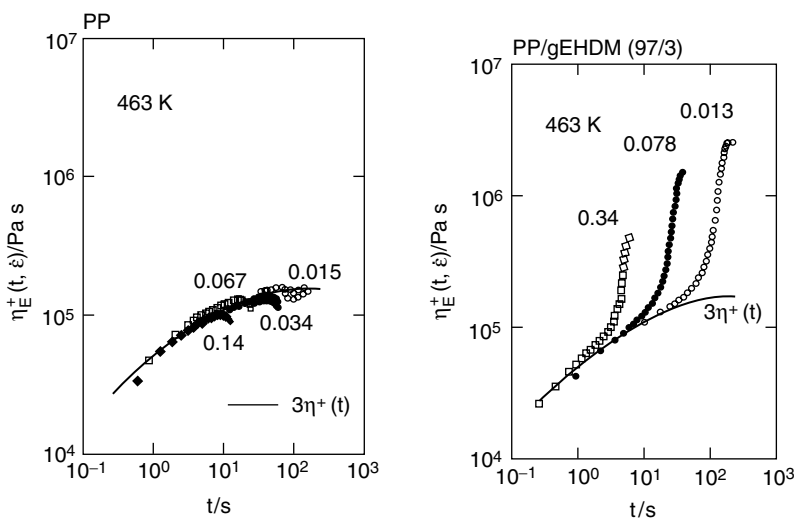


FIGURE 4.15

Time variation of elongational viscosity for PP and foamable PP/crosslinked elastomer blend.⁵⁵

that blending a small amount of crosslinked LLDPE enhanced strain hardening of the elongational viscosity (Figure 4.15) and enhanced extrudate/die swell and elastic modulus, whereas it had little effect on the steady-state shear viscosity. The foams produced from these blends showed higher expansion ratio and more homogeneous cell size distribution. According to the studies by Yamaguchi et al., the conditions under which a small amount of crosslinked polymer enhances the strain-hardening in elongational viscosity of a polymer are (1) the crosslinked polymer has a network chain with a low density of crosslink points; and (2) the precursor of the crosslinked polymer is miscible with the linear polymer.^{56–58} The origin of the resulting rheological properties has been suggested to be the result of the chain stretching of network polymers via trapped entanglements with a linear polymer. Recent work has suggested that the presence of gel-like structures in the amount of at least 70% is required for foaming resins, with the resultant foams having minimal shrinkage.^{56,58}

4.4.2 Modification of Resins to Enhance Foamability

Physical entanglements and entanglements originating from aromatic ring interactions are believed to be responsible for the foamability of LDPE and PS, respectively. Contrary to the case for LDPE, the role of strain hardening has not been clearly defined for PS. Both resins are easy to foam and do not require any further modification.⁶ However, for other resins such as PP, HDPE, and PET, long-chain branching modification in the polymerization reactor or by post-reactor reactive extrusion has been used to enhance foamability and broaden the processing window during extrusion foaming;

foamability in such cases is usually related to enhanced melt strength and strain hardening or extrudate swell. Other methods proposed in the literature to enhance foamability include:

- Introduction of bimodality as with a high MW component in a bimodal MWD PS resin
- Nonreactive blending of immiscible polymers, e.g., LLDPE + LDPE
- Reactive processing, e.g., grafting of styrene on PP; compatibilization of PP/PET blends through functionalized polyolefins and coagents; incorporation of a dispersed crosslinked polymeric phase in a polymeric matrix as, for example, in certain thermoplastic vulcanizates; PP blends with crosslinked diene based elastomers; LLDPE containing small amounts of cross-linked LDPE; PP + crosslinked EHDM

Specific methods that have been used to improve the foamability of PP are

- Long chain branching through low temperature free radical modification with radiation or peroxides in the absence of oxygen
- Controlled crosslinking, grafting with multifunctional monomers, coagents, vinyl silanes, or styrene (by irradiation or peroxides)

Modified PP resins are characterized by high melt strength and drawability in a Rheotens apparatus and can be foamed to very low densities (0.05 g/cc).^{59,60}

A significant body of literature exists describing the post-reactor modification of linear PET resins to increase MW and broaden the MWD for foaming and extrusion blow molding applications.⁶¹ Modification is carried out through the use of suitable multifunctional chain extenders with anhydride or glycidyl functionality which are able to react with the polymer end groups during solid stating or, alternatively, when added during a reactive extrusion process. Reactions of polyester end groups with anhydride and epoxy functionalities are shown in [Figures 4.16](#) and [4.17](#), respectively. The production of extrusion foamable polyesters modified by solid state polyaddition with a premixed multifunctional modifier, e.g., pyromellitic dianhydride (PMDA) is discussed in a series of patents and publications.⁶²⁻⁶⁴ These resins are distinguished from non-foamable resins by increased MW, as measured by intrinsic viscosity I.V. (>0.9 dl/g), increased melt strength, high extrudate swell, increased complex viscosity with higher shear sensitivity, and increase in storage modulus. Post-reactor modification by reactive extrusion of PET carried out using PMDA or other branching additives also results in significant increase in zero shear viscosity, increase in melt strength and die swell, increase in molecular weight, and increases in the polydispersity ratio M_z/M_n from about 4.5 up to 11. Property changes depend on the choice of process conditions and additive concentration and its type of carrier.^{65,66} Foams with densities of 0.2 g/ml were obtained by injecting hydrogenated chlorofluorocarbons in the primary extruder of a tandem line.⁶⁵ In another patent on PET foaming,⁶⁶ isopentane was injected into the

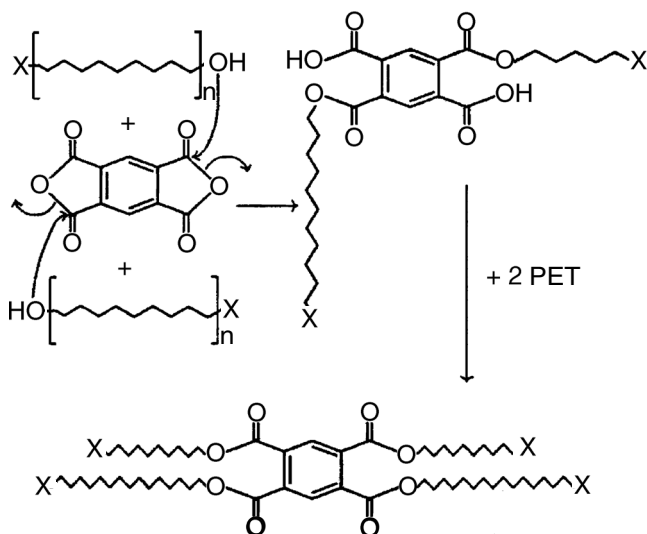


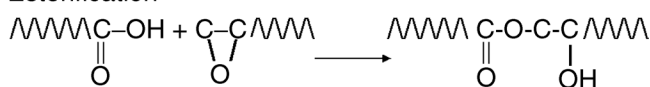
FIGURE 4.16

Esterification of PET with PMDA.⁶⁴

molten blend of PET and PMDA to produce rod-shaped foams. The expansion of the extrudate was proportional to the amount of PMDA added (up to 0.4% by weight); the density values for the PMDA modified foams ranged from 0.35 to 0.13 g/ml vs. 0.7 g/ml when no PMDA was used.

In a recent publication⁶⁵ it was shown that production of low-density PET foams by one-step reactive modification/gas injection foaming is feasible at process conditions not significantly different than those employed in the

Esterification



Etherification

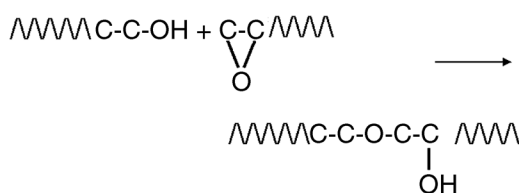


FIGURE 4.17

PET end group reactions with epoxides.⁶⁷

simple PET reactive modification with low MW additives. In initial experiments PET was chain extended with a dianhydride, benzophenone tetracarboxylic anhydride (BTDA, solid, tetrafunctional), and a triepoxide, triglycidyl isocyanurate (TGIC, solid, trifunctional), in a 40 : 1 L : D SSE. It was assumed that only initial OH groups react with dianhydrides and only initial COOH groups react with epoxides at the process conditions. Table 4.3 shows that changes in the reactive extrusion related parameters (die pressure, extrudate swell) and product characteristics (melt flow index and melt strength) as a result of increasing MW and MWD depend on the type of the modifier. A one-step reactive extrusion/foaming with 2–3 phr isobutane injected at 19 L : D length was carried out with the PET and the PET/BTDA system under the same operating conditions (Figure 4.18). The unmodified PET showed 120% expansion with only a few irregular cells; by contrast the BTDA modified extrudate showed 540% expansion, low density of 0.13 g/cc, and uniform cells. Enhanced foamability of PET may be obtained through the addition of a lower melting temperature polymer such as PP. In this case it has been shown that proper compatibilization of the immiscible blend through a functionalized polyolefin and a coagent is important to produce foams with lower density and smaller cell size (Figure 4.19).⁶⁷

With respect to reactive blending as a means of enhancing foamability, low density and uniform cell structure foams were successfully produced from blends containing LLDPE and peroxide crosslinked LDPE (xLDPE) in a batch foaming process.⁶⁸ It was shown that high loadings (50%) of xLDPE were necessary to bring up properties (including melt strength) to foamable levels (Figure 4.20). Blending a small amount (10 wt%) of xLDPE also resulted in significant improvements in LLDPE foam extrusion processability and product quality; foams had larger expansion, uniform cell structure, and ~30% density reduction versus the unmodified LLDPE. Blending recycled xLDPE foam with LLDPE was also effective in producing foamable resins, opening new applications for recycling xLDPE foams.

TABLE 4.3

PET Extrusion Characteristics with Different Modifiers (Solid Extrudates)⁶⁷

Additive	Die Pressure (Mpa)	Die Temperature (°C)	Extrudate Appearance	Average Die Swell (Std. Dev.)	Melt Flow Index (g/10 min), Initial Reading	Melt Flow Index (g/10 min), Average	Melt Strength (10 ⁻³ N)
No additive	0.96	270.6	Smooth, soupy	0.82 (0.04)	>200	>200	Not measurable
BTDA	3.38	274.1	Smooth	2.65 (0.19)	5.18	6.69	13.0
TGIC	15.20	279.6	Wavy, variable diameter	3.07 (0.11)	1.06	1.09	332.0

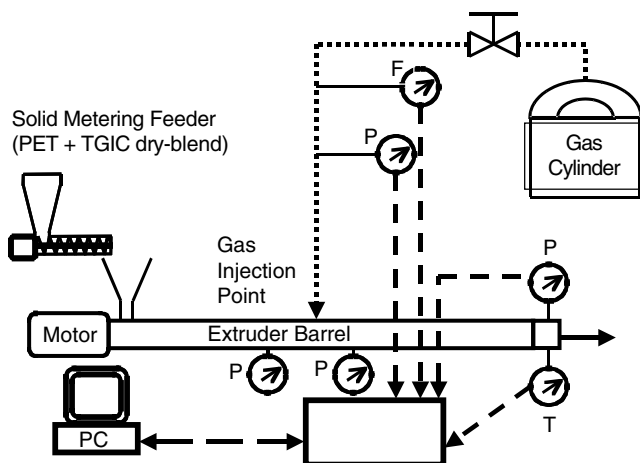


FIGURE 4.18
One step reactive extrusion/foaming of PET.

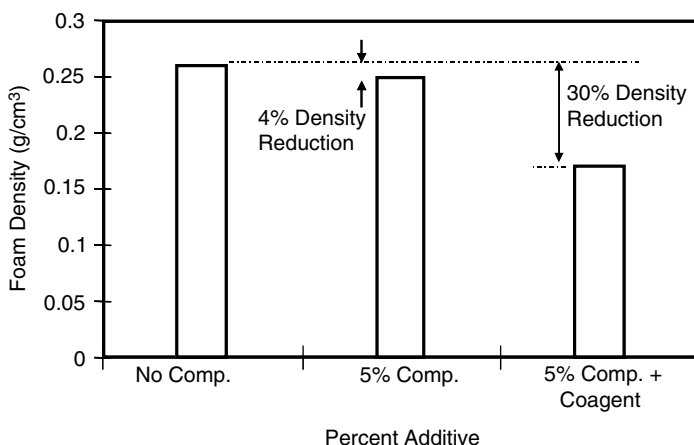


FIGURE 4.19
Foam density of 80 : 20 (PET : PP) blend as a function of additive content.

4.5 Concluding Remarks

The objective of this chapter was to summarize the importance of certain properties of physical blowing agents and polymeric resins that are used to produce low density foams by PBA injection in extruders. Emphasis was placed on (a) the importance of solubility of the PBA in the polymer melt, and (b) the viscoelastic characteristics of the polymer melt.

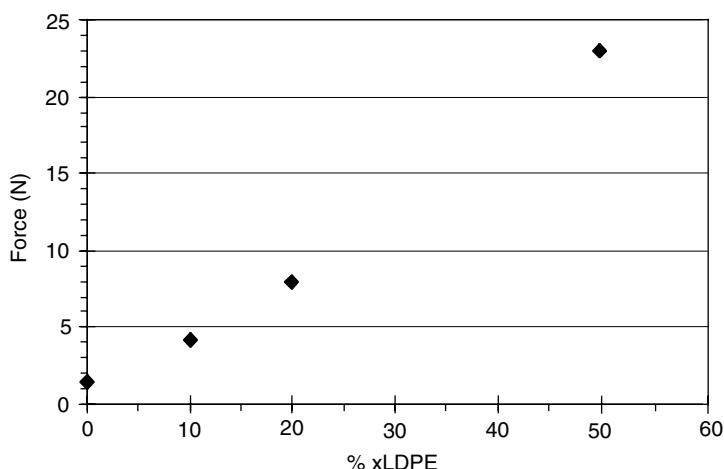


FIGURE 4.20

LLDPE resin property enhancement—melt strength vs. added xLDPE (170°C; die L/D = 10; draw ratio = 100).⁶⁸

With respect to current efforts in the field of PBAs, activities mostly focus on the commercialization of foams containing alternative environmentally friendly PBAs that are nonflammable and nontoxic. The best examples are atmospheric gases, particularly supercritical gases such as CO₂, which has already been used with polystyrene, and water, which has been used in certain thermoplastic vulcanizates. Commercialization of such foams may require modification of extrusion process conditions as well as changes or adjustments in the polymer formulation to accommodate the lower solubility and different permeability of the alternatives versus conventional PBAs. The alternative PBAs are often used in combination with other low boiling point liquids (e.g., alcohols) to balance solubility and diffusivity requirements. As a result of such activities, the need has emerged to measure accurately solubilities of the PBAs in the melt under extrusion conditions and the concomitant effects on the viscosity of the gas laden polymer. Such data are necessary to assist the process and die design requirements; this has led to the development of a variety of in-line/on-line instrumentation. Adoption of alternative PBAs has presented more challenges in the case of multiphase, multicomponent systems (immiscible polymer blends, thermoplastic elastomers, composites) where solubilities and diffusivities of the PBA in the various phases may differ.

With respect to efforts in the field of enhancing the foamability of a variety of resins, the recognition of the importance of structural modification to enhance melt strength has led to the commercial availability of several resins, such as PP, PET, and miscellaneous polyolefins that are now foamable to low densities. Modification can be accomplished in the polymerization reactor by irradiation, by reactive extrusion, or through polymer/polymer blending. In addition to the production of conventional closed-cell foam structures,

such techniques are currently under evaluation for the production of open cell structures with high fluid absorption characteristics.

Acknowledgments

The authors would like to express their appreciation to Dr. S.K. Dey of the Polymer Processing Institute for his contributions to the measurement of the “dynamic” solubility of the blowing agents.

References

1. Khemani, K.C., Extruded polyester foams, in *Polymeric Foams*, ed. K.C. Khemani, American Chemical Society, Washington, D.C., 54–80 1997.
2. Handa, Y.P. and Zhang, Z., New pathways to microcellular and ultramicrocellular polymeric foams, Symposium on Porous, Cellular and Microcellular Materials, *ASME Intern. Mech. Eng. Congr. Exp.*, 82, 1, 1998.
3. Martini-Vvedensky, J., Suh, N.P., and Waldman, F.A., U.S. Patent 4,473,665, 1984.
4. Trexel Inc., Technical literature on MuCell process, Woburn, MA.
5. Throne, J.L., *Proceedings of Foam Conference 96*, LCM Public Relations, Somerset, NJ, 2, 1996.
6. Gendron, R. and Daigneault, L.E., Rheology of thermoplastic foam, in *Foam Extrusion: Principles and Practice*, ed. S.T. Lee, CRC Press, Boca Raton, FL, 2000.
7. Wang, W.C., Kramer, E.J., and Sachse, W.H., Effects of high-pressure CO₂ on the glass transition temperature and mechanical properties of polystyrene, *J. Polym. Sci., Polym. Phys. Ed.*, 20, 1371, 1982.
8. Wissinger, R.G. and Paulaitis, M.E., Glass transition in polymer/CO₂ mixtures at elevated pressures, *J. Polym. Sci., Part B: Polym. Phys.*, 29, 631, 1991.
9. Dey, S.K., Jacob, C., and Biesenberger, J.A., Effect of physical blowing agents on crystallization temperature of polymer melts, *Proceedings of 1994 SPE ANTEC*, San Francisco, CA, 2197, 1994.
10. Handa, Y.P., Kruus, P., and O'Neill, M., High-pressure calorimetric study of plasticization of poly(methyl methacrylate) by methane, ethylene, and carbon dioxide, *J. Polym. Sci., Part B: Polym. Phys.*, 34, 2635, 1996.
11. Zhang, Z. and Handa, P.Y., CO₂-assisted melting of semicrystalline polymers, *Macromolecules*, 30, 8505, 1997.
12. Anon., Acceptable exposure limit lowered, Health Hazard Alert, Office of Health, U.S. Department of Energy, Washington, D.C., 92–1, September 1992.
13. Gabriele, M.C., New foam extrusion technology is “environmentally friendly,” *Plast. World*, 42, 30, 1996.
14. Jacob, C. and Dey, S.K., Inert gases as alternative blowing agents for extruded low density polystyrene foam, *J. Cell. Plast.*, 31, 38, 1995.

15. Paquet, A. and Vo, C.V., Foams 99 Conference, Parsippany, NJ, October 1999.
16. Moulinie, P., Gendron, R., and Daigneault, L.E., Gas solubility as a guide to physical blowing agent selection, Proceedings of the Foamplas '98 Conference, 123, 1998.
17. Han, C.D., Dispersed flow of gas-charged polymeric systems, in *Multiphase Flow in Polymer Processing*, Academic Press, New York, 1981.
18. Stiel, I.L. and Harnish, D.F., Solubility of gases and liquids in molten polystyrene, *AIChE J.*, 22, 117, 1976.
19. Sato, Y. et al., Solubilities of carbon dioxide and nitrogen in polystyrene under high temperature and pressure, *Fluid Phase Equilib.*, 125, 129, 1996.
20. Durrill, P.L. and Griskey, R.G., Diffusion and solution of gases in thermally softened or molten polymers: Part I. Development of technique and determination of data, *AIChE J.*, 12, 1147, 1966.
21. Durrill, P.L. and Griskey, R.G., Diffusion and solution of gases in thermally softened or molten polymers: Part II. Relation of diffusivities and solubilities with temperature, pressure and structural characteristics, *AIChE. J.*, 15, 106, 1969.
22. Park, C.B. and Cheung, L.K., A study of cell nucleation in the extrusion of polypropylene foams, *Polym. Eng. Sci.*, 37, 1, 1997.
23. Xie, H. and Simha, R., Theory of solubility of gases in polymers, *Polym. Int.*, 44, 348, 1997.
24. Van Krevelen, D.W., *Properties of Polymers*, 2nd ed., Elsevier, Amsterdam, 1976.
25. Berens, A.R. and Huvar, G.S., Interactions of polymers with near critical carbon dioxide, in *Supercritical Fluid Science and Technology*, ACS, Washington, D.C., 1989.
26. Elkovitch, M.D., Lee, L-J, and Tomasko, D.L., Proceedings of 56th SPE ANTEC, Atlanta, GA, 1855, 1998.
27. Elkovitch, M.D., Lee, L-J, and Tomasko, D.L., Proceedings of 57th SPE ANTEC, New York, 2811, 1999.
28. Lee, M., Tzoganakis, C., and Park, C.B., Effects of supercritical carbon dioxide on PE/PS blend viscosity and morphology, Proceedings of 56th SPE ANTEC, Atlanta, GA, 2570, 1998.
29. Lee, M., Tzoganakis, C., and Park, C.B., Extrusion of PE/PS blends with supercritical CO₂ in a twin-screw extruder and a twin/single tandem system, Proceedings of 57th SPE ANTEC, New York, 2806, 1999.
30. Simha, R. and Moulinie, P., Statistical thermodynamics of gas solubility in polymers, in *Foam Extrusion: Principles and Practice*, ed. S.T. Lee, CRC Press, Boca Raton, FL, 2000.
31. Lundberg, J.L., Wilk, M.B., and Huyett, M.J., Sorption studies using automation and computation, *I&EC Fundam.*, 2, 1, 37, 1963.
32. Micheals, A.S., Vieth, W.R., and Barrie, J.A., Solution of gases in polyethylene terephthalate, *J. Appl. Phys.*, 34, 1, 1, 1963.
33. Rein, D.H. et al., CO₂ diffusion and solubility in a polystyrene-polybutadiene block copolymer with a highly oriented lamellar morphology, *Macromolecules*, 23, 4456, 1990.
34. Dagli, S.S., Staats-Westover, R.F., and Biesenberger, J.A., Measurement of gas solubility and relationship to extruded foam properties: a new apparatus and some data on nitrogen in polyolefins, Proceedings of 47th SPE ANTEC, New York, 889, 1989.

35. Wong, B. and Handa, Y.P., A high-pressure electrobalance based in-situ technique for determining the solubility and diffusivity of gases in polymers, Proceedings of 55th SPE ANTEC, Toronto, Canada, 1979, 1997. Also in *J. Polym. Sci., Part B: Polym. Phys.*, 36, 2025, 1998.
36. Kamiya, Y., Hirose, T., Mizoguchi, K., and Naito, Y., Gravimetric study of high-pressure sorption of gases in polymers, *J. Polym. Phys.*, 24, 1525, 1986.
37. Thomas, Y. et al., In-line NIR monitoring of composition and bubble formation in polystyrene/blowing agent mixtures, *J. Cell. Plast.*, 33, 516, 1997.
38. Sahnoune, A. et al., Application of ultrasonic sensors in the study of physical foaming agents for foam extrusion, *J. Cell. Plast.*, 37, 429, 2001.
39. Tsujimura, I., Zenki, T., and Ishida, M., Visual analysis of bubble nucleation in foam extrusion die, Proceedings of PPS-14, Yokohama, Japan, 1998.
40. Biesenberger, J.A. and Sebastian, D.H., *Principles of Polymerization Engineering*, John Wiley & Sons, New York, 1983.
41. Todd, D.B., Private communication, Polymer Processing Institute, Newark, NJ, November 1999.
42. Park, C.B., Continuous production of high-density and low-density micro-cellular plastics in extrusion, in *Foam Extrusion: Principles and Practice*, ed. S.T. Lee, CRC Press, Boca Raton, FL, 2000.
43. Zhang, Q., In-line measurement of solubility of physical blowing agents in thermoplastic melts as related to extrusion foaming, Ph.D. thesis, New Jersey Institute of Technology, 2000.
44. Zhang, Q., Xanthos, M., and Dey, S.K., Effects of process conditions on the dissolution of carbon dioxide in PS in foaming extruders, *Intern. Polym. Proc.*, 16, 223, 2001.
45. Xanthos, M., Yilmazer, U., Dey, S.K., and Quintans, J., Melt viscoelasticity of polyethylene terephthalate resins for low density extrusion foaming, *Polym. Eng. Sci.*, 40, 3, 554, 2000.
46. Xanthos, M., Tan, V., and Ponnusamy, A., Measurement of melt viscoelastic properties of polyethylene and their blends—a comparison of experimental techniques, *Polym. Eng. Sci.*, 37, 6, 1102, 1997.
47. Bradley, M.B. and Phillips, E.M., Proceedings of 48th SPE ANTEC, Dallas, TX, 36, 717, 1990.
48. Meissner, J., Raible, T., and Stephenson, S.E., Rotary clamp in uniaxial and biaxial extensional rheometry of polymer melts, *J. Rheol.*, 25, 1, 1, 1981.
49. Meissner, J. and Hostettler, J., A new elongational rheometer for polymer melts and other highly viscoelastic liquids, *Rheol. Acta*, 33, 1, 1, 1994.
50. Japon, S., Leterrier, Y., and Mason, J. A. E., Recycling of poly(ethylene terephthalate) into closed-cell foams, *Polym. Eng. Sci.*, 40, 8, 1942, 2000.
51. McLeish, T.C.B., Larson, R.G., Molecular constitutive equations for a class of branched polymers: the pom-pom polymer, *J. Rheol.*, 42, 1, 81, 1998.
52. Doi, M. and Edwards, S.F., *The Theory of Polymer Dynamics*, Clarendon, Oxford, 1986.
53. Wagner, M.H., Rubio, P., and Bastian, H., The molecular stress function model for polydisperse polymer melts with dissipative convective constraint release, *J. Rheol.*, 45, 6, 1387, 2001.
54. Yilmazer, U., Xanthos, M., Bayram, G., and Tan, V., Viscoelastic characteristics of chain extended/branched and linear polyethylene terephthalate resins, *J. Appl. Polym. Sci.*, 75, 3171, 2000.

55. Yamaguchi, M. and Suzuki, K-I., Rheological properties and foam processability for blends of linear and crosslinked polymer blends, *J. Polym. Sci., Part B: Polym. Phys.*, 39, 18, 2159, 2001.
56. Yamaguchi, M. and Miyata, H., Strain hardening behavior in elongational viscosity for binary blends of linear polymer and crosslinked polymer, *Polym. J. (Tokyo)*, 32, 2, 164, 2000.
57. Abe, S. and Yamaguchi, M., Study on the foaming of crosslinked polyethylene, *J. Appl. Polym. Sci.*, 79, 2146, 2001.
58. Folland, R. et al., Low density extruded polypropylene foams, Proceedings of SPE FOAMS 2002 Conference, Houston, TX, 1, 2002.
59. Mispreuve, H. et al., Novel high melt strength polymers for foam applications, Proceedings of SPE FOAMS 2002 Conference, Houston, TX, 9, 2002.
60. Xanthos, M. and Dey, S.K., Foam extrusion of polyethylene terephthalate (PET), in *Foam Extrusion: Principles and Practice*, ed. S.T. Lee, CRC Press, Boca Raton, FL, 2000.
61. Al Ghatta, H.A.K., Severini, T., and Astarita, L., Polyester foams and their manufacture, World Patent WO 9,312,164, 1993.
62. Al Ghatta, H.A.K., Process for production of high molecular weight polyesters from resins with low intrinsic viscosity, World Patent WO 9,308,226, 1993.
63. Al Ghatta, H.A.K. and Pizzetti, M., Continuous production of high-molecular-weight polyesters, and fibers therefrom, World Patent WO 9,325,600, 1993.
64. Khemani, K.C., Jaurez-Garcia, C.H., Boone, G.D., Foamable polyester compositions having a low level of unreacted branching agent, U.S. Patent 5,696,176, 1997.
65. Khemani, K.C., Rheologically improved polyesters for foams, Proceedings of 56th SPE ANTEC, 1934, 1998.
66. Hayashi, M., Amano, N., Taki, T., and Hirai, T., Process for producing polyester foam resin and polyester resin foam sheet, U.S. Patent 5,000,991, 1991.
67. Zhang, Q., Dhavalikar, R., Wan, C., Dey, S.K., and Xanthos, M., Sequential reactive blending/foaming of PET in extrusion equipment, Proceedings of SPE FOAMS 2002 Conference, Houston, TX, 47, 2002.
68. Zhang, Q., Dey, S.K., and Xanthos, M., Batch and continuous foaming of blends of LLDPE and cross-linked LDPE, Proceedings of SPE FOAMS 2002 Conference, Houston, TX, 19, 2002.

Foam Stability in Flexible Polyurethane Foam Systems

X.D. Zhang, R.A. Neff, and C.W. Macosko

CONTENTS

5.1	Introduction
5.2	Fundamentals of PU Foams
5.3	Cell Opening Mechanisms
5.3.1	Aqueous Foam
5.3.1.1	Film Rupture Mechanisms
5.3.1.1.1	Capillary-wave mechanism
5.3.1.1.2	Nucleation of Pores
5.3.1.1.3	Solute Transport Mechanism
5.3.1.1.4	Solid Particle Defoaming
5.3.1.2	Factors for Short-Term Stability
5.3.1.2.1	Film Drainage
5.3.1.2.2	Prevention of Local Thinning
5.3.2	Critical Review of Proposed Cell Opening Mechanisms in Flexible Polyurethane Foam
5.3.2.1	Urea Precipitation (Solid Particle Defoaming)
5.3.2.2	Surfactant Phase Separation (Insoluble Liquid Droplets Defoaming)
5.3.2.3	Foam Matrix Viscosity Rise
5.3.2.4	Surface Phase Transition
5.3.2.5	Spontaneous Film Rupture
5.3.2.6	Extensional Thinning and Rupture
5.3.2.6.1	Bingham Plastic
5.3.2.6.2	Extensional Thinning
5.3.2.6.3	Cell Opening Mechanism
5.4	Controlling Cell Opening in Flexible Polyurethane Foam
5.4.1	Silicone Surfactant: Surface Rheology Effect
5.4.2	Other Formulation Ingredients: Bulk Rheology Effect
5.5	Summary
	References

5.1 Introduction

The addition polymerization reaction of diisocyanates with alcohols was discovered by Dr. Otto Bayer and coworkers in 1937. This discovery set up the fundamental chemistry for the polyurethane industry, which exceeded 4 billion pounds by 1994 in the U.S. alone.¹ Through a variety of starting materials, polyurethanes are now formulated into a wide variety of end uses including both nonfoam and foam applications. Nonfoam applications include coatings, adhesives, sealants, and elastomers. Among the numerous foam applications are rigid foam for insulation or construction, semirigid foam for various automotive interior applications, and flexible foam for cushioning. Flexible polyurethane foam can be either molded or produced continuously on a conveyor in a slabstock process. Of all the applications for polyurethanes, flexible slabstock foam accounts for the largest volume produced. Depending on the formulation, a wide range of densities and mechanical properties are available for flexible polyurethane foam. Such versatility is an advantage shared by no other type of cushioning material.

The process that produces polyurethane foam is complex and involves simultaneous gas generation, polymerization, and phase separation. A unique cell structure results (see Figure 5.1) comprised of struts (of thickness on the order of microns) and window films (of thickness on the order of tenths of microns). This cell structure is in contrast to that of low density thermoplastic foam, whose cell membranes and struts are of similar and uniform thickness and are well represented by intersecting planes.² Low density rigid foam, whether polyurethane or thermoplastic, is typically closed celled. In such materials, the blowing agent remains trapped and good insulating properties are retained. However, without sufficient porosity (air flow), flexible polyurethane foam would have an undesirable pneumatic feel upon compression, in addition to exhibiting shrinkage after production. Shrinkage results as the foam temperature cools from its maximum exotherm of about 160°C to room temperature.³ The diffusion of carbon dioxide out of the foam cells (which occurs faster than the diffusion of air into the cells) also contributes to shrinkage. Thus, for flexible polyurethane foam, a high content of open cell windows is required in order to obtain both dimensional

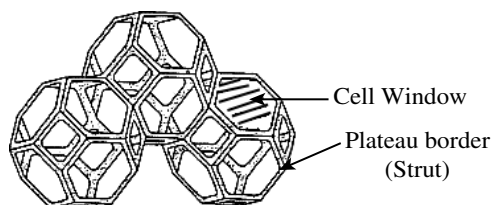


FIGURE 5.1

Illustration of structural features in a foam cell.

stability and the desired mechanical properties for cushioning. Molded flexible polyurethane foam normally requires a crushing operation in order to open the cell windows. In slabstock foam, the porosity results from a sudden and rapid cell opening event occurring within the process, which is unique to its special chemistry.

In the slabstock foam process, the foam initially goes through a stage where the continuous phase is a flowable liquid. Liquid foam is intrinsically unstable; thus the liquid film separating bubbles can become thin and rupture. Without proper control of film thinning, gas bubbles will coalesce, possibly leading to foam collapse. One key to foam stability is preventing localized thinning within the thin film. This can be accomplished through either the Marangoni effect, which is driven by interfacial properties, or the bulk rheological properties of the continuous phase. Most of the previous film rupture studies were conducted on aqueous foams where interfacial properties are dominant, while bulk rheology is less important. In polyurethane foams, both interfacial properties and bulk properties are important in providing foam stability. Nevertheless, concepts from the considerable volume of available literature on aqueous foams are still relevant in order to understand the early stages of the polyurethane foaming process.

In flexible polyurethane foam, a silicone surfactant is added to alter the interfacial properties. The surfactant controls the rate of window film thinning (through drainage into the struts) and prevents rupture by localized thinning until the cell opening event occurs. Thus the surfactant helps to control the open cell content. The timing of the cell opening event is critical—if it occurs too early (before the struts have developed adequate strength through bulk rheology), the struts will fail and the foam will collapse. If the event occurs too late, then the polymer in the cell windows will have strengthened to the point where few or none of the cell windows will rupture. The correct timing of cell opening is obtained through proper balance of polymerization (gelling) and gas generation (blowing). Catalysts are added to promote both of these reactions, and adjustment of these additive levels normally provides the proper chemical balance.

The mechanism by which the extraordinary cell opening event occurs in slabstock foam has been postulated in much recent scientific literature. Critical reviews of this literature, in addition to relevant literature covering aqueous foam, are included in this chapter. The cell opening mechanism is then clarified, in order to explain all of the observed phenomena. Finally, a discussion of the roles of catalysts and surfactants is provided to illustrate the functions of the tools available to a foam manufacturer for controlling cell opening.

5.2 Fundamentals of PU Foams

The formation of flexible polyurethane foam is an intricate process employing two simultaneous reactions: urethane formation, which produces a

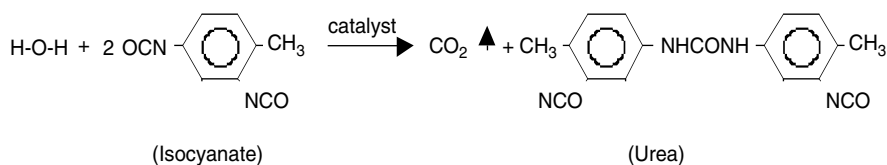
covalent polymer network, and CO₂ blowing, which secondarily forms polyurea.^{3,4} The reaction of the isocyanate group with active hydrogen-containing compounds to form urethanes is the basis of polyurethane chemistry. In water-blown flexible polyurethane foams, two active hydrogen-containing compounds are involved, water and polyol. The reaction between isocyanate and polyol (secondary alcohol used in this study) is called the gelling reaction. Usually, the polyol and isocyanate used are polyfunctional, and this reaction leads to crosslinked polymers as shown in Figure 5.2.

Over 90% of the foam volume is the carbon dioxide generated from the reaction of an isocyanate with water. This reaction is called the gas-producing reaction or blowing reaction. A flexible foam formulation can contain many additives to provide the desired properties of the final product. The basic ingredients include polyol, water, isocyanate, silicone surfactant, and catalyst. The formulation used in this study is listed in Table 5.1. A detailed discussion of these ingredients can be found in the literature.^{1,5}

The nonionic silicone surfactant is used to achieve stable cells. It can retard drainage flow in cell windows and prevent cell coalescence until the material gains sufficient strength to be self-supporting. The stabilization of cell windows has a great effect on the cell opening event and thus affects the porosity of the final foam product.

Catalysts are used for both the blowing reaction and the gelling reaction. The tertiary amine catalyst can form a complex in which the tertiary nitrogen

A. Blowing Reaction:



B. Gelling Reaction:

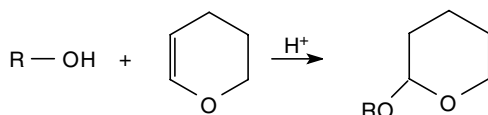
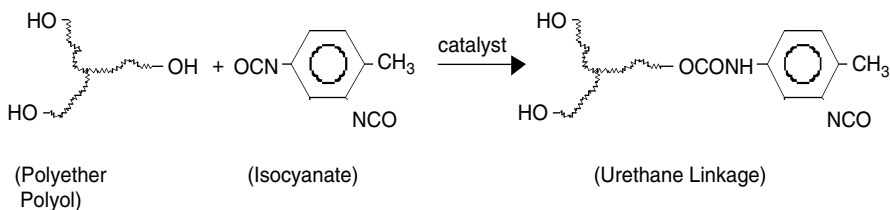


FIGURE 5.2

Chemical reactions during polyurethane foam formation.

TABLE 5.1

Typical Flexible Foam Formulation

Component	Description	Company	Parts by Weight
Polyol (Voranol™ 3137)	A 3100 Mw polyether polyol with functionality of 3, 87% propylene oxide and 13% ethylene oxide	Dow Chemical	100
Water	Deionized water	U of Minnesota	2–6
Isocyanate (Voramate™ T-80)	An 80:20 mixture of the 2,4- and 2,6-isomers of toluene diisocyanate	Dow Chemical	40–60
Silicone surfactants	Silicone-polyether copolymer	OSi Specialty	0.2–5
Amine catalyst (Dabco® 33LV)	33% triethylenediamine in 67% dipropylene glycol	Air Products	0.1–1.0
Tin catalyst T-9	Stannous octoate catalyst	Air Products	0.0–0.5

donates electrons to the carbonyl carbon of the isocyanate group. Thus the amine catalyst can accelerate both the isocyanate–water (blowing reaction) and isocyanate–hydroxyl reaction (gelling reaction). Organometallic tin catalysts are used primarily to accelerate the reaction of isocyanate with hydroxyl groups (gelling reaction). These catalysts are more active than the amine catalysts and thus are used in smaller amounts. The overall mechanisms of catalysis by the tertiary amine catalyst and the organometallic tin catalyst are discussed by Herrington and Hock.¹ By adjusting the catalyst's level and ratio, the desired balance between gelling reaction and blowing reaction can be achieved.

5.3 Cell Opening Mechanisms

In the past 30 years, many researchers have studied the foaming process, and various hypotheses have been proposed on the cell opening mechanism. Some researchers attempted to extend classical aqueous foam defoaming mechanisms to polyurethane foams. Others attributed the polyurethane foam cell rupture to a specific factor in the polyurethane system. In this section, various cell opening mechanisms are discussed and examined. Aqueous foam mechanisms are reviewed, and mechanisms previously and currently proposed for polyurethane systems are discussed in the context of the aqueous foam literature and more recent work.

5.3.1 Aqueous Foam

Liquid foam is a thermodynamically unstable system. Liquid cannot support stress and will flow under external forces such as gravity and capillary pressure. Aqueous foam systems have been studied extensively and a rich

literature regarding film rupture and film stability can be found in this area. A brief summary of aqueous film rupture mechanisms and factors that control short-term stability are reviewed here.

5.3.1.1 Film Rupture Mechanisms

To achieve foam stabilization, it is imperative to understand the mechanism of film rupture. Several mechanisms of rupture of liquid films have been proposed.

5.3.1.1.1 Capillary-wave mechanism

This is the most widely used mechanism for film rupture in liquid foam systems and emulsion systems. This mechanism assumes that in an ideal liquid film with no heterogeneous structures such as particles and droplets, the film will rupture by the growth of surface waves on the film surfaces. The waves originated from thermal motion will grow rapidly when the film reaches a critical thickness. This model was proposed by Vrij.⁶ The original model has been greatly modified. The most recent modification by Sharma and Ruckenstein considers the effects of film thinning on the growth of the surface waves.⁷ The mean film thickness at rupture (h_{cm}) is calculated by the following equation:

$$h_{cm} = \left(\frac{0.015A^2(2\xi_0)^{0.164}}{24\pi^2\mu\sigma v_{t,c}} \right)^{0.24} + 797R^{0.25} - 209$$

where $v_{t,c}$ is the film thinning velocity, ξ_0 is the thermal wave amplitude, A is the Hamaker constant, μ is the liquid matrix viscosity, σ is the surface tension, R is the film radius in cm, and the final film thickness calculated from this equation is in angstroms.

5.3.1.1.2 Nucleation of Pores

This mechanism was proposed by Derjaguin and Gutop.⁸ It is used primarily to explain rupture of ultra-thin films between two surfactant monolayers. The driving force for nucleation of pores is the decrease of the surface energy that occurs when two interfaces merge. This is opposed by the edge energy of the pore periphery, which can be described as the line tension. Above a critical pore size, the deduction of surface energy will overcome the increase of the edge energy and the pore will grow and cause film rupture. Below this pore size, the pore will shrink and film will remain stable.

5.3.1.1.3 Solute Transport Mechanism

The solute transport mechanism was investigated experimentally and theoretically by Ivanov et al.⁹ When solute transfers across the film by diffusion

process, an instability can develop. For systems with high levels of soluble gas, transport of gas across the film can cause significant instability and lead to the growth of capillary waves and cause film rupture at greater thickness.

5.3.1.1.4 Solid Particle Defoaming

The presence of solventphobic solid particles can destabilize a liquid foam system. For example, silica particles are often used as an important part of commercial antifoaming agents.^{10,11} The defoaming mechanism for solid particles was proposed by Frye and Berg¹² (Figure 5.3).

When the thickness of the liquid film is smaller than the particle size, the particle will bridge the film as shown in Figure 5.3. If the particle is solventphobic, then the contact angle will be larger than 90° . This will cause liquid drainage away from the particle and start the dewetting process, which causes thinning and rupture of the film. The rate of dewetting is directly related to the contact angle and hence the degree of solventphobicity of the particle.

When the solid particle is solventphilic, the contact angle will be less than 90° . This small contact angle will prevent dewetting and film rupturing. Solventphilic particles will actually increase the stability of many foam systems.¹⁴ This stabilization effect is mainly attributed to two factors. First, particles can increase the viscosity of the liquid matrix and reduce the drainage rate. Slower drainage will increase the lifetime of a foam system. The second stabilization factor is that solid particles can stabilize the foam system by introducing a structural force.^{15,16} The oscillatory structural forces occur when solid particles are confined between two surfaces of a thin film. Each

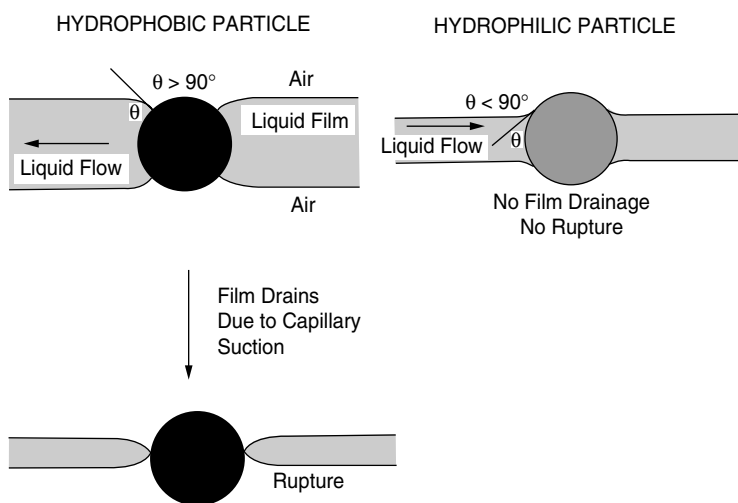


FIGURE 5.3

Schematic representation of liquid film rupture process by hydrophobic particles.¹³ (Reprinted by courtesy of Marcel Dekker, Inc.)

www.iran-mavad.com

surface will induce ordering among the neighboring particles. When the two film surfaces approach, the two structured zones next to the surfaces will overlap. This structured particle array between film surfaces will require more energy for the film to thin further, since thinning of the film will disrupt packing of the particles. This is the origin of the structural force in a solid dispersion system. This effect tends to stabilize the film.

5.3.1.2 Factors for Short-Term Stability

Maintenance of proper foam stability is important to avoid catastrophic coalescence of the bubbles and foam collapse. Much literature exists in the area of aqueous foam stability, most in the area of long-term stability, where disjoining pressure within the film is the key for film stability. During polymeric foam formation, short-term stability and stability under expansion are important. Long-term stability in time scale of hours and above is not relevant.

Two factors are important in short-term foam stability: film drainage rate and ability to prevent local thinning in liquid film. Drainage rate determines how long the film can remain above the critical rupture thickness and what percentage of the film is below the critical rupture thickness. Localized thinning can be detrimental to film stability and needs to be controlled to provide uniform film thinning and foam stability.

5.3.1.2.1 Film Drainage

In the foam matrix, the liquid lamella will drain to the Plateau borders under capillary suction and gravity.¹⁷ How fast liquid drains out of the film will determine film thickness and foam density.

Liquid in thin films will drain into the Plateau border (Figure 5.2) under capillary pressure. Assuming the liquid lamella is a plane-parallel film with a tangential immobile surface, the axisymmetric drainage rate V_{Re} can be described by the Reynolds equation:

$$V_{Re} = -\frac{dh}{dt} = \frac{2\Delta p h}{3\eta R^2}$$

where h is the film thickness, η is the bulk viscosity, R is the radius of the film, and Δp is the pressure drop that drives film draining. This pressure drop is a combination of Plateau border suction and disjoining pressure. However, in actual foaming process, liquid film surfaces are not immobile since the bubbles are constantly subject to shearing and stretching. Surfactant diffusion will limit the surfactant surface coverage.

For films with a mobile surface, drainage will cause the movement of the surface layer and a surfactant surface concentration gradient will be generated. The surfactant surface concentration gradient will cause a surface ten-

sion gradient along the surface that will retard the film drainage. This effect is called the Gibbs–Marangoni effect and is reviewed by Scriven and Sternling.¹⁸ The surface tension gradient can be affected by the diffusion of surfactant along the surface as well as the diffusion of surfactant from the bulk. Thus the surface rheology of the film, such as surface viscosity, becomes important since it will affect the surface diffusion of the surfactant. The drainage can be obtained by solving the Navier–Stokes equations under the lubrication approximation accounting for the mobile surface.¹⁹

$$V_o = \frac{dh}{dt} = \frac{h^3 \Delta p}{24 \eta R^2} \left[\sum_{n=1}^{\infty} \frac{(6\eta + \eta_s k_n^2 M h) J_2(\lambda_n)}{(6\eta + 6M + \eta_s k_n^2 M h) \lambda_n^3 J_1(\lambda_n)} \right]^{-1}$$

where J_0 , J_1 and J_2 are Bessel functions, eigenvalues λ_n are solutions of equations $J_0(\lambda_n) = 0$ and $k_n = \lambda_n/R$. The surface mobility of the film is accounted for by surface viscosity η_s and mobility parameter M . The mobility parameter M includes the contributions of both bulk and surface diffusion to the Marangoni effect and is defined as the following:

$$M = \frac{3D\eta}{\gamma \left(\frac{\partial \lambda}{\partial c} \right)_0} \left[1 + \frac{2D_s \left(\frac{\partial \Gamma}{\partial c} \right)_0}{Dh} \right]$$

where D and D_s are the bulk and surface diffusion coefficients of surfactant, respectively. C is the surfactant concentration in the bulk and Γ is the surface excess concentration of the surfactant on the air/liquid interface. Increasing either D or D_s will cause a faster drainage rate since it will increase the mobility parameter and reduce the surface tension gradient. Interfacial viscosity will change the D_s value and the ability to maintain a surface tension gradient. This is one of the reasons high interfacial viscosity can help foam stabilization. The analysis for drainage rate in a thin liquid film with constant area is shown in the above section. It will be impractical to obtain all the parameters shown in these equations. However, the analysis indicates which factors will contribute to film drainage.

5.3.1.2.2 Prevention of Local Thinning

The other key to foam stability is the prevention of local thinning and rupture of liquid films under deformation. This can be accomplished by either the Gibbs–Marangoni effect or bulk rheology effect.

The short-term foam stability can be provided by the Gibbs–Marangoni effect or the dilational film elasticity of foam lamella. Prevention of local thinning will reduce the rupture thickness of the liquid film and increase foam stability. Variables like surface shear viscosity, surface dilational viscosity, and surface transport can affect both the drainage rate of the liquid

film and the ability to prevent local thinning in the film. Without the minimum level of surface elasticity or surface viscosity, foam will be unstable upon any disturbance. Local thinning can be a result of drainage or a sudden disturbance force. Local thinning of the film will result in an increase of surface area at the thinning point. The surfactant concentration in this area will decrease. As a result, a surface tension gradient is established. This surface tension gradient will tend to pull the two surfaces together. A second function of the surface tension gradient is that it will promote surface transportation of surfactant into the thinning point. This surfactant transportation will drag the underlying layer of the liquid into the thinning point as well. As a result, the thinning point is “healed.” There has been little attempt to measure the dilational film elasticity for personal wash products.

Bulk rheology can have a significant effect on local thinning as well. For aqueous foams, the bulk rheology is usually Newtonian and low viscosity. In this system, the Gibbs–Marangoni effect is the key mechanism for uniform thinning. When bulk viscosity is high, the surface effect becomes less significant. Viscosity of the continuous phase and its extensional rheological behavior become more important. In general, strong extensional thinning systems will promote localized thinning of films and lead to film rupture and bubble coalescence. On the other hand, strain hardening of the foam matrix is shown to have a positive effect on foam stability of thermoplastic foams.²⁰

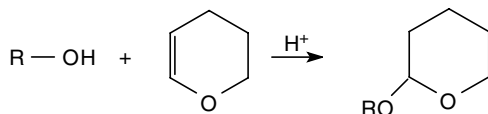
5.3.2 Critical Review of Proposed Cell Opening Mechanisms in Flexible Polyurethane Foam

5.3.2.1 Urea Precipitation (Solid Particle Defoaming)

In a polyurethane foam system, the urea precipitation occurs a few seconds before the cell opening. These particles are stiffer than the liquid matrix and may cause rupture of the film. This hypothesis was originally proposed by Rossmly and coworkers.²¹ This mechanism is a direct extension of the classical solid particle defoaming mechanism and is consistent with the fact that the cell opening always occurs after the urea precipitation occurs regardless of the formulation used. However, the urea precipitation is linked to the matrix by urethane linkages and is unlikely to dewet the surrounding liquid. It is also known that the highly polar urea groups have high surface energy and will be wetted by the low surface energy liquid matrix. As a result, the urea precipitate defoaming mechanism should not be valid.

To test this mechanism, two experiments were performed. In the first experiment, water was reacted with toluene diisocyanate in a flask to generate solid urea particles. These solid particles were then collected. Solid particles of 0.2 pphp were added into a surfactant solution in polyol. Foam column tests were performed to test the stability of liquid foam with and without the addition of the urea particles. The result of this experiment shows that the foam system with urea solid particles has a higher stability and longer foam life than that without the urea particles.

The second test was performed using a similar idea to the first test, except the particles were made inside an end-capped polyol. The end-capping was prepared by capping the hydroxyl group with dihydropyran:²²



350 g of Voranol 3137 polyol, 100 index of dihydropyran, 400 mL methylene chloride, and 0.1 g p-toluenesulfonic acid were placed in a 2000 mL flask. The mixture was stirred using a 1.5 in. magnetic stir bar for 2 h at room temperature; 0.5 g sodium bicarbonate and 50 g of 4 molecular sieves were added to the flask and allowed to stir overnight to neutralize the acid and remove residual water. After filtering, the mixture was placed in a rotary evaporator and heated to 70°C to remove the methylene chloride. The mixture was then placed in a flask and stored under vacuum overnight to remove traces of volatile components. The completion of end-capping can be monitored by the disappearance of the hydroxyl group (3450 cm⁻¹).

Water (0.25 pphp) and isocyanate (100 index) were added to a surfactant solution in end-capped polyol and toluene. The end-capping prevented reaction between polyol and isocyanate, and toluene was added to keep the viscosity of the solution low and the same for solutions with and without urea particles. The solutions with urea particles showed significantly higher stability than those without urea particles using the static foam column test. This again shows that a small amount of *in situ* formed urea particles enhances the stability of the liquid film system. The solid dewetting mechanism does not apply in a flexible polyurethane foam system.

5.3.2.2 Surfactant Phase Separation (Insoluble Liquid Droplets Defoaming)

Insoluble liquid droplets can dewet the film and cause foam rupture in much the same way as the solid particles. The complication in liquid droplet defoaming is that the liquid droplets are deformable and can spread along the film surface. This will create some problem for the liquid droplets to properly bridge the film. There are numerous studies on how insoluble liquid droplets spread and bridge the film.^{12,13} Once the insoluble liquid droplets bridge the film, they will either stabilize or destabilize the film. If the three-phase contact angle is larger than 90°, then these droplets will destabilize the film and cause poor foam stability.

For the polyurethane foam, one mechanism proposes that the cell opening may be due to the silicone surfactant added.^{23,24} This mechanism assumes a decrease in solubility of the surfactant in polyol with increasing temperature. As the temperature rises above a critical value, the surfactant will phase separate and act like a defoamer.

This mechanism suggests a simple model. The surfactant structure will affect the critical temperature of surfactant phase separation and cell opening time. At a different cell opening time, the modulus of the foam material will be different, thus resulting in a different final foam porosity. The effect of the silicone surfactant on cell opening will be easy to predict.

In order to test this hypothesis, two experiments were performed. First, surfactant was dissolved in polyol and the temperature of the solution was controlled. The cloud point was not observed in the temperature range of 0 to 110°C. Also, the solubility of the surfactant was observed to increase with temperature. These observations oppose the proposed theory.

To further examine the surfactant phase separation hypothesis, element mapping of silicon was obtained for final cured foams. The surfactant distribution could be obtained because silicon is present only in the surfactant. A Jeol Electron Probe Microanalyzer 8900 was used for Si mapping. As electrons struck the surface of the sample in a vacuum chamber, x-rays were emitted by the sample. The concentration of silicon at each point was determined by measuring the intensity of x-rays at the characteristic wave length for silicon. Two samples were used in this study: sample A was a collapsed foam made by adding silicone oil, a commercial defoamer; sample B was a normal open cell foam made with a silicone surfactant. Results are shown in Figure 5.4. The silicon concentrations are indicated by the brightness of the pixels. In sample A, silicone oil is shown to be phase separated into micrometer size spherical particles. In sample B, silicone surfactant is shown to be very homogeneously distributed. No bulk segregation with a large enough size to cause film rupture can be observed. This experiment shows that the silicone surfactant is quite homogeneously distributed in the cured open cell foam. It appears that no surfactant phase separation in the bulk occurred. Thus the surfactant phase separation mechanism is also not likely valid.

5.3.2.3 Foam Matrix Viscosity Rise

This hypothesis suggests that as the urea phase separates, a rapid increase in the foam matrix viscosity will occur. Higher viscosity will limit the movement of the surfactant diffusion to the surface and reduce the surface tension gradient-driven transport “self-healing” by the Marangoni effect. Once the stabilizing mechanism is disturbed, the film will experience local thinning and rupture. Generally, the drainage rate of a thin liquid film will decrease linearly as the viscosity of the system increases. Higher bulk viscosity will further increase the surface tension gradient since bulk diffusion will be lower. Thus, the rise of foam matrix viscosity alone cannot explain the cell opening event.

5.3.2.4 Surface Phase Transition

In some systems, as the temperature of the foam reaches a critical temperature, the surfactant layer will experience a surface phase transition. This surface phase transition will disrupt foam stability. It will lead to faster

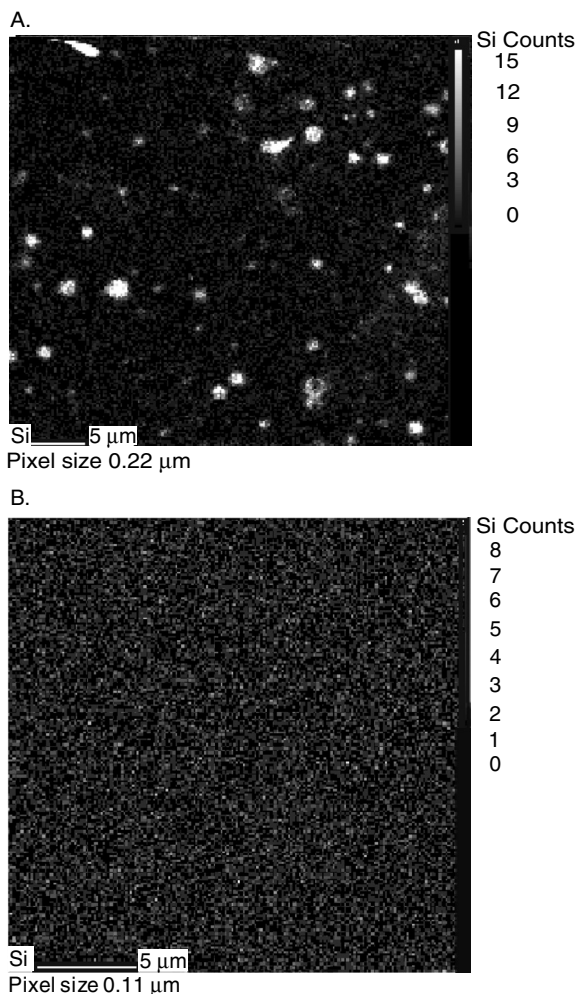


FIGURE 5.4

(A) Silicon map for Foam A (with silicone oil); (B) Silicon map for Foam B (with silicone surfactant).

drainage rate and results in film rupture.²⁵ This mechanism is theoretically sound and surface phase transition does occur for some systems. In these systems, the surfactant layer is typically a rigid layer with high intermolecular interactions since the system temperature is below the melting point of the surfactant. This rigid layer will give an immobile boundary condition for the drainage flow and will create foams with great stability. When the system temperature rises above the melting point of the surfactant, the surfactant surface layer will experience a phase transition and will become mobile. As a result of the mobile interface, the foam system will have faster drainage rate and poor foam stability. This is the basis for the surfactant

surface phase transition mechanism. In a polyurethane foam system, the silicone surfactant is very mobile even at room temperature. A rigid surfactant surface layer never exists. When the system temperature is raised, there will not be a phase transition. Thus, the surface layer phase transition mechanism may not be suitable for a polyurethane foam system.

5.3.2.5 Spontaneous Film Rupture

As mentioned previously, spontaneous film rupture, and specifically the capillary wave mechanism, is most often employed to explain film rupture in liquid foam and emulsion systems. Therefore, it will be considered here for the flexible polyurethane foam system. However, one limitation of this mechanism is that it is normally applied to homogeneous films. This is especially significant in the case of the flexible polyurethane foam system, which can have inhomogeneities such as phase-separated urea. Neff⁵ applied the relatively recent model of Sharma and Ruckenstein⁷ to estimate the upper bound for the critical film thickness at rupture for flexible polyurethane foam. He calculated this to be 15 nm, which is in the thickness range for black films.

Using light interference microscopy, the thinnest film found in polyurethane is thicker than 150 nm. This is an order of magnitude higher than the value estimated by Neff. Thus the spontaneous rupture mechanism is not valid for polyurethane foam systems.

5.3.2.6 Extensional Thinning and Rupture

The first attempt to quantify the internal cell opening time was done by Neff.⁵ Using a parallel-plate rheometer, Neff recorded the normal force that a polyurethane foam exerted on the plate during the reaction. Different stages during foaming are identified and shown in Figure 5.5.

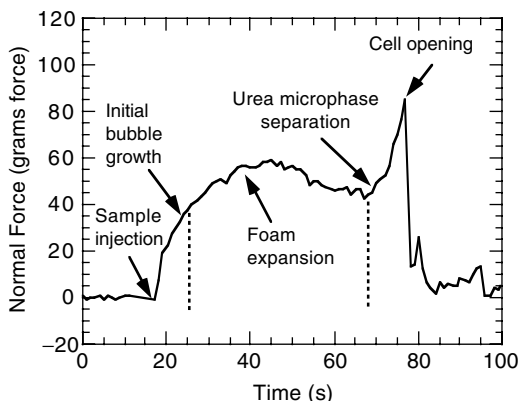


FIGURE 5.5

A typical normal force profile during polyurethane foaming.

www.iran-mavad.com

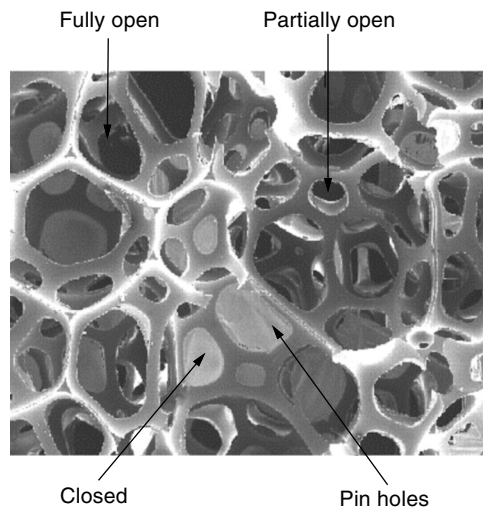


FIGURE 5.6

Different states of cell windows in polyurethane foams.²⁶

The sudden drop in the normal force is a result of the sudden stop of foam expansion due to cell opening. The onset of cell opening occurs several seconds after the onset of urea phase separation and the timing does not depend on the structure of the surfactant. This implies that cell opening is triggered by urea precipitation. However, urea particles cannot cause cell rupture by the dewetting mechanism. In water-blown foam, the particles are generated within the matrix and are chemically grafted to the matrix through urethane linkages. Neff proposed that the precipitated urea will trigger cell opening by affecting the rheological properties of the foam matrix. This is the Bingham plastic mechanism. Most suspensions show strong shear thinning and extensional thinning behavior rather than the Bingham plastic behavior. An extensional thinning mechanism is also discussed in the following.

5.3.2.6.1 Bingham Plastic

Figure 5.6 shows the different states of cell windows observed in polyurethane foams. Some cell windows have completely disappeared without any debris. This suggests that the material is capable of flow at least in the early stage of the cell opening period. The fact that the material has solidlike behavior and is capable of flow suggests that the material is described by a Bingham plastic model.^{27,28} The material behaves as a solid until a yield stress is reached; then the material yields and flows as if it were a liquid. This mechanism was proposed by Neff in 1995 and is shown schematically in Figure 5.7.

Window films are stretched during urea microphase separation. Urea aggregates formed in the film may act as stress concentrators and local

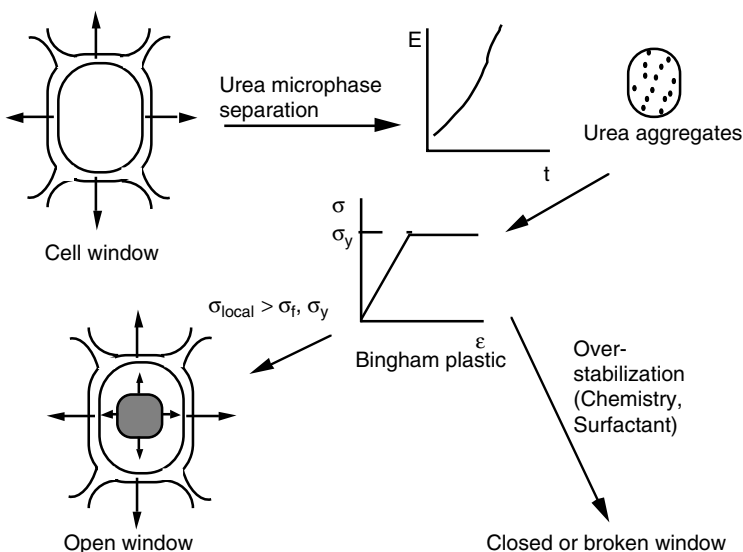


FIGURE 5.7
Proposed model for cell opening.⁵

thinning will occur. The thinned part of the film may form a hole. The hole will grow in the film, and the material flows back to the Plateau's borders. The material keeps stiffening rapidly after the onset of cell opening. The film will lose its flowability. The holes formed earlier will have enough flowability and will form fully open cell windows, while films ruptured later cannot flow very well and result in the torn-off films or partially open films. However, there is no experimental data performed to show that the phase separated polyurethane system behaves as a Bingham plastic.

5.3.2.6.2 Extensional Thinning

True Bingham plastics are rare. The more common behavior for a solid suspension is shear thinning or extensional thinning behavior. Figure 5.8 describes the development of the foam matrix during foaming. When the foam is in a liquid state, expansion of the liquid thin film will cause the film to thin down uniformly until a black film (film thickness less than 60 nm) is reached. Then the surface waves will cause spontaneous film rupture. To reach a black film, a much longer time than the foaming process is needed. When the foam is cured to an elastomer foam, then the expansion will only stretch the film and the film will relax back to the original state once the stress is released as the pressure inside the foam bun releases to the atmosphere. The cell windows rupture when the foam matrix is a pastelike material due to the precipitation of the urea aggregates.⁵ The foam matrix becomes a suspension with urea particles since the crosslinked covalent network is not yet formed.

It is known that most suspensions display shear thinning behavior.²⁷ To verify this, a model compound is made to simulate a phase separated material. 100 g of Voranol 3137, 2 parts water, and 70 index toluene diisocyanate (TDI) were placed in a beaker and mixed. The reactants were allowed to react for 24 h with a magnetic stir bar in the beaker. This material will be similar to the foam material at cell opening time for higher water part foams (4–6 parts). Since the limiting reactant TDI will be consumed mainly by water, polyol will have low conversion and the system will be practically a urea suspension in polyol. Shear viscosity is tested using parallel plate geometry with serrated surfaces. This compound shows significant shear thinning behavior (Figure 5.9). This means the foam matrix will have higher viscosity at low stress and lower viscosity at high stress.

As seen in Figure 5.10, the cell windows usually have a dimple shape. Cell windows are found to be dimple shape using the light interference microscopy method and is discussed later in this text. Once the urea phase separation occurs, the cell window will exhibit shear thinning behavior. The thinner part of the window (edges) will have much lower viscosity than the thicker part of the cell window (center). As a result, the film thinning is localized to the edge of the cell window. The localized thinning will cause the cell windows to thin rapidly and form pinholes. The cell windows containing pinholes can further develop into partially open and fully open cell windows depending on the matrix viscosity and time available for cell opening. This is why the cell opening always happens a few seconds after urea phase separation regardless of what surfactant is added into the system.

A cell window between growing bubbles, however, experiences a biaxial expansion motion rather than a simple shear. It is known that some shear thinning material actually exhibits an extensional thickening effect.²⁷ Therefore, it is important to prove that the phase separated polyurethane matrix

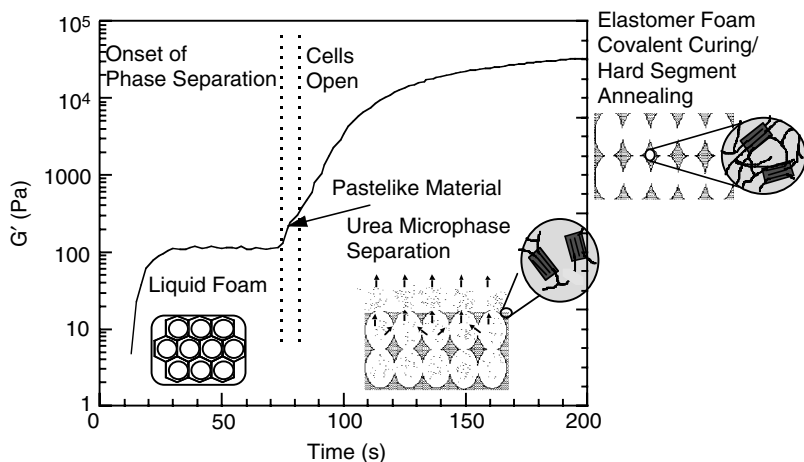


FIGURE 5.8

Foam morphology and modulus development during foaming reaction.

www.iran-mavad.com

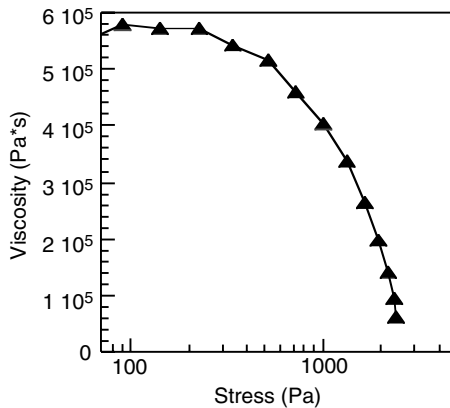


FIGURE 5.9
Shear viscosity of the model compound.

shows extensional thinning as well. This test was performed on a lubricated squeeze flow apparatus.

A lubricated squeeze flow apparatus has been used to obtain biaxial viscosity data.^{28,29} By proper choice of the lubricant viscosity, a sample under compression will experience biaxial extension without shear on the plate surfaces.²⁷ By applying different weights on the top plate, the sample will experience different stresses and deform at different extension rates. Figure 5.11 shows a schematic of the lubricated squeezing geometry.

The model compound is tested using this instrument and a strong extensional thinning behavior is observed (Figure 5.12). Thus, the phase separated model compound does exhibit extensional thinning behavior and can cause cell window rupture as illustrated in Figure 5.10. In a transient extensional viscosity test, no strain hardening is observed.³⁰ Since the shear viscosity is performed in a strain-controlled rheometer, a very limited stress range is

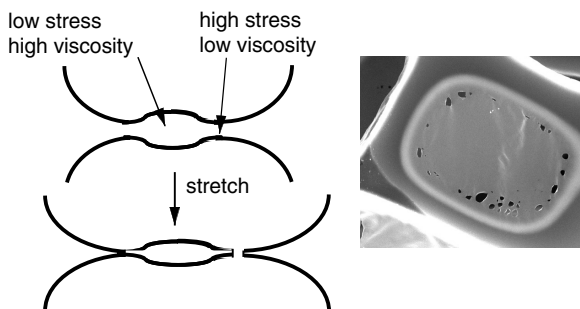


FIGURE 5.10
Schematic of the localized film thinning due to the extensional thinning behavior of the foam matrix.

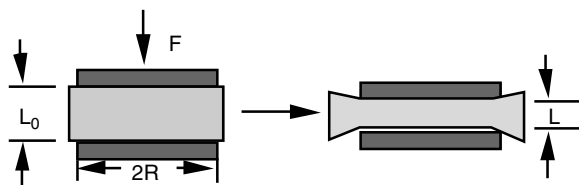


FIGURE 5.11

Schematic of the lubricated squeezing geometry.

covered and detailed correlation between shear and extensional viscosity data cannot be performed.

5.3.2.6.3 Cell Opening Mechanism

Foam formation occurs with a high exotherm. As the temperature of the foam bun gets higher, heat will be lost from the top surface of the foam bun to ambient air. As a result of the heat loss, the temperature at the top surface is lower than that of the center. This lower temperature profile will yield slower reaction kinetics and delayed urea phase separation. When the internal cell opening occurs, the top surface of the foam remains liquid. The foam will continue to expand until the internal pressure is high enough to break the liquid surface layer. This is the skin blow-off time. Cell opening is a continuous process between the internal cell opening time and the skin blow-off time. In other words, as long as foam expansion continues, the cell opening will continue.

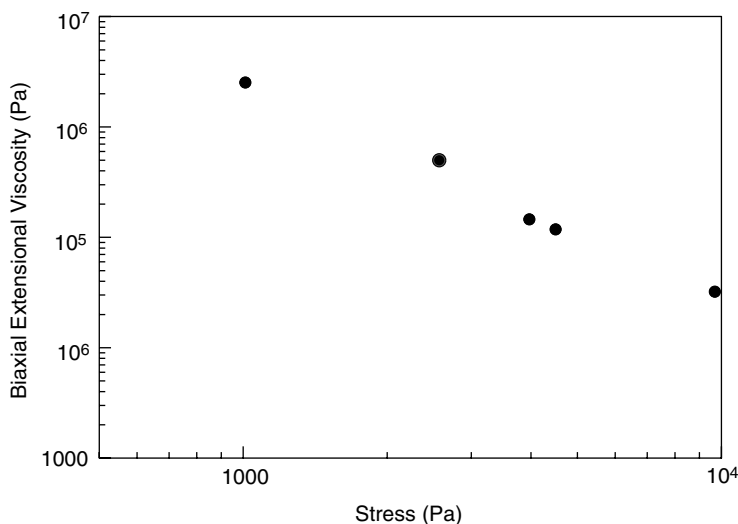


FIGURE 5.12

Biaxial extensional viscosity of the model compound.

www.iran-mavad.com

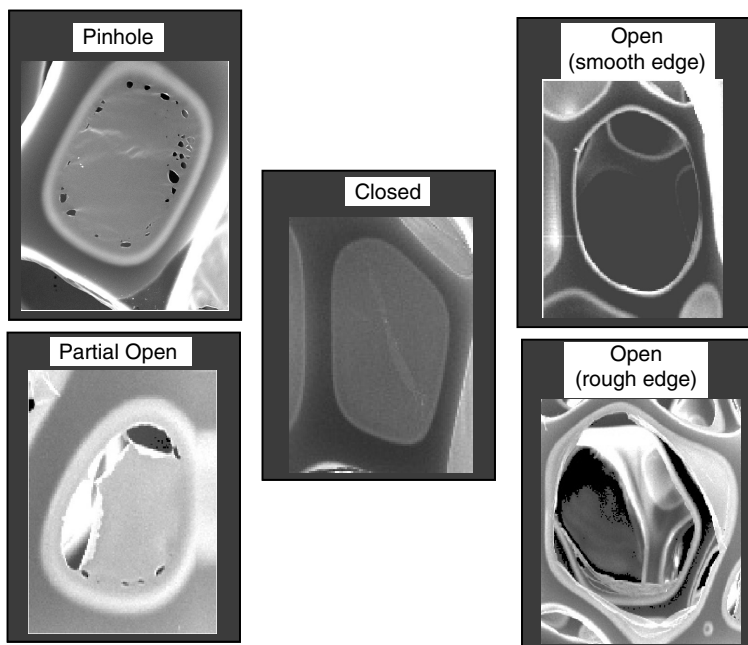


FIGURE 5.13
Various states of cell windows.

SEM shows that the cell windows are in various states. Windows with only small pinholes were observed. Fully open windows and partially open windows were also observed. In some fully open windows, the film debris is totally missed. Other fully open windows show the film debris wrinkling at the strut edge. Images of the different states of cell windows are shown in Figure 5.13.

Partially open windows showed both drained-off (circular) holes and torn-off holes. These various states of the cell windows imply that the cell windows are in a transient status from liquid to solid during the cell opening period.

It is known that different surfactant types and concentrations provide different rates of liquid film drainage.³¹ At the onset of cell opening, the cell window will have a thickness distribution. The window thickness distribution could change the fraction of broken cell windows and air flow. Figure 5.14 shows how cell windows with different morphologies are obtained. The thinner windows will rupture first when the foam matrix viscosity is low. At this stage, the foam matrix still has high flowability. As a result, the ruptured cell window flows back to the struts, and smooth edges will be obtained. The medium thickness windows will form pinholes later in the foaming process when the viscosity of the matrix is higher. At this point, the window has only limited flowability due to the high viscosity. As a result, pinholes will remain with limited growth or connected by tearing the mate-

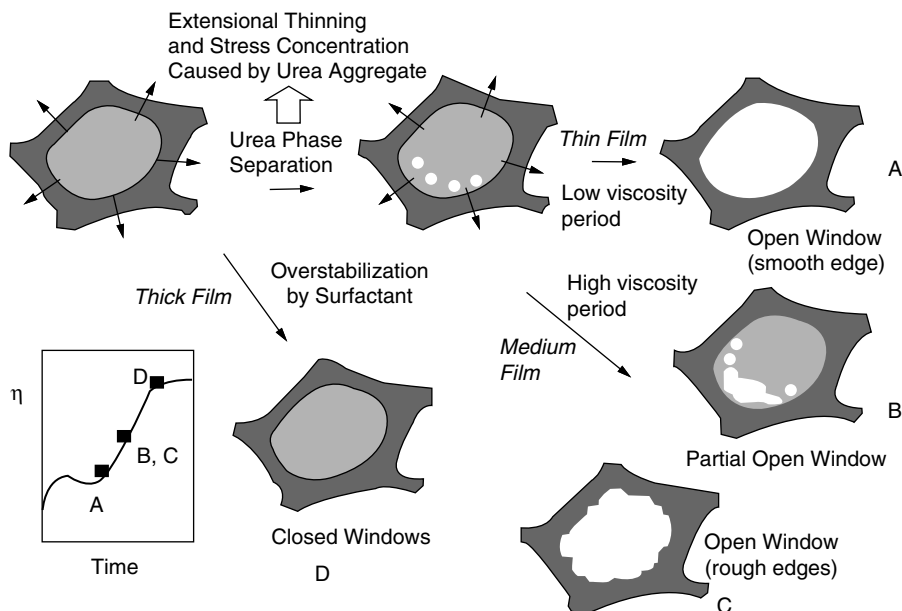


FIGURE 5.14
Cell window status development.

rial between them to form partially open cell windows and cell windows with rough edges. Finally, the very thick windows will not open since the time for window thinning is less than the time for gel reaction. These windows will remain closed after the foam is cured.

5.4 Controlling Cell Opening in Flexible Polyurethane Foam

Polyurethane foams have a variety of applications depending on their density and mechanical properties.¹ High density polyurethane foams (10–20 lb/ft³) are used in applications such as carpet backing, whereas low density foams have applications in furniture (e.g., foam in mattress), transportation (e.g., car seats), and packaging. Many physical properties of flexible polyurethane foam, such as mechanical response for cushioning, are highly affected by its air flow.³² It can be significantly affected by both reaction-related additives and silicone surfactants.

Air flow is difficult to control in practice because the role of silicone surfactant in the cell opening process has not been completely elucidated. The cells in polyurethane formed by carbon dioxide are unstable unless a silicone surfactant is used. The silicone surfactant is shown to have significant effects on the macroscopic cellular structure such as cell size and foam

air permeability. A typical surfactant is a copolymer composed of a silicone backbone and poly(ethylene oxide-co-propylene oxide) grafts. The amount of surfactant, the backbone length, frequency and composition of the grafts are varied for different polyurethane formulations.¹ The surfactant must stabilize the carbon dioxide bubbles; yet, in flexible polyurethane foam, the “windows” between the cells must rupture during polymerization to prevent shrinkage of the product. Some trends have been observed between the structure of the surfactant and the air permeability of the final foam product. Decreasing the molecular weight of the silicone backbone of the surfactant seems to increase the percentage of open cell windows. However, when the backbone is too short, the cells will collapse before the material is strong enough to support itself. Is this controlled by solubility or mobility of the surfactant in the reacting mixture? Understanding the role of silicone surfactant during foaming, especially its effect on the ruptured cell window percentage and air permeability of the final foam product, can help us design new surfactants and better control the macroscopic cellular structure.

Additives that change the reaction kinetics can also play important roles in cell opening. Since the urea separation and extensional thinning of the bulk liquid is the trigger for cell opening, controlling the balance between blowing reaction and gelling reaction to achieve proper bulk viscosity and rheological profile at urea phase separation time is a very effective way to control the degree of cell opening. A common practice in industry is to tune polyol structure, catalyst level, water level, and so forth in order to alter the cell opening process.

5.4.1 Silicone Surfactant: Surface Rheology Effect

Traditionally, it is believed that the silicone surfactant can lower surface tension, emulsify incompatible formulation ingredients, promote nucleation of bubbles during mixing, and stabilize cell windows.^{1,3} Among these functions, cell window stabilization is the most important. During foaming, the bubbles initially introduced by mechanical mixing will grow. As the volume fraction of the gas bubbles exceeds 74%, the spherical bubbles will distort into multisided polyhedra and cell windows are formed. Due to capillary forces, the liquid pressure inside the Plateau borders will be lower than that in the cell windows. This pressure difference will cause cell window thinning by sucking liquid from the windows into the struts. Without adding silicone surfactant, this drainage rate will be such that film rupture and bubble coalescence occur rapidly. It is shown in this chapter that the silicone surfactant added can retard the cell window drainage rate. Different surfactant structures will have different abilities to retard drainage, resulting in different cell window thickness distributions at the time of cell opening.²⁶ The porosity or the air permeability of the solid polyurethane foam is significantly affected by the structure of the silicone surfactant used in the formulation. Thus, it is essential to find the optimized silicone surfactant that will result in foam products with desired physical properties. For example, foam

TABLE 5.2
Designed Surfactant Series

Surfactant Structure	X	Y	Polyether Percentage	Siloxane Backbone Length
MD _x D' _y Ma	119	21	75	140
MD _x D _y M	85	15	75	100
MD _x D' _y M	51	9	75	60
MD _x D' _y M	54	6	66	60
MD _x D' _y M	57	3	50	60
MD _x D'' _y Mb	51	9	88	60

^a Branched copolymer of polydimethylsiloxane and polyether where: M = CH₃, D = (CH₃)₂Si-O, D' = (CH₃)RSi-O, R = 60% propylene oxide and 40% ethylene oxide polyether, 1500 Mw, acetoxy capped.

^b D'' = (CH₃)R'Si-O, R' = 60% propylene oxide and 40% ethylene oxide polyether, 4000 Mw, acetoxy capped.

used in filters needs high air permeability and durability, while insulation foam needs low air permeability and low flammability. However, the relationship between silicone surfactant structure and final foam properties is not well understood.

A series of surfactants (Table 5.2 and Figure 5.15) were designed to study the effects of surfactant structures on the cell opening event and the final open cell percentage.

The surfactants were prepared by reacting the polysiloxane backbone with polyether branches by Witco Corporation, OSi Specialties Group. Two variables were changed: the surfactant backbone length and the polyether branch percentage. The silicone backbone length is defined as x + y. The polyether branch percentage is defined as (y * Mw_{polyether}/Mw). Figure 5.15 describes the surfactant structure in terms of the backbone length and polyether branch percentage.

The ruptured window percentage of a foam is directly related to its air permeability.²⁶ Using the formulation listed in Table 5.1 with different surfactants, the air permeability of the resulting foam products are determined and listed in Table 5.3.

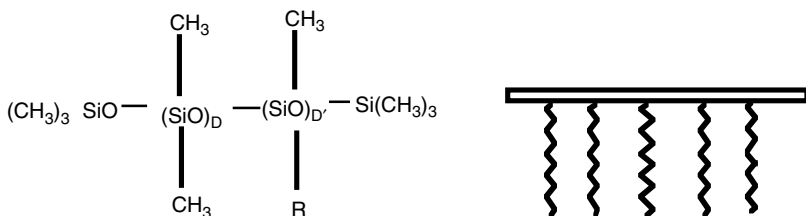


FIGURE 5.15

Typical silicone surfactant structure. [M, D_x, D'_y, M, and D' are the units that are connected to polyether branches.]

TABLE 5.3

Air Permeability for Foams Made with Different Surfactants

Surfactant	MD ₁₁₉ D' ₂₁ M	MD ₈₅ D' ₁₅ M	MD ₅₁ D' ₉ M	MD ₅₄ D' ₆ M	MD ₅₇ D' ₃ M	MD ₅₁ D'' ₉ M
Air Flow (CFM)	0.3	0.9	1.9	1.0	Collapse	Collapse

It is believed that different surfactants have different drainage retardation abilities, thus resulting in different cell window thickness distributions at the time of cell opening. This will cause the final foam product to have a different percentage of ruptured cell windows as well as a different thickness distribution for the remaining windows. To verify this, the cell window thickness in the cured solid foam was measured for foams made with two different surfactants. Surfactants with different backbone lengths (MD₈₅D'₁₅M and MD₅₁D'₉M) were used since they result in foams with the same cell size and different air permeability.

The cell window thickness was determined using the light interference method. The incident light is normal to the cell window. Light was reflected from the top surface and the bottom surface of the cell window. The two reflected beams had interference due to their difference in optical paths. The optical path difference was directly related to the cell window thickness. This path difference then leads to the various interference colors observed. Figure 5.16 shows a sample image as well as the thickness profile.

The thickness profile shows a dimple formation, which is a strong indication of the existence of a surface tension gradient. The thickness of the thin part of the window was recorded. Fifty windows were tested for foams made with these two surfactants. Figure 5.17 shows the thickness distribution of remaining cell windows.

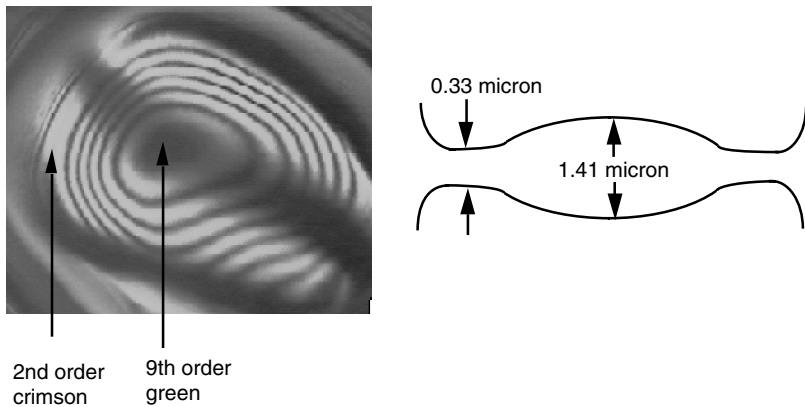


FIGURE 5.16

A cell window thickness profile determined by light interference microscopy. (Left: interference pattern of the cell membrane; Right: cross section of window and thickness profile.)

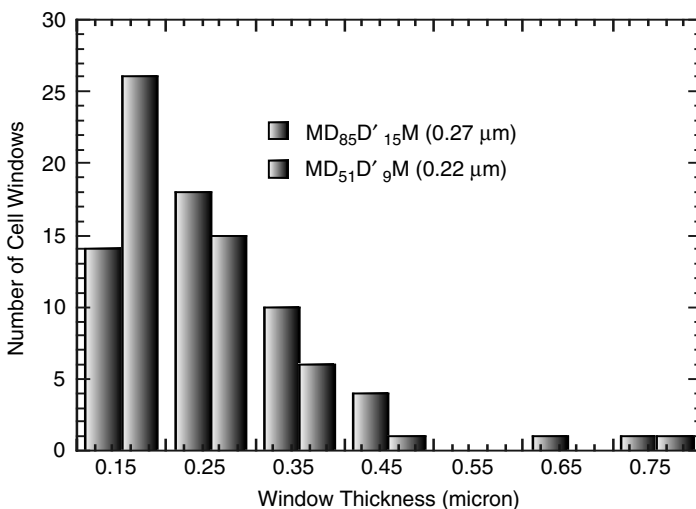


FIGURE 5.17

Window thickness distribution for foams made with different surfactants.

Different distributions are observed: foam made with surfactant MD₈₅D'₁₅M has a higher film density toward the thicker films, while foam made with surfactant MD₅₁D'₉M has a higher film density toward the thinner films. The average thickness for foam made with surfactant MD₈₅D'₁₅M is also thicker than that with surfactant MD₅₁D'₉M. The ruptured cell window percentage is counted for these two foams. Foam made with surfactant MD₈₅D'₁₅M has a rupture cell window percentage of 18%. Foam made with surfactant MD₅₁D'₉M has a higher rupture cell window percentage of 32%.

It is observed that by simply varying the surfactant used in the formulation, foams with different cell window thickness and different percentages of ruptured cell windows can be obtained. This verifies the importance of the cell window drainage rate.

Polyurethane foam develops from a shaving-cream-like liquid foam to a solid foam in about 2 min. It is very important for the surfactant to stabilize the foam lamella before the gelation of the foaming material. This is accomplished by establishing a surface tension gradient along the foam lamella and reducing the rate of thinning of the cell window. A schematic diagram is shown in [Figure 5.18](#).

Due to the capillary suction in the Plateau border, the liquid inside the lamella will drain into the Plateau border. Without the addition of surfactant, the gas/liquid interface cannot support any stress and this interface will have a slip boundary condition. The thin liquid film will rapidly thin and lead to cell window rupture and foam collapse. When a silicone surfactant is added, a surface tension gradient will develop along the gas/liquid interface and this interface can have a finite surface stress. As the bubbles are expanding, the film is expanding. This expansion, in addition to surfactant depletion, will lead to reduction of the surfactant concentration on the

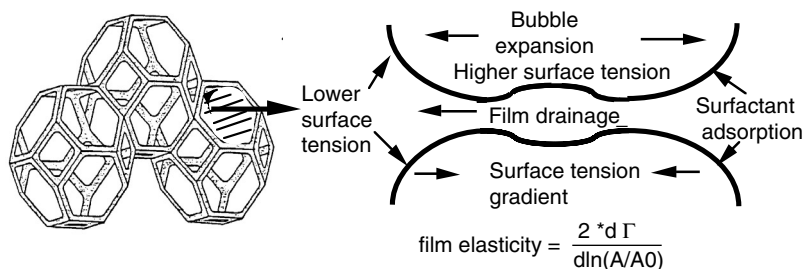


FIGURE 5.18

Schematics of cell window drainage and surface tension gradient formation.

gas/liquid interface. As a result, the surface tension will increase as the bubble expands. Meanwhile, the Plateau border experiences much less expansion and retains a low surface tension value. Thus, a surface tension gradient will exist along the film surface. The surface tension gradient will establish a surface stress and will reduce the drainage flow rate. This surface tension gradient is related to a physical parameter, the dynamic film elasticity, which is defined as the rate of surface tension increase as the film area expands. The effect of surface elasticity on thin liquid film drainage rate was investigated by Malhotra and Wasan using a numerical simulation.³³ A significant effect of the surface elasticity was observed. A large surface elasticity leads to lower surface mobility and lower film thinning rate. Measuring the film tension of the surfactant solution can provide information on the film elasticity and the surface tension gradient. The surface tension gradient will determine the boundary condition for the drainage flow in cell windows and the short-term foam stability.

The film rheometer is used to measure the film elasticity of different surfactants.³⁴ The Gibbs elasticity was obtained by recording the surface tension after the sudden expansion of a bubble. The Gibbs elasticity for different surfactant solutions are listed in Table 5.4.

The Gibbs elasticity of the silicone surfactant solution is not affected by the structure of the surfactants. In a polyurethane foam system, bubbles grow at a finite rate of about 0.02 mm³/min rather than sudden expansion. The finite expansion rate allows some surfactant diffusion and adsorption to reduce surface tension as the bubble expands. As a result, the dynamic film elasticity obtained under the finite expansion rate is always lower than the Gibbs elasticity that is obtained by sudden expansion. Figure 5.19 shows

TABLE 5.4

Gibbs Elasticity for 0.2 wt% Surfactant Solution in Voranol 3137

	MD ₁₁₉ D' ₂₁ M	MD ₈₅ D' ₁₅ M	MD ₅₁ D' ₉ M	MD ₅₄ D' ₆ M
Gibbs Elasticity (dyne/cm)	22.6	23.1	23.1	26.0

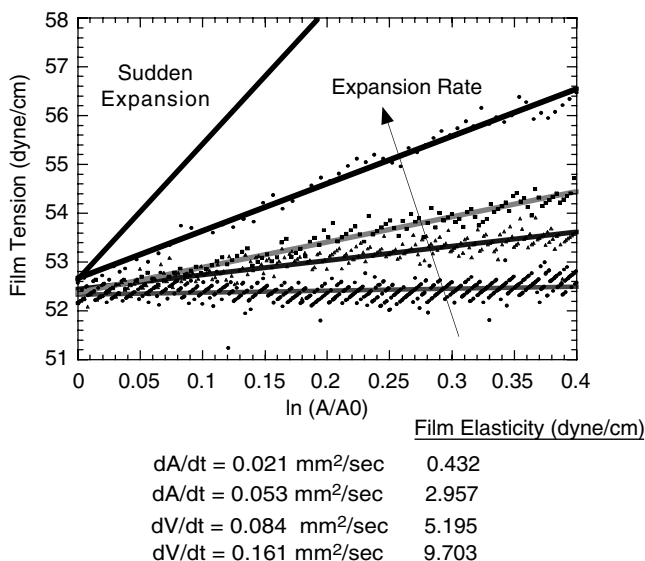


FIGURE 5.19

Effect of bubble expansion rate on dynamic film elasticity of 0.2 wt% MD₅₁D'₉M solution in Voranol 3137.

that as the expansion rate increases, the dynamic film elasticity increases because of the decreased time for surfactant diffusion and adsorption.

The information above shows that the film rheometer can give accurate, reproducible results. Next, the dynamic film elasticity of different surfactants were evaluated with an expansion rate of 0.084 mm²/sec, which is close to the actual polyurethane foam system. The higher the dynamic film elasticity, the higher a surface tension gradient can be obtained in the expanding cell window.

As shown in Figure 5.20 and Figure 5.21, as the silicone backbone length of the surfactant increases, the surface elasticity increases. The film tension after expansion is determined by the overall surfactant mobility including both bulk mobility and surface mobility. The larger surfactant will have a lower surface mobility, which will lead to a lower overall mobility. The fact that a larger surfactant has higher film elasticity suggests that the surface diffusion is significant for a thin liquid film. As a result, a higher surface tension gradient and lower surface mobility can be obtained for foams made with these larger silicone surfactants. This will give a slower drainage rate and smaller open cell window percentage in the cured polyurethane foam. On the other hand, when the percentage of polyether is varied, the observed trend is less clear.

The surfactant with very low film elasticity results in a collapsed foam due to its low drainage retarding ability. The surfactant with reasonable elasticity will result in a stable foam. When the polyether percentage of the surfactant is too high (90%), the film elasticity test cannot be performed since the bubble

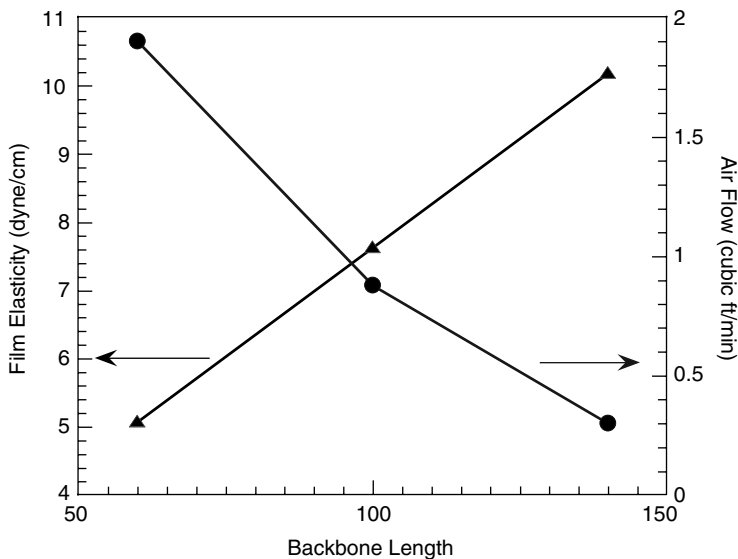


FIGURE 5.20

Effect of silicone backbone length of silicone surfactant on dynamic film elasticity. (1 wt% surfactant solution in Voranol 3137 as well as air permeability of the cured solid polyurethane foam. Polyether percentage is kept constant at 75%.)

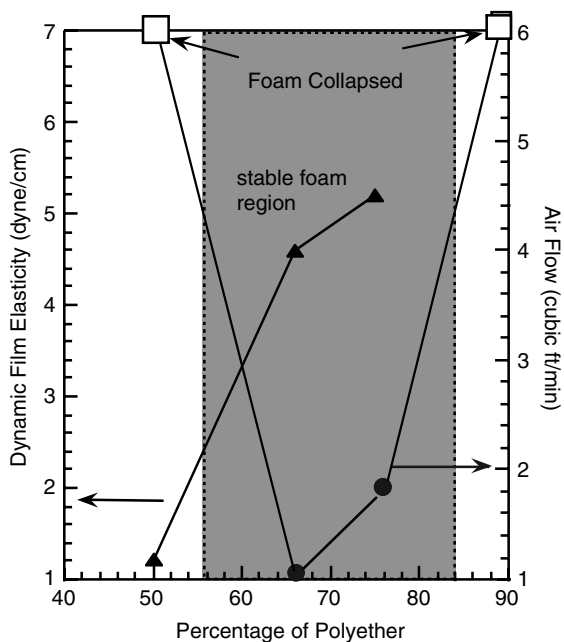


FIGURE 5.21

Effect of polyether percentage of silicone surfactant on surface tension of 0.2 wt% surfactant solution in Voranol 3137 as well as air permeability of the cured solid polyurethane foam. Silicone backbone length is kept constant at 60 (SiO) units.

www.iran-mavad.com

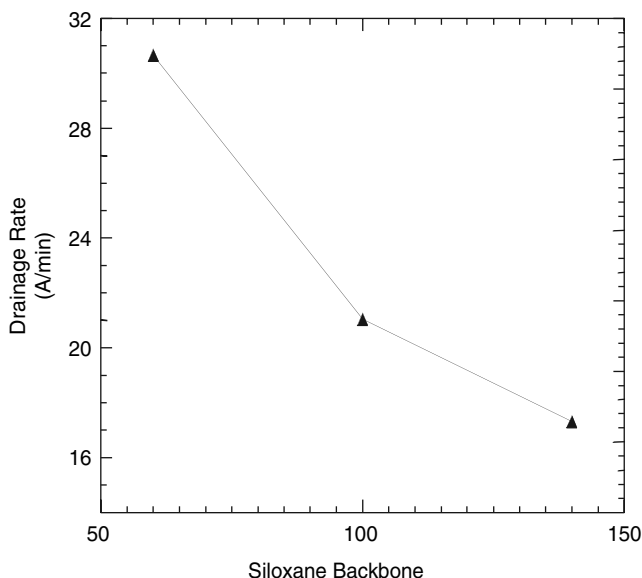


FIGURE 5.22

Effect of silicone backbone length of the surfactants on vertical film drainage rate 1 wt% surfactant solution in Voranol 3137.

on the tip of the capillary is highly unstable. This surfactant will cause polyurethane foam collapse since the surfactant is not sufficiently surface active and no surface tension gradient can be obtained.

As discussed above, a film with a higher elasticity has a higher surface tension gradient along the film to retard drainage. As a result of the slower drainage rate, a thicker film will be obtained. The higher the film elasticity, the thicker the average cell window and the lower the percentage of ruptured cell windows. As discussed in the previous sections, the remaining cell window thickness in the cured solid foam is measured for foams made with different surfactants and different film elasticities. Surfactants with different backbone lengths ($MD_{85}D'_{15}M$ and $MD_{51}D'_9M$) are used since they result in foams with the same cell size. Figure 5.17 shows the thickness distribution of the remaining cell windows. $MD_{85}D'_{15}M$ has a higher film elasticity value (7.1 dyne/cm) than that of $MD_{51}D'_9M$ (5.2 dyne/cm). Polyurethane foam made using a surfactant with a high elasticity has thicker films than that of a foam made using a surfactant with a low elasticity. Also, a different distribution is observed: foam with a high elasticity has a higher film density toward the thicker films, while foam with a low elasticity has a higher film density toward the thinner films.

The short-time foam stability for different surfactant solutions can be evaluated by obtaining the actual thinning rate of thin liquid. Since there are many vertical lamellae in a foam, where gravity plays an important role, a vertical film drainage test is performed.³⁴ The results of the vertical film drainage test for different surfactant solutions are shown in Figure 5.22.

TABLE 5.5

Formulations

Unit: pphp^a

Formulations	A1	A2	A3
Voranol 3137 ^b	100	100	100
Water	4.0	4.0	4.0
Dabco 33LV ^c	0.30	0.30	0.30
Dabco T-9 ^d	0.32	0.24	0.16
Silicone surfactant	1.0	1.0	1.0
Voranate T-80 index	110	110	110

^a Parts per hundred parts polyol (by weight).^b A 1000 equivalent weight triol containing 13% ethylene oxide, 87% propylene oxide and all secondary hydroxyl groups.^c 33% triethylenediamine in dipropylene glycol.^d Stabilized stannous octoate.

As shown, the drainage rate slows as the backbone length of the surfactant is increased. In vertical films, the drainage flow toward the Plateau borders creates a stretching motion along the surface. A surface tension gradient along the film will form to counteract the stretching drainage flow. The higher the surface tension gradient a surfactant can establish, the slower the drainage will be. It is shown that the surfactant with the longer silicone backbone can provide a higher surface tension gradient, and a slower film drainage rate will be obtained.

Silicone surfactant must provide short-time stability for the reacting polyurethane foam system before the matrix material solidifies. Such stabilization is realized by establishing a surface tension gradient along the film surface and reducing the rate of drainage. The ability to build a surface tension gradient is characterized by the dynamic film elasticity measured using the film rheometer. Both bulk mobility and surface mobility have significant effects on the film elasticity. The higher the overall surfactant mobility (mobility parameter M), the lower the film elasticity will be. Drainage rate and foam stability are observed to increase as the film elasticity increases. It is shown that a surfactant with a longer backbone will have a lower overall mobility, higher film elasticity, and slower drainage rate and will result in thicker films and a lower ruptured window percentage. When the silicone content is varied, the surfactant performance will vary significantly. Surfactants with very high silicone content give very low film elasticity and low foam stability. Surfactants with very low silicone content are not surface active enough and also give low foam stability. As a result, a surfactant with either a high or a low silicone content results in a collapsed foam system.

5.4.2 Other Formulation Ingredients: Bulk Rheology Effect

Cell opening can be manipulated by additives that change the reaction kinetics. As previously shown, urea phase separation and extensional thinning of the bulk liquid are key in triggering cell opening. Thus the degree

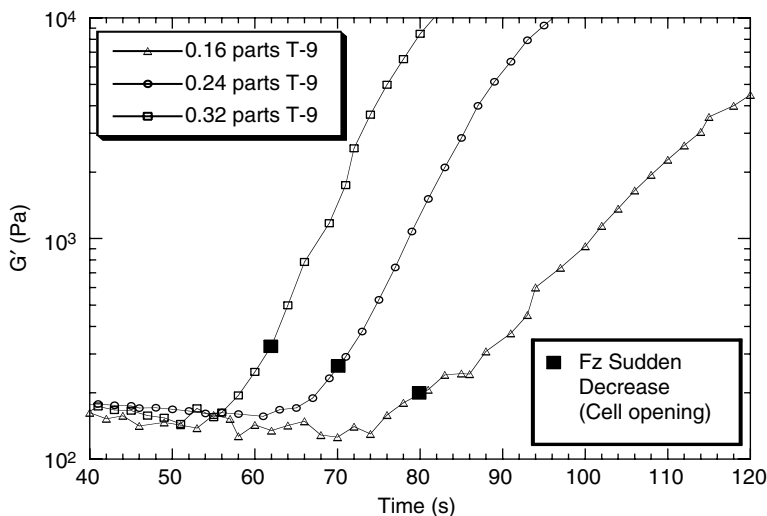


FIGURE 5.23

Modulus rise for foams made with different tin catalyst levels.

of cell opening is effectively controlled through proper balance of the blowing and gelling reactions, which in turn determine the bulk rheology at the time of urea phase separation. Accordingly, it is common to adjust formulation variables such as polyol structure, catalyst package, and water level in order to control cell opening. The effect of tin catalyst on cell opening is shown in the example here. The tin catalyst concentration was changed within the formulation, which is given in Table 5.5. This change will alter the chemistry of the system. The same surfactant type and concentration were employed at all times. Air flow and cell opening data for all the formulations are given in Table 5.6.

In this series, the time to cell opening onset (t_0) changes significantly with formulation. This shows that the foaming chemistry has a significant influence on the cell opening process. One important observation is that the cell opening always happens a few seconds after the modulus sudden increase (Table 5.6 and Figure 5.23).

TABLE 5.6

Time to Cell Opening, G' at Cell Opening and Air Flow

Formulation #	t_0 (sec)	t_r (sec)	G' at t_0 (Pa)	Air Flow (CFM)
A1	62	53	102	0.07
A2	70	64	82	0.32
A3	80	74	60	4.60

t_0 : Time to normal force sudden decrease (internal cell opening time).

t_r : Time to modulus sudden increase (blow-off time).

Sudden decrease in normal force was not observed because the foam collapsed.

Air flow could not be measured due to foam collapse.

www.iram-mavad.com

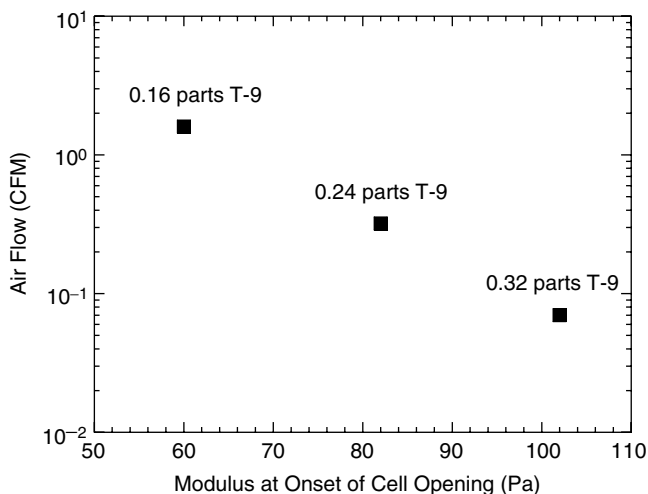


FIGURE 5.24

Air flow vs. G' cell opening time for foams made with different tin catalyst levels.

G' variation at the cell opening onset is higher at high tin catalyst levels. This is due to the different reaction kinetics as well as the different blowing reaction to gelling reaction ratio. As more tin catalyst is added to the system, the overall reaction kinetics will be faster as observed from the modulus development profiles. More importantly, the relative ratio between the gelling and blowing reactions will increase as the tin catalyst level increases. This implies that the foam matrix will be more crosslinked at the cell opening time when the tin catalyst level is high. As a result, a higher modulus at cell opening time is observed for foams made with higher tin catalyst levels. This leads to lower air permeability since a higher gelling reaction increases the strength of the foam matrix and less film rupture will occur. Figure 5.24 shows this trend.

It is shown that the rheology of the matrix material plays a very important role in controlling the degree of cell opening. The higher the bulk viscosity at cell opening time, the more stable the films are and the lower the open cell percentage will be.

5.5 Summary

Flexible polyurethane foam is produced in a process with complex chemistry involving simultaneous gas generation, polymerization, and urea phase separation. The cell opening event, which occurs suddenly during the process by which foam for slabstock applications is produced, is especially remarkable. This process leads to a stable, but porous, material with desirable

mechanical properties. We have comprehensively reviewed and tested previously proposed explanations for the cell opening event, including theories originating from both the aqueous foam and polyurethane literature. A new mechanism was proposed that explains both the resulting distributions of cell window structures and results of *in situ* measurements such as online rheometry. In addition, the roles of silicone surfactant and catalysts in the cell opening event were illustrated.

Spontaneous film rupture mechanisms were eliminated since the observed window film thickness in polyurethane foams is too large. Furthermore, a uniform distribution of surfactant within cured foams was demonstrated; thus cell opening also was not explained by phase separation of surfactant. Urea phase separation leads to a heterogeneous morphology and sudden viscosity increase of the foamed liquid. However, the mere presence of solid urea particles will not cause cell opening since the particles will not dewet from the liquid. This was illustrated in a liquid foam stability experiment with added polyurea particles. It was further shown that after phase separation, the foamed liquid exhibits strong extensional thinning. As this change in rheology occurs during foam expansion, it leads to cell windows that are torn, partially open, or completely missing. Such features were previously observed by microscopy. The silicone surfactant impacts the process by retarding film drainage and increasing film elasticity. Using light interference microscopy, the cell window thickness distribution was measured for foams employing a series of designed surfactants. Film elasticity, an indicator of the drainage rate, was measured on surfactant/polyol mixtures through use of a film rheometer. Structure–performance correlations were thus made with respect to surfactant structure. Surfactants producing films with higher elasticity resulted in thicker films within foams and more closed cells. Catalysts were shown to further affect the cell opening event by modifying the bulk rheology of the foamed liquid at the time of cell opening.

References

1. R.M. Herrington and K. Hock, *Flexible Polyurethane Foams*, The Dow Chemical Company, Midland, MI, 1991.
2. E.A. Blair, *Resinography of Cellular Plastics*, *ASTM STP*, 414, 84, 1967.
3. J.H. Saunders and K.C. Frisch, *Polyurethanes: Chemistry and Technology*, Applied Science Publishers, London, 1962.
4. G. Woods, *Flexible Polyurethane Foam: Chemistry and Technology*, Applied Science Publishers, London, 1987.
5. R.A. Neff, *Reactive Processing of Flexible Polyurethane Foam*, Ph.D. thesis, University of Minnesota, 1995.
6. A.J. Vrij, *Disc. Faraday Soc.*, 42, 44, 1958.
7. A. Sharma and E. Ruckenstein, *Langmuir*, 3, 760, 1987.
8. B.V. Derjaguin and Y.V. Gutop, *Kolloidn. Zh.*, 24, 431, 1962.
9. I.B. Ivanov, K.D. Danov, and P.A. Kralchevsky, *Coll. Surf. A*, 152, 161, 1999.

10. P.K. Prud'homme and S.A. Khan, *Foams*, Marcel Dekker, Inc., New York, 1988.
11. S. Ross and G. Nishioka, *Coll. Polym. Sci.*, 255, 560, 1977.
12. G.C. Frye and J.C. Berg, *J. Coll. Int. Sci.*, 130(1), 54, 1989.
13. R.D. Kulkarni, E.D. Goddard, and P. Chandar, in *Foams: Theory, Measurements and Applications*, R.K. Prud'homme and S.A. Khan, Eds., Marcel Dekker, Inc., New York, 1996.
14. J.B.M. Hudales and H.N. Stein, *J. Coll. Int. Sci.*, 140(2), 307, 1990.
15. A.D. Nikolov, P.A. Kralchevsky, I.B. Ivanov, and D.T. Wasan, *J. Coll. Int. Sci.*, 133, 13, 1989.
16. A.D. Nikolov, D.T. Wasan, N.D. Denkov, P.A. Kralchevsky, and I.B. Ivanov, *Prog. Colloid Polym. Sci.*, 82, 87, 1990.
17. I.B. Ivanov, *Coll. Polym. Sci.*, 252, 982, 1974.
18. L.E. Scriven and C.V. Sternling, *Nature*, 187, 186, 1960.
19. I.B. Ivanov, *Thin Liquid Films*, Marcel Dekker, Inc., New York, 1988.
20. P. Spatel and C.W. Macosko, Poster Section, The Society of Rheology 74th Annual Meeting, Minneapolis, October, 2002.
21. G.L.W. Rossmly, H. Schator, M. Wiemann, and H.J. Kollmeier, *J. Cell. Plast.*, 17, 319, 1981.
22. C.B. Reese, in *Protective Groups in Organic Chemistry*, J.F.W. McOrnie, Ed., Plenum Press, New York, 104, 1973.
23. D.L. Schmidt, in *Foams*, R.K. Prud'homme and S.A. Khan, Eds., Marcel Dekker, Inc., New York, 1996.
24. W. Grabowski and M.C. Desnier, *J. Cell. Plast.*, 31(3), 39, 1995.
25. R.E. Stevens and S.A. Snow, Personal communication, 1995.
26. K. Yasunaga, R.A. Neff, X.D. Zhang, and C.W. Macosko, *J. Cell. Plast.*, 32, 427, 1996.
27. C.W. Macosko, *Rheology: Principles, Measurements and Applications*, VCH Publishers, Inc., New York, 1994.
28. R.W. Whorlow, *Rheological Techniques*, Ellis Horwood Ltd., London, 1992.
29. S. Chatraei, C.W. Macosko, and H.H. Winter, *J. Rheol.*, 25, 433, 1981.
30. X.D. Zhang, Role of Silicone Surfactant in Polyurethane Foaming Process, Ph.D. thesis, University of Minnesota, 1998.
31. P.J.M. Baets and H.N. Stein, *Langmuir*, 8, 3099, 1992.
32. R.E. Jones and P. Fesman, *J. Cell. Plast.*, 1(1), 200, 1965.
33. A.K. Malhotra and D.T. Wasan, *Chem. Eng. Commun.*, 55, 95, 1987.
34. X.D. Zhang, C.W. Macosko, H.T. Davis, A.D. Nikolov, and D.T. Wasan, *J. Coll. Int. Sci.*, 215(2), 270, 1999.

Flexible Polyurethane Foams

J. Bicerano, R.D. Daussin, M.J.A. Elwell, H.R. van der Wal, P. Berthevas, M. Brown, F. Casati, W. Farrissey, J. Fosnaugh, R. de Genova, R. Herrington, J. Hicks, K. Hinze, K. Hock, D. Hunter, L. Jeng, D. Laycock, W. Lidy, H. Mispreuve, R. Moore, L. Nafziger, M. Norton, D. Parrish, R. Priester, K. Skaggs, L. Stahler, F. Sweet, R. Thomas, R. Turner, G. Wiltz, T. Woods, C.P. Christenson, and A.K. Schrock

CONTENTS

- 6.1 Historical Background
 - 6.1.1 Application and Markets
- 6.2 Basics of Chemistry
 - 6.2.1 Overview
 - 6.2.2 Polymerization Reaction
 - 6.2.3 Gas-Producing Reaction
- 6.3 Foam Components
 - 6.3.1 Polyol
 - 6.3.2 Further Discussion of Copolymer Polyols (CPPs)
 - 6.3.3 Isocyanates: Broad Overview
 - 6.3.4 Isocyanates: In-Depth Review of TDI Manufacturing Processes
 - 6.3.4.1 Introduction
 - 6.3.4.2 Nitration of Toluene to DNT
 - 6.3.4.3 Hydrogenation of DNT to TDA
 - 6.3.4.4 Phosgenation of TDA to TDI
 - 6.3.5 Prepolymers
 - 6.3.6 Isocyanate Index
 - 6.3.7 Fillers
 - 6.3.8 Water
 - 6.3.9 Surfactants
 - 6.3.10 Catalysts
 - 6.3.11 Additives
- 6.4 Fundamentals of Foaming

- 6.4.1 Introduction
- 6.4.2 Bubble Nucleation
- 6.4.3 Bubble Growth
- 6.4.4 Bubble Packing
- 6.4.5 Cell Opening
- 6.5 Classical Physical Picture of Morphology
 - 6.5.1 Heterophasic Nature of Flexible Polyurethane Foams
 - 6.5.2 Analytical Tools for Characterizing Flexible Polyurethane Foams
 - 6.5.3 Essential Aspects of Classical Physical Picture of Morphology
- 6.6 Research Frontiers in Microstructure and Property Development
 - 6.6.1 Synopsis
 - 6.6.2 Key Aspects of Morphology Development during Reactive Processing
 - 6.6.3 Reaction Kinetics: Understanding Copolymerization
 - 6.6.4 Phase Separation Kinetics: Understanding the Evolution of Polymer Morphology
 - 6.6.5 Solidification: Understanding the Arrest of Phase Separation
 - 6.6.6 Post-Reaction Analyses: Understanding Properties in End-Use Applications
 - 6.6.7 Summary: Overview of Polymer Microstructure and Morphology Development
- 6.7 Foam Preparation
 - 6.7.1 General Considerations
 - 6.7.2 Slabstock Foams
 - 6.7.3 Molded Foams
 - 6.7.4 Carpet Backing Foams
- 6.8 Evaluation and Testing of Basic Foam Properties
- 6.9 Evaluation and Testing of Foam Durability
- 6.10 Control of Noise and Vibrations
- 6.11 Flammability
- 6.12 Recycling
- 6.13 Polyurethane Foams from Renewable Resources
- 6.14 Summary and Conclusions
- References

6.1 Historical Background

Polyurethanes are chemically complex polymers, usually formed by the reactions of liquid isocyanate components with liquid polyol resin components.

Although these products are all termed “polyurethanes,” other identifiable chemical linkages may also be present (such as urea, allophanate, and biuret). The fundamental addition polymerization reaction of diisocyanates with alcohols to produce high polymers was discovered in 1937 by Otto Bayer and coworkers in the laboratories of the German I. G. Farben Industrie.¹ From their early work pulling “High quality fibers and bristles . . . from the polymer melt” came the further research and experimentation that led to the first laboratory-produced flexible polyurethane foam in 1941.²

The first pilot plant production of flexible polyurethane foam was announced in Germany in 1952.³ Commercial production began in 1954.^{4,5} Using the German technology, numerous companies worldwide raced to introduce polyurethanes commercially to fill many industrial and consumer needs. The first foams were based primarily on the reaction of an aromatic isocyanate with a polyester polyol. However, these foams proved unable to withstand many in-use temperature and humidity conditions and often failed by crumbling away.^{6,7} Better performance was obtained with foams based on polyether polyols. These polyols, introduced by BASF Wyandotte and The Dow Chemical Company in 1957, produced a flexible foam that was less affected by hydrolysis and was more comfortable and considerably more durable. By 1958, the combination of polyether polyols, new catalysts, and new silicone-based surfactants made possible the so-called one-shot foam technology, which paved the way for commercial quantities of more economic foams with significantly improved physical properties.⁸

In the early 1960s, Dow was first to introduce ethylene-oxide-capped polyols for flexible foam. The resulting faster reactivity (due to the presence of primary hydroxyl groups) permitted the fast cure needed for hot cured and high resiliency foams. Dow was also the first to produce amine-capped polyether polyols. Continuing advances in polyol development and processing by the polyurethanes industry have played an important role in the expansion of the technological applications and markets for polyurethane foams.

Concurrent with the advances in the development of polyols, whole families of diisocyanates have come on the global scene. By the early 1950s, the two basic starting products were toluene diisocyanate (TDI) and diphenylmethane diisocyanate (MDI). These two isocyanates remain the most widely used in the polyurethanes industry. However, many additional isocyanates (including several aliphatic isocyanates) have also gained acceptance since then for various applications.

6.1.1 Applications and Markets

The greatest advantage offered by polyurethanes is their versatility, both in their finished product properties and in their ease of production and application. [Figure 6.1](#) is a product chart for flexible polyurethane foams. With proper choice of isocyanate and polyol, products can be made with

properties ranging from the downy softness of very low-density flexible foams to the high strength of elastomeric bubble-free castings. The phenomenal success of polyurethanes in capturing applications previously held by alternative cushioning materials is recorded in a large number of references.⁹

Polyurethane foams can be generated from liquid components on the job site by pouring, frothing or spraying. However, more commonly, foams are produced in large quantities in plants designed specifically for the desired type of foam. Foam formulations can be mixed by hand or by machinery designed specifically for that purpose. They can be molded to shape or produced in large bunstock form for later cutting and fabrication.

Their high mechanical strength allows these foams to endure rigorous fabrication processes. Contemporary flexible polyurethane foams are also resistant to moisture, odor formation, and normal cleaning procedures, and are considerably more resistant to degradation than older latex-based foams, and hence easily used in modern upholstery applications. Their potential uses and multiplicity of properties are practically endless.

Such versatility has resulted in the rapid expansion of their markets. The major markets are cushioning materials in furniture, bedding, carpet underlay, automotive, and packaging applications. With the very broad range of available firmness (load-bearing capacity) and resiliency (including also

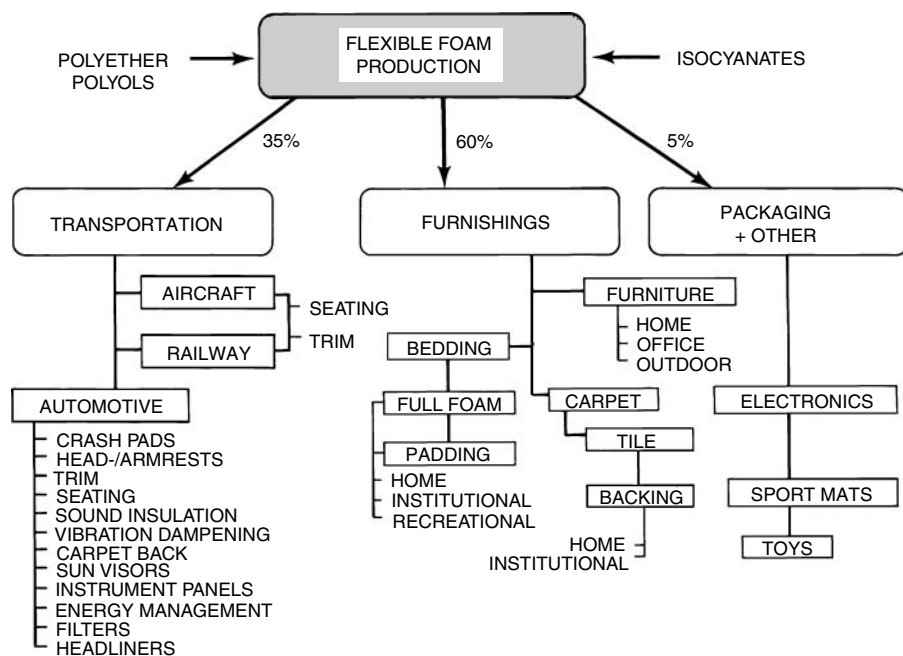


FIGURE 6.1

Applications of flexible polyurethane foams.

“specialty” foams such as semiflexible, semirigid, and integral skin foams), these foams offer degrees of comfort to humans and protection to inanimate objects not approached by any other single cushioning material.

Most flexible polyurethane foams reach consumers through their use in products such as upholstered furniture, mattresses, automobiles, and clothing. Consumers also benefit from their use in all forms of public transportation and commercial seating. From a modest commercial start in the early 1950s, these foams have grown in sales volume to occupy the sixth position among all major plastics sold today. The growth of the industry was slow in the beginning. It gained momentum gradually as the advantages of these new foams became more evident. The total global sales volume was only about 400 million lb in 1960. The industry exceeded the 1.5 billion lb mark by 1970. It continued growing to over 9 billion lb by 1995.¹⁰

6.2 Basics of Chemistry

6.2.1 Overview

Polyurethane chemistry is based on the reactions of isocyanates with active hydrogen-containing compounds. Isocyanates have one or more of the highly reactive $\text{-N}=\text{C}=\text{O}$ (isocyanate) group. This group reacts readily with hydrogen atoms that are attached to atoms more electronegative than carbon. Of the many compounds fitting this description, those that are of primary interest for polyurethane-forming reactions are listed in [Table 6.1](#).

The normal reactions of isocyanates involve addition to the carbon-nitrogen double bond. A nucleophilic center from an active hydrogen-containing compound attacks the electrophilic carbon. The active hydrogen atom then adds to the nitrogen atom. Electron-withdrawing groups attached to the isocyanate molecule increase the reactivity of the NCO group toward nucleophilic groups. Electron-donating groups reduce reactivity. Thus, in most reactions, aromatic isocyanates are more reactive than aliphatic isocyanates. Steric hindrance on the isocyanate and/or on the active hydrogen compound affects the reaction. Extensive reviews of isocyanate reactions are available.¹¹

Flexible polyurethane foam formation involves many ingredients. The two competing reactions (polymerization and gas-producing reaction) are discussed below.

6.2.2 Polymerization Reaction

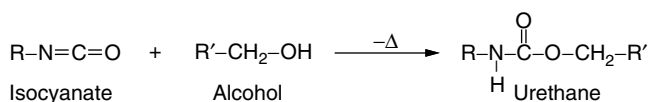
Polymerization occurs via an addition reaction ([Structure 6.1](#)) between an isocyanate and an alcohol. Its heat of reaction is roughly 24 kcal/mol of urethane.¹² Depending on the choice of starting materials, the R and R'

TABLE 6.1

Active Hydrogen Compounds Ordered by Decreasing Isocyanate Reactivity

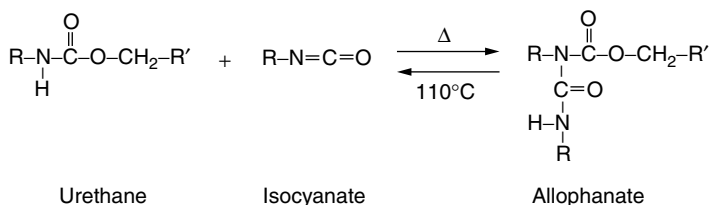
Active Hydrogen Compound	Typical Structure	Reaction Rate Uncatalyzed at 25°C
Primary Aliphatic Amine	R-NH_2	100,000
Secondary Aliphatic Amine	$\text{R}_2\text{-NH}$	20,000–50,000
Primary Aromatic Amine	Ar-NH_2	200–300
Primary Hydroxyl	$\text{R-CH}_2\text{-OH}$	100
Water	H-O-H	100
Carboxylic Acid	$\begin{array}{c} \text{O} \\ \\ \text{R-C-OH} \end{array}$	40
Secondary Hydroxyl	$\begin{array}{c} \text{R} \\ \\ \text{R-CH-OH} \end{array}$	30
Ureas	$\begin{array}{c} \text{O} \\ \\ \text{R-NH-C-NH-R} \end{array}$	15
Tertiary Hydroxyl	$\begin{array}{c} \text{R} \\ \\ \text{R-C-OH} \\ \\ \text{R} \end{array}$	0.5
Urethane	$\begin{array}{c} \text{O} \\ \\ \text{R-NH-C-O-R} \end{array}$	0.3
Amide	$\begin{array}{c} \text{O} \\ \\ \text{R-C-NH}_2 \end{array}$	0.1

groups may also contain isocyanate or isocyanate-reactive groups respectively. When extended to polyfunctional reactants, this reaction provides a direct route to crosslinked polymers.



(Structure 6.1)

The hydrogen on the nitrogen atom of the urethane group is capable of reacting with additional isocyanate to form an allophanate group (Structure 6.2).

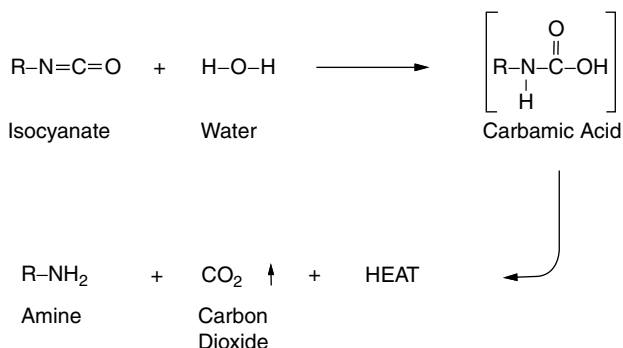


(Structure 6.2)

The formation of allophanate is a high temperature, reversible reaction. If actually formed in normal flexible foams, the allophanate linkage can crosslink the polymer further. The catalysts generally used in foam formulations do not promote this reaction, and temperatures greater than 110°C are necessary for significant allophanate formation. Other comments on the likelihood of allophanate formation can be found elsewhere.¹³

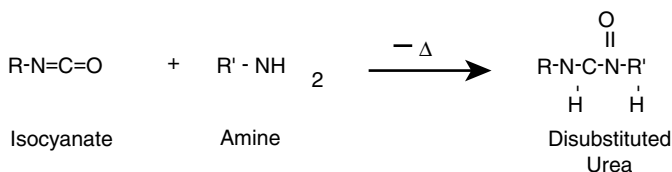
6.2.3 Gas-Producing Reaction

A polymer must be expanded or “blown” by the introduction of bubbles and a gas to make a foam. A convenient source of gas is the CO₂ produced from the reaction of an isocyanate group with H₂O (Structure 6.3). The total heat release is roughly 47 kcal/mol of H₂O.



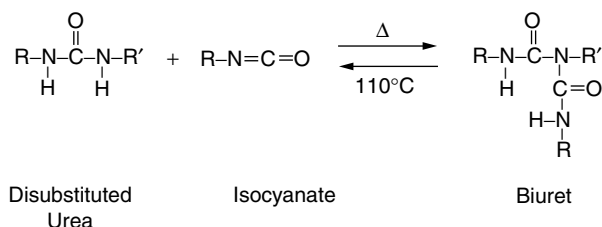
(Structure 6.3)

The intermediate product of this reaction is a thermally unstable carbamic acid which decomposes spontaneously to an amine and CO₂. Diffusion of CO₂ into bubbles previously nucleated in the reacting medium causes expansion of the medium to make a foam. Further reaction of the amine with additional isocyanate gives a disubstituted urea, as shown in [Structure 6.4](#).



(Structure 6.4)

Again, if the isocyanate and amine molecules are polyfunctional, a crosslinked polymer will result. Another conceptual method of crosslinking the polymer is by the reaction of a hydrogen from the disubstituted urea with a free isocyanate group to form a biuret linkage (Structure 6.5).¹⁴ However, since this reaction is also reversible, there is some debate about whether allophanates and biurets actually exist in the final polyurethane foam.¹⁵



(Structure 6.5)

Blowing can also be achieved by physical addition of a low-boiling non-reactive liquid to a foam formulation. Historically, the most commonly used physical blowing agents were the chlorofluorocarbons, urethane-grade methylene chloride, and trichloroethane. The vaporization of these liquids by heat from the exothermic reactions produces gas molecules which diffuse into the nucleated bubbles and contribute to foam expansion. Nowadays, CO₂ produced from the reaction of isocyanate with H₂O (see above) and/or CO₂ introduced physically as a liquid is the predominant blowing agent. Small amounts of methylene chloride are still used in South America, but even there liquid CO₂ is the auxiliary (physical) blowing agent of choice. Liquid CO₂ has the advantages of being cheap, readily available, familiar, and derived from existing industrial processes; and simply supplementing the CO₂ that is already generated by the reaction of water with isocyanate without introducing yet another type of compound into the formulation.

6.3 Foam Components

Flexible polyurethane foam recipes normally contain many ingredients selected to aid in achieving the desired grade of foam.¹⁶ Table 6.2 lists the

TABLE 6.2

Formulation Basics for Flexible Polyurethane Foams

Component	Parts by Weight
Polyol	100
Inorganic Fillers	0–150
Water	1.5–7.5
Silicone Surfactant	0.5–2.5
Amine Catalyst	0.1–1.0
Tin Catalyst	0.0–0.5
Chain-Extender	0–10
Cross-linker	0–5
Additive	Variable
Auxiliary Blowing Agent	0–35
Isocyanate	25–85

most common ingredients and typical concentration ranges used in the production of flexible polyurethane foam.

6.3.1 Polyol

Polyol is a source of hydroxyl or other isocyanate reactive groups. Processing and properties of the resultant foam can be markedly influenced by the choice of starting polyol structure. Polyether-type polyols are used in 90% of the flexible foams produced today. Most of the remaining 10% are made from polyester-type polyols.

The polyether polyols may be broadly grouped into the following categories:

- Polyoxypropylene diols.
- Polyoxypropylene triols.
- Polyoxypropylene tetrols and higher analogs.
- Ethylene oxide capped diols, triols, tetrols, and higher analogs.
- Random and block copolymers of the above in which the polyol is made with both ethylene oxides and propylene oxides. When the oxides are fed as a mixed feed, the products are termed heteropolyols.
- Graft or “copolymer” polyols (CPPs) which contain stable dispersions of a solid particulate polymeric phase in the liquid polyol phase. Because of the critical importance of CPP in flexible polyurethane foam technology, the preparation of CPPs will be discussed in some detail in the next subsection.
- Crosslinkers, which are typically short-chain polyfunctional molecules added to increase load bearing and/or initial foam stability.

There are so many polyol variations partially because what works well in a given commercial plant or geographic location may not work well in another location with seemingly identical conditions. The exact polyol composition

will be selected to tailor the foam for a given application and to allow its processing in commercial plants that differ widely in capabilities.

A polyether polyol is the polymeric reaction product of an organic oxide and an initiator compound containing two or more active hydrogen atoms. The active hydrogen compound in the presence of a base catalyst initiates ring opening and oxide addition. Oxide addition is continued until the desired molecular weight is obtained. If the initiator has two active hydrogens, a diol results. If a trifunctional initiator such as glycerine is used, oxide addition produces chain growth in three directions, and a triol results. These reactions are exothermic. The addition of propylene oxide, for example, releases approximately 22 kcal/mol. Many initiator compounds,¹⁷ as well as blends of these compounds,^{18,19} are used for the manufacture of flexible foam polyols. In practice, side reactions may preclude the production of a pure polyol from a chosen initiator. Many additional references²⁰ discussing the synthetic chemistry, manufacturing processes, and properties of polyether polyols are available.

Polyether polyols can be “filled” with other organic polymers to produce viscous white to off-white fluids useful in making foams of higher hardness than can be obtained by using the unmodified polyols alone. Filled polyols also aid foam processing by improving cell openness. The filler polymer is normally formed by *in situ* polymerization of monomers in a polyol base, through free radical or step addition processes.²¹ The successful preparation of stable colloidal dispersions requires particles to have some type of steric stabilization to prevent flocculation.²² This stabilization is typically provided by a “grafting” process in which either the base polyol or a special added stabilizer molecule copolymerizes with the monomers to form a copolymer.

There are two important composition classes of graft copolymer polyols. Chain-growth copolymer polyols are obtained by using steric stabilization to prepare dispersions in nonaqueous media via free radical polymerization^{21,23} and include styrene-acrylonitrile copolymers which are the most widely used graft copolymer polyols. Step-growth copolymer polyols include the Polyharnstoff dispersion (PHD) polyols^{20hh,24} which are dispersions of polyurea particles in conventional polyols, and the polyisocyanate polyaddition (PIPA) polyols^{20hh,25} which are dispersions of polyurethane particles in conventional polyols. In addition to these two major classes of copolymer polyols, filled polyols based on dispersions of cured epoxy resins,^{26,27} polyisocyanurate particles,²⁸ and melamine-based copolymers^{29,30} in conventional base polyols have also been reported.

6.3.2 Further Discussion of Copolymer Polyols (CPPs)

CPPs are used both to increase flexible foam load bearing and as processing aids to help in cell opening. CPPs are made by free radical polymerization of ethylenically unsaturated monomers in a polyol. The most commonly used monomers are styrene (S) and acrylonitrile (AN). An important CPP property is its load-bearing efficiency which is related to the volume fraction of rigid polymer in the polyol.^{31,32}

The viscosity of the final CPP is related to the volume fraction of polymer and the initial viscosity of the carrier polyol.³³ The particle size distribution determines the maximum packing volume fraction of particles and also the maximum attainable solids level for a liquid CPP.³⁴ CPPs can be made by a semi-batch or a continuous process.

In the semi-batch process, all ingredients are fed to a batch reactor with a certain ramp profile. In the continuous process, all ingredients are fed at a constant rate into a continuously stirred tank reactor. The semi-batch process produces rather narrow and uniform particle size distributions. In the continuous process, the particle size distribution is broader, resulting in lower final CPP viscosities at a given particle volume fraction as a result of having a higher maximum particle packing volume fraction.

The amount and structure of the SAN-polyol grafts created during the process also play an important role in the rheology of the final CPP. When the particles are very small, the protective layer of polyol surrounding the particles begins to contribute to the final CPP viscosity, and the cell opening efficiency is also affected adversely. Particles that are too large (with diameters on the length scale of a foam strut) cause foaming instabilities. It is important to design CPPs with optimum particle size distributions.

The key to the “high solids” CPP process is the design of the stabilizer system in order to deliver the optimum particle size distribution in combination with the lowest possible levels of the unwanted serum phase polymer. The free radical polymerization of S and AN in polyol automatically results in some “natural” SAN-polyol grafting, through the presence of some unsaturated polyol species and by direct radical attack of the polyol chain. Inert organic solvents and/or chain transfer agents are being used to limit the formation of unwanted SAN-polyol grafts in the serum phase. The use of solvents limits the SAN molecular weight through particle swelling and generally results in smoother particle surfaces. The use of a chain transfer agent reduces the SAN molecular weight and is especially useful for the “high solids” CPPs. A chain transfer agent allows control over the molecular weight of the polymer present in both the serum phase and the particle. The major part of the reaction happens in the solid SAN particles. Controlling the molecular weight of the SAN phase allows some control over the fine balance between solid phase and serum phase polymerization. (A higher SAN molecular weight will result in a higher reaction rate. The grafting reaction only happens in the serum phase. Too fast a polymerization will limit the grafting reaction and thus the production of new material to support the stabilization of the growing particle surface.)

Generally, the particle stabilizer precursors (macromer) are polyether polyols containing some sort of unsaturation induced by reacting a polyether polyol with an ethylenically unsaturated monomer. There are many examples of these materials in the patent literature; for instance, the coupling of vinyltrialkoxysilane with a polyether polyol³⁵ or creating a vinyl-capped polyol via unsaturation through the use of dimethyl m-isopropylbenzylisocyanate.³⁶ It has also been shown³⁷ that a stabilizer can be a high molecular

weight polyether polyol without induced unsaturation. The natural grafting by radical chain transfer to the polyether polyol and through the allyl alcohol alkoxylates present in the polyether polyols is adequate for obtaining sufficient SAN polyol grafts to support the dispersion polymerization.

A “seed” is often used to increase the efficiency of the stabilizer. The seed is a low solids CPP produced by reacting higher levels of macromer with the S and AN in the polyol carrier. The seed product made in this way contains very small particles in combination with a high level of SAN-polyol grafts. These SAN-polyol grafts are especially important to support the dispersion polymerization process.

The first CPPs were produced by using azo-type initiators such as 2,2'-azobis(isobutyronitrile). However, because of the difficulties in handling these materials and the degradation products that are formed, the industry is moving towards organic peroxy-type initiators. Peroxide initiators have a stronger hydrogen abstraction tendency towards the polyether polyol, resulting in more SAN grafting and smaller particle sizes but also in somewhat higher final CPP viscosities. In moving from azo to peroxide initiators, the macromer and seed structure need to be adapted somewhat to compensate for the higher natural grafting levels.

Chain transfer agents are used to obtain stable dispersions at higher solids levels. The polymerization rate inside the particles will be a function of the conversion. Very high rates are seen at high conversions. The Trommsdorff effect (reduced radical termination by low chain mobility) changes the delicate balance between the grafting reaction in the polyol phase and the solid SAN phase. Using a chain transfer agent reduces the molecular weight inside the particles and the final monomer conversion.

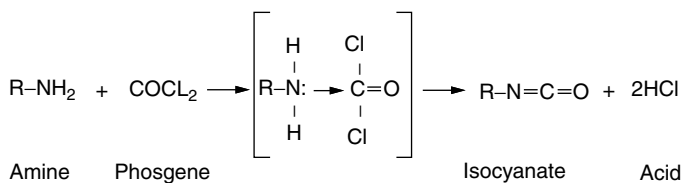
In general, higher monomer conversion leads to higher final CPP viscosities. This effect is thought to be related to the decreasing solubility of the SAN polyol grafts during the residual monomer removal step (forcing soluble SAN-grafts into the solids phase). Another effect is that the molecular weight of the SAN-polyol graft moves towards lower SAN molecular weights (the SAN molecular weight is proportional to the monomer concentration) as the conversion increases, making the SAN-polyol grafts more soluble and increasing the final CPP viscosity.

The use of polystyrene (PS) made by the direct free radical polymerization in the polyol results in high final CPP viscosities, poor monomer conversion, and more difficult particle stabilization, related to the high solubility of PS in the polyol and the lower reactivity of the S radical compared with the AN radical. CPPs based entirely on acrylonitrile result in darkly colored products. The low solubility of polyacrylonitrile (PAN) in polyol, combined with the high reactivity of the AN radical, makes it possible to produce a PAN polymer polyol without using an additional macromer. Unfortunately, the final PAN CPP has a rather high viscosity (natural grafting). The vast majority of the CPPs are based on the copolymers of styrene and acrylonitrile, which provide better CPP characteristics than can be obtained by using either the PS or the PAN homopolymers.

The pre-mixing of all ingredients is important in both the continuous process and the semi-batch process.³⁸ The concentration of unreacted monomers at any point in the reactor should be low because the solubility of the formed particles in the unreacted monomers causes particle destabilization. The reactors for both type of process are normally equipped with a (pitched) turbine blade agitator and the reaction mixture is fed into the high shear zone. The reaction temperatures range from 90 to 140°C.

6.3.3 Isocyanates: Broad Overview

The isocyanate permits the NCO groups to react with functional groups from the polyol, water, and crosslinkers in the formulation. All isocyanates used in industry today contain at least two NCO groups per molecule. The most commercially viable methods of producing isocyanates involve amine phosgenation, as shown in Structure 6.6:



(Structure 6.6)

The reaction is normally carried out in a chlorinated aromatic solvent chosen for its utility in removing excess phosgene in later purification steps.^{11d} The process is complicated by several side reactions.³⁹ Many reviews of isocyanate manufacturing processes are available.⁴⁰

More than 90% of flexible polyurethane foams are based on TDI. The global production capacity for TDI exceeds 1.5 million metric tons. The two most important isomers of TDI are shown in Figure 6.2. An 80:20 blend ratio of the 2,4-TDI and 2,6-TDI isomers, respectively, is obtained by the standard manufacturing process. Other mixture compositions, as well as the pure isomers, can be obtained by modifications of this process and/or by purification. Detailed reviews of typical TDI manufacturing processes are available.⁴¹ Because of the central role of TDI in the fabrication of flexible polyurethane foams, a review of these processes will also be provided below.

2,4-TDI is more reactive than 2,6-TDI. Within a given isomer, steric hindrances affect the relative reactivities of the positions.^{11b,42} Varying the isomer ratios can have dramatic effects on both polymer and foam properties.⁴³ Higher-load-bearing foams can be prepared by using the 65:35 blend ratio of the 2,4-TDI and 2,6-TDI isomers, respectively. Catalyst adjustments necessary to overcome the lower reactivity of this blend ratio have been described.⁴⁴ In some systems, adding a modified TDI or a polymeric diphenylmethane diisocyanate (PMDI) to the TDI reduces the hardness of the foam

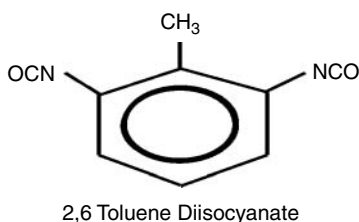
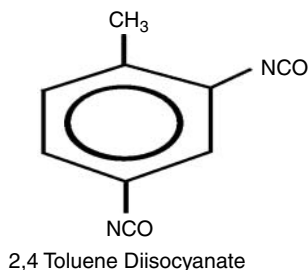


FIGURE 6.2
Isomers of TDI.

by interfering with the alignment of the polyurea hard segments and the effective degree of hard and soft phase separation.

Various forms of MDI are used in high resiliency, semiflexible, and micro-cellular foams. MDI is prepared from aniline, formaldehyde, and phosgene. The undistilled crude reaction mixture resulting from the phosgenation of the polyamine mixture contains varying amounts of di, tri, and higher functional isocyanates. Market demand for the pure MDI isomers dictates that the reactions be optimized for maximum production of two-ring material. Detailed reviews of typical MDI manufacturing processes are available.⁴⁵ PMDIs are differentiated by viscosity, functionality, and reactivity and have lower vapor pressure than TDI. Blends of PMDI with TDI are also used, as mentioned above.

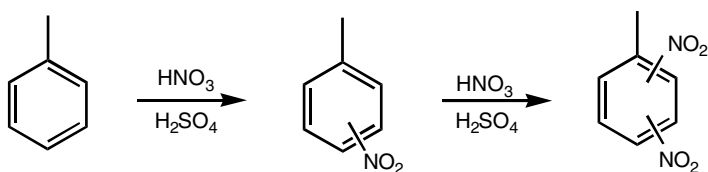
6.3.4 Isocyanates: In-Depth Review of TDI Manufacturing Processes

6.3.4.1 Introduction

In 1848, Wurtz first synthesized two aliphatic isocyanates (methyl and ethyl isocyanate) by reacting the alkyl sulfates with potassium cyanate.⁴⁶ Shortly thereafter, Hoffman prepared an aromatic isocyanate by pyrolysis of the symmetrical diphenyloxamide.⁴⁷ Use of phosgene for conversion of an amine to an isocyanate was first carried out by Hentschel⁴⁸ and has become the process of choice for production of the major commercial aromatic isocyanates including TDI.^{11a,c,49} Current commercial TDI production involves a sequence of three process steps which will be reviewed below: (a) nitration of toluene to dinitrotoluene (DNT), (b) reduction of DNT to toluene diamine (TDA), and (c) phosgenation of TDA to TDI.

6.3.4.2 Nitration of Toluene to DNT

Most commercial toluene nitration processes use a mixture of acids ($\text{HNO}_3/\text{H}_2\text{SO}_4$). The nitronium cation is formed by reaction of nitric acid with the stronger acid (sulfuric acid). Nitration of toluene follows as a bimolecular reaction involving aromatic electrophilic substitution with the nitronium cation, NO_2^+ .⁵⁰ Under typical mixed acid nitration conditions (65–98% HNO_3 , 80% H_2SO_4), toluene is substituted as 57.5% *ortho*, 4.0% *meta*, and 38.5% *para*, as shown in Structure 6.7.⁵¹



(Structure 6.7)

Subsequent reaction leads to a mixture of DNT isomers. Tillet⁵² determined the isomeric mixtures of DNTs produced from each of the three nitrotoluene compounds. The *o*-nitrotoluene reacts with nitric acid/sulfuric acid to give 2,4-DNT (66.5%), 2,6-DNT (33.2%), and 2,3-DNT (0.3%). The *m*-nitrotoluene upon further nitration leads to 3,4-DNT (55%), 2,3-DNT (25%), 2,5-DNT (18.6%), and 2,4-DNT (1.4%). The *p*-nitrotoluene gives rise to 2,4-DNT (99.7%) and 3,4-DNT (0.3%).

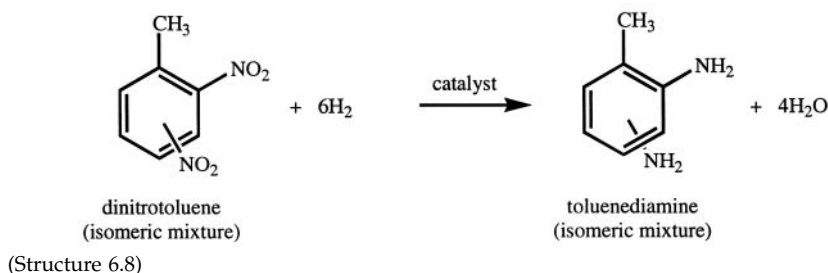
The DNT product distribution thus includes isomers in which the nitro groups are *ortho* and *para* to each other and which upon hydrogenation produce *o*-TODA and *p*-TDA. In the final TDI product mixture, the *meta* isomers are preferred. The *o*-TDA and *p*-TDA compounds are considered byproducts and are normally removed by distillation from the product mixture. Since nitration of *m*-nitrotoluene is most responsible for the formation of the undesirable *o*- and *p*-DNT derivatives, attenuation of *m*-nitrotoluene in the first nitration of toluene is crucial to reduce formation of the undesired *o*- and *p*-DNTs.

Nitrocresols and nitrophenols are other impurities formed in the nitration of toluene. Several proposed mechanistic routes may account for their formation.⁵³ The cresols are very reactive with respect to aromatic electrophilic substitution and readily nitrated under conditions of mixed acid nitration to the di- and trinitrocresols. These phenolic impurities are commonly removed by aqueous extraction. The wastewater process stream is then treated by purification processes.⁵⁴

In addition to the classical mixed acid method for toluene nitration, new methods such as the use of lanthanide(III)triflates as catalysts are under development.⁵⁵

6.3.4.3 Hydrogenation of DNT to TDA

The overall product reaction pathway for DNT reduction is shown in Structure 6.8. In typical commercial processes, the isomeric mixture of DNTs is comprised of roughly 20% 2,6-DNT and 80% 2,4-DNT. The hydrogenation product mixture contains a similar isomeric ratio (~20% 2,6-TDA and ~80% 2,4-TDA).



Several processes have been commercialized for both gas and liquid phase hydrogenation of nitro compounds. In general, DNT hydrogenation is mediated by either Raney nickel or noble metal (e.g., palladium or platinum) on carbon catalysts. In reductions of DNT with palladium on carbon, it has been proposed that iron facilitates reduction by improving dispersion of the metal phase and aiding in hydrogen transfer.⁵⁶

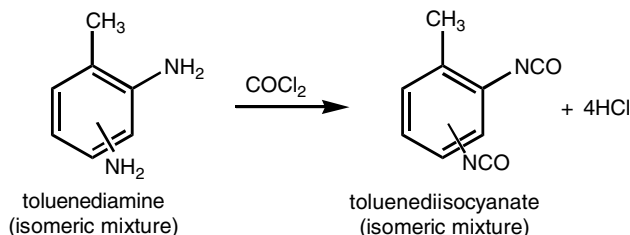
It has been reported that the use of tetrahydrofuran in the hydrogenation of DNT over Raney nickel results in less byproduct formation than the use of alcoholic solvents.⁵⁷

Musolino et al. developed methods to quantify major intermediates in catalytic hydrogenation of 2,4-DNT⁵⁸ and proposed a general mechanism based on the analytical results.⁵⁹ Westerterp et al.⁶⁰ proposed a mechanism with two parallel reaction pathways.

6.3.4.4 Phosgenation of TDA to TDI

Amines react with excess phosgene to give an initial reaction mixture comprised largely of carbamyl chlorides and amine hydrochlorides. Undesired secondary reactions are initiated when amines react with the product (isocyanates) to form ureas. Amine phosgenation reaction yields are not only reduced by the formation of ureas, but the yield losses are compounded by further reactions of the urea byproducts. The overall reaction is illustrated in Structure 6.9.

TDI purity, particularly with respect to reduction of chloride compounds and high molecular weight isocyanate byproducts, was the major goal of early work on TDI process improvements. A TDA phosgenation process incorporating the use of low initial reaction temperatures and high phosgene to TDA mole ratios was thus developed.⁶¹



(Structure 6.9)

Many highly efficient mixing devices were designed by the 1960s to improve the initial reaction of TDA with phosgene, typically using an initial temperature lower than 60°C at the point of mixing of the TDA solution with the phosgene solution to produce a mixture of TDA dihydrochloride and carbamyl chlorides in a first reaction stage.⁶² In these early inventions, completion of the reaction was then achieved by heating the initial reaction mixture to 100–200°C in a second reaction stage. Latourette and Johnson⁶³ and Denton et al.⁶⁴ showed that good yields may also be obtained at significantly higher initial reaction temperatures by optimizing some of the other process parameters.

Many inventors have patented impingement, jet, and venturi mixers that combine the amine and phosgene solutions at high flow velocities to reduce byproduct formation.⁶⁵ Others have proposed the use of mechanical mixing devices to reduce mixing times in the first stage of the reaction.⁶⁶ In general, mechanical mixing devices provide high shear at the point of contact of the amine solution with the phosgene solution. High shear mixing may also be attained by using a multistage rotary pump.⁶⁷ High speed mixing devices may be combined with mixing temperatures below 90°C to improve overall reaction yields.⁶⁸

Preparation of TDA dihydrochloride prior to reaction with phosgene eliminates the need for highly efficient mixing and reduced initial reaction temperatures. Relative rates of reaction of TDA dihydrochlorides with phosgene were investigated by Soos and Petnehazy.⁶⁹ The TDA dihydrochloride reaction is heterogeneous due to the insolubility of the amine salts. The reaction of TDA dihydrochloride with phosgene results in improved overall TDI yields.⁷⁰ Overall TDI yields as high as 96% have been reported by this so-called salt phosgenation process.

Partial conversion of the TDA to a mixture of hydrochlorides may also be carried out to improve yield relative to phosgenation of the free TDA.⁷¹ Immediately prior to the initial mixing of the phosgene solution with the amine solution, the TDA hydrochloride salts may also be formed *in situ* by addition of HCl to the phosgene solution.⁷² The addition of HCl to prevent byproduct formation has also been utilized in the second stage of phosgenation.⁷³ The formation of TDA dihydrochloride and subsequent phosgenation to TDI can be carried out in the absence of a reaction solvent.⁷⁴

Salts other than hydrochloride salts may also be formed prior to reaction of TDA with phosgene in order to improve reaction yields. For example, sulfur dioxide salts of TDA have been prepared and phosgenated to provide TDI with improved yields.⁷⁵

Dimethylformamide has been reported to catalyze the phosgenation reaction of TDA.⁷⁶ The use of tetra-N-substituted thioureas has been shown to decrease the reaction time of the phosgenation reaction.⁷⁷ Other N,N-disubstituted amides such as dimethylacetamide have been used as weak bases to remove HCl and decompose the carbamyl chlorides to reduce overall reaction times.⁷⁸

Staged-temperature phosgenation of TDA in dichlorobenzene with non-ylphenol polyethylene oxide increased the TDI yield from 73 to 84%.⁷⁹ The typical solvents for commercial phosgenation of TDA are chlorohydrocarbons, such as chlorobenzene and dichlorobenzene.⁸⁰ Numerous reaction solvents have been reported to facilitate the reaction of TDA with phosgene and improve the overall yield of TDI.⁸¹

Gas-phase phosgenation of TDA has also been described by several groups.⁸² Its advantages include the small amounts of excess phosgene (less than one equivalent) required and the relatively high overall yields. Following phosgenation of the diamine to the diisocyanate, phosgene and solvent are removed to provide a crude TDI. The crude TDI is then distilled to provide a colorless TDI product of relatively low viscosity.

6.3.5 Prepolymers

Prepolymers are liquid intermediates between the monomers and a final polymer. They are formed by reacting an excess of either polyol or isocyanate so that the product is still a liquid and contains the reactive functional group of the reagent in excess.

The use of prepolymers offers several advantages. Since the vapor pressure of a free isocyanate is reduced according to its mole fraction, there is a reduced vapor hazard because of increased molecular weight of the isocyanate component. Increased viscosity leads to better mixing of foam components. There may be improved hard segment formation arising from pre-reaction of some chain extenders that are incompatible with normal foam components. Pre-reacting some of the ingredients under precisely regulated conditions may also result in improved control of desired or undesired side reactions.

Hydroxyl-tipped prepolymers were popular in the early days of polyurethanes. Most prepolymers in use today are isocyanate tipped. A strict prepolymer is formed when just enough isocyanate is added to react with all available hydroxyl sites. If excess or residual free isocyanate monomer is present, the product is called a quasi-prepolymer. Just like the other types of isocyanates, the final prepolymer can react to form all of the normally expected structures. A typical procedure for prepolymer preparation has been described.⁸³ The key variables involved in producing low-free-isocyanate prepolymers have been discussed.⁸⁴ Stable, non-gelling prepolymers can only

be prepared when the stoichiometry, moisture, base contamination, and temperature are all closely controlled. Many additional reviews and foaming procedures are available.⁸⁵

6.3.6 Isocyanate Index

The amount of isocyanate required to react with the polyol and any other reactive components of the formulation is calculated in terms of theoretically stoichiometric equivalents. This amount may then be adjusted upwards or downwards, depending on the foam system and the required final properties. The amount of isocyanate used relative to the theoretical equivalent amount is known as the isocyanate index.

$$\text{Isocyanate Index} \equiv 100 \cdot \frac{\text{Actual amount of isocyanate used}}{\text{Theoretical amount of isocyanate required}}$$

Increasing the isocyanate index over a reasonable range has a pronounced effect in increasing the hardness of the final foam. This effect is related directly to increased covalent crosslinking resulting from the more complete consumption of the isocyanate reactive sites caused by the presence of excess isocyanate groups. The isocyanate index normally ranges from 105 to 115 (where foam hardness can be controlled readily and safely) in flexible slab-stock foam formulations. There is, however, a point beyond which foam hardness does not increase and other physical properties begin to suffer.

6.3.7 Fillers

Finely divided inert inorganic fillers are often added to foam formulations to increase density, load bearing, or sound attenuation. All other foam physical properties are generally sacrificed. Typical results have been described in the literature.⁸⁶ Depending on the nature of the filler, the overall cost of the final foam may be reduced.

Typical fillers include the many grades of barium sulfate and calcium carbonate. Care must be taken to dry the fillers or to know the precise water content available and factor that information into the formulation calculations. Normal concentrations used are from 20 to 150 parts per hundred parts of polyol. The fillers are heavy and will settle out of a polyol mixture unless constant agitation is used. Due to their abrasive nature, mineral fillers can also increase wear on machinery components. Calcium carbonate fillers have a significant effect on the gelling reaction and necessitate a rebalancing of the blowing and gelling reactions. A general review of fillers for plastics applications is available.⁸⁷

6.3.8 Water

Water is a source of active hydrogens. Only demineralized water should be used for foam production. Isocyanate reacts with water to provide CO₂ gas

(blowing agent) and polyurea molecules. The CO_2 gas diffuses into nucleated bubbles and aids foam expansion. The polyurea molecules enter into and contribute to the properties of the final polymer. The compatibility of water with various polyether polyols has been studied.⁸⁸

The amount of water used in the formulation is one of the most important variables at the disposal of a flexible polyurethane foam manufacturer who wants to optimize the properties of a foam for a given application. The typical effects of the water level in the formulation on the morphology, density, and stiffness (modulus) of a flexible polyurethane foam will be discussed and illustrated later. It suffices to say, at this point, that if all other factors are kept constant, the use of a larger amount of water in the formulation normally results in an increased foam modulus because of the increasing volume fraction of the polyurea-rich hard phase, and a decreased foam density because of the generation of a larger amount of the CO_2 blowing agent.

6.3.9 Surfactants

Almost all flexible polyurethane foams are made with the help of silicone-based nonionic surfactants. Surfactants lower the surface tension. They emulsify incompatible formulation ingredients. They promote the nucleation of bubbles during mixing. They stabilize the rising foam by reducing stress concentrations in thinning cell walls. They counteract the defoaming effect of any solids added (such as fillers) or formed (such as precipitated polyurea structures) during the foaming reaction.

The stabilization of cell walls is the most important of these functions. By doing this, the surfactant prevents the coalescence of rapidly growing cells until those cells have attained sufficient strength through polymerization to become self-supporting. Cell coalescence would otherwise lead to total foam collapse. Surfactants also help to control the precise timing and the degree of cell opening.

The judicious choice of a surfactant or surfactant combination for any given foam requires literature review, supplier consultation, and small-scale foaming tests.⁸⁹ Many additional extensive discussions of surfactant production methods, surfactant selection, influence of surfactant type and amount on foam structure and properties, and other aspects of surfactant technology are available in the literature.⁹⁰

6.3.10 Catalysts

Virtually all commercially manufactured flexible polyurethane foams are made with the aid of at least one catalyst. Among the many classes of compounds investigated, the amines and the organometallics have been found to be the most useful. Various combinations of catalysts are used to establish an optimum balance between the chain propagation (isocyanate with hydroxyl) reaction and blowing (isocyanate with water) reactions. The

polymer formation rate and the gas formation rate must be balanced so that gas is entrapped efficiently in the gelling polymer and the cell walls develop sufficient strength to maintain their structure without collapse or shrinkage. Catalysts are also important for assuring completeness of reaction or “cure” in the finished foam.

The selection of a catalyst system for a particular grade of foam is a complex task requiring literature review, supplier consultation, and small-scale foaming tests.^{91,92} Further refinement is usually needed at full commercial production scale.

Tertiary amines are the most commonly used flexible polyurethane foam catalysts. Generally regarded as blowing catalysts, most amines also offer some contribution to the polymerization reaction.⁹³ The catalytic activity of amines is due to the presence of a free electron pair on the nitrogen atom. Steric hindrance about the nitrogen atom and the electronic effects of substituent groups are the main factors influencing the relative catalytic activity of various amines. In some foam systems, combinations of various amines are used in an attempt to balance the polymerization and blowing reactions so that the foaming process can be adequately controlled. The type and concentration of amine catalyst(s) can be selected to satisfy process requirements such as cream times, rise profiles, gel times, and even cure of the outer surface skin. The choice of amine may also affect the foam properties such as air flow and load bearing through influences on the primary and secondary foam reactions.⁹⁴ In general, the requirements for good catalytic activity include that the catalyst should be a strong nucleophile capable of attacking the carbon of the isocyanate group, capable of readily forming an active hydrogen amine complex, and soluble in water (forming stable hydrogen bonds with water). Detailed reviews of amine catalysis are available.⁹⁵

The polymerization reaction between the isocyanate and a polyol is promoted by organometallic catalysts.⁹⁶ Of the many available metals, tin compounds such as stannous octoate are the most widely used. These compounds act as Lewis acids and are generally thought to function by interacting with basic sites in isocyanate and polyol compounds.

In recent years, a growing desire for better in-mold flowability and faster curing along with a need to balance foam reactivities in the dual-hardness process has led to the development of delayed action catalysts.⁹⁷ These are compounds that are not very active at room temperature. They become effective when the initial reaction exotherm warms up the foaming mass. The most common approach is to use a tertiary amine salt in a suitable solvent such as a low-molecular-weight glycol or water. Tertiary amine salts with organic acids such as carbonic, formic, acetic, 2-ethylhexanoic, and lactic acids have been introduced. Catalyst activity, phase separation, and metal corrosion problems have been reported when acid-blocked amines are formulated with normal amine catalysts in the presence of water. Other types of delayed action catalyst include the thermosensitive catalysts whose activities increase dramatically with increasing temperature.

6.3.11 Additives

Various additives may be incorporated into a foaming system to impart specific desired properties. A general review of additives for plastic products is available.⁹⁸ The following are the more common types of additives used in flexible polyurethane foams: colorants,⁹⁹ UV stabilizers,¹⁰⁰ fire retardants,¹⁰¹ bacteriostats,¹⁰² plasticizers, cell openers, antistatic agents,¹⁰³ compatibilizers,¹⁰⁴ and auxiliary blowing agents.¹⁰⁵

6.4 Fundamentals of Foaming

6.4.1 Introduction

Foams are three-dimensional agglomerations of gas bubbles separated from each other by thin sections of the host medium. For finished open-celled flexible polyurethane foams like that shown in Figure 6.3, the void areas are artifacts of expanded gas bubbles introduced into the reacting medium early in its existence. In classical discussions of foams, physical chemists identify cell walls and struts as lamellae and Plateau borders. Polyurethane foam chemists usually call them windows and struts. Foams can be further characterized as having a very large surface area per unit volume and a widely variable cellular structure. The properties of a foam result from both the geometry of the cells and the properties of the polymer. The formation of a flexible polyurethane foam is an intricate process using unique hardware, multiple ingredients, and at least the two simultaneous reactions discussed above. Successful foam preparation requires the formation, growth, and stabilization of gas bubbles in the reacting medium.

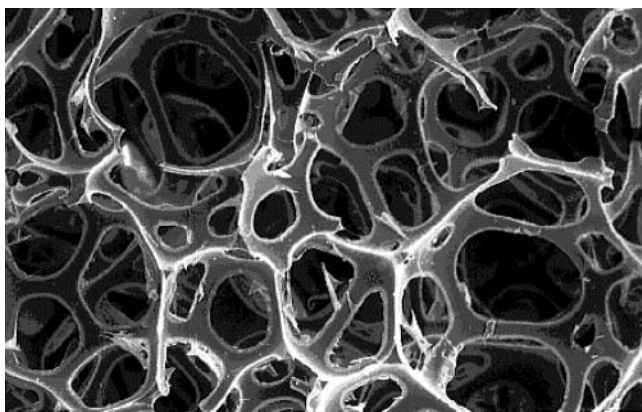


FIGURE 6.3

Open-celled flexible polyurethane foam. (Original magnification $\times 50$.)

6.4.2 Bubble Nucleation

The development of bubbles within a liquid is called nucleation. For polyurethane foams, the gas in the bubbles has several potential sources; namely, dissolved gases in the liquid reactants, low-boiling liquids added as auxiliary blowing agents, gases such as CO_2 produced by the reactants, and gases released from thermally decomposable additives. In addition, air or other gases may be entrained into the system by mechanical mixers or frothing devices. The number and size of any entrained bubbles are important to foam performance since gas from the other sources may preferentially diffuse into these sites.

The development of the fundamental understanding of bubble dynamics began with Young¹⁰⁶ and Laplace¹⁰⁷ in the early nineteenth century. Plateau is also credited with a major share of our knowledge about foams.¹⁰⁸ An excellent review of bubble dynamics has been published by Bikerman.¹⁰⁹

Foams can be described conceptually in terms of either a dispersion model or a condensation model. In a dispersion model, the gas would be present in a large separate phase such as in the head space of a vessel. With sufficient added work, aggregate molecules of the gas can be entrained and dispersed uniformly throughout the continuous liquid phase. A common example is the meringue topping on a lemon pie. (Meringue is the French word for the foam formed by whipping air into a mixture of egg whites and sugar.) In a condensation model, soluble gas molecules are forced to condense to form a bubble as the solute is dissolved in a continuous liquid phase. Again, with added work, the soluble gas molecules of a sufficiently supersaturated liquid may be caused to aggregate and condense into a bubble within the continuous liquid phase. An interesting apparent example of this model is the foam that forms on a glass of beer.

See Yazdi and Beckman¹¹⁰ for a review of nucleation theory in the context of bubble nucleation in polymer mixtures. Nucleation requires an input of energy. For example, the impossibility of self-nucleating CO_2 from a supersaturated solution of polyol and TDI was demonstrated by Kanner and Decker.¹¹¹ A bubble of CO_2 in a liquid will differ from an equal number of gas molecules in solution by its possession of enough surface energy to produce that bubble as a new phase. Foams can, therefore, be characterized as being thermodynamically unstable until other events (such as polymer gelation) provide permanent stabilization.

LaMer¹¹² has reviewed how the introduction of various interfaces within a gas-saturated liquid phase can greatly facilitate nucleation. Major changes in the number of cells per unit volume and the average cell size can result from apparently small changes in dissolved gas content. Bessette and Sundstrom have shown that, for a given volume of foam, a larger number of cells results in a more viscous and more stable foam.¹¹³ The impact of cell count on foam physical properties has been discussed extensively.¹¹⁴

In practice, both entrainment and supersaturation are done by foam manufacturers. Some bubble air into the polyol day tank to make an entrained

gas/polyol mixture of reduced density which is then pumped into the mix-head. Others simply ensure that the polyol is at equilibrium with dry air of atmospheric pressure and use the pressure drop after high pressure impingement mixing to cause bubble nucleation. In low pressure stirred mixing, air can be injected into the mixhead, and cavitation on the low pressure side of a multipin mixer will induce nucleation. The polyols must be near saturation with air to produce foams with high cell count (small cell size).

6.4.3 Bubble Growth

Producing spherical bubbles in a desired liquid is only the first step towards arriving at a useful foam. The initial mixture of reaction components has a low viscosity which would result in an unstable foam without input of additional energy. The possible fates of a foamed system include the flocculation and/or sedimentation of the bubbles (possibly followed by a return to phase-separated polymer and gas phases) as alternatives to the desired polymer gelation that produces a stable dry foam. Unless permanent stabilization occurs soon after formation, the foam disintegrates. In polyurethane foams, the energy for bubble growth comes from the exothermic and gas-producing reactions. Factors promoting bubble expansion include the production of CO₂ gas, the volume expansion work provided by an increasing temperature, and bubble coalescence.

An important consequence of the existence of a surface free energy in gas bubbles is the presence of a pressure difference across the curved gas-liquid interface. This pressure difference under a concave curved meniscus gives rise to the well-known capillary elevation effect on a liquid in a small tube. If the curved liquid surface fully encloses a volume of gas, a bubble results. The pressure excess ΔP of the gas in the bubble is given by the Laplace equation, where γ is the surface tension of the liquid and r_c is the critical radius of the bubble:

$$\Delta P = \frac{2\gamma}{r_c}$$

It is evident from this equation that the pressure inside a bubble is inversely proportional to the radius of the bubble. In real foams, there is always a distribution of bubble sizes so that the pressures in different bubbles will not be the same. This will lead to the diffusion of gas molecules from regions of higher pressure (small bubbles) to regions of lower pressure (large bubbles). The rate at which diffusion proceeds will be proportional to the pressure difference, the permeability, and the thickness of the liquid film separating bubbles of unequal size. Therefore, each bubble will grow or shrink depending on its diameter and the diameters of the bubbles in its environment. The rate at which a small bubble shrinks and disappears then depends mainly on its radius and the permeability of the gas through the liquid separating adjacent bubbles.

The net observation in a static system is that, with time, the average bubble size in a polydisperse system will increase while the total number of bubbles will decrease. A common example of this event can be found in a bubble bath, as illustrated by Clark and Blackman.¹¹⁵ Similar data were presented by Smith.¹¹⁶ Frensdorff reported the same phenomena in a model polyurethane foam system.¹¹⁷ For actual polyurethane-based foams, there is some argument that diffusion between bubbles is not a major factor in bubble growth¹¹⁸ because that mechanism is expected to be very slow compared with the rate of gas diffusion from the gas-saturated liquid phase into the bubbles.

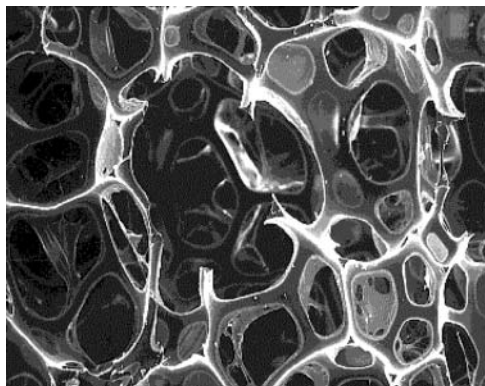
The Laplace equation shows that a low liquid surface tension favors low pressure differences between bubbles of different sizes. Lowering the system surface tension is then expected to lead to better bubble stability and smaller average cell size.

If coalescence were the only growth mechanism, fine-cell foam would not exist. Coalescence taken to the extreme would result in one bubble. The mutual approach of two bubbles requires pushing aside the liquid phase between them. The viscosity of this moving liquid affects the rate at which the liquid layer thins. Ideally, the viscosity of a thick section of the liquid would be low enough to allow the bubbles to come together quickly and then become high enough as a thin film to overcome coalescence. If the thin film viscosity could be made high enough, coalescence would not occur.

6.4.4 Bubble Packing

The bubbles in a polyurethane foam grow with continued reaction. As their volume fraction exceeds 74%, they lose their spherical shape and begin distorting into polyhedra. Matzke reviewed over 300 years of literature debating the theoretically preferred and actually observed polyhedral shapes in real foams.¹¹⁹ Early polyurethane researchers described these polyhedra as being approximate pentagonal dodecahedra.^{114a} However, pure structures of that type have 12 five-sided membranes and would not be expected to account for all available physical space. Real polyurethane foams also show some four-sided and six-sided cells and may be better approximated by Lord Kelvin's 14-faced tetrakaidecahedron space filling models.^{120,121} The real and approximate geometries are compared in Figure 6.4. Actual counts of the number of faces per cell closely match 14, as predicted by Duchartre.¹²² A distribution of cell sizes is usually found.

Bubble stability during growth is a complex function of surfactant effects, rate of gas evolution, viscosity, pressure, and presence of cell-disrupting agents. As growing spherical cells are squeezed into polyhedra, the liquid phase is initially redistributed between the tetrahedral interstices and the bubble surfaces. With continued cell volume growth, cell wall thinning takes place and polymer is drained from the lamellae into the unique structural features known as Plateau borders (see Figure 6.5). There is strong curvature



PENTAGONAL DODECAHEDRON

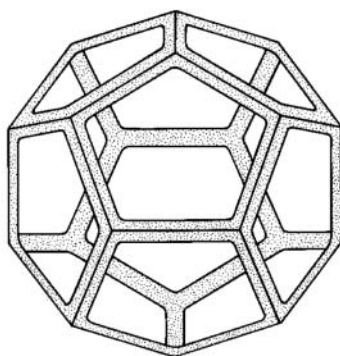


FIGURE 6.4

Examples of real foam geometry (left) and approximate cellular shape (right).

in the surface of a lamella at the edges where bubbles meet. The thinning of the cell windows is promoted by gravity, capillary suction into Plateau borders, and foam volume expansion. The effects of gravity and capillary suction forces may be additive in some parts of a lamella and opposite to each other in other parts.

The means by which foams stabilize themselves is a much debated subject. The lack of understanding arises in part from the experimental and theoretical difficulties of elucidating the intimate details of the molecular events occurring in foams. Kitchener and Cooper reviewed the major theories of foam stabilization.¹²³ The four theories with reasonable applicability to flexible polyurethane foams emphasize the importance of the surface viscosity,¹²⁴ surface elasticity,¹²⁵ film elasticity,¹²⁶ and surface transport.¹²⁷ These theories are actually quite similar and complementary. They vary mainly in their details. Implicit in each theory is the assumption that the rupture of a thinning window is preceded by a pronounced local thinning at some spot on

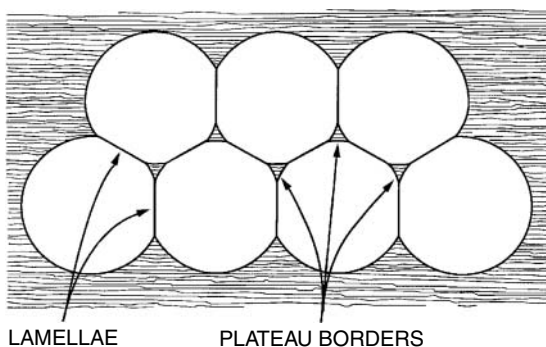


FIGURE 6.5

Schematic illustration of the structural features of a foam.

the film. This localized thinning results from drainage or from the action of a sudden force (such as a thermal, pressure, or vibrational shock). Localized thinning in a film will result in an expansion of the surface in that area, causing dilution of the locally absorbed surfactant. The expanded film element will thus possess a higher non-equilibrium surface tension.

To summarize, Figure 6.6 provides an idealized model for bubble nucleation, growth, and packing in polyurethane foams. The cells are produced by gas diffusion into bubbles that are nucleated or stirred into the system at the time of mixing. Their size is related to the total amount of blowing agent available, the exotherm, and the degree of stabilization (as by a surfactant). The total number of cells produced is governed by the dissolved gas content and the amount of gas stirred in. Ultimate stabilization of the polyhedral framework occurs as a result of the chemical reactions that occur up to the point of polymer gelation, when all film movement and expansion (except that induced by outside physical forces and leading to anisotropy) ceases. At this point, the foam may or may not possess enough open cells to make it a useful product.

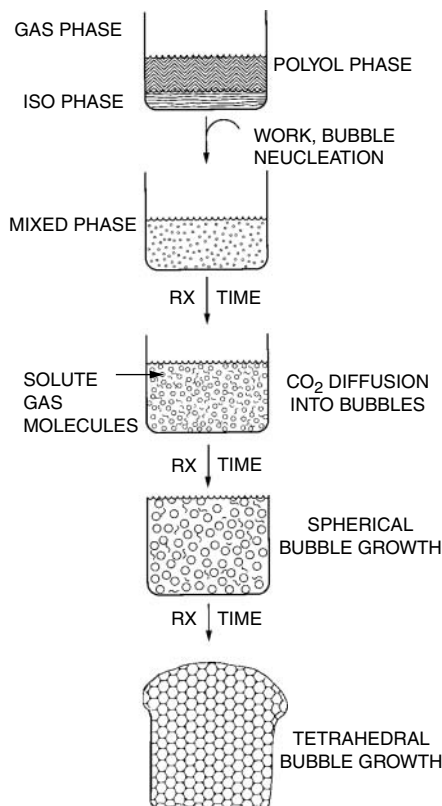


FIGURE 6.6

Model for bubble nucleation and growth.

6.4.5 Cell Opening

It is desirable to have a large fraction of the cell windows rupture through a natural balance of physical and chemical forces in flexible polyurethane foam production. A stable and nonshrinking foam may result if this happens near the chemical gel point of the reacting system. When enough windows are open, the foam will have less pneumatic character and will be more suitable for comfort cushioning applications. It has also been postulated that a more completely open-celled foam will have better fatigue resistance.¹²⁸ As Figure 6.7 indicates, cell opening is very complex and formulation dependent. The major theories are that cell opening results from steam formation,¹²⁹ urea precipitation,¹³⁰ or balanced catalysis,¹³¹ or is due in part to some particle effects.¹³² The literature also teaches that surfactants, through their influence on bubble nucleation and stability, are important contributors to controlled cell opening.¹³³ The importance of viscosity in controlling the drainage of polymer from cell windows has also been discussed.^{118,134} It has also been reported that foam cells can be opened by the precisely timed application of a physical shock such as the release of internal pressure from a mold.¹³⁵

Classical concepts regarding cell opening in flexible foams have been reviewed (see Saunders and Frisch¹³⁶). Conceptually, the opening of cells would occur to a large extent just as the foam reaches its full rise. At that time, the foamed polymer would have reached high viscosity with very low elasticity. The high viscosity would not permit the foam structural elements to flow fast enough to expand and relieve the increasing cell gas pressure. Low elasticity in the cell window membranes would likewise prohibit reversible stretching of cell windows. Under such conditions, the cell window membranes burst, leaving an interconnected open-celled network. The polymer in the cell struts must have enough strength to endure this event and prevent splits or catastrophic foam collapse.

Attaining this ideal natural balance is a complex task due to the large number of formulation and equipment variables in common use. Shrinkage

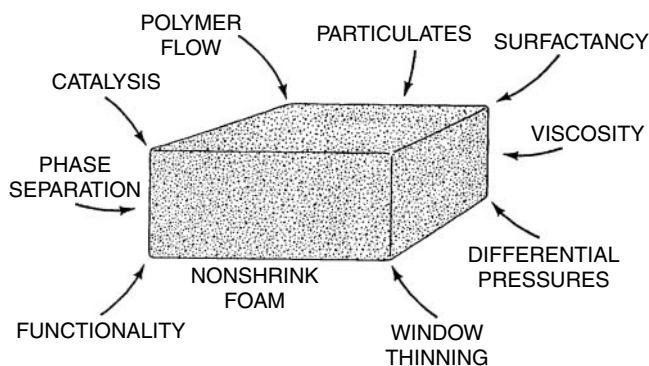


FIGURE 6.7

Factors affecting cell opening in flexible polyurethane foam formation.

in a flexible foam results when a large population of cells with intact windows remains at the end of foam manufacture. Just after production, such cells are filled with hot, pressurized CO₂. As the foam cools, the internal gas pressure diminishes, and CO₂ diffuses out of the cells roughly 15 times faster than air diffuses into the cells.^{118,137} The net result is a partial vacuum in the cell. When taken over a population of closed cells, this partial vacuum causes the foam to shrink and thus lose its physical dimensions.

A unique method for the automatic detection of cell opening has been described.¹³⁸ A more accurate understanding of the cell opening mechanism in conventional slabstock and hot-molded flexible polyurethane foams began with the work of Rossmly et al.¹²⁹ They observed that a high polymer molecular weight was not present at the time of cell opening. Shortly before cell opening, infrared spectroscopy showed negligible formation of urethane bonds and sudden appearance of strong urea-related absorption.¹³⁹ Coinciding with that event, a visible phase separation occurred in the bulk liquid.¹²⁸ The macrophase separation was identified as the precipitation of an agglomerated polyurea phase that was noted to increase the viscosity of the bulk liquid momentarily to a level consistent with the onset of a chemical gel. Small-angle x-ray studies revealed that the macrophase separation was accompanied by a microphase separation attributed to the formation of a bidentate hydrogen-bonded urea hard phase. Furthermore, cell opening was noted to occur only after a critical amount of hard phase had formed. In practical terms, the degree of cell openness can be regulated by adjusting the catalyst package.

The ingredients of higher reactivity used in high resiliency slabstock and molded foams make these foams more susceptible to having closed cells and shrinkage. During foam rise, the primary hydroxyl capped polyols and crosslinkers compete successfully with the water, resulting in higher levels of urethane and urea bond (and thus molecular weight) formation. The bidentate hydrogen bonded urea structures form to a lesser degree and appear only as a microphase. The macrophase separation of urea domain agglomerates does not occur and thus that potential cell opening mechanism is not available. In molded foams, cell opening due to continuing volume expansion is limited due to the restricted volume of the mold cavity. Cell opening in high resiliency molded foams is thus more dependent on the chemical methods that can be used to influence it.

In summary, cell opening in a flexible polyurethane foam is a complex physical and chemical event. It is influenced by the kinetics of chemical reactions and of cell growth, the type and concentration of surfactant, the morphology of thinning cell window membranes, phase separation, the presence of any cell-disrupting agents, and possibly contributions from physical stresses as in mechanical or vacuum crushing. The proper combination of these factors at the right moment in a foam's history leads to the desired type of foam. Further discussions of cell opening mechanisms are available.¹⁴⁰

6.5 Classical Physical Picture of Morphology

6.5.1 Heterophasic Nature of Flexible Polyurethane Foams

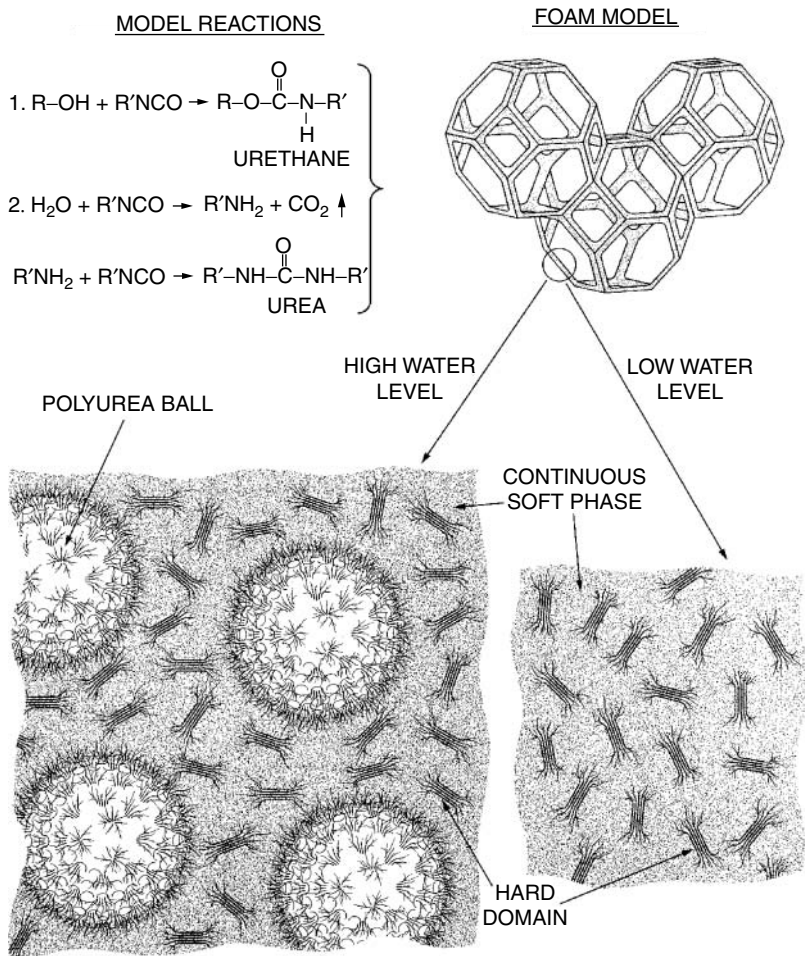
The properties of a flexible foam depend both on the macroscopic cell geometry and on the morphology of the polymer in its structural elements. Numerous reviews of the effects of cell geometry on foam properties are available.¹¹⁴ Much of the following discussion of the effects of polymer morphology is condensed from the literature.^{32,139,141}

Figure 6.8 illustrates how the reactions occurring during the manufacture of an unfilled conventional slabstock polyurethane foam lead to multiphase morphology formation. The existence of a heterogeneous (phase-separated) morphology in polyurethanes was suggested as early as 1966.¹⁴² Historically, it has generally been conceptualized to consist of discrete hard phase rich regions dispersed within a continuous soft polymer phase. It is also seen that the amount of water in the formulation can affect the morphology significantly, as discussed below.

The water-isocyanate reaction proceeds much faster than the polyol-isocyanate reaction in the early stages of a slabstock foam,^{130,143} due in part to the low reactivity of the secondary hydroxyls present in most slabstock-grade polyols. This disparity in reaction rates leads to the formation of polyurea oligomers. These oligomers continue to grow until they phase separate from the continuous liquid phase because of their different symmetry, thermodynamic incompatibility with liquid phase, and ability to form strong hydrogen bonds.^{141m,n} A detailed review of hydrogen bonding in polyurethanes is available.^{141l} In the lower portion of Figure 6.8, hard phase rich regions are represented by clustered thick lines. These features are tied into the matrix by covalent attachment to the polymer chains shown fading off into the continuous phase.

Water is completely soluble in the formulation. It reacts with the isocyanate to form urea species that are initially found totally in solution at low formulation water levels. At a certain concentration or molecular weight, these species suddenly separate out as the hard phase rich regions, indicated in the lower right-hand portion of Figure 6.8. When the water concentration exceeds the solubility of water in the blend of polyol, isocyanate and additives, discrete and stable droplets of water are formed in the mixture.^{141m} With continuing reaction, these regions of locally high water concentration give rise to locally high urea oligomer concentrations. Once a certain molecular weight is reached, these high urea oligomer concentrations separate into macrophase urea agglomerates,¹⁴¹ⁿ and a third phase consisting of agglomerated polyurea hard phase rich regions (polyurea balls shown in the lower left-hand portion of Figure 6.8) develops.

The continuous soft phase polymer results when the polyol-isocyanate reaction proceeds past the chemical gel point. The covalent links between the soft phase and the polyurea hard segment rich regions are urethane bonds.



MORPHOLOGY MODELS

FIGURE 6.8

Conceptual representation of polyphase structure in conventional slabstock polyurethane foams.

Evidence for the existence of this polyphase structure in slabstock polyurethane foams was reported first by Lidy et al.¹⁴⁴ and later confirmed by Turner and Wilkes.^{141h}

Macrophase polyurea agglomerates (urea balls) are not found in typical high-resiliency foams, where the primary hydroxyl-capped polyol and low molecular weight crosslinker compete successfully with water in isocyanate-consuming reactions. Water is also typically totally soluble in such polyol/isocyanate/additive blends, so that polyurea oligomers are dispersed much more uniformly in the continuous phase. The polyol reacts earlier with the

isocyanate to give prepolymer species. (Note that the solubilities and the relative reactivities in typical high-resiliency foams are quite different from those in the typical slabstock foams that were discussed in an earlier paragraph of this subsection. Water has a higher solubility in the types of polyols used in typical high-resiliency foams. These polyols also react faster than the ones used in typical slabstock foam formulations because of the reduced steric hindrance of their primary hydroxyl caps as well as the increased compatibility due to the high local concentration of their ethylene oxide repeat units.) These species react further with water and with the isocyanate groups in growing hard segments, to couple these segments with the continuous phase and further prevent agglomeration and macrophase separation. Crosslinker molecules also react with hard segments to further build molecular weight, disrupt symmetry, and thus hinder hydrogen bonding between hard segments.

When the water level is increased, the sizes of both the hard segment rich regions and the urea precipitates should increase. Both structures will contribute to an increase in the load bearing capacity of the foam. The efficiency and the permanence of load bearing enhancement may, however, differ between these two types of structures.^{141h}

An additional reinforcing phase may be present if the foam has been formulated to contain particulate fillers. Variations in this polyphase morphology can often account for the wide range of bulk physical properties attainable in flexible polyurethane foams.

6.5.2 Analytical Tools for Characterizing Flexible Polyurethane Foams

Many tools of analytical science are useful in investigating the morphologies of flexible polyurethane foams.^{139,141} This section discusses some tools that were especially useful in elucidating the “classical” features of the morphology summarized above.

Fourier-transform infrared (FTIR) spectroscopy is used to study the formation and structure of polyurethane foams.^{143–145} FTIR has been particularly useful in studying the time-related aspects of foam reaction kinetics and morphology development.¹⁴⁶

Dynamic mechanical spectroscopy (DMS) measures the ability of a viscoelastic material to store and dissipate mechanical energy. It thus provides information concerning stiffness and phase separation. Two excellent instructional reviews on the use of DMS with polyurethanes are available.^{147,148} The application of DMS and related techniques to flexible polyurethane foams is a fairly new endeavor,^{141e,149} while DMS has been used routinely to characterize both linear and crosslinked polyurethane elastomers. Many other references¹⁵⁰ are also helpful in interpreting foam data. DMS of typical flexible polyurethane foams made from three different conventional slabstock foam formulations are provided in Figure 6.9. Despite the possibility of formation of a more complex morphology, polyurethane foam DMS behavior

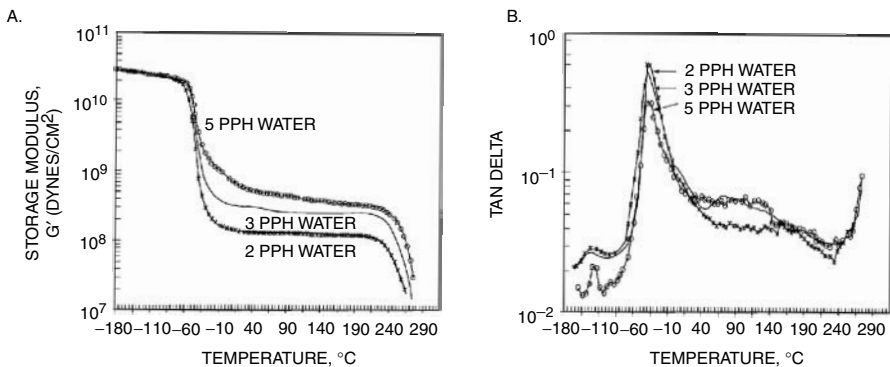


FIGURE 6.9

Examples of the dynamic mechanical spectra of flexible polyurethane foams, for foams made from three different conventional slabstock foam formulations. The theoretical hard segment weight fraction calculated from the foam composition under the assumption of complete reaction of water, polyol, and isocyanate is 0.21 for H₂O at 2 pphp (parts per hundred polyol), 0.26 for H₂O at 3 pphp, 0.30 for H₂O at 4 pphp, and 0.34 H₂O at 5 pphp.

is usually strikingly similar to that of polyurethane elastomers. The shear storage modulus G' is a measure of polymer stiffness. At low temperatures, molecular movement is essentially frozen, G' is high, and the polymer has nearly perfect elasticity. The loss tangent $\tan(\delta)$ is at a minimum, indicating that nearly all of the energy stored in deforming the sample is recovered when the stress is removed. A sharp transition occurs from a glassy state to a rubbery state at a low temperature (typically, but not always, somewhere in the range of -50 to -30°C). This transition is assigned to the onset of molecular motion in the soft phase. In this region, G' decreases sharply with a corresponding sharp increase in $\tan(\delta)$. The maximum in $\tan(\delta)$ is generally quoted as the soft phase glass transition temperature (T_g). T_g is related to the chemical structure and the molecular weight of the pure soft segment.¹⁵¹ Upscale shifts of T_g may result from the chain-immobilizing effects of a second phase.^{151a,d,152} Then follows a “rubbery plateau,” extending to the temperature range normally assigned to dissociation of microdomains of polyurea hard block rich regions.¹⁵³ This dissociation leads to a gradual decrease in G' . Increasing the water level increases G' in the plateau region since a larger volume fraction of the polyurea-rich hard phase is formed because of the increasing water-isocyanate reactions per unit volume. Finally, sample degradation takes place via thermal scission of covalent chemical bonds and G' drops precipitously.

T_g normally increases with decreasing molecular weight of the polyol since soft segments are connected to hard segments, so that lowering the polyol molecular weight increases the topological constraints on large-scale cooperative motions of soft segments. T_g can be modified further by the presence of urea groups resulting from the water reaction. It can be broadened by blending polyols. It can be both lowered and broadened by using plasticizers.

Polyurethane “shape memory polymer” foams^{151h,i} are fascinating examples of the unusual performance characteristics that can be obtained by tailoring the soft segment so that its T_g is near or slightly above room temperature. These foams are sometimes alternatively referred to as “memory,” “viscoelastic,” “low recovery,” “slow recovery,” “low resiliency,” or “pressure relief” foams. They manifest reversible switching behavior (flexible \leftrightarrow rigid transitions) with small changes in temperature near room temperature. Body heat is normally sufficient to cause them to soften and conform to the shape of the area that is being contacted. This behavior provides a unique feel and absence of “fight-back,” making them the preferred materials in many comfort cushioning and health care applications. Since a polymer will absorb significant amounts of energy at its T_g , they also have excellent energy absorption properties, resulting in their use in many applications where it is important to dampen noise and vibrations. In practice, making a flexible foam with a low resiliency near room temperature requires the use of a ~ 700 molecular weight poly(propylene oxide) triol. Triols with higher molecular weights will result in a lower T_g . Blends are often used to widen the low resiliency response and delay the hardening of the foam as the use temperature decreases. Plasticizers can also broaden the glass transition and extend the low resiliency response to lower use temperatures. Slow recovery is probably due to increased hydrogen bonding in these foams, consistent with the observation that the effect is reduced or totally lost if the foam is placed in a very humid area or is allowed to get wet.

Hard phase dissociation occurs at a higher temperature for a polyurea than for the corresponding polyurethane. For a given type of hard phase, the dissociation temperature increases with increasing segment length. The observation that the foam polymers exhibit fairly temperature-insensitive moduli over a broad temperature range in DMS offers indirect support for the presence of a virtual as well as covalent crosslinked network. The typical position, sharpness, intensity, and insensitivity of the glass transition argue for a well-segregated phasic structure with little phase mixing. The co-continuity of the hard phase with the soft phase (see below) is related to the coextension of both phases throughout the specimen. This is to be distinguished from phase mixing, which refers to the presence of segments of each type “buried” within regions rich in the other phase.

Energy dissipation by hysteresis upon repeated deformation cycles is related to $\tan(\delta)$ as measured by DMS. It increases with increasing phase mixing and soft segment linearity. It decreases with increasing covalent cross-linking in the soft phase.

Differential scanning calorimetry (DSC) is useful in confirming the soft phase T_g and in evaluating the other thermal response characteristics of foams.¹⁵⁴

Optical microscopy (OM),¹⁵⁵ scanning electron microscopy (SEM),¹⁵⁶ and transmission electron microscopy (TEM), can all be used to study the cellular structures of foams. The maximum possible magnification and the amount

of effort required to prepare the samples and to run the experiments both follow the order TEM>SEM>OM.

SEM and TEM are also used routinely in characterizing the polymer morphology in polyurethane foams, just as in many other types of multiphase materials. On the other hand, the use of some of the more recently developed techniques of microscopy to characterize the polymer morphology is growing gradually but is not yet routine. The most important such relatively new tool is atomic force microscopy (AFM) which is being used to study the polymer morphology in polyurethane foams^{90p,157} and elastomers.¹⁵⁸

Wide-angle x-ray scattering (WAXS) is useful in detecting the possible presence of crystalline ordering, especially in the hard phase.^{150a,151,159}

Small-angle x-ray scattering (SAXS) provides information on the total content and average size of hard phase rich regions and the thicknesses of “interphase” regions between hard and soft phases.^{160,161}

Recent advances have made it possible to conduct dynamic (synchrotron) SAXS, dynamic FTIR and dynamic rheometry simultaneously during polyurethane foam formation, allowing the simultaneous study of the kinetics of polymerization, hard phase formation, phase separation, and stiffness development.^{162,163} These recent advances at the frontiers of research on microstructure and property development in polyurethane foams merit a more detailed discussion, which will be provided in the next section.

6.5.3 Essential Aspects of Classical Physical Picture of Morphology

Figure 6.10 summarizes the general events leading to a flexible polyurethane foam. A simplified model of the types of morphological features found in

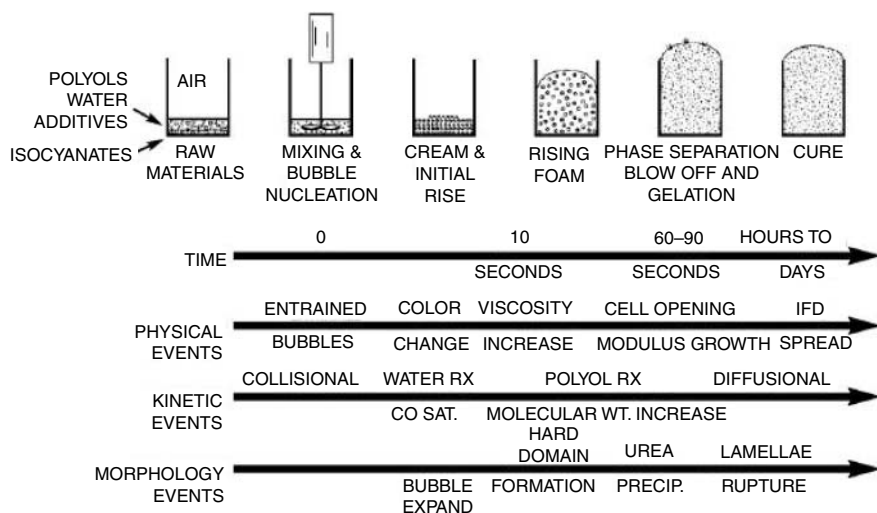


FIGURE 6.10

Summary of the general types of events that take place during flexible polyurethane foam formation.

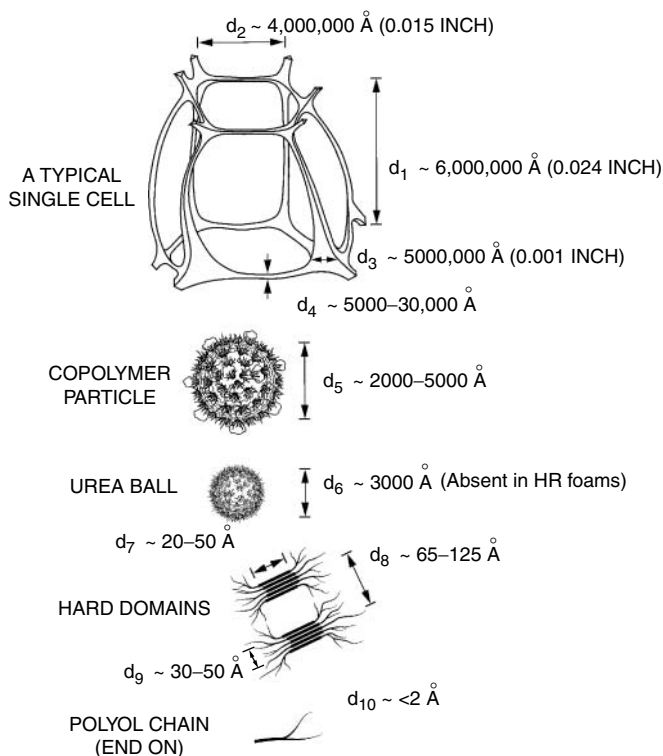


FIGURE 6.11

Simplified model for morphological features found in flexible polyurethane foams.

TDI-based flexible polyurethane foams is provided in Figure 6.11. We will refer to the perspective provided by Figures 6.8 and 6.11 as the “classical” model. It was developed mainly as the result of *postmortem* analyses; that is, analyses where the morphologies of a foam and of the polymer within the structural elements of this foam are characterized and the properties of the foam are measured after the fabrication of the foam has been completed. For the benefit of readers who may be interested in delving into the frontiers of research, the next section will discuss the important new fundamental insights that are being obtained by using dynamic (*in situ*) measurements to study morphology and property development.

6.6 Research Frontiers in Microstructure and Property Development

6.6.1 Synopsis

Flexible copoly(ether-urethane urea) foam is a multiphase cellular material. It contains nonlinear segmented $-(H_mS)_n$ - multiblock copolymer chains where

H_m represents a polyurea hard segment with a degree of polymerization m ; S is the poly(ether-urethane) soft segment; and n is the degree of polymerization of the block copolymer.^{139,141e,i} Polyether and polyurea blocks are joined via covalent urethane links. The process by which the block copolymer microstructure and resultant morphology evolve is reaction-induced phase separation.¹⁶⁴ The final morphology of the polymer is strongly dependent upon the kinetic competition between the rates of polymerization, phase separation, solidification, and the inherent connectivity between the phases. Various morphologies can be accessed through control of the rates of polymerization and phase separation.

A refined description of the physical events during flexible polyurethane foam formation, deduced from such *in situ* real-time experiments,¹⁶³ is shown in Figure 6.12. In this example, a typical water-blown copolyurethaneurea foam is made by using a polyether polyol, TDI, or MDI as the isocyanate, and water (which reacts with the isocyanate to form polyurea hard segments) as the chain extender. MST denotes the microstructural phase transition, p_{NCO} is the fraction of conversion of the NCO groups, Φ is the volume fraction, N is the degree of polymerization, χ is the Flory-Huggins interaction parameter quantifying the deviations of a mixture from ideal mixing, and the Bergh-

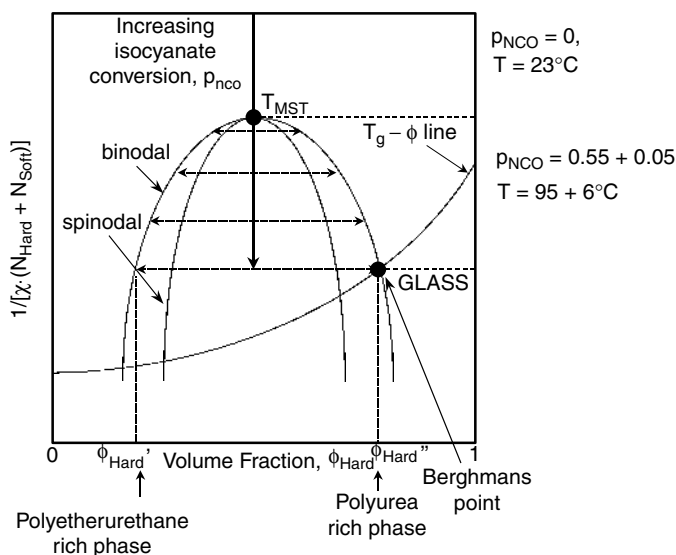


FIGURE 6.12

A refined description of some of the key physical events that take place during flexible polyurethane foam formation, as deduced from *in situ* real-time experiments. A typical water-blown copolyurethaneurea foam is made by using a polyether polyol, TDI, or MDI as the isocyanate, and water (which reacts with the isocyanate to form polyurea hard segments) as the “chain extender.” MST denotes the microstructural phase transition, p_{NCO} is the fraction of conversion of the NCO groups, Φ is the volume fraction, N is the degree of polymerization, χ is the Flory-Huggins interaction parameter, and the Berghmans point is the point at which the glass transition temperature of the hard phase reaches the temperature of the reacting mixture.

mans point is the point at which the glass transition temperature of the hard phase reaches the temperature of the reacting mixture. The onset of vitrification takes place at the Berghmans point, so that the microphase separation is intercepted and arrested by the vitrification of the phase that is richer in hard segment. The product χN is similar to an effective temperature, so that the effect of the rapid increase of N and hence decrease of $1/(\chi N)$ during polymerization resembles the effect of applying a temperature quench.

Only the soft phase is assumed to be continuous, and discrete hard phase domains (resembling those shown in Figures 6.8 and 6.11) are assumed to be dispersed in this soft matrix, in the classical model of the morphology. However, Figure 6.12 indicates that the MST occurs preferentially by spinodal decomposition, which can lead to hard phase co-continuity. ("Spinodal decomposition" refers to the process of spontaneous and continuous phase separation and growth that occurs in the unstable region of the phase diagram beneath the spinodal curve in Figure 6.12. It results from the fact that the mixture is unstable to infinitesimal concentration fluctuations in this region, so that phase separation does not require the "nucleation" of finite-sized regions of concentration inhomogeneity.) This relatively recent comprehension that the hard phase often manifests a significant amount of co-continuity with the soft phase is important in understanding and predicting the properties of polyurethane flexible foams and elastomers.

The interpretation of the mechanical properties of polyurethane elastomers, which are dense materials, is not complicated by the need to deconvolute the effects of the cellular structure as in foams. The effects of any hard phase co-continuity are, therefore, generally easiest to identify unambiguously in the observed elastic properties (moduli) of polyurethane elastomers. See Ryan et al. for an example.¹⁶⁵

6.6.2 Key Aspects of Morphology Development during Reactive Processing

The reactive processing of a flexible copoly(ether-urethane urea) foam from liquid monomers and oligomers involves a complex combination of chemical and physical events.¹⁶⁶ From room temperature and in less than 5 min, a liquid mixture of low molar mass components is transformed into a material with a supramolecular architecture of a "solid" foam. The copolymerization proceeds via the simultaneous reactions of a diisocyanate with polyether polyol and water. The copolymerizing mixture is blown into foam by the cogeneration of CO_2 gas evolved from the water-diisocyanate reaction. As copolymerization proceeds, the core of the foam becomes insulated by the surrounding polymerizing mixture, creating, in effect, a quasi-adiabatic environment. In the initial 5 min of the copolymerization, the reactive mixture experiences an exotherm of 110 to 140°C, depending upon the specifics of the composition of the formulation, an approximately 30-fold volume expansion for a foam with a density of 32 kg/m³, and a $\sim 10^6$ -fold viscosity increase. These physical changes are illustrated in Figure 6.13.¹⁶⁷

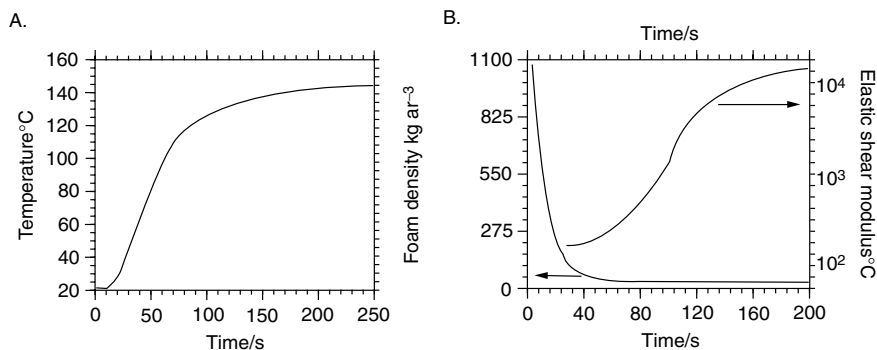


FIGURE 6.13

(A) Adiabatic temperature rise profile and (B) the rapid changes in density and elastic shear modulus during a typical flexible polyurethane foaming process. (Copyright 1994 American Chemical Society. Reprinted with permission from Elwell, M.J., Mortimer, S., and Ryan, A.J., *Macromolecules*, 27, 5428, 1994.)

Investigation of the intimate and complex competition between copolymerization, macrophase separation and microphase separation, and solidification processes, requires the use of *in situ*, time-resolved analytical methods.^{146,149,163,166–168} However, when such studies are conducted under isothermal conditions and thus ignore the importance of the process thermal history, they lead to erroneous results. The realization that analytical investigations must be conducted under forced-adiabatic conditions^{166a,168a,b} was crucial to making significant progress in understanding how the polymer microstructure and architecture actually evolves.

Structure and morphology development can be divided into four categories:

1. The copolymerization itself, and the subsequent development of the polymer microstructure and architecture.
2. Macrophase and microphase separation processes, and their associated kinetics.
3. The solidification processes of vitrification, chemical gelation, and crystallization, and how they impact the development of the macroscopic properties.
4. The polymer morphology of the foam, *post-reaction*, four weeks after it has made. It is at this point that *postmortem* as opposed to *in situ* analyses are conducted. Only by appreciating and understanding how the prevailing morphology evolved (*in situ* and *postmortem* investigations) is it possible to understand, control, and subsequently improve the end use performance as defined in terms of certain foam properties.

6.6.3 Reaction Kinetics: Understanding Copolymerization

Fast reactions put certain limitations on the techniques that can be employed for their analysis.^{168c} Time-resolved FTIR spectroscopy is the technique of choice. The use of a forced-adiabatic reaction cell in combination with a FTIR spectrophotometer was reported first by Artavia and Macosko^{168a} and has since been adapted by other research groups. A wide range of information can be obtained from such experiments, as shown for example in Figure 6.14.^{163b} Such investigations on slabstock foams have demonstrated that the

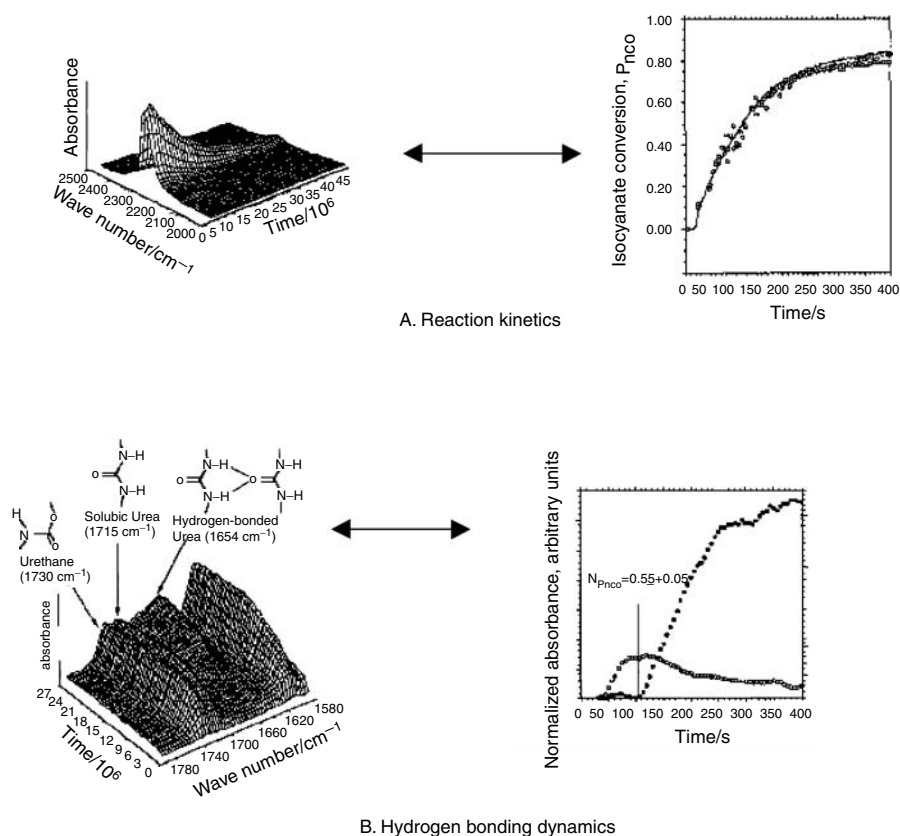


FIGURE 6.14

Time-resolved FTIR data obtained under forced-adiabatic reaction conditions during the formation of flexible polyurethane foam from a polyether triol (number-average molecular weight of 6000 g/mol), water, and an isomeric mixture of MDI. **(A)** Copolymerization kinetics in terms of the fraction of isocyanate conversion, p_{NCO} , versus time, determined from the decay of the NCO stretch band (2270 cm^{-1}). **(B)** Hydrogen bonding dynamics, in relation to the microphase separation transition, derived from the variations with time of the carbonyl absorbances associated with soluble polyurea (1715 cm^{-1}) (○) and hydrogen-bonded urea (1654 cm^{-1}) (●). (Copyright 1997 Wiley-VCH Verlag. Reprinted with permission from Stanford, J.L., Ryan, A.J., and Elwell, M.J., in *Processing of Polymers*, ed. H.E.H. Meijer, vol. 18 of *Materials Science and Technology: A Comprehensive Treatment*, VCH Publishers, Weinheim, Germany, 1997, chap. 9.)

formation of urethane and soluble urea moieties occurs simultaneously in the initial stages of the reaction, as opposed to sequentially.

In early stages of copolymerization, the reaction mixture comprises polyether, isocyanate-terminated polyether oligomers, water, polyurea homopolymer, and some copoly(ether-urethane urea) block copolymer that contains the urethane linking group. Such mixtures are similar to ternary polymer blends.^{167,168j} Reaction between the monomers and oligomers results in both a molecular weight increase (N) and a concomitant change in the values of the interaction parameters (c). The onset of microphase separation of the polyurea hard segment sequence lengths occurs midpoint in the reaction at an isocyanate conversion fraction of $p_{\text{NCO}} = 0.55 \pm 0.05$.¹⁶⁶ FTIR spectroscopy is capable of providing much information on the reaction chemistry and the sequence of chemical events, both prior to and after microphase separation of the urea hard segments. However, it does not provide any indication of the mechanism(s) of phase separation, the length scales of the evolving morphology, or the extent of microphase separation.

6.6.4 Phase Separation Kinetics: Understanding the Evolution of Polymer Morphology

The structure development kinetics must be probed by time-resolved forced-adiabatic synchrotron SAXS measurements to investigate the real-time morphological changes during fast bulk copolymerization. The use of this technique to investigate the structure development kinetics in both conventional and model MDI-based flexible copoly(ether-urethane urea) foams was first reported by Elwell, Mortimer, and Ryan.¹⁶⁷ This was later followed by McClusky et al.,^{168d} and more recently by Li et al.^{168i,j} who further developed the technique and the subsequent analysis and also extended the interpretation and understanding of the scattering data that are obtained.

Figure 6.15 illustrates the wealth of polymer microstructure and morphological information that can be obtained from *in situ* time-resolved synchrotron SAXS measurements.^{163b} There have been many studies on the morphology and properties of flexible copoly(ether-urethane urea) foams based upon TDI and MDI. Different research groups have observed particulate^{149b,166a,b,d,168d,h,169} and bicontinuous^{146c,157b,163a,c,166c,e,167,168i,j} hard segment structures in a wide range of systems. The evidence suggests strongly that phase separation proceeds with kinetics associated with spinodal decomposition. Vitrification of the polyurea rich phase arrests and preserves a bicontinuous morphology shortly after the onset of microphase separation.

Li et al.^{168j} also investigated high resiliency foam formulations that incorporate chain extenders of low molar mass and crosslinking agents. Their *in situ* studies showed that incorporation of such components delays the onset of microphase separation. The extent of disruption to urea group assembly and development of hydrogen bond interactions is a function of the chemical structure of the chain extender or crosslinking agent.

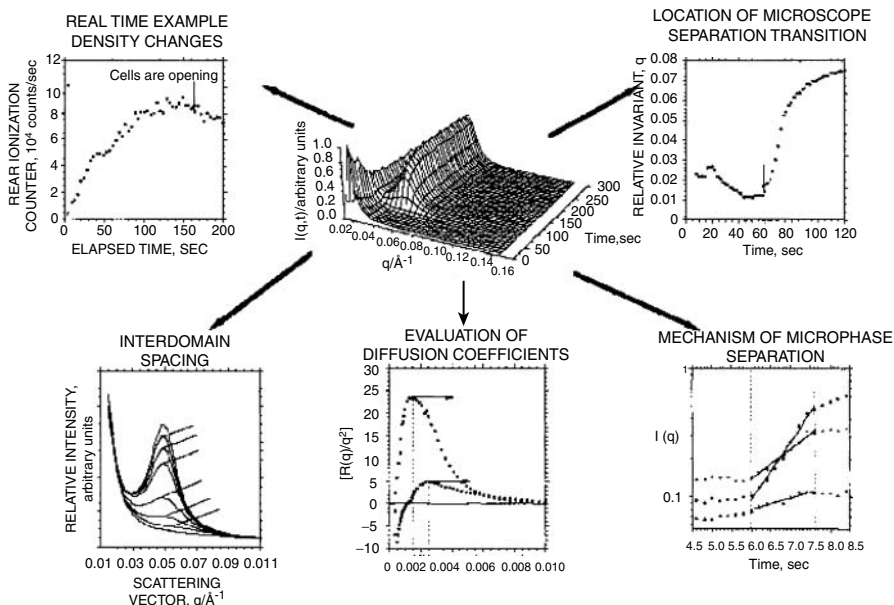


FIGURE 6.15

Application of time-resolved SAXS to the study of structure development in reactive polymer systems. Three-dimensional SAXS data from a flexible polyurethane foam-forming system, comprising 38% by weight of polyurea hard segments, provide information on macroscopic density changes, microphase separation, and domain size scale, with simultaneous cell formation and copolymerization. The $I(q)$ versus time plot shows data obtained at scattering vector values of $q = 0.036$ (+), 0.050 (○), and 0.076 (▲). (Copyright 1997 Wiley-VCH Verlag. Reprinted with permission from Stanford, J.L., Ryan, A.J., and Elwell, M.J., *Processing of Polymers*, ed. H.E.H. Meijer, vol. 18 of *Materials Science and Technology: A Comprehensive Treatment*, VCH Publishers, Weinheim, Germany, 1997, chap. 9.)

6.6.5 Solidification: Understanding the Arrest of Phase Separation

Dynamic rheometry has been employed to investigate the development of polymer modulus, the nature of the connectivity between the hard and soft segments, and the macroscopic stability of the foam beyond the onset of cell opening.¹⁶⁶ The development and use of an adiabatic rheometer was reported first by Mora et al.^{166b,168b} As illustrated in Figure 6.16,^{149b} there are four regions of differing rheological behavior: (1) bubble nucleation; (2) liquid foam and microphase separation; (3) stiffening of the polymer, hard segment vitrification, and cell opening; and (4) chemical gelation.

In slabstock foams, the storage modulus begins to increase at the onset of the microphase separation of the polyurea hard segments. The increase in stiffness is derived from the growth in the interconnecting physical network of hydrogen-bonded, polyurea hard segments. Cookson et al.¹⁷⁰ showed that the onset of microphase separation coincided with a sharp increase in the normal force, and cell opening coincided with the apex of the peak in the normal force measured during foaming, as illustrated in Figure 6.17.

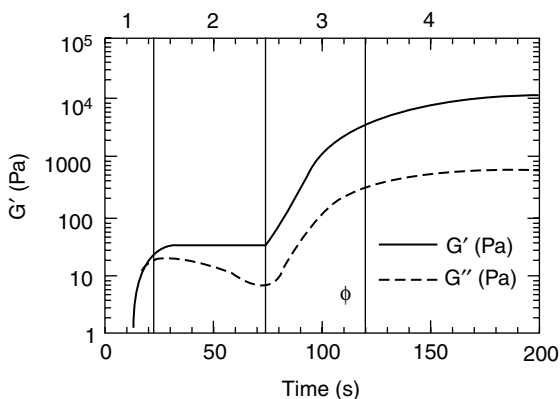


FIGURE 6.16

Modulus build in a flexible slabstock foam. Four regions of behavior are indicated: (1) initial bubble growth, (2) bubble network, (3) polymer stiffening, and (4) final curing. Cell opening occurs a few seconds after the onset of Region 3. (Copyright 1995 Society of the Plastics Industry [now held by the Alliance for the Polyurethanes Industry]. Reprinted with permission from Neff, R. and Macosko, C.W., *Proceedings of Polyurethanes 1995*, Society of the Plastics Industry, Chicago, 344–352, September 1995.)

The sudden stiffening of the polymer in the absence of the covalent network results in a brittle material. This material has insufficient tensile and shear strength to accommodate the additional strain resulting from the continued expansion of the foam. Consequently, the cell windows undergo rupture and blow-off takes place. Catastrophic collapse occurs if the foam is too weak to support its own weight after cell rupture, while under other

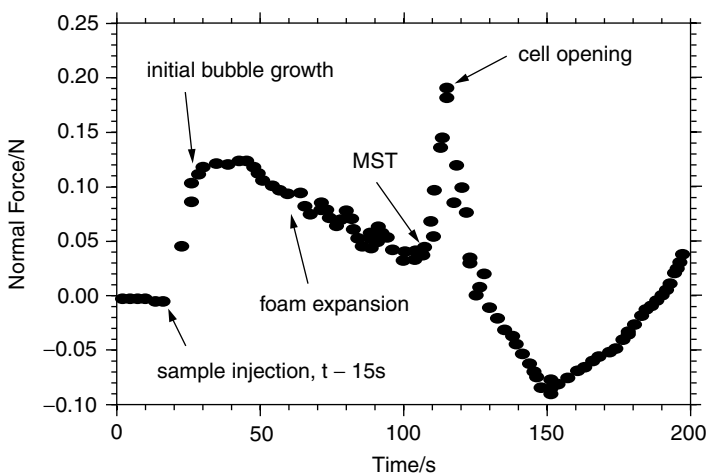


FIGURE 6.17

Example of normal force versus time during polyurethane foam formation, illustrating identification of microphase separation transition (MST) and cell opening.

circumstances there may even be no blow-off or cell opening. Li et al.^{168j} showed that the incorporation of chain extenders and crosslinking reagents delayed the onset of microphase separation and that more block copolymer could be formed. The compatibility between the hard segments and soft segments increased. By increasing the degree of connectivity between the hard and soft segments, the stress on the polyurea interconnecting physical network can be spread to the soft segment phase, increasing the overall extensibility and strength of the foamed polymer. The delay in the onset of microphase separation leads to an increase in the molecular weight of the polyether at the time of cell opening. The increase in molecular weight and concomitant increase in viscosity results in a higher degree of closed cells in the foam.

6.6.6 Post-Reaction Analyses: Understanding Properties in End-Use Applications

Postmortem analyses of both MDI-based and TDI-based flexible copoly(ether-urethane urea) foams by scanning transmission x-ray spectromicroscopy and tapping mode AFM have confirmed the presence of a bicontinuous, interconnecting network of polyurea hard segments. Figure 6.18 shows AFM phase images from an MDI-based flexible copoly(ether-urethane urea) foam of Li et al.¹⁶⁸ⁱ and a TDI-based flexible copoly(ether-urethane urea) foam of Rightor et al.^{157b} The lighter phases are rich in polyurea. The hard segment rich regions appear to be interconnected. These images agree qualitatively with those reported by Hamley et al.^{163c} They are also consistent with the hypothesis that arresting phase separation by vitrification of the hard segment rich phase prevents the evolution of a morphology comprising dispersed isolated domains such as those exemplified by the equilibrium morphologies (e.g., spheres, cylinders, and lamellae) of diblock and triblock copolymers.

6.6.7 Summary: Overview of Polymer Microstructure and Morphology Development

In summary, the reactive processing of a flexible polyurethane foam from liquid monomers and oligomers involves a complex combination of chemical and physical events. In early stages of copolymerization, the reaction mixture comprises polyether, isocyanate terminated polyether oligomers, water, polyurea homopolymer, and some copoly(ether-urethane urea) block copolymer that contains the urethane linking group. The copolymerizing mixture is blown into foam by the cogeneration of CO₂ gas evolved from the water-diisocyanate reaction. As copolymerization proceeds, the core of the foam becomes insulated by the surrounding polymerizing mixture, creating, in effect, a quasi-adiabatic environment. Reaction between the monomers and oligomers results in both a molecular weight increase and a change in the interaction parameters, resulting in a reaction-induced

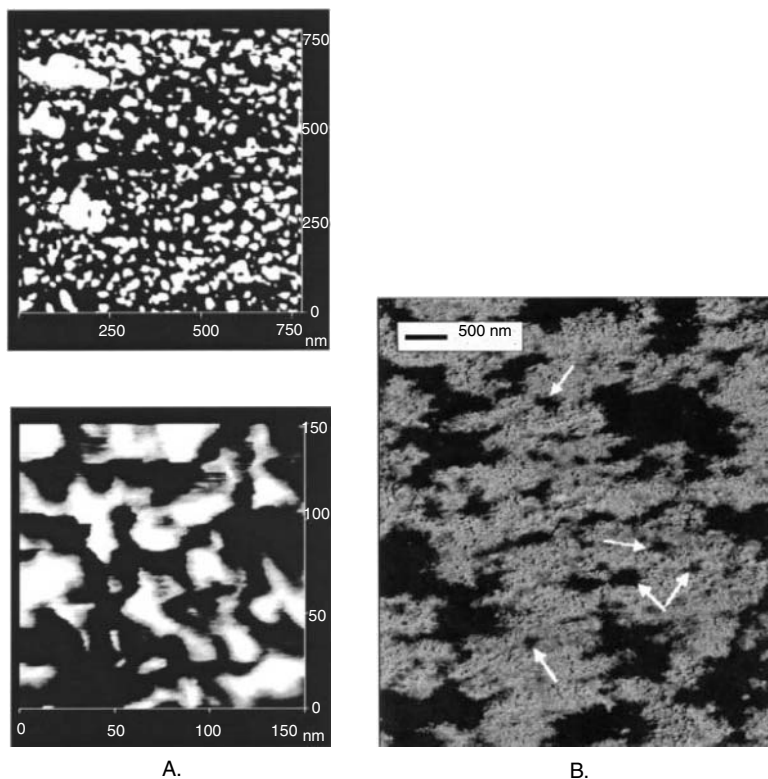


FIGURE 6.18

(A) AFM tapping mode phase images of an MDI foam at low (top) and high (bottom) magnifications. (Copyright 2002 American Chemical Society. Reprinted with permission from Li, W., Ryan, A.J., and Meier, I.K., *Macromolecules*, 35, 5034, 2002.) (B) High magnification ($5 \times 5 \mu\text{m}^2$) AFM phase image of a TDI foam. The arrows indicate some of the larger polyol-rich regions present within urea aggregates. (Copyright 2002 American Chemical Society. Reprinted with permission from Richtor, E.G. et al., *Macromolecules*, 35, 5873, 2002.)

phase separation process. The onset of microphase separation of the polyurea hard segment sequence lengths occurs midpoint in the reaction, at isocyanate conversion fraction $p_{\text{NCO}} = 0.55 \pm 0.05$. The evidence suggests strongly that phase separation proceeds with kinetics associated with a spinodal decomposition.

At the onset of microphase separation, the system becomes both spatially and chemically heterogeneous, separating the functional groups. The microphase-separated polyurea hard segments continue to grow. Association of these urea moieties takes place via the formation of hydrogen bonds. Hydrogen bonding is thus a parasitic process, not the driving process of microphase separation. As copolymerization proceeds further, the concentration of copoly(ether-urethane urea) block copolymer continually increases until the microphase separation is arrested by vitrification. The copoly(ether-urethane urea) block copolymer evolves via the formation of a urethane

group between the respective polyether and the polyurea blocks. It effectively acts as a surfactant for the immiscible hard polyurea and soft polyether segments. The strength of the interactions between the multi-block copolymer and the homopolymer phases controls the overall degree of mixing and the driving force for interfacial segregation.

The storage modulus begins to increase at the onset of microphase separation of polyurea hard segments. The increase in stiffness is derived from the growth in the interconnecting physical network of hydrogen-bonded, polyurea hard segments. Cell opening occurs within 5 to 10 sec after the onset of modulus increase. The sudden stiffening of the polymer in the absence of a covalent network results in a brittle material that has insufficient tensile and shear strength to accommodate the additional strain resulting from the continued expansion of the foam. As a direct consequence, the cell windows undergo rupture and blow-off occurs.

Vitrification of the polyurea-rich phase at a phase composition whose T_g is equal to the temperature of the surrounding medium arrests and preserves the bicontinuous morphology shortly after the onset of microphase separation. This results in a foam whose internal polymer morphology comprises a bicontinuous interconnecting physical network of hydrogen-bonded polyurea hard-segment sequence lengths within a crosslinked poly(ether urethane).

6.7 Foam Preparation

6.7.1 General Considerations

Polyurethanes are usually processed quite differently from other major polymers. Most thermoplastics are polymerized in large factories by chemical manufacturers and then sold to processors as pellets or powders. The pellets or powders are then converted to useful end products by fabrication methods involving heating, shaping under pressure, cooling, and packaging. The properties of the plastic thus produced are controlled by the properties of the base polymer. By contrast, the polymerization of polyurethanes is more often carried out by independent outside processors who often possess enough skill to achieve wide variations in the properties of products made from just a few base resins. In addition to providing the raw materials, the chemical manufacturer is often required to provide advice, technical information, and even manpower assistance to the processor.

There is a vast number of variables in the formation of polyurethane foams. Many of these variables can have dramatic effects on the foam properties. For example, the typical effects of varying the water level in the formulation on the density of the resulting foam are illustrated in Figure 6.19. As was discussed earlier, the reaction of H_2O with isocyanate produces both polyurea compounds which remain in the foam and CO_2 , which acts as a blowing

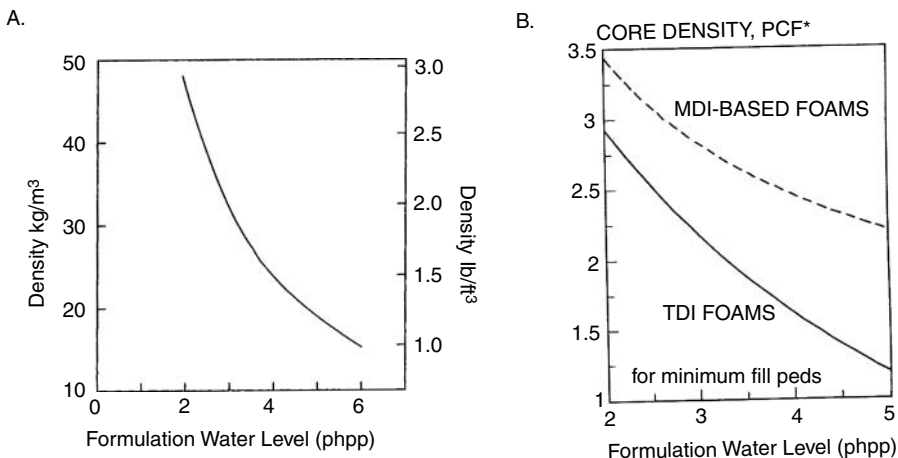


FIGURE 6.19

Typical effects of varying the water level in the formulation on the density of the resulting foam. The reaction of H_2O with isocyanate produces both polyurea compounds which remain in the foam and CO_2 which acts as a blowing agent. Increasing the amount of H_2O in the formulation increases the production of the CO_2 blowing agent and hence decreases the density of the foam. Consequently, in the absence of auxiliary blowing agents, the amount of H_2O in the formulation determines the foam density. **(A)** Results for typical slabstock foam formulations. **(B)** Results for typical TDI-based and MDI-based molded foam formulations. The units (phpp) denote parts per hundred parts polyol.

agent. Increasing the amount of H_2O in the formulation increases the production of the CO_2 blowing agent and hence decreases the density of the foam. Consequently, in the absence of auxiliary blowing agents, the amount of H_2O in the formulation determines the foam density.

The complexity of foam formulations makes the development or selection of recipes that will give good results at a minimum cost difficult. This task requires not only knowledge of polyurethane chemistry but also skill in the operation of dispensing machines of various types, and in the technology and art of evaluating final products. Over the roughly 40-year commercial history of polyurethanes, many successful methods for foam production have been developed and recorded in the literature. Many of the best foam recipes are commercially available from suppliers as fully formulated systems, which are often attractive to manufacturers who (because of volume requirements, in-house technical limitations, equipment, or other restraints) limit their involvement to the final mixing and distribution of the polyurethane materials.

The chemical reaction between a polyol and an isocyanate begins immediately when the two ingredients are mixed in the presence of suitable catalysts. Once started, the polymerization is exothermic up to its completion. Whichever method of mixing and dispensing is used, there are certain basic requirements for satisfactory foam production:

- *Temperature conditioning.* The viscosity, density, and chemical reactivity of polyols and isocyanates vary significantly with temperature. Controlling the temperature is, therefore, essential to the reproducible processing of polyurethane foams.
- *Accurate metering or weighing.* To make a foam reproducibly, the ingredients must be mixed together consistently in the proportions required by the formulation.
- *Freedom from contaminants.* Contamination is defined as the presence of any of the vast number of possible unintended foreign materials in the foam preparation system. Defects in polyurethane foams are often eventually linked to contaminants.
- *Effective mixing.* Incomplete mixing can produce a foam that has both cosmetic and physical defects.
- *Curing environment.* In general, flexible polyurethane foams do not develop their ultimate properties until some hours or days after initial mixing. Many foams cure satisfactorily and develop properties simply through storage at room temperature. Other systems may benefit from a post-cure heating cycle. The optimum processing and curing conditions must be investigated for each type of flexible foam.

Foaming at different scales often produces foams with different cell sizes and hence different resultant properties from the same starting formulation.^{114a,171} Commercial flexible polyurethane foam development typically proceeds through three stages:

- *Cup foaming.*¹⁷² Foaming on this small “laboratory” scale typically requires 1 worker, approximately 1 gal of materials, and 1 day of work.
- *Box foaming.*¹⁷³ Foaming on this intermediate “laboratory” scale typically requires 1 worker, approximately 1 to 5 gal of materials, and 1 day of work.
- *Machine foaming.*¹⁷⁴ Foaming on this “production” scale typically requires a number of workers that varies as a function of the size and the complexity of the machine, approximately 5 to 55 gal of materials, and 1 to 5 days of work.

Flexible foams are made commercially by various fabrication processes, as will be discussed briefly in the next three subsections. Typical block flow diagrams for slabstock and molded foam processes are available.¹⁷⁵

6.7.2 Slabstock Foams

More than half of all flexible polyurethane foam is produced as slabstock buns. Slabstock foam is in high demand because of its wide application and

large volume usage. Simple and adaptable manufacturing processes, coupled with the wide array of products that can be produced with high quality, have made these foams economical and versatile choices for many markets. Process and formulation changes that slabstock foam manufacturers made in the 1990s will allow the industry to continue to produce these products while also addressing the environmental concerns of customers and the public.

Approximately 1.5 billion lb (680 million metric tons) of flexible slabstock foam were produced in North America during 1994.¹⁷⁶ The U.S. market breaks down into furniture (40%), bedding (15%), transportation cushioning (12%), carpet underlayment (25%), and packaging (5%). The balance is used in textiles, household goods, and miscellaneous other applications.

Most slabstock foams are made on continuous foam machines, but discontinuous box foaming is viable in less-developed countries or for low-volume specialty foams.

Slabstock foam buns can be cut into a variety of desired shapes after curing. The foam pieces cut from the bun can then be used “as is,” or cut, sewn, glued, or stapled to each other or to other objects or materials. The relative ease of fabrication helps ensure the complete cushioning of delicate objects, allows manufacturers to produce complex sizes and shapes, and makes flexible slabstock foam one of the most adaptable among all cushioning and comfort products. Cushioning and comfort properties can be tailored to meet the requirements of various applications by simply modifying the formulation used to produce the foam. Formulation changes (whose effects are well understood) can be made easily, to increase or decrease the density and the load-bearing characteristics of the foam (resulting in a softer or harder foam). Additives can be used to modify the polymer chemistry and cell structure and allow manufacturers to fine-tune the properties. Other additives can modify foam flammability, dissipation of static electricity, and many other important properties. Mechanical processes such as partially crushing the foam to open cells or to cause foam densification can modify foam characteristics after a foam has been produced, to meet the needs of specialized applications.

There are four main types of flexible polyurethane slabstock foam: conventional, high resiliency, filled,¹⁷⁷ and high load bearing.¹⁷⁸ The properties can be tailored to the requirements of various applications by properly selecting the level and type of polyol and the other formulation components. The most important properties are the density, hardness, and porosity. The hardness grades that are typically specified for conventional flexible polyurethane foams in North America are listed in [Table 6.3](#). The formulation variables that most affect the key properties are the isocyanate index, amount of water, amount of auxiliary blowing agent, and catalyst level and type. Recent formulation changes, dictated by environmental considerations, have resulted in formulations that use a higher water level and a lower isocyanate index. There is growing belief that these changes may be detrimental to long term fatigue (loss of load bearing) resistance. Research is in progress to further elucidate the causes of fatigue. An improved understanding of the fundamental nature

TABLE 6.3

Hardness Grades for Conventional Flexible Slabstock
Foams in North America

Foam Grade	Density Range (lb/ft ³)	Indentation Force Deflection (lb/50 in. ²)
Supersoft	1.0–1.8	10–20
Soft	1.0–1.5	20–30
Intermediate	1.2–1.4	30–40
Hard	1.2–3.0	>40

of fatigue in foams will enable the design of foam structures and polymer morphologies that result in improved fatigue resistance.^{31,179}

6.7.3 Molded Foams

In contrast to the large buns produced in conventional slabstock foams, molded foams are made one at a time in production plants designed specifically for the repetitive (batch) production of discrete foam shapes. These plants often operate two or three working shifts per day and may produce more than one style or part. Molding involves pouring the reacting mixture into a suitable mold, closing the mold, and allowing the foam to fill the mold. In addition to replicating the internal dimensions of the mold, the final product can also permanently record its part or style number and incorporate physical inserts of various types. A vast variety of intricate shapes can be molded successfully. With the appropriate selection of the starting isocyanate and polyol and with the selective use of additives, it is possible to form flexible molded foam products meeting very different performance specifications. It is also possible to “foam in place” various reinforcements or otherwise produce foams with multiple zones of hardness.

Molded foams find application in all forms of transportation seating and trim parts, as well as in some upholstered furniture,¹⁸⁰ bedding, packaging, and novelty items. While a small percentage of the seating cushions used in automobiles today is cut from slabstock foam buns,¹⁸¹ most are made from molded foams. Typical methods of constructing a final automobile seat assembly have been reviewed.¹⁸²

Molded foam production is considerably more complicated than slabstock foam production, because of factors such as the use of formulations of higher reactivity, pour-pattern limitations, the discrete size of each individual shot, the need to open and close a mold lid mechanically, the choice of release agent, mold temperature latitudes, and the available curing cycle. Foam formulations used for molded and slabstock foams differ mainly with respect to their catalyst packages and the compositions of their polyols. More reactive polyols of higher molecular weight are generally used to enable the production of molded foams with good cure behavior and rapid property development.

The two major molding techniques used in the polyurethane industry are the hot cure and the cold cure (or high resiliency) processes. The hot cure molding process was established commercially more than 30 years ago. High temperature is applied to the mold during the cure cycle, driving the foaming reaction to a sufficient degree of surface cure to permit the foam to be demolded in a timely manner and then subjected to additional downstream fabrication steps. The newer high resiliency foam molding process utilizes ingredients (especially polyols) of higher reactivity so that less oven curing (and hence less externally applied energy) is needed. The essential differences between hot and high resiliency molding are summarized in Table 6.4. Detailed discussions of other processing and physical property differences are available.¹⁸³

Most flexible polyurethane foam molding is done in cast aluminum molds, but there has also been some use of reinforced epoxy molds. Molds are usually made in two sections, with mechanical opening and closing of the lid. A mold release agent (most often, a commercial blend of various natural and synthetic waxes) is used to help remove a polyurethane foam article from a mold. Mold release agents can be characterized as water based or solvent based. Detailed review articles are available.¹⁸⁴ Recent developments in water-based systems have been reported.¹⁸⁵

Specialty molded foams include semiflexible, semirigid, and integral-skin types of foams. In general, semiflexible molded foams are used in instrument panels, arm rests, console covers, door panels, and other foam parts found in automobile interiors. If the mold is lined with a preformed plastic skin or textile fabric, dispersed foam will adhere to it and simplify the assembly requirements of many composite products. Technology for directly foaming onto a cover material preformed into a seat cushion mold has existed since 1955.¹⁸⁶ Recent developments in vacuum-assisted foam-in-place technology

TABLE 6.4

Essential Differences between Hot Cure and High Resiliency Flexible Polyurethane Foam Molding Technologies

	Hot Cure	High Resiliency
Isocyanate	80/20 TDI	80/20 TDI Blends with MDI Polymeric MDI MDI prepolymers
Polyol		
Molecular Weight (g/mole)	2800–3500	4500–6500
Ethylene Oxide Capping	Yes	Yes
Copolymer Polyol	Optional	Optional
Cure Oven	180–300°C	75–200°C
Temperature	(356–572°F)	(165–392°F)
Postcuring	No	Optional
Mold Temperature	25–45°C	50–70°C
At Pour	(77–113°F)	(122–158°F)

for auto seating have been discussed.¹⁸⁷ Alternative schemes for bonding the cover fabric to the foam pad have been developed.¹⁸⁸

6.7.4 Carpet Backing Foams

An adhesive backing is required to anchor the tufts in manufacturing tufted carpets. The most popular carpet backing systems are based on styrene-butadiene latexes which give good tuft-lock at low cost. Another backing approach is the application of a resilient foam backing over the anchor coat. Foamed materials used for this backing are poly(vinyl chloride) (PVC) plastisols, polyurethanes, EVA, and latex.

The concept of forming a flexible polyurethane foam directly on the back of a carpet was described as early as 1959.¹⁸⁹ Advantages in improved tuft-lock, energy absorption, heat and sound absorbance, non-slip character, and appearance retention time of the carpet face were recognized rapidly. Commercial success for polyurethanes came at the expense of traditional backing materials (foamed rubber latex and foamed PVC).¹⁹⁰

Polyurethane raw materials are more expensive than latex. Nonetheless, advantages in processing, physical properties, and durability have resulted in polyurethanes becoming the foams of choice.¹⁹¹ A processing advantage is lower energy consumption due to the lower curing oven operating temperatures. Unlike polyurethane foams, large amounts of water must be evaporated in latex foams. In addition to their physical property and plant capital advantages, frothed polyurethanes are also more energy efficient than alternative backings.¹⁹² Detailed reviews of the processes and applications for mechanically frothed polyurethane foams are available.^{191,193}

6.8 Evaluation and Testing of Basic Foam Properties

Properties are tested to characterize a foam and thus determine its suitability for applications of interest, as well as for quality control. The historical development of basic test methods for flexible polyurethane foams can be found elsewhere.¹⁹⁴

ASTM D 3574-95 presents a standard method for conditioning foam samples and testing the basic physical properties:¹⁹⁵ density, indentation force deflection, compression force deflection, constant deflection compression set, tensile strength, tear resistance, airflow, and resilience. Some of these tests have been automated successfully.¹⁹⁶ Most of these basic foam properties have also been the subject of math modeling exercises.^{114a,197}

ASTM D 3574-95 calls for conditioning a sample by waiting for 1 week or longer after fabrication and then storing the undistorted foam at a specified temperature (generally $23^{\circ}\text{C} \pm 2^{\circ}\text{C}$) and humidity (generally $50\% \pm 5\%$ relative humidity) for 12 h prior to testing. In some tests, mechanical condition-

ing is also used in an attempt to obtain data under conditions resembling the actual performance of a product in service.

The density measurement provides an apparent or bulk density (and not the true polymer density). A representative sample is measured carefully and weighed accurately. The bulk density (normally reported in pounds per cubic foot or kilograms per cubic meter) is simply the weight of the sample divided by its volume. The relative density (or the solid volume fraction) of the foam is defined as its bulk density divided by the true density of the solid (dense) polymer from which it is made. The void fraction is defined as $[1 - (\text{relative density})]$. The relative density is relevant both to cost and to load bearing. Higher relative densities generally result in improved load bearing at higher cost. A typical example of how foam properties vary with density¹⁹⁸ and simple models for such dependences³¹ have been presented.

The indentation force deflection (IFD) test measures the load-bearing properties. The force required to depress a circular plate into the foam (indentation resulting from a specified force, force required to reach a specified indentation) is measured. The results can depend on the temperature and relative humidity conditions under which the foam was made, cured, and tested. Detailed discussions of such effects are available.¹⁹⁹

The compression force deflection (CFD) test is similar to the IFD test. The force required to compress the foam to a specified level is measured and reported for a plate large enough to apply force across the entire top surface of a $50 \times 50 \times 20$ mm foam sample.

Variations on these basic load-bearing tests include changes in sample dimensions and indenter foot area. Such changes affect the results of the tests.²⁰⁰

In the constant deflection compression set test, three samples are placed between metal plates and compressed to 50%, 75%, or 90% of their original thickness. They are held at 70°C for 22 h, removed, allowed to recover for 30 min, and remeasured. The results are normally reported as a percentage of the original thickness.

The tensile test measures the stiffness and strength under tension. Samples are generally die-cut and are “dogbone” or “dumbbell” shaped. The sample is pulled at a constant rate until it breaks. The stiffness (modulus of elasticity) is defined as the initial slope of the stress/strain curve in the linear region of ideal elasticity where Hooke’s law holds. The force recorded at the breaking point is the tensile strength. The maximum extension of the sample as a percentage of its original length is the elongation at break.

Another measure of foam strength is tear resistance. A sample is slit at one end. The force required to continue this tear at a constant rate is measured. The results are highly rate dependent. Tear strength is not necessarily related to tensile strength in foams. The results have also been found to vary with the sharpness of the sample cutting die.

The air flow test^{114a} measures cell openness (porosity). Air is pulled through a sample of standard thickness and its flow rate is observed. Air flow is very sensitive to the orientation of the sample within the foam. Air flow is generally reported both parallel to and perpendicular to the foam rise direction.

In molded foams, air flow through the surface skin is also of interest and can be measured.²⁰¹

Resilience is measured in a ball rebound test where a steel ball is dropped on a foam sample and the height of rebound is measured visually.²⁰² The results of this test have been correlated to overall cushion comfort.^{201a,203}

Fogging refers to formation of a light-scattering film on interior glass surfaces. It is important for foams used in the automotive industry. Volatile ingredients in interior trim parts may contribute to the film. A sample is typically placed in an apparatus and heated at a desired temperature to promote the release of volatile components. These components are then condensed on a cooled glass plate and subjected to quantification by gravimetry or light reflectance loss measurement. The details of fogging test methods²⁰⁴ and the key variables influencing the test results^{204a,205} have been documented extensively.

6.9 Evaluation and Testing of Foam Durability

The techniques for measuring fatigue at the laboratory scale²⁰⁶ fall in two classes: static fatigue and dynamic fatigue. Within each class, individual tests vary in the degree of loading or deflection, use of indentation or full size deflection, use or absence of shear, sample thickness, number of cycles, rate of application of flex, and recovery or rest period after flexing. The sample type also varies. Measurements from the tests (including height loss, load loss, physical appearance, or loss in other properties) vary considerably. Some standard test methods for commonly used laboratory tests are summarized below.

Two types of static fatigue tests are commonly used. (1) The constant deflection compression set test is used most often. It is described in ASTM D 3574-95, Test I1.²⁰⁷ It is similar to the simple constant deflection compression set test. The sample is removed and allowed to recover when the compression time is complete. Its height is measured. The results are provided as a percentage of the original height. (2) The constant load creep test measures the reversible change in the shape of a sample with time under a sustained load. A foam block is placed under a weight platform. The platform is loaded to the desired mass and lowered onto the foam. The percentage of vertical deflection (creep) is measured over 10 min and plotted versus time. A creep rate (slope of curve showing the data) is calculated. It varies with the percent penetration into the foam. A high creep rate corresponds to cushion comfort loss.^{11c,208}

Dynamic fatigue tests simulate the alternating loads experienced by foam seating cushions under actual service conditions. Two general types of tests have been used; namely, those in which the sample is indented to a fixed percentage of its thickness by an oscillating indenter, and those in which the sample is loaded and unloaded repeatedly with an indenter exerting a fixed

load. Tests such as the constant load pounder, in which the extent of indentation increases as the foam softens, have reportedly shown a high correlation with height loss (and to a lesser extent, also with hardness loss) in the end use performance of foams. Two laboratory-scale dynamic testing protocols are commonly used by furniture and automotive foam suppliers: (1) constant-load pounding and (2) roller-shear. A standardized constant-load-pounding fatigue test, ISO 3385-1975(E), is a common choice for many furniture and automotive foam application areas.²⁰⁹ Another frequently used test protocol is the ASTM D 3574-95, test I3. The Jounce test is used to assess fatigue performance for seating cushions.²¹⁰ The standard roller-shear test and a suggested method of equipment construction are described in ASTM D 3574-95.²¹¹ A modified roller-shear test, the Caster fatigue test, which is used in carpet backing applications, gives the best correlation with actual use performance.²¹² A Society of the Plastics Industry study reports excellent correlation between the laboratory roller-shear procedure and field evaluations of fatigue²¹³ but the absolute accuracy was unsatisfactory.

There is an extensive body of literature describing the results of experiments probing into the effects of various chemical and physical factors affecting foam durability as measured by the types of fatigue tests that were summarized above.^{114a,214} Most importantly, recent research has begun to deconvolute fatigue effects due to the cellular nature of the foam from those that are due to the polymer used in the foam. The main cellular factor influencing fatigue is found to be the density. If all other factors are kept constant, loadbearing retention under fatigue decreases with decreasing density. Increased foam hardness (a larger foam storage modulus) attained by increasing the hard segment volume fraction (for example, by increasing the water level in the formulation) or by incorporating SAN CPP particles in the polyol is also usually detrimental to fatigue performance. Consequently, in general, if high durability is needed simultaneously with a higher modulus in a certain grade of foam, then the foam density should also be increased.

6.10 Control of Noise and Vibrations

The ability to control noise and vibrations is crucial to the use of foams in vehicle seats^{214g,h} as well as in many of the trim parts of vehicles. The noise and vibrations present inside an automobile contribute to occupant discomfort by creating a harsh environment. They have become a major consumer concern as cars have become smaller and lighter. Interior noise levels of up to 70 decibels have been reported.²¹⁵

Grades of specialty molded foams that are helpful in reducing this discomfort are called noise and vibration harshness (NVH) foams. Many new car and truck models will insulate noisy mechanical parts with shields padded on the noise-receiving side with molded NVH foam. Commercial examples of such applications of molded NVH foams have been presented.²¹⁶ On

the other hand, recent advances in cutting and contouring technology have won new NVH applications for conventional slabstock foams.²¹⁷

Air flow, cell size, and density are the main factors influencing the effectiveness of sound absorption by simple cut sheets of foam.²¹⁸ Increasing the cell count improves sound absorption at all frequencies. Optimum air flow ranges between 0.1 and 1.0 ft³/min at 0.5 in. of water pressure. Increasing the relative density generally improves sound absorbance, but does so less than the previous two factors. The effects of foam thickness, cutting profile, and surface treatment have also been studied.²¹⁹ Fundamental mechanisms and experimental methods of measuring sound absorption by flexible foams have been reviewed.²²⁰ A review of the patent literature prior to 1986 is available.²²¹ The physiological effects of noise and vibrations on humans have been described.²²²

6.11 Flammability

The flammability of flexible polyurethane foams is important because their growing use in upholstered furniture and bedding presents the possibility that they could contribute to a life and safety hazard. Since these foams consist of carbon, nitrogen, hydrogen, and oxygen atoms, an entirely non-combustible foam cannot be made. Furthermore, furniture and cushion foams are normally very low in solid volume fraction. The high void space fraction results in a large surface area which allows a free oxygen pathway into the foam. It also creates thread-like struts that can be heated easily by adjacent heat sources. Even small ignition sources such as a match or a cigarette may hence warm small polymer fibrils in certain types of uncovered polyurethane foams to their ignition point.²²³ However, since the foam is always used as a filler in an upholstered cushion, there is no way for smoldering cigarettes or flaming ignition sources to reach the foam without first penetrating the upholstered cover. Consequently, foam involvement in fires is related to the lack of resistance of the cover to ignition, and flammability assessment must be done on the specific construction used to make the article rather than on any single component of the upholstered furniture.²²⁴ There are many standards and regulations in different parts of the world regarding the ignition resistance of upholstered furniture and cushion items.

Although a life and safety hazard results from ignition of the entire upholstered cushion, significant efforts have been made by the flexible polyurethane foam industry to improve the fire resistance of uncovered foams. Several methods are prominent in improving the fire resistance of foams. (1) Addition of fire retardants¹⁰¹ (especially phosphorus-containing and/or halogen-containing ones) during foam preparation. Halogens interrupt the free radical reactions involved in combustion. Phosphorus helps form a barrier that restricts the organic material in the foam from feeding the flame. (2) Addition of fillers along with the fire retardants. The most effective fillers

are melamine²²⁵ and hydrated alumina.^{224b} (3) Protection of the foam by fire-resistant upholstery fabric or by liners between the upholstery fabric and the foam cushion.^{224c}

Many tests exist to evaluate flammability. The basic objective of these tests is to screen the performance of new materials and formulations. They range from bench or laboratory-scale tests to full-scale tests on entire rooms or buildings. Laboratory-scale tests are generally used to compare the ignitability and the burn rate of small specimens. Their results can vary widely, depending on the orientation of the specimen, the size of the flame source, and the amount of radiant energy. Furthermore, laboratory-scale tests cannot be used to predict performance under actual fire conditions. The performance in a real fire situation can vary markedly from that observed in small-scale tests. In fires involving building materials, there are many parameters that affect the course of a real fire, and many additional hazards (such as smoke) can arise. Most deaths in fires result from asphyxiation due to lack of oxygen or from inhalation of smoke or toxic vapors.²²⁶ For these reasons, full-scale tests are generally needed to measure both flame spread and smoke density. In recent years, many national standard and insurance organizations have been involved in developing a unified set of tests.²²⁷ New tests continue to evolve.

6.12 Recycling

The typical life cycle of polyurethane products is shown in [Figure 6.20](#). Petroleum-derived chemicals are converted into rigid and flexible foams, reaction injection molded (RIM) and cast elastomers, and other products.²²⁸ Flexible polyurethane foams are thermoset polymers. It is worth emphasizing that no foamed thermoplastics of any kind have yet found use as adequate replacements for flexible polyurethane foams in practice. While thermosets have historically not generally been associated with recycling, a lot of recycling of flexible polyurethane foams actually occurs, to conserve and recover as much as possible of the invested energy and other resources. The strategies include material recycling (recovery by foam rebond²²⁹ and regrind²³⁰ processes), chemical recycling (recovery of chemicals by polymer breakdown through hydrolysis,²³¹ glycolysis,²³² or pyrolysis²³³), and energy recovery by combustion technologies such as the rotary kiln/fluidized bed²³⁴ and the high temperature gasification processes.

Virtually all process scrap from flexible slabstock foam cutting operations and molded foam seating production is recycled by a rebonding process into high-quality carpet underlay. Other uses for rebond foams include seating and cushioning applications such as gym mats, seat inserts, headrests, and school bus and golf cart seats. Additional rebond uses are being developed, including sound absorption firewall, door, and automotive carpet pads. Post-consumer foam scrap is less widely recycled because of the diversity of location and the lack of a collection infrastructure. Several companies in the

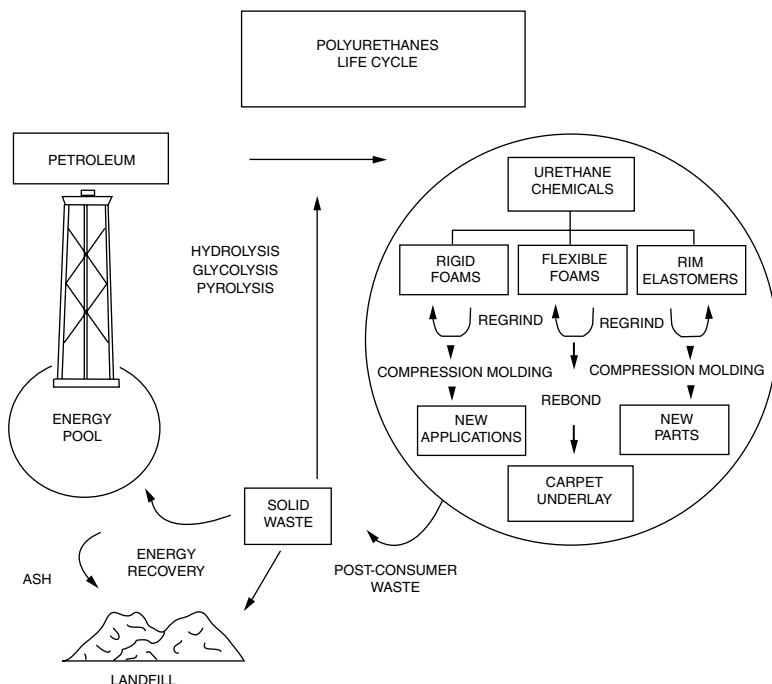


FIGURE 6.20

Typical life cycle of polyurethane foam and elastomer products.

U.S. have found it profitable to collect scrap foam from furniture, bedding, and carpet underlayment and process it into rebond foam. The volume of scrap collected has increased steadily as the value of the scrap is being recognized.

The formation of the Polyurethane Recycle and Recovery Council by the Polyurethane Division of the Society of the Plastics Industry (now the Alliance for the Polyurethanes Industry, a business unit of the American Plastics Council) underscores the importance of the recycle issue to the industry.²³⁵ This industry group sponsors recycling programs in flexible and rigid foams. Its membership includes all of the major suppliers to the polyurethane industry. The flexible foam programs are focused on post-consumer scrap, including the separation and recycling of flexible foam from automotive shredder operations, the evaluation of energy recovery options, and the possibilities for adding scrap regrind to flexible slabstock and molded foam production.

6.13 Polyurethane Foams from Renewable Resources

Efforts to reduce the dependence of flexible polyurethane foam production on petroleum-based precursor materials by using renewable feedstocks con-

stitute a new research frontier. For example, John et al.²³⁶ described the reaction of polyols based on inexpensive soybean-based vegetable oils (as replacements for conventional polyols) with TDI and MDI to produce flexible slabstock polyurethane foams. Crude soybean oil does not contain hydroxyl groups. It did not generate any foam. However, it contains 95 to 97% triglycerides and a fatty acid composition with a high level of unsaturation. It was functionalized by introducing hydroxyl groups at some of these sites of unsaturation, to obtain polyols which were reacted with isocyanates to make foams. Just like foams obtained from conventional polyols, the properties of these foams could be changed by controlling variables such as water content, isocyanate index, and catalysts.

6.14 Summary and Conclusions

Polyurethanes are chemically complex polymers. They were first synthesized early in the twentieth century. They are usually formed by reactions of liquid isocyanate components with liquid polyol resin components. Their greatest advantage is versatility, both in the finished product properties and in their ease of production and application. By proper choice of isocyanate and polyol, products can be made with properties ranging from the downy softness of very low-density flexible foams to the high strength of elastomeric bubble-free castings.

The phenomenal success of flexible polyurethane foams in capturing applications previously held by alternative cushioning materials is recorded in an extensive body of literature. Such foams are now ubiquitous and hard to avoid in the civilized world. Commercial production involves many formulation ingredients (such as polyols, isocyanates, water, auxiliary blowing agents, catalysts, surfactants, additives, and fillers) and at least the two main competing reactions (polymerization and gas-producing reaction). Many variables are, hence, at the disposal of a manufacturer who wants to optimize the properties of a foam for any one of a vast number of potential applications. The potential applications are often only limited by our imagination.

Considerable understanding has been developed on the fundamentals of foaming and on analytical characterization, morphologies, properties, and practical performance characteristics of flexible polyurethane foams. The most important progress in the fundamentals in recent years has involved the development of a new understanding (differing from the “classical” one at the level of its basic qualitative physical picture) of the evolution and final form of the polymer morphology in the solid portion of the foam. This progress has been paralleled by improvements in methods for the fabrication of slabstock, molded, and carpet backing foams.

Future progress in two areas should augment the environmental friendliness of flexible polyurethane foams and thus help them to continue to flourish in a world that places increasing emphasis on sustainable development.

While thermosets have historically not generally been associated with recycling, a lot of recycling of flexible polyurethane foams actually occurs, to conserve and recover as much as possible of the invested energy and other resources. Efforts to reduce the dependence of flexible polyurethane foam production on petroleum-based precursor materials by using renewable feedstocks constitute a new research frontier.

References

1. Bayer, O., *Mod. Plast.*, 24, 149–152, 250–262, 1947.
2. Bayer, O., *Ang. Chem.*, 59, 257–272, 1947.
3. Hochtlen, A., *Kunststoffe*, 42/10, 303–310, 1952.
4. Brochhagen, F.K., *Kunststoffe*, 44/12, 555–558, 1954.
5. Tenhoor, R.E., *Chem. Eng. News*, 41, 94–104, 1963.
6. Winkler, J., *SPE J.*, 12/11, 23–25, 1956.
7. Ferrari, R.J. et al., *Ind. Eng. Chem.*, 50/70, 1041–1044, 1958.
8. Frisch, K.C., *J. Macromol. Sci. Chem.*, A15(6), 1089–1112, 1981.
9. (a) *Mod. Plast.*, 32/3, 106–108, 214–216, 1954. (b) Editorial, *Chem. Week*, 75/10, 82–84, 1954. (c) *Mod. Plast.*, 32/12, 102–104, 212–215, 1955. (d) Beutel, A.C. et al., *Harvard Graduate School Report*, Polyurethane Associates, Cambridge, MA, 1956. (e) Editorial, *Br. Plast.*, 29/1, 5–9, 39, 1956. (f) *Ind. Eng. Chem.*, 48/9, 1383–1388, 1956. (g) *Mod. Plast.*, 35/1, 115–121, 238–247, 1957. (h) Buist, J.M. and Lowe, A., *Plast. Int. Trans.*, 27, 13–27, 1959. (i) Editorial, *Br. Plast.*, 34/8, 408–417, 1961. (j) Erlich, V.L., *Mod. Text. Mag.*, 44/2, 37–40, 1963. (k) Saunders, J.H. and Frisch, K.C., *Polyurethanes Chemistry and Technology, Part II: Technology*, Interscience, New York, 1964. (l) Bender, R.J., *Handbook of Foamed Plastics*, Lake Publishing, Libertyville, IL, 1965. (m) Frisch, K.C. and Saunders, J.H., *Plastic Foams, Part I*, Marcel Dekker, New York, 1972. (n) Oertel, G., *Kunststoffe*, 71, 2–7, 1981. (o) Allport, D.C., *Plast. Rub. Proc. Appl.*, 4/2, 173–180, 1984. (p) Oertel, G., *Polyurethane Handbook*, Hanser, New York, 1985. (q) Woods, G., *The ICI Polyurethanes Book*, John Wiley & Sons, Chichester, England, 1987. (r) Ulrich, H., *An Encyclopedia of Chemical Technology*, 3rd ed., John Wiley & Sons, New York, 1982, vol. 23, 576–608.
10. (a) Nortman, P.B., *Plast. Tech.*, 42–49, December, 1960. (b) Wouters, R.P., *Conference Papers, UTECH 88*, Crain Communications, London, 1988. (c) Manno, P.J., *Conference Papers, UTECH 90*, Crain Communications, London, 1990, 5–8. (d) Anon., *Facts and Figures of the U.S. Plastics Industry*, Society of the Plastics Industry, Washington, D.C., 1990, 51–54. (e) Manno, P.J., *1991 U.S. Foamed Plastics Markets and Directory*, Technomic, Lancaster, PA, 1991, 5–9.
11. (a) Pinner, S.H., *Plastics (London)*, 11, 206–211, 215, 1947. (b) Cooper, W., Pearson, R.W., and Darke, S., *Ind. Chem.*, 3, 121–126, 1960. (c) Saunders, J.H. and Frisch, K.C., *Polyurethanes: Chemistry and Technology*, Robert E. Krieger Publishing, Huntington, NY, 1978. (d) Sayigh, A.A.R., Ulrich, H., and Farrissey, W.J., *Condensation Monomers*, Wiley-Interscience, New York, 1972, 369–476. (e) Satchell, D.P.N. and Satchell, R.S., *Chem. Soc. Rev.*, 4/2, 231–250, 1975. (f) Richter, R. and Ulrich, H., *The Chemistry of Cyanates and Their Thio Derivatives, Part 2*, ed. S. Patai, John Wiley & Sons, New York, 1977.

12. Lovering, E.G., Laidler, K.J., *Can. J. Chem.* 1962, 40, 26–30.
13. (a) Smith, H.A., *J. Appl. Polym. Sci.*, 7, 85–95, 1963. (b) Smith, H.A., *J. Polym. Sci.: Part A-1*, 6, 1299–1306, 1968. (c) Hartley, F.D., Cross, M.M., and Lord, F. W., *Advances in Polyurethane Technology*, ed. J.M. Buist and H. Gudgeon, Macclaren and Sons, London, 1968, 127–140. (d) Cole, K.C. et al., *Proceedings of the SPI-31st Annual Technical/Marketing Conference*, Technomic, Lancaster, PA, 1988, 2–10. (e) Spirkova, M., Kubin, M., and Dusek, K., *J. Macromol. Sci.-Chem.*, A27(4), 509–522, 1990. (f) Dusek, K. and Spirkova, M., *Cell. Polym.*, 9/2, 69–83, 1990.
14. Kurzer F., *Chem. Rev.*, 56, 95–197, 1955.
15. Saunders, J.H. and Hansen, R.H., *Plastic Foams, Part I*, Marcel Dekker, New York, 1972, 23–108.
16. Abbate, F.W., *Plast. Cmpd.*, 9/4, 20, 23–24, 26–27, 1986.
17. Hill, B.G., *Chemtech*, 613–616, October, 1973.
18. Sparrow, D.J. and Thorpe, D., *Telechelic Polymers, Vol. 2: Synthesis and Application*, ed. E.J. Goethals, CRC Press, Boca Raton, FL, 1989, 203.
19. Friedli, H.R., *Reaction Polymers*, ed. W.F. Gum, W. Riese, and H. Ulrich, Hanser, Munich, 1992, 68.
20. (a) Dege, G.J., Harris, R. L., and MacKenzie, J. S., *J. Am. Chem. Soc.*, 81, 3374–3379, 1959. (b) Simons, D.M. and Verbanc, J.J., *J. Polym. Sci.*, 44, 303–311, 1960. (c) Steiner, E.C., Pelletier, R. R., and Trucks, R.O., *J. Am. Chem. Soc.*, 86, 4678–4686, 1964. (d) Fogiel, A.W., *Macromolecules*, 2/6, 581–587, 1969. (e) Livigni, R.A. et al., *Polyethers*, ACS Symposium Series No. 6, ed. E.J. Vandenberg, American Chemical Society, Washington, D.C., 1975, 29–31. (f) Stanford, J.L. and Stepto, R.F.T., *Br. Polym. J.*, 6, 124–132, 1977. (g) Miller, D.R., Valles, E.M., and Macosko, C.W., *Polym. Eng. Sci.*, 19/4, 272–283, 1979. (h) Barksby, N. and Allen, G.L., *Proceedings of the Polyurethanes World Congress 1993*, Technomic, Lancaster, PA, 1993, 445–450. (i) Carr, R.H., Hernalsteen, J., and Devos, J., *J. Appl. Polym. Sci.*, 52/8, 1015–1022, 1994. (j) David, D.J. and Staley, H.B., *Analytical Chemistry of the Polyurethanes, Vol. 16, Part III*, Wiley-Interscience, New York, 1969, 291–292. (k) Earing, M.H. to Wyandotte Chemical Company, U.S. Patent 3,271,462, 1966. (l) General Tire Corporation, U.S. Patent 3,278,457, 1966. (m) Cuscurida, M. to Jefferson Chemical Corporation, U.S. Patent 3,393,243, 1968. (n) McKellar, R.L. and Musolf, M.C. to Dow Corning Corporation, U.S. Patent 3,485,861, 1969. (o) Herold, R.J. and Linigim, R. A., *Polymerization Kinetics and Technology*, Advances in Chemistry Series No. 128, American Chemical Society, Washington, D.C., 1973. (p) Bleijenberg, K.C., *Conference Papers, UTECH 88*, Crain Communications, London, 1988, 185–187. (q) Schuchardt, J.L. and Harper, S.D., *Proceedings of the SPI-32nd Annual Technical/Marketing Conference*, Technomic, Lancaster, PA, 1989, 360–364. (r) Heuvelsland, A.J. to Dow Chemical Company, U.S. Patent 5,010,187, 1991. (s) Hinz, W., *Proceedings of the SPI/ISOPA Polyurethanes World Congress 1991*, Technomic, Lancaster, PA, 1991, 519–523. (t) Penati, A., Maffezzoni, C., and Moretti, E., *J. Appl. Polym. Sci.*, 26, 1059–1071, 1981. (u) Baize, T. H., *Ind. Eng. Chem.*, 53/11, 903–906, 1961. (v) Powell, D.G., Puig, J.E., and van Leuwen, B.G., *J. Cell Plast.*, 8/2, 90–99, 1972. (w) Gaylord, N.G., ed., *Polyethers, Vol. 1: Polyalkylene Oxides and Other Polyethers*, Interscience, New York, 1963. (x) Furukawa, J. and Saegusa, T., *Polymerization of Aldehydes and Oxides*, Interscience, New York, 1963, 125–208. (y) Newton, R.A., *Kirk-Othmer Encyclopedia of Chemical Technology*, 3rd ed., John Wiley & Sons, New York, 1982, vol. 18, 633–645. (z) Schauerte, K. et al., *Polyurethane Handbook*, ed. G. Oertel, Hanser, New York, 1985, 42–50. (aa) Hampton, H.A., Hurd, R., and Shearing, H.J., *J. Oil Col. Chem. Ass.*, 43, 96–123, 1960. (bb) Yost, C. W., Plank, C.A., and

- Gerhand, E.R., *Ind. Eng. Chem. Prod. Res. Dev.*, 6/2, 113–115, 1967. (cc) Yen, Y.C., *Process Economics Program Report No. 45*, Stanford Research Institute, Menlo Park, CA, 1968. (dd) Wright, P. and Cumming, A.P.C., *Solid Polyurethane Elastomers*, Gordon and Breach, New York, 1969, 66–68. (ee) Guibert, R.M., Plank, C.A., and Gerhard, E.R., *Ind. Eng. Chem. Prod. Res. Dev.*, 10/4, 497–500, 1971. (ff) Christianson, L.R., Dheming, M., and Ochoa, E.L., *J. Cell Plast.*, 13/2, 111–117, 1977. (gg) Hampton, H.A., Hurd, R., and Shearing, H.J., *J. Oil Col. Chem. Ass.*, 43, 96–123, 1960. (hh) Sparrow, D.J. and Thorpe, D., *Telechelic Polymers, Vol. 2: Synthesis and Application*, ed. E.J. Goethals, CRC Press, Boca Raton, FL, 1989, 181–228.
21. Barrett, K.E.T., *Dispersion Polymerization in Organic Media*, John Wiley & Sons, London, 1975.
 22. Napper, D.H., *Polymeric Stabilization of Colloidal Particles*, Academic Press, London, 1983.
 23. (a) Kuryla, W.C. et al., *J. Cell. Plast.*, 2/2, 84–96, 1966. (b) Bamford, C.H. and Tipper, C.F.H., *Free Radical Polymerization*, Elsevier, New York, 1976. (c) Kahrs, K.H. and Zimmermann, J.W., *Makromol. Chem.*, 58, 75–103, 1962. (d) Critchfield, F.E., Koleske, J.V., and Priest, D.C., *Rubber Chem. Tech.*, 45, 1467–1484, 1972. (e) Cloetens, R. et al., *Proceedings of the SPI/FSK Polyurethanes World Congress*, Technomic, Lancaster, PA, 1987, 480–489. (f) Ramlow, G.G., Heyman, D.A., and Grace, O.M., *J. Cell Plast.*, 19/4, 237–242, 1983. (g) Shears, J.H. et al., *Proceedings of the 1996 SPI Polyurethanes Conference*, Technomic, Lancaster, PA, 1996, 150–155. (h) Yen, Y.C. and Tsao, T.S., *Process Economics Program Report No. 45A*, Stanford Research Institute, Menlo Park, CA, 1982, 119–152.
 24. (a) Spitler, K.G. and Lindsey, J.J., *J. Cell Plast.*, 17/1, 43–50, 1981. (b) Vehlwald, P. and Volland, R., *Kunststoffe*, 73/8, 439–443, 1983. (c) Koshute, M.A. and Freitag, H.A., *Proceedings of the SPI/FSK Polyurethanes World Congress*, Technomic, Lancaster, PA, 1987, 502–507.
 25. (a) Reischl, A., Muller, H., and Wagner, K. to Bayer, U.S. Patent 4,260,530, 1981. (b) Rowlands, J.P. to Interchem International S.A., U.S. Patent 4,374,209, 1983. (c) Pickin, K., *Urethanes Tech.*, June 23–24, 1984. (d) Carroll, W.G. and Farley, P. to Imperial Chemical Industries, U.S. Patent 4,452,923, 1984. (e) Carroll, W.G. to Imperial Chemical Industries, U.S. Patent 4,554,306, 1985. (f) Pal, J.M., Cosman, J.P., and Tan, K. to Dow Chemical Company, U.S. Patent 5,068,280, 1991. (g) Wujcik, S.E., Christman, D.L., and Grace, O.M. to BASF Corporation, U.S. Patent 5,179,131, 1993. (h) Van Veen, K.J. and Blair, G.R. to Woodbridge Foam Corporation, U.S. Patent 5,292,778, 1994. (i) Yeakey, E.L. and Cuscurida, M. to Arco Chemical Company, U.S. Patent 4,785,026, 1988.
 26. Knight, J.E., *Proceedings of the SPI-27th Annual Technical/Marketing Conference*, Technomic, Lancaster, PA, 1982, 225–227.
 27. van der Wal, H.R., *Proceedings of the SPI/FSK Polyurethanes World Congress*, Technomic, Lancaster, PA, 1987, 493–497.
 28. Narayan, T. and Patton, J.T. to BASF Wyandotte Corporation, U.S. Patent 4,326,043, 1982.
 29. Sam, F.O., Stefani, D., and Gallo, B., *Proceedings of the Polyurethanes World Congress 1993*, Technomic, Lancaster, PA, 1995, 62–69.
 30. Kageoka, M., Tairaka, Y., and Kodama, K., *Proceedings of the 1995 SPI Polyurethanes Conference*, Technomic, Lancaster, PA, 1995, 62–69.
 31. Gibson, L.J. and Ashby, M.F., *Cellular Solids*, 2nd ed., Cambridge University Press, Cambridge, England, 1997.

32. Gier, D.R. et al., *Polyurethanes Expo '98*, Technomic, Lancaster, PA, 1998, 227–237.
33. Macosko, C.W., *Rheology: Principles, Measurements, and Applications*, John Wiley & Sons, New York, 1994.
34. Lee, D.I., *J. Paint Tech.*, 42, 579, 1970.
35. Cloetens, R.C., Lidy, W.A., and Thanh, H.P. to Dow Chemical Company, U.S. Patent 4,883,832, 1989.
36. Moore, D.R., Plowman, K.R., and Neill, P.L. to Dow Chemical Company, U.S. Patent 5,494,957, 1996.
37. Lidy, W.A. and Thanh, H.P. to Dow Chemical Company, U.S. Patent 4,831,076, 1989.
38. Langdale-Smith, R.A. to Union Carbide Corporation, U.S. Patent 4,208,314, 1980.
39. Wright, P. and Cumming, A.P.C., *Solid Polyurethane Elastomers*, Gordon and Breach, New York, 1969, 68–70.
40. (a) Sittig, M., *Amines, Nitriles and Isocyanates, Processes and Products*, 1969, Noyes Development Corporation, Park Ridge, NJ, 1969. (b) Ozaki, S., *Chem. Rev.*, 72/5, 457–496, 1972. (c) Ranney, M.W., *Isocyanates Manufacture*, Noyes Data Corporation, Park Ridge, NJ, 1972. (d) Ulrich, H., *Introduction to Industrial Polymers*, Hanser, Munich, 1982, 83–84.
41. (a) Eldib, I.A., *Hydrocarbon Proc. Petrol. Ref.*, 42/12, 121–127, 1963. (b) Chadwick, D.H. and Cleveland, T.H., *Kirk-Othmer Encyclopedia Of Chemical Technology*, 3rd ed., John Wiley & Sons, New York, 1982, vol. 13, 789–818. (c) Lunde, K.E. and Bratt, L.C., *Process Economics Program Report No. 1*, Stanford Research Institute, Menlo Park, CA, 1963.
42. (a) Bailey, M.E., Kirss, V., and Spaunburgh, R.G., *Ind. Eng. Chem.*, 48/4, 794–797, 1956. (b) Lenz, R.W., *Organic Chemistry of Synthetic High Polymers*, Interscience, New York, 1967, 180–185. (c) Bender, R. J., *Handbook of Foamed Plastics*, Lake Publishing Corporation, Libertyville, IL, 1965, 130. (d) McGinn, C.E. and Spaunburgh, R.C., Symposium on Isocyanate Polymers, Paper No. 38, American Chemical Society Meeting, Atlantic City, NJ, September 1956, 16/2.
43. (a) Gmitter, G.T. and Gruber, E.E., *SPE J.*, 13/1, 27–31, 1957. (b) Berger, S.E. et al., *SPE J.*, 17/2, 170–173, 1961. (c) Smith, C.H. and Petersen, C.A., *SPE J.*, 18/4, 455–459, 1962. (d) Misprenue, H. et al., *J. Cell. Plast.*, 24/4, 348–358, 1988. (e) Nierzwichi W. and Walczynski, B., *J. Appl. Polym. Sci.*, 41, 907–915, 1990. (f) Aneja, A., Wilkes, G.L., and Rightor, E.G., *J. Polym. Sci. Polym. Phys. Ed.*, 41, 258–268, 2003.
44. Vargas, J.B., Loefgren, B.C., and Kato, H., *Proceedings of the SPI-18th Annual Urethane Division Technical Conference*, Technomic, Lancaster, PA, 1972, 17–35.
45. (a) Yen, Y.C., *Process Economics Program Report No. 1-A*, Stanford Research Institute, Menlo Park, CA, 1968–1973. (b) Twitchett, H.J., *Chem. Soc. Revs.*, 3, 209–230, 1974. (c) Chono, M., Fukuoka, S., and Kohno, M., *Proceedings of the SPI-6th International Technical/Marketing Conference*, Technomic, Lancaster, PA, 1983, 394–398.
46. A. Wurtz, *Ann.*, 71, 326, 1849.
47. A. W. Hofmann, *Annales*, 74, 9, 1850.
48. W. Hentschel, *Berichte*, 17, 1284, 1884.
49. (a) Saunders, J.H. and Slocombe, R.J., *Chem. Rev.*, 43, 203, 1948. (b) Arnold, R.G., Nelson, J.A., and Verbanc, J.J., *J. Chem. Ed.*, 34, 158, 1957.
50. Melander, L., *Nature*, 163, 599, 1949.
51. Roberts, R.A. et al., *J. Am. Chem. Soc.*, 80, 4285, 1958.

52. Tillet, J.G., *J. Am. Chem. Soc.*, 5142, 1962.
53. (a) Bennett, G.M. and Youle, P.V., *J. Chem. Soc.*, 1816, 1938. (b) Titov, A.I., *Uspekhy Khimii*, 27, 845, 1958. (c) Hanson, C., Kaghazchi, T., and Praat, M.W.T., *ACS Symp. Ser.*, 22, 132, 1976.
54. (a) Carr, R.V.C. et al. to Air Products, U.S. Patent 4,604,214, 1986. (b) Baur, K.G. to BASF, European Patent 503,387, 1992.
55. Waller, F.J. et al., *Chem. Ind.*, 75, 289, 1998.
56. Pinna, F. et al., *J. Catal.*, 150, 356, 1994.
57. Beckhaus, H., Waldau, E., and Witt, H. to Bayer, German Patent 3,611,677, 1987.
58. (a) Neri, G. et al., *J. Mol. Catal. A: Chem.*, 111, 257, 1996. (b) Musolino, M.G. et al., *J. Chromatogr. A*, 818, 123, 1998.
59. (a) Musolino, M.G. et al., *Stud. Surf. Sci. Catal.*, 108, 239, 1997. (b) Neri, G. et al., *Ind. Eng. Chem. Res.*, 34, 2226, 1995. (c) Neri, G. et al., *J. Mol. Catal. A: Chem.*, 95, 235, 1995.
60. (a) Westerterp, K.R. et al., *Chem. Eng. Sci.*, 43, 2229, 1988. (b) Janssen, H.J. et al., *Ind. Eng. Chem. Res.*, 29, 1822, 1990. (c) Westerterp, K.R., Janssen, H.J., and van der Kwast, H.J., *Chem. Eng. Sci.*, 47, 4179, 1992. (d) Molga, E.J. and Westerterp, K.R., *Chem. Eng. Sci.*, 47, 1733, 1992.
61. Allied Chemical, British Patent 1,007,785, 1965.
62. (a) Gemassmer, A.M. et al. to Bayer, British Patent 901,377, 1962. (b) Bayer, British Patent 761,590, 1954. (c) Bayer, British Patent 761,592, 1954. (d) Vaganay, J. and Wevert, S., French Patent 1,071,629, 1954. (e) Nicholas, A.J. and Twitchett, H.J. to ICI, British Patent 1,034,285, 1966. (f) Kantyka, T.A. and Toynce, C. to ICI, British Patent 806,903, 1959. (g) Cleveland, T.H. to Mobay, British Patent 979,259, 1965. (h) Slocombe, R.J., Flores, H., and Cleveland, T.H. to Monsanto, U.S. Patent 2,680,127, 1954. (i) Bloom, A., Freyermuth, H.B., and Normington, J.B. to GAF, U.S. Patent 2,847,440, 1958. (j) Boehme, O., Mott, F., and Pfirschke, J. to Bayer, U.S. Patent 2,875,225, 1959. (k) Maeda, S., Yamori, K., and Kaminaka, H. to Sumitomo, U.S. Patent 3,184,494, 1965.
63. Latourette, H.K. and Johnson, O.H., U.S. Patent 2,908,703, 1959.
64. Denton, W.I., Hammond, P.D., and Wood, J.A. to Olin, U.S. Patent 3,287,387, 1966.
65. (a) Upjohn, British Patent 1,238,669, 1968. (b) Gemassmer, A.M. et al. to Bayer, British Patent 901,377, 1962. (c) Beck, T.R. to Du Pont, U.S. Patent 2,822,373, 1958. (d) Van Horn, I.B. to Mobay, U.S. Patent 3,507,626, 1970. (e) Horn, P., Koehler, W., and Bittler, R. to BASF, U.S. Patent 4,128,569, 1978.
66. (a) Ewald, R.M. to Mobay, U.S. Patent 3,321,283, 1967. (b) Irwin, C.F. to Du Pont, U.S. Patent 337,167, 1975.
67. Mitrowsky, A. et al. to Bayer, U.S. Patent 3,947,484, 1976.
68. (a) Gemassmer, A.M. to Bayer, U.S. Patent 3,188,337, 1965. (b) Nicholas, A.J. and Twitchett, H.J. to ICI, U.S. Patent 3,465,021, 1969. (c) Yamamoto, R. et al. to Mitsui, U.S. Patent 4,422,976, 1983.
69. Soos, R. and Petnehazy, I., *Periodica Polytechnica*, 15, 119, 1971.
70. (a) Delfs, D. and Muenz, F. to Bayer, German Patent 942,145, 1956. (b) Bircher, B.J. and Wild, J.H. to ICI, British Patent 1,050,555, 1966. (c) Irwin, C.F. to Du Pont, U.S. Patent 2,644,007, 1953.
71. Suzuki, S. et al. to Mitsubishi, U.S. Patent 3,484,472, 1969.
72. Lomax, R. and Twitchett, H.J. to ICI, British Patent 1,120,770, 1968.
73. (a) Cooper, J.R. to Du Pont, French Patent 1,368,031, 1964. (b) Cooper, J.R. to Du Pont, U.S. Patent 3,234,253, 1966.

74. (a) Fuchs, W., Platz, R., and Vogt, V. to BASF, U.S. Patent 3,960,916, 1976. (b) Fuchs, W., Platz, R., and Vogt, V. to BASF, U.S. Patent 3,978,105, 1976.
75. Hardy, E.E., U.S. Patent 2,839,559, 1958.
76. Pagano, A.S. to Rohm and Haas, U.S. Patent 3,746,746, 1973.
77. Bircher, B.J., Dodman, D., and Wild, J.H. to ICI, British Patent 1,085,824, 1967.
78. (a) Stauffer, British Patent 1,114,085, 1963. (b) Stamm, W. to Stauffer, U.S. Patent 3,440,268, 1969.
79. Arndt, O., Semler, G., and Schaeffer, G. to Hoechst, U.S. Patent 3,835,172, 1974.
80. (a) Flores, H. to Monsanto, U.S. Patent 2,680,129, 1954. (b) Irwin, C.F. and Swamer, F.W. to Du Pont, U.S. Patent 2,757,183, 1956. (c) Hettich, B.V. and Latourette, H.K. to FMC, U.S. Patent 3,226,410, 1965.
81. (a) Vaganay, J. et al. to Tolochimie, German Patent 1,175,666, 1964. (b) Michelet, J. and Alheritiere, L. to Tolochimie, French Patent 1,469,105, 1967. (c) Alheritiere, L. and Repper, M. to Tolochimie, French Patent 1,476,755, 1967. (d) Burkhardt, T. and Findeisen, K. to Bayer, French Patent 2,329,051, 1975. (e) Clifford, B.H. and Hargreaves, J.R. to ICI, British Patent 1,037,933, 1966. (f) Thomas, R.M. and Blaich, M.C. to Olin, U.S. Patent 3,119,856, 1964. (g) Clifford, B.H. and Hargreaves, J.R. to ICI, British Patent 1,054,328, 1967. (h) Bloom, A., Freyermuth, H.B., and Normington, J.B. to GAF, U.S. Patent 2,911,429, 1959. (i) Bloom, A., Freyermuth, H.B., and Normington, J.B. to GAF, U.S. Patent 2,875,226, 1959. (j) Skiles, B.F. to Du Pont, U.S. Patent 2,908,704, 1959. (k) Bloom, A., Freyermuth, H.B., and Normington, J.B. to GAF, U.S. Patent 2,999,873, 1961.
82. (a) Biskup, K., Koenig, C., and Waldau, E. to Bayer, European Patent 570,799, 1993. (b) Joulak, F., Revelant, D., and Vacus, P. to Rhone-Poulenc, European Patent 593,334, 1994. (c) Armand, J. et al. to Rhone-Poulenc, European Patent 699,657, 1996.
83. Anon., *Preparation of Prepolymers, Laboratory to Full-Scale Production*, The Dow Chemical Company, Form No. 109-00895-290-SAI.
84. (a) Heiss, H.L. et al., *Ind. Eng. Chem.*, 51/8, 929-934, 1959. (b) Wall, J.R., *Chem. Eng. Prog.*, 57/10, 48-51, 1961. (c) Saunders, J.H. and Frisch, K.C. *Polyurethanes, Chemistry and Technology, Part II. Technology*, Interscience, New York, 1964, 8-43. (d) Martin, R.A., Hoy, K.L., and Peterson, R.H., *Ind. Eng. Chem., Prod. Res. Dev.*, 6/4, 218-222, 1967. (e) Peebles, L.H., *Macromolecules*, 7/6, 872-881, 1974. (f) Wang, T. and Lyman, D.J., *Polym. Bul.*, 27, 549-555, 1992.
85. (a) Saunders, J.H. and Frisch, K.C. *Polyurethanes, Chemistry and Technology, Part II, Technology*, Interscience, New York, 1964, 8-49. (b) Gemeinhardt, P.G., *Handbook of Foamed Plastics*, ed. R.J. Bender, Lake Publishing Corporation, Libertyville, IL, 1965, 173-208. (c) Zwolinski, L.M. and Frink, J.W., *J. Cell. Plast.*, 8/1, 20-29, 1972. (d) Brydson, J.A., *Plastics Materials*, Butterworth Scientific, London, 1982, 709-712. (e) Hartley, F.D., Cross, M.M., and Lord, F.W., *Advances in Polyurethane Technology*, ed. J.M. Buist and H. Gudgeon, H., Maclaren and Sons, London, 1968, 135-136. (f) Klempner, D. and Frisch, K.C., *Handbook of Polymeric Foams and Foam Technology*, Hanser, Munich, 1991, 53-54. (g) Elwell, R.J. et al. to Dow Chemical Company, U.S. Patent 5,114,989, 1992.
86. (a) Ferrigno, T.H., *SPE J.*, June, 638-640, 1960. (b) Byall, R.D., paper presented at American Chemical Society Meeting, Rubber Chemistry Division, Oct. 20, 1965. (c) Reilly, A.F., *Chem. Eng. Prog.*, 63/5, 104-108, 1967. (d) Currier, V., *Plast. Tech.*, 12/8, 35-37, 1966. (e) Doyle, E.N., *The Development and Use of Polyurethane Products*, McGraw-Hill, New York, 1971, 77-82.

87. Katz, H.S. and Milewski, J.V., *Hand Book of Fillers for Plastics*, Van Nostrand Reinhold, New York, 1987.
88. Tabor, R.L. et al., *Proceedings of the SPI-34th Annual Technical/Marketing Conference*, Technomic, Lancaster, PA, 1992, 514–528.
89. Hersch, P., *Plast. Tech.*, 13/12, 49–53, 1967.
90. (a) Bryant, R.M. and Stewart, H.F., *J. Cell Plast.*, 9/2, 99–102, 1973. (b) Plumb, J.B., Atherton, J.H., *Block Copolymers*, ed. D.C. Allport and W.H. Janes, John Wiley & Sons, New York, 1973, 305–353. (c) Brydson, J.A., *Plastics Materials*, Butterworth Scientific, London, 1982, 730–766. (d) Boudreau, R.J., *Mod. Plast.*, 133–147, January 1967. (e) Frey, J.H., *Proceedings of the 1995 SPI Polyurethanes Conference*, Technomic, Lancaster, PA, 1995, 224–229. (f) Snow, S.A., Fenton, W.N., and Owen, M.J., *J. Cell. Plast.*, 26/2, 172–182, 1990. (g) Burkhart, G., Schlons, H.-H., and Zellmer, V., *Proceedings of the SPI-34th Annual Technical/Marketing Conference*, Technomic, Lancaster, PA, 1992, 359–363. (h) Burkhart, G., Klietsch, J., and Zellmer, V., *Proceedings of the SPI/ISOPA Polyurethanes World Congress 1991*, Technomic, Lancaster, PA, 1991, 127–131. (i) Grabowski, W. and Desnier, M.C., *Proceedings of the Polyurethanes World Congress 1993*, Technomic, Lancaster, PA, 1993, 81–88. (j) Brune-Fischer, A., Burkhart, G., and Zellmer, V., *Proceedings of the 1994 SPI Polyurethanes Conference*, Technomic, Lancaster, PA, 1994, 267–273. (k) Brune, A., Klietsch, J., and Zellmer, V., *Conference Papers, UTECH 96*, Crain Communications, London, 1996, Paper 12. (l) Dahm, M., *Cellular Plastics*, National Academy of Sciences–National Research Council Publication 1462, 52–63, 1967. (m) Rossmly, G. R. et al., *J. Cell. Plast.*, 13/1, 26–35, 1977. (n) Woods, G.W., *Flexible Polyurethane Foams, Chemistry and Technology*, Applied Science, New Jersey, 1982, 68–72. (o) Stevens, R.E. et al., *Proceedings of the Polyurethanes World Congress 1997*, Technomic, Lancaster, PA, 1997, 118–129. (p) Kaushiva, B.D. et al., *Polymer*, 41, 285–310, 2000.
91. Brecker, L.R., *Plast. Eng.*, March, 39–42, 1977.
92. Rusch, T.E. and Raden, D.S., *Plast. Compd.*, 61–74, July/August 1980.
93. Listemann, M.L. et al., *Proceedings of the Polyurethanes World Congress 1993*, Technomic, Lancaster, PA, 1993, 595–608.
94. (a) Winkler, J., *SPE J.*, 12/11, 23–26, 1956. (b) Alzner, B.G. and Frisch, K.C., *Ind. Eng. Chem.*, 51/5, 715–716, 1959. (c) Gmitter, G.T., Gruber, E.E., and Joseph, R.D., *SPE J.*, 15/11, 957–960, 1959. (d) Listermann, M.L. et al. to Air Products and Chemicals Inc., U.S. Patent 5,508,314, 1996.
95. (a) Burkhart, G., Kollmeier, H.J., and Schloens, H.H., *J. Cell. Plast.*, 20/1, 37–41, 1984. (b) Malwitz, N. et al., *Proceedings of the SPI-30th Annual Polyurethane Technical/Marketing Conference*, Technomic, Lancaster, PA, 1986, 338–353. (c) Malwitz, N. and Kresta, J.E., *Proceedings of the SPI/FSK Polyurethanes World Congress*, Technomic, Lancaster, PA, 1987, 826–836.
96. (a) Anon., *Plast. Tech.*, 8/4, 26–32, 1962. (b) Sandridge, R.L., Gemeinhardt, P. G., and Saunders, J.H., *SPE Trans.*, 3/2, 117–122, 1963. (c) Mack, G.P., *Mod. Plast.*, 42/4, 148–160, 194, 1964.
97. (a) Letts, J.B., Gerkin, R.M., and Martineau, P., *Proceedings of the SPI/ISOPA Polyurethanes World Congress 1991*, Technomic, Lancaster, PA, 1991, 174–181. (b) Diblitz, K. and Diblitz, C., *Proceedings of the Polyurethanes World Congress 1993*, Technomic, Lancaster, PA, 1993, 619–624. (c) Derderian, E.J. et al., *Proceedings of the 1994 SPI Polyurethanes Conference*, Technomic, Lancaster, PA, 1994, 274–279. (d) Casati, F.M.H., Arbir, F.W., and Raden, D.S., *Proceedings of the SPI-27th Annual Technical/Marketing Conference*, Technomic, Lancaster, PA, 1982,

- 35–48. (e) Casati, F.M.H., Arbir, F.W., and Tylenda, E.J., *Proceedings of the SPI-6th International Technical/Marketing Conference*, Technomic, Lancaster, PA, 1983, 161–171.
98. Stepek, J. and Daoust, H., *Additives for Plastics*, Springer-Verlag, New York, 1983.
99. (a) Miley, J.W. and Moore, P.D., *Proceedings of the SPI-26th Annual Technical Conference*, Technomic, Lancaster, PA, 1981, 83–86. (b) Moore, P.D., Miley, J. W., and Bates, S.H., *Proceedings of the SPI-27th Annual Technical/Marketing Conference*, Technomic, Lancaster, PA, 1982, 255–261. (c) Bates, S.H. and Miley, J.W., *Proceedings of the SPI-30th Annual Technical/Marketing Conference*, Technomic, Lancaster, PA, 1986, 160–165. (d) Bates, S.H., Moore, P.D., and Miley, J. W., *Proceedings of the SPI/FSK Polyurethanes World Congress*, Technomic, Lancaster, PA, 1987, 916–921. (e) Miley, J., *Pure & Appl. Chem.*, 68/7, 1423–1428, 1996. (f) Vielee, R.C. and Haney, T.V., *Coloring of Plastics*, ed. T.G. Webber, Wiley-Interscience, New York, 1979, 191–204.
100. (a) Davis, A. and Sims, D. *Weathering of Polymers*, Applied Science, London, 1983, 222–237. (b) Beachell, H.C. and Ngoc Son, C.P., *J. Appl. Polym. Sci.*, 7, 2217–2237, 1963. (c) Nevskii, L.V. and Tarakanov, O.G., *Soviet Plast.*, 9, 47–48, 1967 (translation of *Plast. Massy.*, 9, 1966). (d) Bieneman, R.A., *Polyurethane Technology*, Interscience Publishers, New York, 1969, 230–231. (e) Bellettini, A.G. and Harrison, J.R., *Cell. Polym.*, 3, 241–247, 1984. (f) Capocci, G., *Proceedings of the SPI-30th Annual Polyurethane Technical/Marketing Conference*, Technomic, Lancaster, PA, 1986, 220–227. (g) Rabek, J.F., *Photostabilization of Polymers*, Elsevier, London, 1990. (h) Valentine, C., Craig, T.A., and Hager, S.L., *Proceedings of the SPI-34th Annual Technical/Marketing Conference*, Technomic, Lancaster, PA, 1992, 149–155. (i) Sutton, R.G. and Steever, J.A., *J. Cell. Plast.*, 19/6, 372–374, 1983.
101. (a) Lyons, J.W., *The Chemistry and Uses of Fire Retardants*, Robert Krieger Publishing, Malabar, FL, 1987. (b) Babiec, J.S. et al., *Plast. Tech.*, June, 47–50, 1975. (c) Treadwell, K. to M&T Chemicals Inc., U.S. Patent 3,635,821, 1972. (d) Cobbledick, D.S. and Norman, A.J. to Gencorp Inc., U.S. Patent 3,810,851, 1974. (e) Cobbledick, D.S. and Norman, A.J. to General Tire and Rubber Company, U.S. Patent 3,876,571, 1975. (f) Molbert, R.A. to General Tire and Rubber Company, U.S. Patent 3,884,849, 1975. (g) Fabris, H.J. and Maxey, E.M. to General Tire and Rubber Company, U.S. Patent 3,925,266, 1975. (h) Cobbledick, D.S. to General Tire and Rubber Company, U.S. Patent 3,931,062, 1976. (i) Stone, H., *Proceedings of the 1978 Fire Retardant Chemicals Association Meeting*, Houston, TX, March 12–15, Fire Retardant Chemicals Association, Westport, CT, 1978, 257–273. (j) Woods, G.W., *Flexible Polyurethane Foams, Chemistry and Technology*, Applied Science, NJ, 1982, 88. (k) Grace, O.M., Mericle, R.E., and Taylor, J.D., *J. Cell. Plast.*, 21/5, 311–317, 1985. (l) Natoli, F.S. et al., *Proceedings of the SPI/ISOPA Polyurethanes World Congress 1991*, Technomic, Lancaster, PA, 1991, 762–765. (m) Wujcik, S.E. et al., *Proceedings of the SPI-34th Annual Technical/Marketing Conference*, Technomic, Lancaster, PA, 1992, 672–677. (n) Bhatnagar, V. M., *Fire Retardant Formulations Handbook*, vol. 1, Progress in Fire Retardancy Series, Technomic, Lancaster, PA, 1972. (o) *Handbook of Flame Retardant Chemicals and Fire Testing Services*, Technomic, Lancaster, PA, 1992. (p) Kuryla, W.C. and Papa, A.J., *Flame Retardancy of Polymeric Materials*, vol. 3, Marcel Dekker, New York, 1975, 1–133.
102. (a) Darby, R.T. and Kaplan, A.M., *Appl. Microbiol.*, 16/6, 900–905, 1968. (b) Kapan, A.M. et al., *Dev. Ind. Microbiol.*, 9, 201–217, 1968. (c) Rei, N.M., *J. Coated*

- Fab.*, 8, 21–32, 1978. (d) Tamborini, S.M., Mahoney, C.J., and McEntee, T.C., *Proceedings of the SPI-27th Annual Technical/Marketing Conference*, Technomic, Lancaster, PA, 1982, 308–313. (e) Baseman, A.L., *Plast. Tech.*, 9, 33–37, 1966. (f) Patarcity, R., Stern, E., and Murthy, U., *Proceedings of the SPI-6th International Technical/ Marketing Conference*, Technomic, Lancaster, PA, 1983, 142–144. (g) Brophy, J.F., *Proceedings of the SPI-29th Annual Technical/ Marketing Conference*, Technomic, Lancaster, PA, 1985, 224–229. (h) Battice, D.R., Hales, M.G., *Proceedings of the SPI-29th Annual Technical/Marketing Conference*, Technomic, Lancaster, PA, 1985, 108–112.
103. (a) Knobel, T.M., Kennedy, E.E., and Walker, M.A. to Dow Chemical Company, U.S. Patent 4,618,630, 1986. (b) Sweet, F.H. et al., *J. Cell. Plast.*, 22/2, 139–146, 1986.
104. (a) Kopsheva, L.M., Shamov, I.V., and Tarakanov, O.G., *J. Appl. Chem. USSR*. Translated from *Zh. Prikl. Khim.* (Leningrad), 57/6, 1358–1361, 1984. (b) White, K.B. et al., *J. Cell. Plast.*, 22/3, 331–339, 1986. (c) Hager, S.L. et al., *Proceedings of the SPI-34th Annual Technical/Marketing Conference*, Technomic, Lancaster, PA, 1992, 529–534. (d) Koehler, C.E., McClellan, T.R., and Murray, P.L. to The Upjohn Company, U.S. Patent 4,246,364, 1981. (e) Grube, L.L. and Horner, C.J. to GAF, U.S. Patent 4,444,916, 1984. (f) Wood, R.J. to Stephan Company, U.S. Patent 4,529,744, 1985. (g) Goel, A.B. and Tufts, T.A. to Ashland Oil Incorporated, U.S. Patent 4,579,877, 1986. (h) Graefe, P.U., Gajewski, V.J., and Jimenez, I.A. to Inter-Polymer Research Corporation, U.S. Patent 3,929,730, 1975. (i) Nelson, D.L., Matijega, R.J., and Miller, D.P. to Dow Chemical Company, U.S. Patent 4,585,803, 1986. (j) Majewski, W., Khalil, H., and Wypych, J. to Tremco Ltd., U.S. Patent 5,126,421, 1992. (k) Glynn, K.T. and Doyle, E.N. to Crowley Chemical Company, U.S. Patent 5,104,904, 1992. (l) Wang, D.S.T., *J. Cell. Plast.*, 15/3, 144–151, 162, 1979. (m) Barron, B.G. to Dow Chemical Company, U.S. Patent 3,993,576, 1976. (n) Olstowski, F. and Peffley, R.D. to Dow Chemical Company, U.S. Patent 4,485,031, 1984. (o) Olstowski, F. and Peffley, R.D. to Dow Chemical Company, U.S. Patent 4,485,032, 1984. (p) Carswell, R. to Dow Chemical Company, U.S. Patent 4,981,877, 1991.
105. (a) Klesper, E., *Rubber Age*, Oct., 84–87, 1958. (b) Burt, J.G. and Brizzolara, D.F., *Proceedings of the SPI-18th Annual Technical Conference*, Technomic, Lancaster, PA, 1975, 35–39. (c) Sayad, R.S. and Williams, K.W., *Proceedings of the SPI-24th Annual Urethane Division Technical Conference*, Technomic, Lancaster, PA, 1978, 1–8. (d) Sayad, R.S. and Williams, K.W., *Plast. Tech.*, June, 71–74, 1979. (e) *Handbook for Reducing and Eliminating Chlorofluorocarbons in Flexible Polyurethane Foams*, United States Environmental Protection Agency, 21A-4002, April 1991. (f) Walmsley, G.D. to Hickory Springs Manufacturing Company, U.S. Patent 5,120,771, 1992. (g) Graff, G., *Mod. Plast.*, 70/4, 32–36, 1993. (h) Stone, H. et al. to PMC Incorporated, U.S. Patent 4,906,672, 1990. (i) Farkas, P.V. and Duley, J.A. to Woodbridge Foam Company, U.S. Patent 5,081,162, 1992. (j) Doyle, E.N. and Carson, S., U.S. Patent 5,120,770, 1992. (k) Fiorentini, C. et al., *Proceedings of the 1994 SPI Polyurethanes Conference*, Technomic, Lancaster, PA, 1994, 12–16. (l) Eiben, R.G. et al., *Proceedings of the 1995 SPI Polyurethanes Conference*, Technomic, Lancaster, PA, 1995, 70–73. (m) Fiorentini, C. et al., *Proceedings of the 1995 SPI Polyurethanes Conference*, Technomic, Lancaster, PA, 1995, 491–496. (n) Eiben, R.G., *Conference Papers, UTECH 96*, Crain Communications, London, 1996, Paper 31. (o) Noakes, C.W. and Casagrande, G., *Conference Papers, UTECH 96*, Crain Communications London, 1996, Paper 11. (p) Taverna, M. and Cor-

- radi, P., *Conference Papers, UTECH 96*, Crain Communications, London, 1996, Paper 10. (q) Taverna, M., Meloth, H., and Griffiths, T., *Proceedings of the 1996 SPI Polyurethanes Conference*, Technomic, Lancaster, PA, 1996, 164–168. (r) Franklin, R. et al. to Azko N.V., U.S. Patent 5,030,664, 1991. (s) Bradford, L., Franklin, R., and Williams, B., *Proceedings of the SPI-34th Annual Technical/Marketing Conference*, Technomic, Lancaster, PA, 1992, 668–671. (t) Lichtenberg, F.W., ed., *CFCs and the Polyurethane Industry: A Compilation of Technical Publications, 1986-1988*, Technomic, Lancaster, PA, 1988. (u) Anon., *Eliminating CFCs in Foam Plastics*, The Society of the Plastics Industry, 1989. (v) Lichtenberg, F.W., ed., *CFCs and the Polyurethane Industry, Volume 2: A Compilation of Technical Publications, 1988-1989*, Technomic, Lancaster, PA, 1990. (w) Lichtenberg, F.W., ed., *CFCs and the Polyurethane Industry, Volume 3: A Compilation of Technical Publications, 1990*, Technomic, Lancaster, PA, 1990. (x) Methven, J. M., *RAPRA Review Reports*, 3/1, 1, 5–33, 1990. (y) Zwolinski, L.M., *Conference Papers, UTECH 90*, Crain Communications, London, 1990, 23–24. (z) Dwyer, F.J., Knopeck, G.M., and Zwolinski, L.M., *Proceedings of the SPI-33rd Annual Polyurethane Technical/Marketing Conference*, Technomic, Lancaster, PA, 1990, 400–406. (aa) Decaire, B.R. et al., *Proceedings of the SPI-34th Annual Technical/Marketing Conference*, Technomic, Lancaster, PA, 1992, 2–11. (bb) White, L., *Urethanes Tech.*, 13/4, 42, 1996.
106. Young, T., *Phil. Trans. R. Soc. (London)*, 95, 65–87, 1805.
 107. Laplace, P.S., *Traité de Mécanique Céleste*, vol. 4, Courcier, Paris, 1806.
 108. Plateau, J., *Mem. Acad. R. Sci. Belgique*, 23, Series 2, 1849.
 109. Bikerman, J.J., *Foams: Theory and Industrial Applications*, Reinhold, New York, 1953.
 110. Yazdi, A.V. and Beckman, E.J., *Plast. Eng. (NY)*, 33 (Polymer Devolatilization), 67–102, 1996.
 111. Kanner, B. and Decker, T.G., *J. Cell. Plast.*, 5/1, 32–39, 1969.
 112. LaMer, V.K., *Ind. Eng. Chem.*, 44, 1270–1277, 1952.
 113. Bessette, M.D. and Sundstrom, D.W., *Polym. Proc. Eng.*, 3(1 and 2), 25–35, 1985.
 114. (a) Jones, R.E. and Fesman, G., *J. Cell. Plast.*, 1/1, 200–216, 1965. (b) Harding, R.H., *Resinography of Cellular Plastics*, ASTM STP 414, 1967. (c) Blair, E.A., *Resinography of Cellular Plastics*, ASTM STP 414, 1967. (d) Buist, J.M., Ball, G. W., and Woods, G., *Advances in Polyurethane Technology*, ed. J.M. Buist and H. Gudgeon, Maclaren and Sons, London, 1968, 152–154. (e) Meinecke, E.A. and Clark, R.C., *Mechanical Properties of Polymeric Foams*, Technomic, Lancaster, PA, 1972. (f) Baumhake, R., *J. Cell. Plast.*, 8/6, 304–310, 1972. (g) van Leuwen, B.G. et al., *Advances in Urethane Science and Technology*, vol. 2, Technomic, Lancaster, PA, 1973, 173–202. (h) Berlin, A.A., Shutov, F.A., and Zhitinkina, A.K., *Foam Based on Reactive Oligomers*, Technomic, Lancaster, PA, 1982, 85–87.
 115. Clark, N.O. and Blackman, M., *Trans. Faraday Soc.*, 44, 1–7, 1948.
 116. Smith, C.S., *Met. Rev.*, 9/33, 1–51, 1964.
 117. Frensdorff, H.K., *Rubber Age*, 812–818, August, 1958.
 118. Owen, M.J. and Kendrick, T.C., *J. Colloid Interface Sci.*, 24, 141–150, 1967.
 119. Matzke, E.B., *Am. J. Bot.*, 33/1, 58–80, 1946.
 120. Lord Kelvin, *Phil. Mag.*, 5s24, 503–514, 1887.
 121. Lord Kelvin, *Proc. R. Soc. London*, 55, 1–16, 1894.
 122. Duchartre, P., *Elements de botanique*, Paris, 1867.
 123. Kitchener, J.A. and Cooper, C.F., *Q. Rev. (London)*, 13/1, 71–97, 1959.
 124. Plateau, J., *Mem. Acad. R. Sci. Belgique*, 37, 49, 1869.

125. Marangoni, C., *Nuovo Cimento*, (2), 5–6, 239, 1871.
126. Gibbs, J.W., *Collected Works*, vol. 1, Longmans Green, New York, 1928.
127. Ewers, W.E. and Sutherland, K.L., *Aust. J. Sci. Res.*, A, 5, 697–710, 1952.
128. Blair, E.A., *Resinography of Cellular Plastics*, ASTM STP 414, 1967, 84–95.
129. Rossmly, G.R. et al., *J. Cell. Plast.*, 13/1, 26–35, 1977.
130. Kollmeier, H.J. et al., *Plast. Cmpd.*, July/August, 64–74, 1985.
131. Petrella, R.G. and Kushner, S.A., *Proceedings of the SPI-33rd Annual Technical/Marketing Conference*, Technomic, Lancaster, PA, 1990, 186–190.
132. Patten, W., Seefried, C.G., Jr., and Whitman, R.D., *J. Cell. Plast.*, 10/6, 276–282, 1974.
133. (a) Boudreau, R.J., *Mod. Plast.*, 133–138, 143–147, 234–240, January 1967. (b) Dahm, M., *Cellular Plastics*, National Academy of Sciences–National Research Council Publication 1462, 52–63, 1967. (c) Schwarz, E.G., *Applied Polymer Symposia*, No. 14: *Silicone Technology*, John Wiley & Sons, New York, 1970, 71–93. (d) Battice, D.R. and Lopes, W.J., *J. Cell. Plast.*, 23/2, 158–167, 1987.
134. Turner, R.B., Nichols, J.B., and Kuklies, R.A., *Proceedings of the SPI-31 Annual Technical/Marketing Conference*, Technomic, Lancaster, PA, 1988, 18–21.
135. (a) Cavender, K.D. to Union Carbide Corporation, U.S. Patent 4,579,700, 1986. (b) Cavender, K.D., *J. Cell. Plast.*, 22/3, 222–234, 1986.
136. Saunders, J.H., and Frisch, K.C., *Polyurethanes, Chemistry and Technology, Part I: Chemistry*, Robert Krieger, New York, 1978, 250–255.
137. (a) Ostrogorsky, A.G. and Glicksman, L.R., *Trans. ASME J. Heat Trans.*, 110, 500–506, 1988. (b) Foreman, P.J., *Conference Papers, UTECH 90*, Crain Communications, London, 1990, 268–273.
138. Miller, T.E. and Schmidt, D.L., *J. Cell. Plast.*, 19/5, 326–332, 1983.
139. Armistead, J.P., Wilkes, G.L., and Turner, R.B., *J. Appl. Polym. Sci.*, 35, 601–629, 1988.
140. (a) Artavia, L.D. and Macosko, C.W., *Low Density Cellular Plastics*, ed. N.C. Hilyard and A. Cunningham, Chapman & Hall, London, 1994, 47–55. (b) Yasunaga, K., Neff, R., and Macosko, C.W., *Proceedings of the 1995 SPI Polyurethanes Conference*, Technomic, Lancaster, PA, 1995, 362–370. (c) Zhang, X.D., Davis, H.T., and Macosko, C.W., *J. Cell. Plast.*, 35/5, 458–476, 1999.
141. (a) Seefried, C.G., Jr., Whitman, R.D., and Pollart, D.F., *J. Cell. Plast.*, 10/4, 171–180, 1974. (b) Noshay, A. and McGrath, J.E., *Block Copolymers, Overview and Critical Survey*, Academic Press, New York 1977, 365–389. (c) Gibson, P.E., Vallance, M. A., and Cooper, S.L., *Developments in Block Copolymers-1*, ed. I. Goodman, Applied Science Publishers, London, 1982, 217–259. (d) Wilkes, G.L., Abouzahr, S., and Radovich, D., *J. Cell. Plast.*, 19/4, 248–254, 1983. (e) Turner, R.B., Spell, H.L., and Wilkes, G.L., *Proceedings of the SPI-28th Annual Technical/Marketing Conference*, Technomic, Lancaster, PA, 1984, 244–247. (f) Armistead, J.P., M.S. thesis, Virginia Polytechnic Institute and State University, 1985. (g) Abouzahr, A. and Wilkes, G.L., *Processing Structure and Properties of Block Copolymers*, ed. M.J. Folkes, Elsevier Applied Science Publishers, London, 1985, 165–207. (h) Turner, R.B. and Wilkes, G.L., *Proceedings of the SPI/FSK Polyurethanes World Congress*, Technomic, Lancaster, PA, 1987, 935–940. (i) Creswick, M.W. et al., *Proceedings of the SPI-31st Annual Technical/Marketing Conference*, Technomic, Lancaster, PA, 1988, 11–17. (j) Artavia, L.D. et al., *Proceedings of the SPI/ISOPA Polyurethanes World Congress 1991*, Technomic, Lancaster, PA, 1991, 509–518. (k) Artavia, L.D. and Macosko, C.W., *Low density cellular plastics*, Hilyard, N.C., Cunningham, A., Eds., Chapman & Hall, London, 1994, 22–55. (l) Priester, R.D., Turner, R.B., *Low Density Cellular*

- Plastics*, ed. N.C. Hilyard and A. Cunningham, Chapman & Hall, London, 1994, [chap. 4](#). (m) Lidy, W.A., *UTECH '96-Processing Workshop 3*, Crain Communications, London, 1996. (n) Lidy, W.A. et al., *Proceedings of the 1996 SPI Polyurethanes Conference*, Technomic, Lancaster, PA, 1996, 119–135. (o) Lidy, W.A. et al., *Proceedings of the Polyurethanes World Congress 1997*, Technomic, Lancaster, PA, 1997, 95–117. (p) Mertes, J. et al., *J. Cell. Plast.*, 34, 526–543, 1998.
142. Cooper, S.L. and Tobolsky, A.V., *J. Appl. Polym. Sci.*, 10, 1837–1844, 1966.
 143. (a) Hauptmann, G. et al., *Proceedings of International Conference on Cellular and Non-Cellular Polyurethanes*, Strasbourg, France, June 1980, Carl Hanser Verlag, Munich, Germany, 1980, 617–634. (b) Bailey, F.E. and Critchfield, F.E., *J. Cell. Plast.*, 17/6, 333–339, 1981.
 144. Lidy, W.A., Phan Thanh, H., and Cadole, D., an unpublished presentation at the 1984 Gordon Conference on foams.
 145. (a) Merten, R., Lauerer, D., and Dahm, M., *J. Cell. Plast.*, 4/7, 262–275, 1968. (b) Rossmly, G.R. et al., *J. Cell. Plast.*, 13/1, 26–35, 1977. (c) Menges, G., Schwesig, H., and Hahn, H., *Org. Coat. Plast. Chem.*, 44, 229–233, 1981. (d) Cole, K.C. and Van Gheluwe, P., *J. Appl. Polym. Sci.*, 34, 396–407, 1987. (e) Van Gheluwe, P. et al., *J. Cell. Plast.*, 23/1, 73–85, 1987. (f) Artavia, L.D. and Macosko, C.W., *Proceedings of the SPI-33rd Annual Technical/Marketing Conference*, Technomic, Lancaster, PA, 1990, 554–561.
 146. (a) Cole, K.C. et al., *Proceedings of the SPI-31st Annual Technical/Marketing Conference*, Technomic, Lancaster, PA, 1988, 2–10. (b) Priester, R.D. et al., *J. Cell. Plast.*, 26/4, 346–367, 1990. (c) Elwell, M.J. et al., *Macromolecules*, 29/8, 2960–2968, 1996.
 147. Fuest, R.W. and Palinkas, R.L., *Conference Papers, UTECH 88*, Crain Communications, London, 1988, 32–35.
 148. Clift, S.M., *Proceedings of the SPI-33rd Annual Technical/Marketing Conference*, Technomic, Lancaster, PA, 1990, 547–553.
 149. (a) Neff, R. and Macosko, C.W., *Proceedings of the 1994 SPI Polyurethanes Conference*, Technomic, Lancaster, PA, 1994, 386–392. (b) Neff, R. and Macosko, C.W., *Proceedings of the 1995 SPI Polyurethanes Conference*, Technomic, Lancaster, PA, 1995, 344–352.
 150. (a) Paik Sung, C.S., Hu, C.B., and Wu, C.S., *Macromolecules*, 13/1, 111–116, 1980. (b) Paik Sung, C.S., Smith, T.W., and Sung, N.H., *Macromolecules*, 13/1, 117–121, 1980. (c) Wang, C.B., Cooper, S.L., *Macromolecules*, 16/ 5, 775–786, 1983. (d) Tyagi, D., Structure-property relationships in segmented copolymers, Ph.D. thesis, Virginia Polytechnic Institute and State University, 1985.
 151. (a) Whitman, R.D., Faucher, J.A., and Reding, F.P., *Proceedings of the SPI-7th Annual Technical Conference*, The Society of the Plastics Industry, New York, 1963, Section 2-C, 1–8. (b) Darr, W.C., Gemeinhardt, P.G., and Saunders, J.H., *Ind. Eng. Chem. Prod. Res. Dev.*, 2, 194–199, 1963. (c) Seefried, C.G., Koleske, J. V., and Critchfield, F.E., *J. Appl. Polym. Sci.*, 19, 2493–2502, 1975. (d) Seefried, C.G., Koleske, J.V., and Critchfield, F.E., *J. Appl. Polym. Sci.*, 19, 2503–2513, 1975. (e) Redman, R.P., *Developments in Polyurethane-1*, ed. J.M. Buist, Applied Science Publishers, London, 1978, 47. (f) Tazewell, J.H. et al. to Firestone Tire and Rubber et al; U.S. Patent 4,843,138, 1989. (g) Gilch, H. and Rath, W., *Conference Papers, UTECH 90*, Crain Communications, London, 1990, 179–184. (h) Tobushi, H. et al., *J. Intell. Mater. Struct.*, 12, 283–287, 2001. (i) Kintrup, S., Treboux, J.P.,

- and Misprouve, H., *Proceedings of the 2000 API Polyurethanes Conference*, Technomic, Lancaster, PA, 2000, 91–95.
152. (a) Illinger, J.L. and Schneider, N.S., *Polym. Eng. Sci.*, 12/1, 25–29, 1972. (b) Work, J.L., *Macromolecules*, 9/5, 759–763, 1976. (c) Christenson, C.P. et al., *J. Polym. Sci. Part B: Polym. Phys. Ed.*, 24, 1401–1439, 1986.
 153. (a) Harrell, L.L., *Macromolecules*, 2/6, 607–612, 1969. (b) Lee, H.S. and Hsu, S. L., *Macromolecules*, 22/3, 1100–1105, 1989.
 154. Schneider, N.S. et al., *Macromolecules*, 8/1, 62–67, 1975.
 155. (a) Rhodes, M.B., *Cellular and Noncellular Polyurethanes, International Conference, Strasbourg, France, June, 1980*, Carl Hansen Verlag, Munich, Germany, 1980, 803–819. (b) Rhodes, M.B. and Khaykin, B., *Langmuir*, 2/5, 643–649, 1986. (c) Rhodes, M.B., *Ureth. Tech.*, 5/3, 29–32, V. (d) Rhodes, M.B., *Rub. Plast. News*, 18/3, 27–28, 1988. (e) Rhodes, M.B. and Khaykin, B., *Proceedings of the SPI-32nd Annual Polyurethane Technical/Marketing Conference*, Technomic, Lancaster, PA, 1989, 178–182. (f) Chaffanjon, P. and Verhelst, G., *Proceedings of the SPI/ISOPA Polyurethanes World Congress 1991*, Technomic, Lancaster, PA, 1991, 545–552. (g) Rhodes, M.B., *Proceedings of the SPI-34th Annual Technical/Marketing Conference*, Technomic, Lancaster, PA, 1992, 548–551. (h) Reimann, K.A. et al., *Proceedings of the 1996 SPI Polyurethanes Conference*, Technomic, Lancaster, PA, 1996, 112–118.
 156. (a) Brumfield, H.L. and Estill, W.B., *J. Cell. Plast.*, 5/4, 212–220, 1969. (b) Kanakannatt, S.V., *J. Cell. Plast.*, 9/1, 50–53, 1973. (c) Hilyard, N.C., *Mechanics of Cellular Plastics*, Macmillan, New York, 1982, 107.
 157. (a) Aneja, A. and Wilkes, G.L., *Polyurethanes Expo 2001*, Technomic, Lancaster, PA, 2001, 195–199. (b) Rightor, E.G. et al., *Macromolecules*, 35, 5873–5882, 2002.
 158. Garrett, J.T., Siedlecki, C.A., and Runt, J., *Macromolecules*, 34, 7066–7070, 2001.
 159. (a) Chang, Y.P. and Wilkes, G.L., *J. Polym. Sci. Phys. Ed.*, 13, 455–476, 1975. (b) Bonart, R., Morbitzer, L., and Hentze, G., *J. Macromol. Sci. Phys.*, B3(2), 337–356, 1969. (c) Bonart, R., Morbitzer, L., and Muller, E.H., *J. Macromol. Sci. Phys.*, B9(3), 447–461, 1974. (d) Blackwell, J., Gardner, K.H., *Polymer*, 20, 13–17, 1979.
 160. Clough, S.B., Schneider, N.S., and King, A.O., *J. Macromol. Sci. Phys.*, B2(4), 641–648, 1968.
 161. Koberstein, J.T., Morra, B., and Stein, R.S., *J. Appl. Cryst.*, 13, 34–45, 1980.
 162. McClusky, J.V. et al., *Proceedings of the Polyurethanes World Congress 1993*, Technomic, Lancaster, PA, 507–516.
 163. (a) Elwell, M.J. et al., *Plast. Rub. Comp. Proc. Appl.*, 23/4, 265–276, 1995. (b) Stanford, J.L., Ryan, A.J., and Elwell, M.J., *Processing of Polymers*, ed. H.E.H. Meijer, VCH Publishers, Weinheim, Germany, 1997, chap. 9. (c) Hamley, I.W. et al., *Polymer*, 41, 2569–2576, 2000.
 164. (a) Macosko, C.W., *RIM: Fundamentals of Reaction Injection Moulding*, Hanser, Munich, 1989. (b) Ryan, A.J., *Polymer*, 31, 707, 1990. (c) Yang, W.L.P. and Macosko, C.W., *Makromol. Chem.*, Makromol. Symp. 1989, 25, 23. (d) Girard-Reydet, E. et al., *Polymer*, 39, 2269, 1998. (e) Yamanka, K., Takagi, Y., and Inoue, T., *Polymer*, 30, 1839, 1989. (f) Kim, B.S., Chiba, T., and Inoue, T., *Polymer*, 36, 43, 1995. (g) Pearson, R.A., *Advances in Chemistry Series*, 233, ed. C.K. Riew and A.J. Kinloch, American Chemical Society, Washington D.C., 1993, 405–425.
 165. Ryan, A.J., Stanford, J.L., and Still, R.H., *Plast. Rub. Proc. Appl.*, 13, 99–110, 1990.
 166. (a) Artavia, L.D., Ph.D. thesis, University of Minnesota, 1991. (b) Mora, E. M.Sc. thesis, University of Minnesota, 1991. (c) Elwell, M.J.A., Ph.D. thesis, Victoria

- University of Manchester, United Kingdom, 1993. (d) Neff, R., Ph.D. thesis, University of Minnesota, 1995. (e) Li, W., Ph.D. thesis, University of Sheffield, 2002.
167. Elwell, M.J., Mortimer, S., and Ryan, A.J., *Macromolecules*, 27, 5428, 1994.
 168. (a) Artavia, L.D. and Macosko, C.W., *J. Cell. Plast.*, 26, 490, 1990. (b) Mora, E., Artavia, L.D., and Macosko, C.W., *J. Rheol.*, 35, 921, 1991. (c) Elwell, M.J., *Thermochim. Acta*, 269/270, 145, 1995. (d) McClusky, J.V. et al., *J. Cell. Plast.*, 30, 338, 1994. (e) Bras, W. et al., *Science*, 267, 996, 1995. (f) Elwell, M.J.A. et al., *Polymer*, 37, 1353, 1996. (g) Wilkinson, A.W. et al., *Polym. Comm.*, 37, 2021, 1996. (h) Neff, R. and Macosko, C.W., *Rheologica Acta*, 35, 656, 1996. (i) Li, W., Ryan, A.J., and Meier, I.K., *Macromolecules*, 35, 5034, 2002. (j) Li, W., Ryan, A.J., and Meier, I.K., *Macromolecules*, 35, 6306, 2002.
 169. (a) Neff, R. et al., *J. Polym. Sci., Part B: Polym. Phys.*, 36, 573, 1998. (b) Kaushiva, B.D. and Wilkes, G.L., *J. Appl. Polym. Sci.*, 77, 202, 2000. (c) Kaushiva, B.D. and Wilkes, G.L., *Polymer*, 41, 6981, 2000. (d) Aneja, A. and Wilkes, G.L., *J. Appl. Polym. Sci.*, 85, 2956, 2002.
 170. Cookson, P., Stanford, J.L., and Ryan, A.J., Real-time measurements of structure development during the formation of flexible polyurethane foams, Macro-Group Young Researchers' Meeting, The Royal Society of Chemistry, Annual Conference 2001, University of Strathclyde, Glasgow, April 18–20, 2001.
 171. (a) Harding, R.H., *Resinography of Cellular Plastics*, ASTM STP 414, 1967, 3–18. (b) Blair, E.A., *Resinography of Cellular Plastics*, ASTM STP 414, 1967, 84–95. (c) Buist, J.M., Ball, G.W., and Woods, G., *Advances in Polyurethane Technology*, ed. J.M. Buist and H. Gudgeon, Maclaren and Sons, London, 1968, 152–154. (d) Meinecke, E.A. and Clark, R.C., *Mechanical Properties of Polymeric Foams*, Technomic, Lancaster, PA, 1972. (e) Baumhake, R., *J. Cell. Plast.*, 8/6, 304–310, 1972. (f) van Leuwen, B.G. et al., *Advances in Urethane Science and Technology*, vol. 2, Technomic, Lancaster, PA, 1973, 153–182. (g) Berlin, A.A., Shutov, F.A., and Zhitinkina, A.K., *Foam Based on Reactive Oligomers*, Technomic, Lancaster, PA, 1982, 85–87.
 172. (a) Rusch, T.E. and Raden, D.S., *Plast. Compd.*, July/August, 61–74, 1980. (b) Wooler, A.M., *Cell. Polym.*, 8, 296–320, 1989. (c) Burks, S., Autenrieth, R., and Gutowsky, K., *Proceedings of the SPI33rd Annual Polyurethane Technical/Marketing Conference*, Technomic, Lancaster, PA, 1990, 297–305.
 173. (a) Rosemund, W.R. and Sanders, M.R., *J. Cell. Plast.*, 13/3, 182–193, 1977. (b) Motte, P. and Regnault, J., *Proceedings of the SPI32nd Annual Polyurethane Technical/Marketing Conference*, Technomic, Lancaster, PA, 1989, 691–692.
 174. (a) Davis, B., *Urethanes Tech.*, March, 28–38, 1987. (b) Neary, W.J., *Plast. Tech.*, 11/3, 50–53, 1965. (c) Lerner, A. and Coen, R., *Plast. Tech.*, July, 97–99, 1966. (d) Bowyer, R.L., *International Progress in Urethanes*, vol. 1, ed. K.C. Frisch and A. Hernandez, Technomic, Lancaster, PA, 1977, 272–285. (e) Anon., *How to Buy a RIM Machine*, Gusmer-Admiral, Inc., Lakewood, NJ, 1996. (f) Jennings, R., *Plast. Tech.*, 15/3, 43–46, 1969. (g) Schlueter, K., *J. Cell. Plast.*, 17/1, 51–58, 1981.
 175. Dworkin, D., *SPE J.*, 1269–1275, December 1961.
 176. Anon., End use market survey of the polyurethane industry in the United States, Allegheny Marketing, September 1995.
 177. (a) Currier, V., *Plast. Tech.*, 12/8, 35–37, 1996. (b) Doyle, E.N., *The Development and Use of Polyurethane Products*, McGraw-Hill, New York, 1971, 238. (c) Ferri-gno, T.H., *SPE J.*, 638–640, June 1960.
 178. (a) Ramlow, G.G., Hwymman, D.A., and Grace, O.M., *J. Cell Plast.*, 19/4, 237–242, 1983. (b) Spittler, K.G. and Lindsey, J.J., *J. Cell. Plast.*, 17/1, 43–50, 1981. (c)

- Kuryla, W.C. et al., *J. Cell. Plast.*, 2/2, 84–96, 1966. (d) Heyman, D.A. and Grace, O.M., *Proceedings of the SPI-28th Annual Technical/Marketing Conference*, Technomic, Lancaster, PA, 1984, 257–260.
179. Wolfe, H.W., *Mechanics of Cellular Plastics*, ed. N.C. Hilyard, Macmillan, New York, 1979, 99–145.
 180. (a) Stewart, D.A., Westfall, P.M., and Quarles, P.D., *Proceedings of the 1995 SPI Polyurethanes Conference*, Technomic, Lancaster, PA, 1995, 90–93. (b) Chadwick, F. and McCune, L., *Conference Papers, UTECH 96*, Crain Communications, London, 1996, Paper 33.
 181. (a) Potzsch, R., *Proceedings of the SPI/FSK Polyurethanes World Congress, Aachen*, Technomic, Lancaster, PA, 1987, 887–890. (b) Ubben, R., *Conference Papers, UTECH 90*, Crain Communications, London, 1990, 145–148. (c) Schiffler, C., *Conference Papers, UTECH 96*, Crain Communications, London, 1996, Paper 20.
 182. Brown, M.J., *Proceedings of the SPI-34th Annual Technical/Marketing Conference*, Technomic, Lancaster, PA, 1992, 463–467.
 183. (a) Knibbe, D.E., *J. Cell. Plast.*, 21/4, 264–268, 1985. (b) Lambach, J.L. and Gill, W.A., *Proceedings of the SPI33rd Annual Polyurethane Technical/Marketing Conference*, Technomic, Lancaster, PA, 1990, 165–171.
 184. (a) Green, H.L., *J. Cell. Plast.*, 5/3, 173–175, 1969. (b) Axel, F., *International Progress in Urethanes*, ed. K.C. Frisch and A. Hernandez, Technomic, Lancaster, PA, 1975, 1, 286–291. (c) Kirkland, C., *Plast. Tech.*, 65–70, Sept., 1980. (d) Collins, S.H., *Plast. Cmpd.*, 38–44, March/April, 1983. (e) Cox, D.B., *Urethane Chemistry and Applications*, ed. K.M. Edwards, ACS Symposium Series 172, 1981, 565–573. (f) Lammerting, H., *Uret. Tech.*, 3/1, 38–42, 1986. (g) Sherman, L.M., *Plast. Tech.*, 42–45, August 1995.
 185. (a) Andrews, G.D. and Wasilczyk, G.J., *Proceedings of the SPI 31st Annual Technical/Marketing Conference*, Technomic, Lancaster, PA, 1988, 447–454. (b) Schroder, W., *J. Elast. Plast.*, 20, 200–207, 1988. (c) Wochnowski, H., *Kunststoffe*, 78/8, 680–683, 1989. (d) Block, H.H., *Kunststoffe*, 79/3, 240–242, 1989. (e) Fountas, G., *Elastomerics*, 122/12, 30–31, 1990. (f) Moskowitz, M., *Plast. World*, 49/3, 103, 1991. (g) Andrew, G.D. et al., *Proceedings of the Polyurethanes World Congress 1991*, Technomic, Lancaster, PA, 1991, 877–884. (h) Editorial, *Elastomerics*, 124/2, 29, 1992. (i) Thies, W., *Conference Papers, UTECH 94*, Crain Communications, London, 1994, Paper 15. (j) Michaeli, W. et al., *Kunststoffe*, 86/6, 838–842, 1996. (k) Andrew, G.D., Boyer, T.C., and Olari, J.R., *Proceedings of the 1996 SPI Polyurethanes Conference*, Technomic, Lancaster, PA, 1996, 480–486.
 186. (a) Abernathy, H.H., *Rub. World*, 131/6, 765–769, 1955. (b) Wall, J.R., a paper given before the Cellular Plastics Division, Society of the Plastics Industry, Inc., Detroit, June 1960. (c) Healy, T.T., *Polyurethane Foams*, ed. T.T. Healy, Iliff Books, London, 1963, 75–92. (d) Bishop, A.C., *Plast. Rub.*, 1/9, 381, 1970.
 187. (a) Zick, J., *Proceedings of the SPI/FSK Polyurethanes World Congress*, Technomic, Lancaster, PA, 1987, 570–573. (b) Bayer, H.G., *Proceedings of the SPI/FSK Polyurethanes World Congress*, Technomic, Lancaster, PA, 1987, 574–577. (c) Ostertag, B., *Kunststoffe*, 79/11, 1144–1145, 1987. (d) Zick, J., *Proceedings of the SPI-32nd Annual Technical/Marketing Conference*, Technomic, Lancaster, PA, 1989, 211–215. (e) Ostertag, B., *Proceedings of the SPI-32nd Annual Technical/Marketing Conference*, Technomic, Lancaster, PA, 1989, 209–210. (f) Heiberger, R., Dipietrantonio, B.F., and Katz, J.J., *Proceedings of the SPI-32nd Annual Technical/Marketing Conference*, Technomic, Lancaster, PA, 1989, 44–49. (g) Pierkes, L., *Conference Papers*,

- UTECH 90, Crain Communications, London, 1990, 126–130. (h) Deno, L., *Conference Papers, UTECH 90*, Crain Communications, London, 1990, 142–144. (i) Schneider, F.W. and Grasse, H., *Conference Papers, UTECH 90*, Crain Communications, London, 1990, 149–154. (j) Schneider, F.W., Grasse, H., and Gillham, M., *Proceedings of the SPI-33rd Annual Technical/Marketing Conference*, Technomic, Lancaster, PA, 1990, 32–39. (k) Gill, W.A., Good, R.M., and Hawker, L.E., *Proceedings of the SPI-33rd Annual Technical/Marketing Conference*, Technomic, Lancaster, PA, 1990, 40–45. (l) Murray, D., Deno, L., and Katz, J.J., *Proceedings of the SPI-33rd Annual Technical/Marketing Conference*, Technomic, Lancaster, PA, 1990, 172–176.
188. (a) Kozlowski, E.F. and Kruger, E.R. to Lear Siegler, Inc., U.S. Patent 4,692,199, 1987. (b) Anon., *Seating Technology*, Lear Seating Corporation, 1994. (c) Gabriele, M. and Monks, R., *Plast. Tech.*, 38/4, 15–23, 1992. (d) Anon., *Trim Retention Bonding*, The Woodbridge Group, 1993. (e) Andrew, G.D., Boyer, T.C., and Olari, J.R., *Proceedings of the 1996 SPI Polyurethanes Conference*, Technomic, Lancaster, PA, 1996, 480–486.
 189. Buist, J.M., *Plast. Inst. Trans.*, 27, 13–27, 1959.
 190. Editorial, *Mod. Plast. Int.*, June 14–17, 1973.
 191. Editorial, *Mod. Plast. Int.*, 12–13, August 1978.
 192. Cravens, T.E., *Proceedings of the Carpet Rug Institute Annual Meeting*, Hilton Head, SC, 1975.
 193. (a) Editorial, *Plast. Rub. Wkly.*, March 7, 25–26, 1975. (b) Marlin, L., Durante, A.J., and Schwarz, E.G., *J. Cell. Plast.*, 11/6, 317–322, 1975. (c) Kallert, W., *J. Coated Fab.*, 4, 272–278, 1975. (d) Bobe, J., Hurd, R., and Woods, G., *Proceedings of the SPI-4th International Cellular Plastics Conference*, Society of the Plastics Industry, New York, 1976, 290–295. (e) Hurd, R., *Developments in Polyurethane-1*, ed. J.M. Buist, Applied Science, London, 1978, 211–222. (f) Bez, W. and Quack, G., *Cell. Polym.*, 2, 31–53, 1983. (g) Berthevas, P., *Cell. Polym.*, 4, 179–193, 1985.
 194. (a) Anon., *Rub. Age*, 804–810, August 1956. (b) Editorial, *Br. Plast.*, 34/2, 73–74, 1961. (c) Jones, R.E., Patten, G. and Steingisen, S., *Handbook of Foamed Plastics*, ed. R. Bender, Lake Publishing Corporation, Libertyville, IL, 1965, 52–68. (d) Rogers, T.H., *J. Cell. Plast.*, 4/10, 392–394, 1968. (e) Touhey, W.J., *J. Cell. Plast.*, 4/10, 395–397, 1968.
 195. *Annual Book of American Society for Testing and Materials Standards*, Volume 09.02, D 3574–86, ASTM, Philadelphia, 1990, 320–335.
 196. Graf, W.C. and Schondlowski, H., *Proceedings of the SPI-3rd International Cellular Plastics Conference*, The Society of the Plastics Industry, New York, 1972, 225–236.
 197. (a) Lambert, A., *Eur. J. Cell. Plast.*, 25–35, January 1980. (b) Wang, S.L., Frisch, K.C., and Malwitz, N., *Proceedings of the SPI-30th Annual Technical/Marketing Conference*, Technomic, Lancaster, PA, 1986, 363–368. (c) Lawler, L.F. and Schiffauer, R., *Proceedings of the Polyurethanes World Congress 1993*, Technomic, Lancaster, PA, 1993, 288–296. (d) Ramesh, N.S. and Malwitz, N., *Proceedings Annual Technical Conference—Soc. Plast. Eng.*, 52/2, 1941–1945, 1994. (e) Fabishak, D.M., *J. Cell. Plast.*, 8/2, 82–84, 1972. (f) Schiffauer, R., *Proceedings of the 1994 SPI Polyurethanes Conference*, Technomic, Lancaster, PA, 1994, 225–238. (g) Cavender, K.D. and Kinkelaar, M.R., *Proceedings of the 1994 SPI Polyurethanes Conference*, Technomic, Lancaster, PA, 1994, 248–251. (h) Lederman, J.M., *J. Appl. Polym. Sci.*, 15, 693–703, 1971. (i) Hilyard, N.C. and Collier, P., *Cell. Polym.*, 6/6, 9–26,

1987. (j) Gent, A.N. and Rusch, K.C., *J. Cell. Plast.*, 2/1, 46–51, 1966. (k) Hilyard, N.C., *Low Density Cellular Plastics, Physical Basis of Behaviour*, ed. N.C. Hilyard and A. Cunningham, Chapman & Hall, London, 1994, 235–269.
198. Kreter, P.E., *J. Cell. Plast.*, 21/5, 306–310, 1985.
199. (a) Hogan, J.M. et al., *J. Cell. Plast.*, 9/5, 219–225, 1973. (b) Saotome, K., Matsurbara, K., and Yatomi, T., *J. Cell. Plast.*, 13/3, 203–209, 1977. (c) Woods, G., *Flexible Polyurethane Foams, Chemistry and Technology*, Applied Science Publishers, London, 1982, 119–120. (d) Moreland, J.C., Wilkes, G.L., and Turner, R.B., *Proceedings of the SPI/ISOPA Polyurethanes World Congress 1991*, Technomic, Lancaster, PA, 1991, 500–508. (e) Dounis, D., Wilkes, G.L., and Turner, R.B., *Polymer Preprints*, vol. 35, no. 2, 1994, American Chemical Society, Washington, D.C., 1994, 781–782. (f) Brasington, R., Kinkelaar, M.R., and Cavender, K.D., *Conference Papers, UTECH 96*, Crain Communications, London, 1996, Paper 9.
200. (a) Anon., *Plast. Tech.*, 8/4, 26–32, 1962. (b) Lambert, A., *J. Cell. Plast.*, 10/1, 35–42, 1974. (c) Ashe, W.A. and Grace, O.M., *J. Cell. Plast.*, 25/4, 371–390, 1989.
201. (a) Hartings, J.W. and Hagan, J.H., *J. Cell. Plast.*, 14/2, 81–86, 1978. (b) Rosemund, W.R. and Sander, M.R., *J. Cell. Plast.*, 13/3, 182–193, 1977. (c) Blair, G.R. and Wilson, A.R., *Proceedings of the 1995 SPI Polyurethanes Conference*, Technomic, Lancaster, PA, 1995, 413–417.
202. (a) Jones, R.E. et al., *Plast. Tech.*, 5/9, 55–59, 1959. (b) Polis, S., *Proceedings of the SPI-24th Annual Urethane Division Technical Conference*, Technomic, Lancaster, PA, 1978, 59–69. (c) Time Tech TT502 Ball Rebound Foam Resilience Tester, Time Tech, Inc. Wilmington, DE, 1996.
203. Wolfe, H.W., *Mechanics of Cellular Plastics*, ed. N.C. Hilyard, Macmillan, New York, 1979, 105.
204. (a) McCallum, J.B., *Text. Chem. Color.*, 21/12, 13–15, 1989. (b) American Society for Testing and Materials, D 5393-93, ASTM, Philadelphia, 1993. (c) General Motors Engineering Standard GM9305P, January, 1992. (d) Ford Laboratory Test Method BO-116-03, 1990. (e) Deutsches Institut für Normung (DIN) Test Method DIN 75201R and DIN 75201G. (f) SAE Test Method J1756, 1994.
205. (a) Coupland, F.E., *Proceedings of the SAE International Congress and Exposition*, Detroit, MI, 1988, SAE, Warrendale, PA, Paper 880504. (b) Baatz, G. and Franyutti, S., *Conference Papers, UTECH 94*, Crain Communications, London, 1994, Paper 9. (c) Bradford, L., Pinzoni, E., and Wuestenenk, J., *Proceedings of the 1996 SPI Polyurethanes Conference*, Technomic, Lancaster, PA, 1996, 358–361. (d) Loock, F., Lampe, Th., and Bahadir, A.M., *Kunststoffe*, 83/3, 201–205, 1993.
206. (a) Rothermel, H.M., *Polyurethane Handbook*, ed. G. Oertel, Hanser, New York, 1985, 455–507. (b) Wolfe, H.W., *Mechanics of Cellular Plastics*, ed. N.C. Hilyard, Macmillan, New York, 1979, 99–145. (c) Woods, G., *Flexible Polyurethane Foams, Chemistry and Technology*, Applied Science Publishers, London, 1982, 126–128, 296.
207. *Annual Book of American Society for Testing and Materials Standards*, Volume 09.02, D 3574-95, ASTM, Philadelphia, 1990, 320–335.
208. Campbell, G.A., Report GMR-2662, General Motors Research Laboratories, April 1978.
209. (a) Ashe, W.A., Grace, O.M., and Otten, J.G., *Proceedings of the SPI-25th Annual Urethane Division Technical Conference*, Technomic, Lancaster, PA, 1979, 107–112. (b) Flexible Cellular Materials—Test for Dynamic Fatigue by Constant Load Pounding, International Standard 3385.
210. Hartings, J.W. and Hagan, J.H., *J. Cell. Plast.*, 14/2, 81–86, 1978.

211. American Society for Testing and Materials, D3574-86, ASTM, Philadelphia, 1990.
212. Ashe, W.A., *Proceedings of the SPI-30th Annual Technical/Marketing Conference*, Technomic, Lancaster, PA, 1986, 320-325.
213. Knight, J.E., *Proceedings of the SPI-30th Annual Technology/Marketing Conference*, Technomic, Lancaster, PA, 1986, 48-57.
214. (a) Dwyer, F.J., *J. Cell Plast.*, 12/2, 104-113, 1976. (b) Wolfe, H.W., Brizzolara, D.F., and Bryam, J.D., *J. Cell. Plast.*, 13/1, 48-56, 1977. (c) Beals, B., Dwyer, F.J., and Kaplan, M., *J. Cell. Plast.*, 1/1, 32-41, 1965. (d) Ball, G.W. and Doherty, D.J., *J. Cell. Plast.*, 3/5, 223-232, 1967. (e) Stone, H., *Proceedings of the SPI-27th Annual Technical/Marketing Conference*, Technomic, Lancaster, PA, 1982, 124-137. (f) Saunders, J.H. and Frisch, K.C. *Polyurethanes, Chemistry and Technology, Part 1: Chemistry*, Robert Krieger, New York, 1962, 327-345. (g) Casati, F.M. et al., *Polyurethanes World Congress 1997*, Technomic, Lancaster, PA, 1997, 402-420. (h) Casati, F.M. et al., *Polyurethanes Expo '98*, Technomic, Lancaster, PA, 1998, 417-431. (i) Broos, R., Casati, F.M., and Herrington, R.M., *Polyurethanes Expo '99*, Technomic, Lancaster, PA, 1999, 347-364. (j) Moore, D.R. et al., *Proceedings of the SPI-34th Annual Polyurethanes Technical/Marketing Conference*, Technomic, Lancaster, PA, 1992, 502-511.
215. (a) Bryan, M.E., Tempest, W., and Williams, D., *Appl. Ergonom.*, 9/3, 151-154, 1978. (b) Winklhofer, E. and Thien, G.E., *Proceedings of the SAE International Congress and Exposition*, Detroit, MI, 1985, SAE, Warrendale, PA, Paper 850966. (c) Kryter, K.D., *The Effects of Noise on Man*, Academic Press, New York, 1970. (d) Miller, J.D., *J. Acou. Soc. Am.*, 56/3, 729-763, 1974. (e) Howell, T.M. and Schumacher, R.F., *Proceedings of the SAE International Congress and Exposition*, Detroit, MI, 1985, SAE, Warrendale, PA, Paper 850969. (f) Bagga, K.S. and Repick, E.P., *Proceedings of the SAE International Congress and Exposition*, Detroit, MI, 1985, SAE, Warrendale, PA, Paper 850994. (g) Measurement of Interior Sound Levels of Light Vehicles, SAE Recommended Practice SAE J1477, SAE, Warrendale, PA, Jan., 1986. (h) Stacy, J.M., *Proceedings of the SAE International Congress and Exposition*, Detroit, MI, 1987, SAE, Warrendale, PA, Paper 871260.
216. (a) Costa, C.E.T. and Pauperio, A., *Proceedings of the SPI-32nd Annual Polyurethane Technical/Marketing Conference*, Technomic, Lancaster, PA, 1989, 579-586. (b) MacFarland, D.R., *Proceedings of the SAE International Congress and Exposition*, Detroit, MI, 1994, SAE, Warrendale, PA, Paper 940700.
217. Grande, J.A., *Mod. Plast.*, 30-31, October 1996.
218. (a) Ball, G.L., Schwartz, M., and Long, J.S., *Off. Dig. Fed. Soc. Paint Technol.*, 32/425, 817-831, 1960. (b) Buist, J.M. and Gudgeon, H., *Advances in Polyurethane Technology*, Maclaren and Sons, London, 1968, 159-162.
219. Imai, Y., and Asano, T., *J. Appl. Polym. Sci.*, 27, 183-195, 1982.
220. (a) Moore, R.S., *Encyclopedia of Polymer Science and Technology*, 12, 700-724, 1970. (b) Ludman, W.R., *Proceedings of the Plastics and Rubber Institute Urethanes Group Conference*, London, 1976, G1-G4. (c) Kingsbury, H.B., Cho, K., and Powers, W.R., *J. Cell. Plast.*, 14/2, 113-117, 1978. (d) Eeckhaut, G., Pham, T., and Lockwood, R.J., *Proceedings of the SPI/FSK Polyurethanes World Congress*, Technomic, Lancaster, PA, 1987, 708-711. (e) Gahlau, H.K., *Proceedings of the SPI/FSK Polyurethanes World Congress*, Technomic, Lancaster, PA, 1987, 712-726. (f) Lee, J.R., *Conference Papers, UTECH 88*, Crain Communications, London, 1988, 81-82. (g) Corsaro, R.D. and Sperling, L.H., eds., *Sound and Vibration Damping with Polymers*, ACS

- Symposium Series 424, American Chemical Society, Washington, D.C., 1990. (h) Lutter, H.D., Mertes, J., and Zschiesche, R., *Proceedings of the Polyurethanes World Congress 1991*, Technomic, Lancaster, PA, 1991, 252–256. (i) Lauriks, W., *Low Density Cellular Plastics, Physical Basis of Behaviour*, ed. N.C. Hilyard and A. Cunningham, Chapman and Hall, London, 1994, 319–361.
221. *Polymers in Vibration Damping and Soundproofing*, PB86-858966, National Technical Information Service, Springfield, VA, 1986.
 222. (a) Goldman, D.E. and von Gierke, H.E., *Shock and Vibration Handbook*, ed. C.M. Harris, and C.E. Crede, McGraw-Hill, New York, 1961, 44.1–44.51. (b) McCormick, E.J., *Human Factors Engineering*, McGraw-Hill, New York, 1964, 474–483. (c) Kryter, K.D., *The Effects of Noise on Man*, Academic Press, New York, 1970. (d) Miller, J.D., *J. Acou. Soc. Am.*, 56/3, 729–764, 1974. (e) Griffin, M.J., *Handbook of Human Vibration*, Academic Press, London, 1990.
 223. (a) Wooley, W.D., *Proceedings of Fire and Cellular Polymers*, Elsevier, London, 1984, 37–39. (b) Drysdale, D.D. and Thomson, H.E., *Proceedings of Flame Retardants 90*, Elsevier, London, 1990, 191–205.
 224. (a) Rua, L. et al., Evaluations of the fire performance of flame retarded flexible polyurethane foam in an upholstered furniture application, *J. Consum. Prod. Flamm.*, 7, 99–126, 1980. (b) Szabat, J., *J. Consum. Prod. Flamm.*, 8, 189, 1981. (c) Schuhmann, J. and Hartzell, G., *J. Fire Sci.*, 7, 386–402, 1989. (d) Powell, D., *Fire Prev.*, 27–30, 1989.
 225. Van der Plaats, G., Soons, H., and Snellings, R., The thermal behavior of melamine, DSM Corporate Research and Patents Department, Letter report WdB/GBL/860, February 20, 1990.
 226. Balkon, J., *Proceedings of the SPI-31st Annual Technical/Marketing Conference*, Technomic, Lancaster, PA, 1988, 218–239.
 227. (a) Babrauska, V. and Krasny, J.F., NBS Monograph 173, National Bureau of Standards, Washington, D.C., 1985. (b) Strength, R.S. and Sherman, M., *Proceedings of the SPI-31st Annual Technical/Marketing Conference*, Technomic, Lancaster, PA, 1988, 268–272.
 228. Gum, W.F., *Proceedings of the SPI-33rd Annual Polyurethane Technical/Marketing Conference*, Technomic, Lancaster, PA, 1990.
 229. (a) Hull & Co., *End Use Market Survey of the Polyurethane Industry in the United States and Canada*, prepared for the Society of the Plastics Industry, Inc., Polyurethane Division, May 29, 1990. (b) Saunders, J.H. and Frisch, K.C., *High Polymers*, Vol. XVI, Part II, Interscience, New York, 1964, 849. (c) Roegler, M., *Polyurethane Handbook*, ed. G. Oertel, Hanser, Munich, 1985, 176–177. (d) Woods, G. *The ICI Polyurethanes Book*, John Wiley & Sons, New York, 1987, 203–204. (e) Miyama, S., *Conserv. Recyc.*, 10/4, 265–272, 1987. (f) Kettemann, B.U. et al., *Kunststoffe*, 85/11, 33–35, 1995. (g) Editorial, *Charlotte Observer*, March 26, 1990.
 230. Baumann, B.D. et al., *Proceedings of the SPI-6th International Technical/Marketing Conference*, Technomic, Lancaster, PA, 1983, 139–141.
 231. (a) Gerlock, J., Braslaw, J., and Zimbo, M., *Ind. Eng. Chem. Proc. Des. Dev.*, 23, 545–552, 1984. (b) Campbell, G.A. and Meluch, W.C., *Environ. Sci. Tech.*, 10/2, 182–185, 1976. (c) Meluch, W.C. and Campbell, G.A., U.S. Patent 3,978,128, 1976. (d) Campbell, G.A. and Meluch, W.C., *J. Appl. Polym. Sci.*, 21, 581–584, 1977. (e) Salloum, R.J., *Proceedings of the SPE ANTEC*, Society Of Plastics Engineers, Brookfield Center, Ct., 1981, 491–494. (f) Grigat, E. and Hetzel, H., U.S. Patent 4,051,212, 1977. (g) Niederdelmann, G. et al., U.S. Patent 4,399,236, 1983. (h)

- Mahoney, L.R., Weiner, S.A., and Ferris, F.C., *Environ. Sci. Tech.*, 8/2, 135–139, 1974. (i) Braslaw, J. and Gerlock, J.L., *Ind. Eng. Chem. Pro. Des. Dev.*, 23, 552–557, 1984.
232. (a) Ulrich, H. et al., *Polym. Eng. Sci.*, 18/11, 844–848, 1978. (b) Frulla, F.F., Odinak, A., and Sayigh, A.A.R., U.S. Patent 3,709,440, 1973, and U.S. Patent 3,738,946, 1973. (c) Tucker, B. and Ulrich, H., U.S. Patent 3,983,087, 1976. (d) Ulrich, H. et al., *Elast. Plast.*, 11, 208, 1979. (e) Simioni, F., Bisello, S., and Cambini, M., *Macplas* 8, (47), 52, 1983. (f) Simioni, F., Bisello, S., and Tavan, M., *Cell. Polym.*, 2, 281–283, 1983. (g) Simioni, F., Modesti, M., and Navazzio, G., *Macplas* 12, (88), 127–129, 1987. (h) Simioni, F., Modesti, M., Brambilla, C.A., *Cell. Polym.*, 8, 387–400, 1989. (i) Sheratte, M.B., *Proceedings of the SPI-20th Annual Technical Conference*, Technomic, Lancaster, PA, 1977, 59–60. (j) Kinstle, J.F. et al., *Polym. Preprints*, 24/2, 446–447, 1983. (k) Ulrich, H., *Advances in Urethane Science and Technology*, vol. 5, ed. K.C. Frisch and S.L. Reegen, Technomic, Lancaster, PA, 1978, 49–57. (l) Chapman, T.M., *J. Polym. Sci. A. Polym. Chem.*, 27, 1993–2005, 1989. (m) Grigat, E., *Kunststoffe*, 68/5, 281–284, 1978. (n) Bauer, G., RECYCLE 1990, Davos, Switzerland, May 29–31, 1990. (o) Bauer, G., German Patent 2,738,572. (p) Bauer, G., German Patent 19,512,778.
233. (a) Madorsky, S.L. and Straus, S., *J. Poly. Sci.*, 36, 183–194, 1959. (b) Rapp, N.S. and Ingham, J.D., *J. Polym. Sci.*, A/2, 689–704, 1964. (c) Ingham, J.D. and Rapp, N.S., *J. Polym. Sci.*, A/2, 4941–4964, 1964. (d) Tilley, J.N. et al., *J. Cell. Plast.*, 4/2, 56–66, 1968. (e) Levin, B.C., National Bureau of Standards Report, NBSIR 853267, 1986. (f) Maya, P. and Levin, B.C., *Fire Mater.*, 11, 129, 1987. (g) Wooley, W.D. and Fardell, P.J., *Fire Res.*, 1, 11–21, 1977. (h) Wooley, W.D., *Br. Polym. J.*, 4, 27–43, 1972. (i) Wooley, W.D., Fardell, P.J., and Buckland, I.G., Fire Research Note No. 880, July, 1971. (j) Chambers, J., Jiricny, J., and Reese, C.B., *Fire Mater.*, 5, 133–141, 1981. (k) Braslaw, J., Gealer, R.L., and Wingfield, R.C., *Polym. Preprints*, 24, 434, 1983.
234. Myers, J.I. and Farrissey, W.J., *Proceedings of the SAE International Congress and Exposition*, Detroit, MI, 1991, SAE, Warrendale, PA, Paper 910583.
235. Fosnaugh, J., *Automot. Transp. Int.*, 76, May 1994.
236. John, J., Bhattacharya, M., and Turner, R.B., *J. Appl. Polym. Sci.*, 86, 3097–3107, 2002.

Rigid Polyurethane Foams

H.J.M. Grünbauer, J. Bicerano, P. Clavel, R.D. Daussin, H.A. de Vos,
M.J. Elwell, H. Kawabata, H. Kramer, D.D. Latham, C.A. Martin, S.E.
Moore, B.C. Obi, V. Parenti, A.K. Schrock, and R. van den Bosch

CONTENTS

- 7.1 Introduction
- 7.2 Raw Materials
 - 7.2.1 Isocyanates
 - 7.2.1.1 Introduction
 - 7.2.1.2 Production
 - 7.2.1.3 Properties
 - 7.2.1.4 Products
 - 7.2.2 Polyols
 - 7.2.2.1 Introduction
 - 7.2.2.2 Production
 - 7.2.2.3 Properties
 - 7.2.2.4 Products
 - 7.2.3 Blowing Agents
 - 7.2.4 Additives
 - 7.2.4.1 Catalysts
 - 7.2.4.2 Surfactants
- 7.3 Applications and Markets
 - 7.3.1 Appliance
 - 7.3.1.1 Introduction
 - 7.3.1.2 Processing
 - 7.3.1.3 New Blowing Agents
 - 7.3.1.4 Hydrochlorofluorocarbons
 - 7.3.1.5 Hydrocarbons
 - 7.3.1.6 Vacuum Insulation Panels (VIPs)
 - 7.3.1.7 Markets
 - 7.3.2 Construction
 - 7.3.2.1 Introduction
 - 7.3.2.2 Continuous Production

7.3.2.3 Discontinuous Production

Products and Applications

7.3.2.5 Markets

7.4 Foaming Process

7.4.1 Mixing

7.4.2 Nucleation

7.4.3 Expansion

7.4.4 Rheology

7.4.5 Polymer Morphology

7.5 Physical Properties

7.5.1 Thermal Conductivity

7.5.1.1 K-factor Contributions

7.5.1.2 Condensation

7.5.2 Aging

7.5.2.1 Gas Diffusion

7.5.2.2 Dimensional Stability

7.6 Conclusions

Acknowledgments

References

7.1 Introduction

Urethane foams represent a highly versatile class of expanded thermoset materials that find application in a wide range of industrial products such as carpet backings, mattresses, insulation panels, and refrigerators. Within this spectrum, closed-cell rigid foams are an important sub-class owing to their outstanding thermal insulation properties when expanded with suitable blowing agents of low thermal conductivity.¹⁻⁴ To illustrate, [Figure 7.1](#) compares the thermal insulation performance of rigid polyurethane foam with that of other materials, such as expanded polystyrene, mineral wool, cork, softwood, fireboard, concrete blocks, and bricks. [Figure 7.1](#) clearly shows that to match the insulation performance of 50-mm rigid polyurethane foam other materials need to be applied at much higher thicknesses, ranging from 80 mm (~3 in.) for expanded polystyrene to 90 mm for mineral wool or 1720 mm for bricks. As will be explained in [Section 7.5.1](#), this performance is primarily due to a combination of blowing agent properties, cell size, and cell-morphology. The latter is characterized by fully drained, dodecahedron-shaped cells^{5,6} with void volumes of 95–97% and 100–500 μm cell size. An example is given in [Figure 7.2](#).

Notwithstanding its prime importance, excellent thermal insulation performance is not the only property that makes rigid polyurethane foams an attractive choice in various industrial applications. There are several added advantages which, alone or in combination, are often decisive to the selection

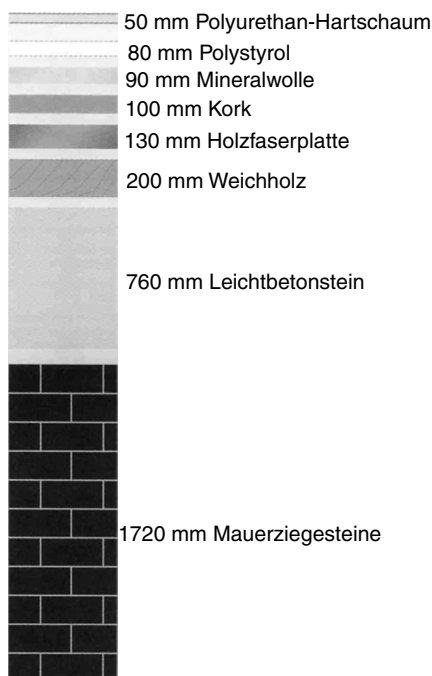


FIGURE 7.1

Example of the relative thicknesses of alternative building materials needed to match the thermal conductivity properties of rigid polyurethane foam at 50 mm. Note that the other materials need to be applied at much higher thicknesses (ranging from 80 mm for expanded polystyrene to 90 mm for mineral wool and 1720 mm for bricks) to match the insulation performance of 50-mm rigid polyurethane foam. (Reprinted with permission from Koschade, R., *Die Sandwichbauweise (How to Build a Steel Sandwich)*, Ernst & Sohn, Berlin, 2000.)

of polyurethane foams in a particular application or process environment.⁷ The most important advantages are their high mechanical strength, their strong adhesive propensity, and, above all, their easy processing. The combination of all three is particularly apparent in, e.g., refrigerators and sandwich panels where rigid polyurethane foam is virtually unmatched.^{1-3,8-10} Easy processability allows “pour in place” manufacturing of foams, even in molds of highly complex shapes and forms. It is most convincingly demonstrated by a lab scale experiment, as visualized in Figure 7.3. Starting from two low viscosity liquids, polyol and isocyanate, the first step of foam preparation consists of mixing and pouring the mixture. After 5–20 sec, the reacting mass takes a creamy appearance which reflects the fact that nucleation of gas bubbles has occurred. Subsequently, the foam rises to achieve its final shape after 30–120 sec. Finally, a curing step (not shown) of several minutes to hours should be taken into account. The appealing simplicity of this pictorial should not conceal that the design of such a system that foams “by itself” often takes years of development and significant investments before all ingredients and sub-processes are fine tuned.

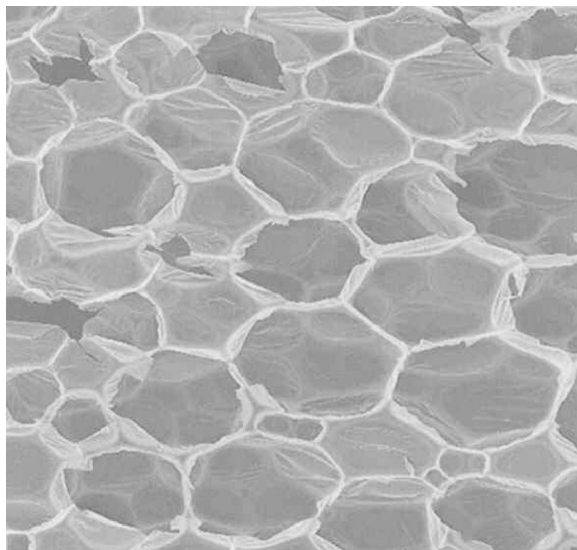


FIGURE 7.2

Cellular structure of rigid polyurethane foam. (Reprinted with permission from Koschade, R., *Die Sandwichbauweise (How to Build a Steel Sandwich)*, Ernst & Sohn, Berlin, 2000.)

From a physical point of view, rigid polyurethane foaming represents an intricate combination of simultaneous processes that starts by mixing two partially miscible liquids, followed by a multiple co-polymerization process involving at least the steps of solidification, vitrification, and chemical network formation. Meanwhile, sufficient gaseous compounds are evolving to expand the reacting mass 30- to 50-fold to achieve a final low density of 20–50 kg/m³ without deteriorating its fine-cell structure. In view of this complexity, it is not surprising that the polyurethane industry has been unable to respond with “drop-in” technology to the challenges imposed by global ozone depletion and global warming issues.^{11–13} On the contrary, these issues have raised a wave of research and development throughout academia and industry which is still going on today. It is the aim of this chapter to provide a concise account of this work by discussing both raw materials, major applications, and new fundamental insights.

7.2 Raw Materials

7.2.1 Isocyanates

7.2.1.1 Introduction

Isocyanate types can be subdivided into aromatic, aliphatic, and cyclo-aliphatic isocyanates. Due to their higher reactivity and favorable economics,

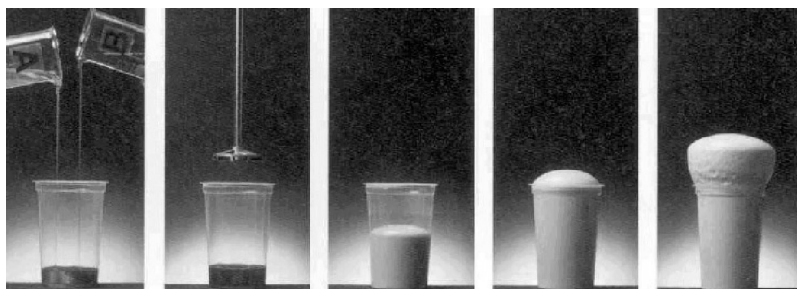


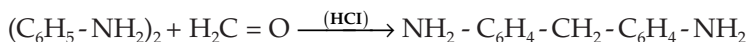
FIGURE 7.3

Lab scale preparation of rigid polyurethane foam. (Reprinted with permission from Koschade, R., *Die Sandwichbauweise (How to Build a Steel Sandwich)*, Ernst & Sohn, Berlin, 2000.)

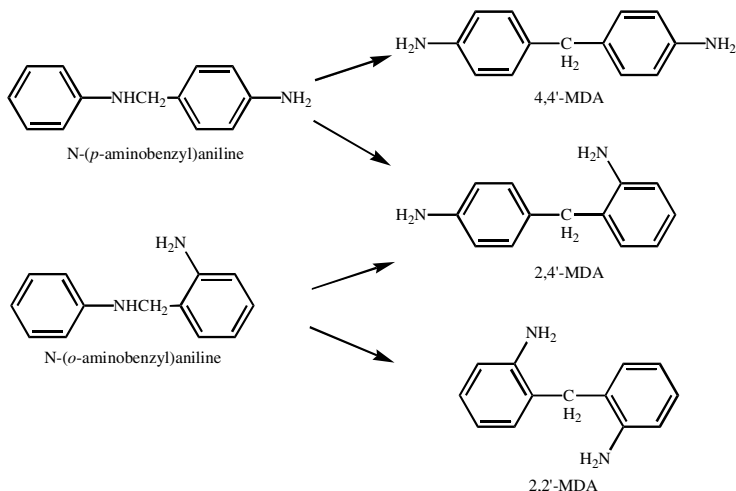
aromatic isocyanates account for more than 95% of isocyanate consumption for rigid polyurethane foams. Early developments were primarily based on toluene diisocyanate (TDI), but this changed during the 1960s when diphenylmethane diisocyanates (MDI) and their polymeric byproducts (pMDI) became available in commercial quantities. Since then, MDI and pMDI production has seen a very significant capacity growth. In 1984, the global use of MDI/pMDI overtook that of TDI and has outperformed the latter ever since.

7.2.1.2 Production

The production of MDI/pMDI is based on aniline and formaldehyde as the main raw materials. Aniline is produced from benzene. The preferred and lowest cost commercial production method is via nitration of benzene to nitrobenzene, using a mixed acid process ($\text{HNO}_3/\text{H}_2\text{SO}_4$)^{22,23} whereby aniline is produced from nitrobenzene via a reduction step.^{24,25} Methylenedianiline (MDA) and a mixture of its oligomers (pMDA) subsequently results from an acid-catalyzed condensation of aniline with formaldehyde:^{26,27}

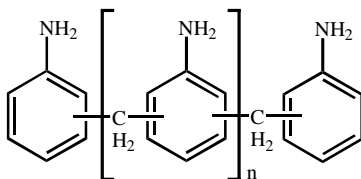


Three MDA isomers are predominantly produced in this reaction process: 4,4'-methylenedianiline (4,4'-MDA), 2,4'-methylenedianiline (2,4'-MDA), and 2,2'-methylene-dianiline (2,2'-MDA). The relative amounts of these products depend on the acid catalyst concentration, the aniline/formaldehyde ratio, and the process temperature ([Structure 7.1](#)):



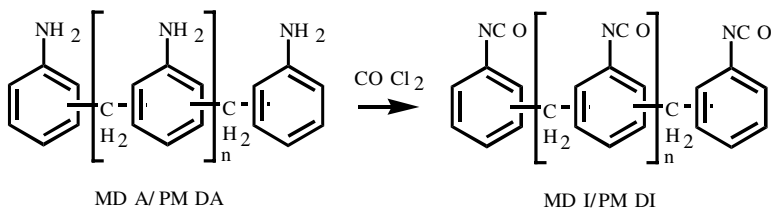
(Structure 7.1)

In addition to the MDA-isomers, the oligomeric mixture of pMDA is largely comprised of compounds with three ($n = 1$) to approximately six ($n = 4$) phenylamino functional groups (Structure 7.2). They are formed via further reactions of the MDA-isomers:



(Structure 7.2)

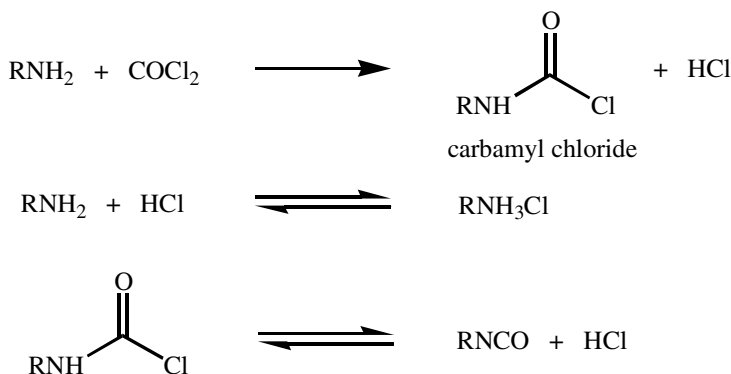
The MDA/pMDA mixture is subsequently phosgenated into the corresponding isocyanate mixture of MDI/pMDI in the presence of an inert solvent (Structure 7.3).



(Structure 7.3)

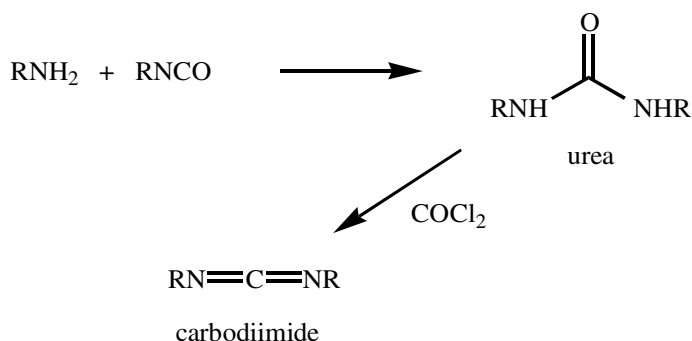
High efficiency initial mixing of the amine solution and the phosgene solution is important for obtaining a high quality, consistent MDI/pMDI product with high yields and low byproduct formation. Important parameters include:

ters are, apart from the relative concentrations of the reactants, reactor design, temperature, and pressure.²⁸⁻³¹ In the initial reaction stage carbamoyl chloride and amino hydrochloride are formed as an intermediate, which are subsequently thoroughly phosgenated in a second process step at high temperatures, yielding the isocyanate product (Structure 7.4):



(Structure 7.4)

Following the reaction of the polymeric amine mixture with phosgene, excess phosgene and acid are removed from the mixture and the solvent is distilled off. Undesired secondary reactions are initiated when amines react with isocyanates to form ureas, which can be dehydrated by phosgene to form carbodiimides (CDIs) (Structure 7.5):



(Structure 7.5)

In the pMDI-process other byproducts can be formed from CDI, such as uretonimine and imino-hexahydro-s-triazine compounds.³² The final MDI/pMDI mixture contains varying amounts of different functionality isocyanates. Monomeric MDI is typically present between 40 and 70% (w/w) in this mixture, with a split between 80 and 98% 4,4'-MDI and 2–20% 2,4'-MDI,

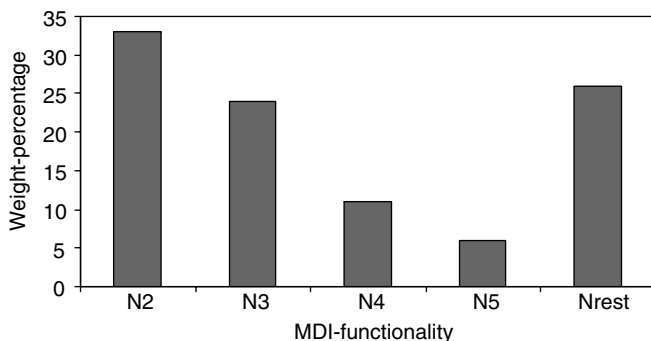


FIGURE 7.4

Typical distribution of MDI and its oligomers in polymeric MDI (pMDI).

sometimes also referred to as para-para and ortho-para MDI, respectively. Oligomeric MDI with more than two NCO groups per molecule is typically present at 30–60% of the total mixture.

In production, pure MDI is separated from the MDI/pMDI product mixture by means of distillation. The bottom product from this distillation is what is known as polymeric MDI (pMDI), which is the isocyanate of choice for the production of rigid polyurethane foam. It usually contains a mixture of pure MDI (N_2) and higher functional isocyanates (N_3 , N_4 , N_5 , N_{rest}), as shown by Figure 7.4. Dependent on market demand and plant capacity, pMDI is sometimes produced as a straight run product by changing the plant operating conditions.

7.2.1.3 Properties

Polymeric MDI products are usually characterized by their NCO content, acidity, and viscosity. The NCO content is defined as the NCO weight as a percentage of total weight and is indicated by %NCO. The molecular weight of a reactive NCO group being 42, the isocyanate equivalent weight (I.E.) is readily calculated from %NCO values via:

$$I.E. = 42 \times 100 / \%NCO$$

The number of NCO equivalents present in a weighed amount of pMDI follows in the usual way (by dividing the total weight through I.E.). Subsequently, the so-called isocyanate index for a given reaction with polyol(s) can be calculated via the equation

$$Index = \frac{Equiv.Isocyanate}{Equiv.Polyol}$$

where the number of equivalents of polyol component is defined by the polyol equivalent weight. The isocyanate index is very important in poly-

urethane chemistry as it quantifies the number of NCO groups available for reaction with polyol(s). Rigid polyurethane foaming is usually carried out at an index of 1.05–1.20 which implies an NCO excess of 5–20% on an equivalent basis. A notable exception is polyisocyanurate foaming which is carried out at index values from 2 to 5 in order to stimulate the trimerization reaction between NCO groups, as discussed in [Section 7.4.3](#).

7.2.1.4 Products

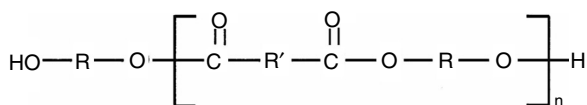
The acidity of pMDI is important for its effect on the reactivity, and hence processing performance, of rigid foam systems which are base catalyzed, and its processing performance. The viscosity of pMDI is linked to its average functionality and oligomeric distribution. As a rule, viscosity increases with decreasing MDI monomer (N_2) content; that is, the higher the viscosity, the higher the average number of NCO groups per molecule. The average number of isocyanate groups per molecule is called the “functionality” of a given pMDI. It ranges from 2.7 to 3.2 in current pMDI products, which corresponds to a viscosity range of 200 to 2000 cps at 25°C. Low viscosity pMDIs (200 cps at 25°C) are used as a standard throughout rigid polyurethane foam applications and in those cases where the flowability of the foam is a key parameter, such as, for instance, in the appliance industry. In the building industry, the preferred pMDI type has a viscosity of 550 to 700 cps at 25°C. High viscosity pMDIs are favored when mechanical strength or curing rate is an important processing parameter. This is typically the case for metal-faced sandwich panels at higher thicknesses, as discussed in [Section 7.3.2.2](#).

A special class of isocyanate products for rigid foams is formed by the modified isocyanates or so-called prepolymers. These are isocyanates which are partially prereacted with polyols. Although there are two types of these prepolymers, only the NCO-terminated polyols, created by the reaction of a polyol with an excess of isocyanate, are of some technical and commercial importance for rigid foams, most commonly in rigid block production to control the exotherm during the foam reaction. It also produces less friable foams and provides better adhesion to substrates. The prepolymer reaction is normally carried out in the absence of catalysts at relatively low temperatures (40–90°C) to prevent side reactions like dimerization, trimerization, or carbodiimide formation. These reactions may create additional heat as well as unwanted gelation and an uncontrolled pressure buildup. Prepolymer reactions are carried out under neutral or mildly acidic conditions to favor chain extension via the urethane reaction and to avoid unwanted gelation through branching.

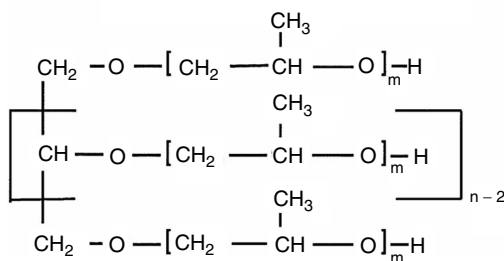
7.2.2 Polyols

7.2.2.1 Introduction

Isocyanates react with any molecular entity possessing active hydrogens, such as hydroxylic, carboxylic, and amine groups. For rigid foams, primary and



Typical polyester polyol



Typical polyether polyol

FIGURE 7.5

Structural formula of typical polyether and polyester polyols. (Reprinted with permission from Grünbauer, H.J.M., Rigid polyurethane foams, in *Polymeric Materials Encyclopedia*, vol. 10, ed. J.C. Salamone, CRC Press, Boca Raton, FL, 1996, 7504-7512.)

secondary hydroxyl group terminated polyether polyols are most important, followed by polyester polyols, which have the oldest application.¹⁻⁴ Both are represented by Figure 7.5, where polyether polyols are seen to provide by far the largest variety of possible molecular structures as far as hydroxyl functionality and molecular weight are concerned. This is expressed in Figure 7.5 by integers m and n , which represent the number of alkoxydes per branch and the number of branches of the polyol, respectively. The latter, usually termed the “functionality” of the polyol, can range from 2 to 8, depending on the original initiator molecule used for alkoxylation. In contrast to polyols for flexible foams, rigid foam polyols are relatively small in comparison to the original initiator molecule. This is due to the requirement of high stiffness of the foamed, rigid end product, which is achieved by means of crosslinking and urea precipitation, as detailed in Section 7.4.5. As a result, the molecular weight of the initiator is sometimes as high as 70% of the total polyol molecular weight. The character of the initiator is thus reflected in the performance of the polyol during rigid foam formation. This gives the polyol formulator the ability to tune polyol blends for desired product performance via selection of suitable polyols and their blends.

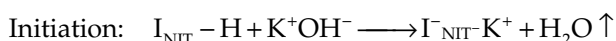
Polyester polyols for rigid foam applications are almost always of aromatic origin and can be characterized in terms of raw material origin. They are produced by condensation of phthalic anhydride, dimethylterephthalate (DMT) or polyethyleneterephthalate (PET) recycle streams with ethylene glycol, diethylene glycol, or triols and higher functional products like pentaerythritol. These moieties are represented in Figure 7.5 by R' and R , respectively. Polyester polyols enjoy a growing interest for rigid polyurethane foam producers due to their relatively low cost as well as the presence of aromatic

groups in their backbones, which gives enhanced flammability performance of the foam.

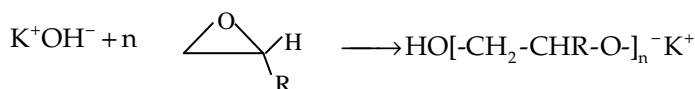
7.2.2.2 Production

Polyether polyols are manufactured by the addition polymerization of alkylene oxides. The main reaction for rigid polyols is the homopolymerization of propylene oxide and, to a lesser extent, the homopolymerization of ethylene oxide and the co- or block-polymerizations of both. Rigid polyols are anionic polymerized. The overall polymerization can be characterized with four typical steps: initiation, propagation, chain transfer, and termination. Catalyst concentration, temperature, and type of alkoxide used determine the reaction rate.

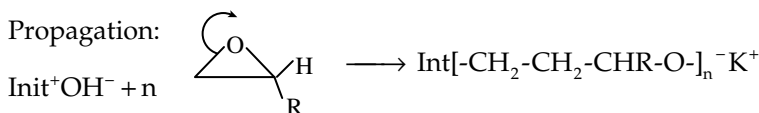
The initiation step is shown below:



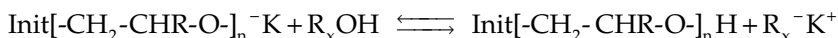
An initiator (e.g., glycerine or sugar) is loaded in the reactor with KOH. Vacuum is applied to force the equilibrium to alkanolate formation. A nucleophile can also be formed from direct reaction of the base with a monomer to form an alkoxide ion:



Diols are initiated with this reaction; a KOH solution is heated and the alkoxides are fed to the reactor. Propagation and chain transfer immediately follow initiation. After the water has been (sometimes partly) removed the monomer is added and propagation and chain transfer will take place at a temperature of 100–120°C.



Chain transfer:

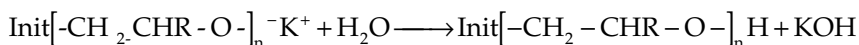


Only a few hydroxyl groups are alkanolated and therefore active to grow. A narrow molecular weight distribution can be obtained for two reasons: the chain transfer reaction and the dependence on the molecular weight of the reaction rate of the growing alkoxide chains. In other words, lower equivalent weight chains grow faster, and hence, narrower distributions are obtained. Because ethylene oxide reacts more quickly than propylene oxide, the copolymer chains will be predominantly terminated by secondary

hydroxyls. If termination by primary hydroxyl is desired, ethylene oxide is loaded to the reactor after complete reaction of propylene oxide.

The reaction is finished or terminated by adding water:

Termination:



After the termination reaction the polyol must be neutralized. Rigid polyols are mostly neutralized with acids; the residual salts are filtered out or left in the polyol. These residual salts (like K-acetate) will catalyze the polyurethane reaction if they are left in the polyol; see [Section 7.2.4.1](#).

7.2.2.3 Properties

Polyol structure is usually quantified in terms of equivalent weight, functionality, chain structure, and primary or secondary hydroxyl end groups. The hydroxyl equivalent weight HEW of a polyol is given by:

$$\text{HEW} = M_{\text{polyol}} / \text{functionality}$$

where *functionality* represents the number of reactive groups per molecule available for alkoxylation of the original initiator. Assuming all available groups have reacted, the functionality corresponds to the nominal number of branches or arms of the final polyol.

In those cases where a mixture of initiators is used, the average functionality is calculated from the molar fractions of each initiator:

$$\overline{\text{functionality}} = \sum_{i=1}^i \left[\left(\frac{\text{moles}_i}{\text{moles}} \right) \cdot \text{functionality}_i \right]$$

The alkoxyde chain structure of the polyol may be varied in a number of different ways, by selecting different alkylene oxides, mostly ethylene oxide (EO) and propylene oxide (PO), or by using homopolymers or block or random copolymers. The structure of the end group is of special importance for the intrinsic reactivity of the polyol. Polyols terminated with primary hydroxyl groups containing ethylene oxide are more reactive with isocyanate than their propylene oxide counterparts which predominantly contain secondary hydroxyl groups. To quantify the number of reactive groups, the hydroxyl number OH_{no} is frequently used. It is defined as the concentration of isocyanate reactive hydroxyl groups per unit weight of polyol, expressed in mg KOH/g.

$$\text{OH}_{\text{no}} = \left(\frac{56.1 * \text{functionality}}{M_{\text{polyol}}} \right) * 1000$$

www.iran-mavad.com

It follows that:

$$HEW = \left(56.1 / OH_{no} \right) * 1000$$

which can be readily used to calculate the total number of equivalents available for reaction with pMDI in a given amount of polyol. The calculation of the isocyanate index from this number and the number of pMDI equivalents is explained in [Section 7.2.1.3](#).

7.2.2.4 Products

Except for high index isocyanurate foams, high functionality sucrose or sorbitol initiated polyols are at the basis of every rigid polyurethane foam. A typical polyol formulation comprises 40–60% of this polyol type, while the remaining additives and polyols are selected to balance the processing needs for the specific application at hand. In the last 10 years, there has been a notable shift toward sorbitol initiated polyol, especially in Europe, where these polyols are widely used. Perceived advantages of sorbitol initiated polyols include improved compatibility with hydrocarbon blowing agents, enhanced flammability performance, higher foam strength, and faster strength build up during the first 10 min after reaction (green strength). As a result, demold times are reduced and thicker panels, up to 20 cm, can be produced on a double band laminator.

A wide variety of polyol components are used to tune processing and performance parameters, such as flowability, demold, adhesion, reaction profiles, and so on. An incomplete listing includes 50 to 100 equivalent weight EO diols as chain extenders and metal adhesion promoters, 500 to 750 equivalent weight PO diols and triols as hydrocarbon compatibilizers, plastic adhesion promoters, viscosity cutters and flow enhancers, and so on. In practice, the improvements always need to be balanced against deteriorated foam strengths, increased demold times, and flammability performance. A special class of polyols in this context is quatrols or 4-functional polyols based on amine initiators such as ethylene diamine and toluene diamine. The amine group gives these polyols a self-catalytic character for reaction with isocyanate. Apart from the advantage of reduced catalyst levels, these polyols are further beneficial in that they yield foams with shorter demold times and increased foam strength versus triol-based counterparts.

Polyester polyols are an important raw material for the production of polyisocyanurate (PIR) insulation panels, especially in North America. These foams derive their excellent flammability performance from the high content of aromatic groups which results from isocyanurate formation in combination with high aromaticity polyester polyols. In other regions, polyester polyols are seeing increased application for the same reason as well as for their relatively low cost. The latter is ultimately connected to the origin of aromatic polyester polyols which are produced from recycled PET bottles, fibers, and x-ray film sheets, or DMT process waste.

7.2.3 Blowing Agents

For almost 30 years, chlorofluorocarbon CFC-11 was the blowing agent of choice for the rigid polyurethane foam industry, due to its high molecular weight, in combination with low toxicity, optimum boiling point (23.8°C), and very low gas K-factor of 7.8 mW/mK. As a result, CFC-11 can be considered the best blowing agent ever used for thermal insulation foam applications: rigid polyurethane foams containing high amounts of CFC-11 could reach K-factors as low as 15-17 mW/mK.¹⁻⁴ This performance level is simply unattainable with current alternatives that have been developed in response to the global issues of ozone depletion and global warming¹¹⁻¹³ raised during the last two decades of the 20th century. The phase-out of CFCs was completed in the developed countries by the first of January 1996,¹³ although several countries voluntarily completed the phase-out much earlier.

New blowing agent technology required identification or development of compounds with low gaseous thermal conductivity. They had ideally to be cheap and also had to show many other characteristics in order to fit within rigid polyurethane foam applications. Characteristics vary widely and include qualities such as being non-toxic, being environmentally acceptable, having zero ozone depletion potential (ODP), having low global warming potential (GWP), being chemically inert, preferably having good solubility in the polyol and isocyanate components, having a usable boiling point (ideally in the range of -10 to 50°C), having a low diffusion coefficient in the PU foam matrix, and of course being readily available in commercial quantities.

Not surprisingly, none of the current alternatives can fully satisfy these requirements. Nevertheless, hydrocarbons, HCFC, and HFC replacements are currently employed by industry. Major European manufacturers have almost completely converted to hydrocarbons while adapting conventional foaming plants to guarantee safety and compliance with environmental regulations. North American manufacturers have chosen HFCs as a replacement for short-term alternative HCFC-141b, which was phased out on January 1, 2003. Both HFC-245fa and HFC-134a blowing agents are considered due to their relatively good insulation performance and low flammability. Both blowing agents are properly handled by utilizing a premix station to assure a constant mixing ratio between polyol and the blowing agent. Other regions follow the Montreal Protocol implementation plan.¹³ Based on local regulations, all blowing agents are still in use. Cyclopentane has been chosen as the main blowing agent by the major original equipment manufacturers (OEMs) in Japan and Latin America, while HCFC-141b is still widely used in India as well as in the other Pacific countries. The aid of international funds such as the United Nations Industrial Organization (UNIDO) has driven the major African and Middle Eastern OEMs to adopt cyclopentane as the preferred blowing agent.

An overview of the different blowing agents and their critical properties and environmentally relevant properties is listed in [Table 7.1](#).

TABLE 7.1

Overview of New Blowing Agents and Their Physical Properties

Compound	Molecular Formula	Molecular Weight (g/mol)	λ_{gas} @25°C mW/mK	Boiling Point (°C)	Vapor Pressure 20°C (bars)	Flammability Limits (% vol. in air)	Indicative Price \$/lb	ODP	GWP 100 yr ITH	HGWP	POCP or SFP	Atmosph. lifetime (yrs)	Phase-out target
CFC-11	C-Cl ₃ F	137.5	7.8	24	0.88	none	n.a.	1.0	4000	1.0	<0.1	50–60	1995
HCFC-141b	CH ₃ C-Cl ₂ F	116.9	9.8	32	0.69	5.6–17.6	~0.9–1.0	0.11	630	0.12	10	8–10	2003
HCFC-22	CHClF ₂	86.5	11.2	-41	8.92	none	~1.0	0.05	1700	0.35	6	13–15	2010
HCFC-142b	CH ₃ C-ClF ₂	100.5	9.8	-10	2.50	6.7–14.9	~1.0	0.06	2000	0.36	5	19–20	2010
HCFC-124	CHClFCF ₃	136.5	12.3	-11	3.27	none	~2.0	0.02	480	0.10	12	5–6	2020
HFC-125	CHF ₂ CF ₃	120	14.0	-48	12.41	none	~2.5–3.0	0	2800	0.58	1	32–35	none
HFC-134	CHF ₂ CHF ₂	102	14.1	-23	4.53	none	~1.8–2.0	0	1000	0.20	8	10–12	none
HFC-134a	CH ₂ FCF ₃	102	14.3	-26	5.62	none	~1.5–1.8	0	1300	0.26	6	14–16	none
HFC-152a	CH ₃ CHF ₂	66	13.8	-25	5.06	3.9–16.9	~2.0–2.5	0	140	0.03	14	1.5–2	none
HFC-245 fa	CHF ₂ CH ₂ CF ₃	134	12.2	15	1.24	8.9–11.2	~3.0–4.0	0	820	0.18	11	7–10	none
HFC-365 mfc	CH ₃ CF ₂ CH ₂ CF ₃	148	10.6	40	0.47	3.5–9.0	~3.0–4.0	0	840	0.18	7	9–12	none
n-Pentane	C ₅ H ₁₂	72	14.6	36	0.65	1.4–8.3	~0.25	0	11	0.002	500	0.03	none
Iso-Pentane	C ₅ H ₁₂	72	13.8	28	0.80	1.4–7.6	~0.25	0	11	0.002	500	0.03	none
Cyclo-Pentane	C ₅ H ₁₀	70	12.6	50	0.34	1.4–7.8	~0.75	0	11	0.002	400	0.05	none
Iso-Butane	C ₄ H ₁₀	58	15.9	-12	2.99	1.8–8.4	~0.3	0	5	0.001	650	0.02	none
n-Butane	C ₄ H ₁₀	58	15.3	-1	2.08	1.6–8.4	~0.3	0	5	0.001	650	0.02	none
Carbon dioxide	CO ₂	44	16.3	-78	56.55	none	n.a.	0	1.0	1.10-4	0	120–200	none
Air	N ₂ /O ₂	28.8	26.5	-193	624.03	none	n.a.	0	0	0	0		none

ODP = Ozone Depletion Potential

GWP = Global Warming Potential

ITH = Infinite Time Horizon

HGWP = Halocarbon Global Warming Potential (R-11 = 1.0)

POCP = Photochemical Ozone Creation Potential (methane = 1)

SFP = Smog Formation Potential (methane = 1)

7.2.4 Additives

7.2.4.1 Catalysts

Polyurethane foaming is a highly complex event which requires delicate balancing of several simultaneously occurring processes, such as foam expansion, network kinetics, and phase segregation. Several types of catalysts are known to influence these processes.^{1-3,33} To clarify the action of various catalysts and to facilitate catalyst selection for practical purposes, the reactions described in Section 7.4.3 are usually distinguished:¹⁻³

- The blowing reaction of pMDI with H₂O to form CO₂ and polyurea
- The gelling reaction of pMDI with polyol to form polyurethane
- The trimerization of pMDI (as well as related reactions, such as carbodiimide and dimer formation)

In preparing formulations for specific processing and application needs, catalysts are thought to balance these reactions, albeit synergistic effects of certain catalyst combinations are known as well. The distinction is nevertheless of some practical use as it provides guidance to the selection of possible combinations for trial and error experiments. This system is therefore used to summarize today's most important catalysts in Table 7.2.

TABLE 7.2

Overview of Frequently Used Catalysts in Rigid Polyurethane Foams

Catalyst Type	Code	Perceived Action
Tertiary amines		
Niax A1	PMDETA	blowing
pentamethyl diethylene triamine		blowing
triethylene diamine	TEDA	gelling
dimethyl cyclohexyl amine	DMCHA	blowing/gelling
triethyl amine	TEA	curing
Quaternary ammonium salts		
2-hydroxy propyl trimethyl ammonium (2-ethylhexoate)	TMR	gelling/curing/trimer formation
2-hydroxy propyl trimethyl ammonium (formiate)	TMR-2	delayed action/trimer formation
Alkali metal carboxylates		
Potassium acetate	K Ac	gelling/trimer formation
Potassium octoate	K Oct	gelling/trimer formation
Sodium N-2-hydroxy, 5-nonylphenol methyl N methyl glicinate	Curithane 52	gelling/trimer formation
Tin complexes		
Stannous octoate	Sn Oct	gelling
Dibutyl tin dilaurate	DBTDL	gelling

Catalysts for rigid polyurethane foam include a range of chemical structures, such as tertiary amines, aromatic amines, quaternary ammonium salts, alkali metal carboxylates, and organo-tin compounds. For the greater part, their catalytic activity is dependent on their basicity, with steric hindrance on the active site playing a secondary role. The activity of tertiary amines is, for example, decreased in the presence of residual acidic compounds in the polyol formulation. This phenomenon is successfully exploited with so-called “delayed action” catalysts which are active only after acid-blocked amine catalyst decomposes during foaming to give active amine. Applied as formic acid salts, these catalysts are active only after decomposition of the formate at some higher temperature. Quaternary ammonium salts are widely used because of their strong gelling and trimerization action, while maintaining a relatively smooth foam rise profile. Alkali metal carboxylates are very active curing and trimerization catalysts. Higher molecular weight carboxylates are giving smoother rise rate profiles but have to be dosed at higher amounts for a given catalytic effect.

Tin complexes are the most powerful gelling catalysts known today. They are not often used in rigid foams, albeit that small quantities are sometimes used to boost gelation. Stannous octoate is hydrolytically unstable, preventing its use in aqueous formulations.

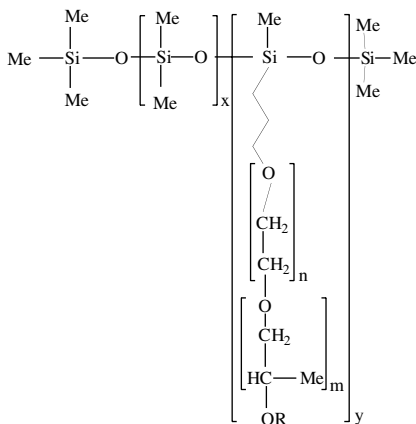
7.2.4.2 Surfactants

The presence of surfactants serves a twofold purpose in polyurethane foaming. First of all, they stabilize the foam immediately after mixing polyol and isocyanate by lowering the surface tension of the emerging gas-liquid interface³⁴ and presumably also by emulsifying the polyol-isocyanate interface. Mechanistically, this effect arises from a preferred accumulation of surfactant molecules at interfaces. A second, equally important role of surfactants is to stabilize the polymerizing liquid-gas interface during the roughly 30- to 50-fold volume increase of a rising foam.³⁵ Here, the mechanism is rather dynamic: the expanding foam continuously creates new surface area of high tension that needs to be stabilized by fast migration of surfactant towards the interface (the Marangoni effect).

The surfactants most commonly used in the polyurethane industry are polydimethyl siloxane-polyether copolymers.³⁶ Since the late 1950s, these so-called “silicone surfactants” almost completely replaced other organic, non-ionic surfactants which were used before.^{37,38} This is largely due to their ability to lower surface tensions to approximately 20 dyne/cm, compared to only 30 dyne/cm for common organic surfactants.³⁹ Today, the largest commercial application of polysiloxane surfactants is their use as additives for the production of polyurethane foam, with a worldwide volume of about 40,000 MT/Y versus a global pMDI capacity of over 3,000,000 MT/Y.

The surface-active character of siloxane surfactants results from high-molecular weight methyl-rich segments,^{40–44} attached to a flexible –O–Si–O–Si– backbone, in combination with polyether chains that are grafted to the same

backbone, either via Si—O—C or Si—C bonds. The latter type is hydrolytically stable⁴⁵ and predominant in polyurethane foam applications. They can be represented as $\text{Me}_3\text{SiO}(\text{Me}_2\text{SiO})_x(\text{RMeSiO})_y\text{SiMe}_3$ where Me represents a methyl group (Structure 7.6) :



(Structure 7.6)

Silicone surfactants are typically added in amounts of 0.4–2.0% w/w of the polyol formulation. To meet specific processing needs of different foam systems, the molecular structure may be tuned by varying the length and the composition of the polydimethylsiloxane backbone or the number, length, and composition of the pendant polyether chains.⁴⁶ Surfactants for rigid foam typically contain 10 to 50 Si-units per molecule while the average molecular weight of a polyether chain ranges from 400 to 1500 g/mol. The ethylene oxide content typically varies from about 50 to 100% and the polysiloxane/polyether ratio lies in the range of 3/1 to 10/1. The total molecular weight of the surfactant amounts to 1500 to 15000 g/mol. In general, surface activity in rigid polyol formulations increases with increasing polysiloxane molecular weight. Increasing the polyether molecular weight has a reducing effect on surface activity but is improving solubility. As a result, emulsification and thereby cell stabilization can be improved. High propylene oxide content tends to increase solubility in isocyanates, whereas high ethylene oxide content tends to increase solubility in polyols, but simultaneously reduce surface activity and flow properties.

7.3 Applications and Markets

Rigid polyurethane foams are employed in a rich variety of industrial products and processes. Among these are various buoyancy applications, such as surfboards and bouys for navigation, and energy absorbing applications,

for example, in shock and explosive blast wave dissipation and as industrial filters and carrier materials for biomedical research purposes. From an industrial point of view, however, none of these applications is nearly as important as their main use in thermal insulation materials. This is the reason why the present section is limited to the use of rigid polyurethane foam in the global appliance and construction market.

7.3.1 Appliance

7.3.1.1 Introduction

The construction of modern domestic refrigerators and freezers would not be possible without the use of polyurethane foam technology.^{14,15} While its high insulation efficiency ensures minimal wall thickness, polyurethane appliance foams allow the use of very little plastic and steel, the structural strength being instead guaranteed by the strength of the foam and its rigidity. The foam also acts as the structural adhesive to bond the inner and outer liners of the refrigerator during the foaming process, and allows ease of application and manufacture. In physical terms, the foam itself is typically characterized by a closed cell content of 95% or higher, low density (30 to 40 kg/m³), and high compressive strength (ca. 150–200 kPa). It is manufactured by pouring, just after mixing, a mixture of polyol and isocyanate into a mold, in most cases between a plastic inner liner material, generally made of high-impact polystyrene (HIPS) or acrylonitrile butadiene styrene copolymer (ABS) and a metal sheet, which will be the external part of the appliance. The location of the foam in the final product is shown in Figure 7.6. A typical mold is shown in Figure 7.7.

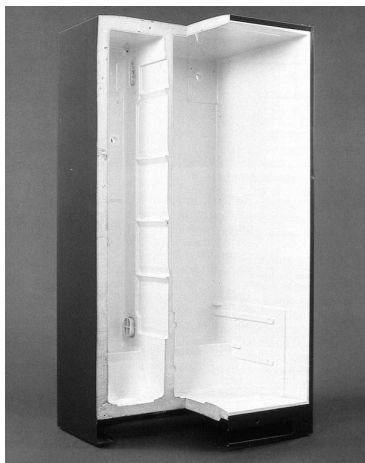


FIGURE 7.6

Appliance foam example, showing a rigid polyurethane foam component inside a refrigerator.

www.iran-mavad.com



FIGURE 7.7

Appliance foam example, showing a refrigerator mold with a refrigerator in the “breakers up” position. (Reprinted with permission from Cannon.)

The formulated polyol often consists of a blend of high functionality sucrose or sorbitol initiated polyols and lower functionality polyols such as glycerine and/or amine initiated polyols. The high functionality polyols in the system are chosen to give the foam its high strength and rigidity, and the low functionality polyols to reduce the viscosity, improve the compatibility of the polyol formulation, and enhance flow characteristics. Other possible types of polyols, such as polyester polyols, or polyaromatic polyamine (PAPA) or toluene diamine (TDA) initiated polyols, may have a positive influence on the thermal conductivity of the foam. Polymeric MDI (pMDI) is commonly used on the isocyanate side. Blowing agent packages have recently shifted from CFC-11 to hydrocarbons, HCFCs, and HFCs. This ongoing development will be described in detail due to its impact on modern appliance technology.

7.3.1.2 Processing

Today's industry standard for appliance manufacturing is a high pressure foaming machine, typically equipped with an L-shaped impingement mix head as described in [Section 7.4.1](#) and depicted by [Figure 7.11](#). The “L” in the mix head design denotes the 90° angle that the foam transverses after mixing, as it exits the mix head. This “L” shape is used to decelerate the liquid mixture prior to its departure from the mix head, decreasing the amount of cell destruction or coagulation prior to the gelling reaction taking place. As discussed in [Section 7.5.1.1](#), small cells are a key ingredient in creating a foam which performs well from a thermal conductivity standpoint.¹⁶ Processing

www.iran-mavad.com

parameters vary by application but normally run between 70 and 170 bar, 15–25°C and 20–90 kg/min. These parameters are varied based on the blowing agent used, the type or size of appliance being filled, and the optimal flow pattern based on the internal dimensions of the appliance.

Foaming operations for refrigerator cabinets and doors consist of both stationary and carousel fixture lines. These fixtures must support the external and internal liners against the pressure generated by the foam flowing into the cavity to fill. The methodology used for cabinet injection depends on the position of the refrigerator during foaming. The “breakers up” position shown by [Figure 7.7](#), with the door opening face on top, is the most commonly used position. This method is considered the most advantageous because the reacting foam can distribute itself more uniformly in the back part of the cabinet, then rise and flow to fill the lateral walls. For this flow position, the flow paths are relatively short. In addition, the foam reaches the farthest areas when its viscosity is rapidly rising, thereby limiting leakage. The “breakers up” foaming technology is typically the foaming position of choice for the industry when building a new plant. The “breakers down” position, with the door opening face on bottom, is sometimes chosen when the mold construction is simpler. In this case, it is extremely important that a proper cabinet seal is achieved to avoid foam leakage.

In the cabinet manufacturing process, the cabinet is quickly pre-assembled, coupling the external metal sheets with a plastic inner liner made of thermoformed HIPS or ABS. The inner and outer materials are then placed into a fixture (or jig) coupled with a mold plug. Once properly set, the cavity between the metal and plastic liners is injected with the proper amount of polyurethane foam. During foaming, the position and number of the injection holes depends on the foaming technology (breakers up or down) as well as the foam reactivity.

Demolding times depend on many factors, such as type of blowing agent employed, foam over-pack, wall thickness, and mold temperature. Demold times as fast as 3–5 min can be obtained with a standard refrigerator’s wall thickness (27–50 mm), while longer demold times are needed when the wall thickness increases. After demolding, the cabinet will continue along the manufacturing assembly line. During this assembly process, the door (previously foamed with a similar process), the compressor unit, and the other elements (condenser, handles, sometimes the top cover) of the refrigerator will be added to the cabinet.

Two types of refrigerator foaming line layouts are currently employed for both breakers up and breakers down technology: carousel lines and stationary jigs lines. Carousel lines comprise a large number of molds in a continuously moving line. The line is composed of a conveyor chain to transport the molds and several stations where the cabinet is first inserted, heated up before foaming, foamed, and finally demolded. Line productivity is dependent on the number of molds. This number is determined by the demolding time and the number of different models produced on the line. Insertion and removal of molds are therefore quite important limiting factors.



FIGURE 7.8

Typical production line for appliances with stationary jigs. (Reprinted with permission from Cannon.)

Stationary jigs lines allow superior productivity if a fast demold foam system is employed. The line is composed of (1) a supply line from the assembling area, (2) a preheating station where the cabinet is heated up to facilitate foam flow, (3) stationary jigs where the cabinets are foamed and kept until curing time is completed, and (4) an exit transport system to bring the cabinet to the final assembling and control stations. In this case, each mold can be equipped with its own mixing head or a single mix head system can move, injecting multiple stationary fixtures. An example is given in Figure 7.8. Compared to the carousel line layout, one of the advantages is that the lighter cabinets are transported instead of the heavier molds, and the line is easily automated, providing the maximum production flexibility. A judicious combination of the mold and the cabinet design can eliminate the bottlenecking of demolding time: each jig demold time can be appropriately set so the longest necessary demold time for thick wall cabinets would not affect the full line speed. Moreover, the availability of two to four plugs already mounted on the fixture system would practically eliminate the time wasted for model change and practically reduce the need for part storage, providing obvious logistical advantages.

Doors can be foamed as an open pour or closed pour process. Both multiple presses and a rotational mold system are currently used in the industry routinely. In either case, the foaming principles are not different from those discussed for the cabinet, though they are often an easier application. Open lid foaming does guarantee an optimum foam distribution due to the ability to adjust the pour pattern of the mix head over the cross section of the door. However, closed pour doors often allow a more complete fill of the dikes and ridges in a door.

7.3.1.3 *New Blowing Agents*

In response to global environmental issues^{11–13} raised during the last two decades of the 20th century, the appliance industry has gone through a considerable effort to replace CFC-11, the traditional blowing agent of choice, by non-ozone-depleting (ODP) blowing agents that, preferably, exhibit low global warming potentials (GWP) as well. At this moment, several replacements are used in commercial plants which deserve special attention due to their current and future (potential) impact on foaming practice in appliances.

7.3.1.4 *Hydrochlorofluorocarbons*

HCFC-141b is no longer used in Western Europe and North America but remains an interim alternative in Latin America, in Eastern Europe, and in the Pacific regions for those manufacturers who have decided not to convert to hydrocarbon blown foams. HCFC-141b has a residual ozone depleting potential (ODP = 0.11; see [Table 7.1](#)), but its low gas K-factor combined with the fact that only minor machine/line modifications were required for its implementation made it a preferred candidate for a certain number of OEMs. Nevertheless, additional cost had to be considered due to the solvent effect of HCFC-141b on thermoplastic liners (ABS or HIPS) which necessitates the use of a protective layer on the inner liner or a modified liner polymer.

Hydrofluorocarbons HFC-245fa, now commercially available, and HFC-134a are the chosen solutions for the medium and longer term in the U.S. and possibly in the Asia-Pacific region, although many signs are observed that hydrocarbons may end up being preferred in this region as well. HFC-245fa has a boiling point of 15°C and new systems blown with this material have insulation properties comparable to HCFC-141b. Work to date has shown about a 2% energy reduction for the switch from HCFC-141b to HFC-245fa. Another alternative in use by some appliance manufacturers is HFC-134a.¹⁷ The primary concern with the HFC-134a is that it provides a higher K-factor at ambient than the other candidates, albeit the difference with HCFC-141b and HFC-245fa diminishes at actual service temperatures because of the absence of condensation effects, as discussed in [Section 7.5.1.2](#). For the same reason, dimensional stability is improved under these conditions; see [Section 7.5.1.2](#). On the other hand, processing and handling of polyol formulation is challenged due to the low boiling point of –26°C.

7.3.1.5 *Hydrocarbons*

The first hydrocarbon systems, launched in 1993, were blown with cyclopentane. Compared to CFC-11 blown foams, their K-factor and density were significantly higher. Since that time, continuous improvement of the hydrocarbon formulations has led to the development of systems with thermal insulation performance similar to 50% reduced CFC-11 systems. More recent developments aimed to rectify the low vapor pressure of cyclopentane, which may cause unwanted condensation at lower temperatures with negative impact on the dimensional stability of cyclopentane blown foams, are discussed in [Section 7.5.1.2](#).

www.iran-mavad.com

Long-term successful experiences in the appliance industry with low boiling blowing agents (LBBA) such as HCFC22/142b and HFC-134a provided the direction for a solution of this problem. This class of blowing agents is loosely defined as having a normal boiling point below ambient (and frequently even below 0°C). Based on their boiling characteristics and processing conditions, the low boiling hydrocarbons appeared to be ideal candidates for use in combination with cyclopentane. The higher vapor pressure was expected to produce foams with superior cell gas pressure, and hence, better foam mechanical strength and dimensional stability. For isomeric butanes, the inferior gas K-factor performance given by Table 7.1, as well as their more critical solubility characteristic,¹⁸ are however limiting their maximum concentration. A judicious combination of these two hydrocarbons does nevertheless yield optimum properties for rigid appliance foam. An additional benefit of cyclopentane/butane blown systems is their excellent flowability. This feature allows the use of 8–10% lower densities versus the latest generation of cyclopentane, while maintaining compressive strength values above the accepted limit to guarantee foam dimensional stability.

The application of cyclopentane/isopentane blends forms an intermediate solution between cyclopentane and cyclopentane/butane technologies. It consists of exploiting the low vapor pressure of iso-pentane to increase the cell pressure and therefore improve the dimensional stability, subsequently allowing a reduction of foam density and weight. This technique can be applied most advantageously when the existing production unit does not allow the use of low boiling hydrocarbon. Machine modifications are not needed and existing polyol/hydrocarbon premixing units can still be utilized. The amount of isopentane used with cyclopentane cannot exceed a certain level to avoid degradation of the insulation properties; see Table 7.1. To be attractive, isopentane levels should, however, be high enough to obtain a sufficient increase of vapor pressure in the cells to allow reduction of the foam weight. In practice, a good compromise has been found with a blend consisting of 8–9 php of cyclopentane and 3–4 php of isopentane.

7.3.1.6 Vacuum Insulation Panels (VIPs)

The technological concept of VIPs is the use of the excellent insulation properties of high vacuum. Panels 15–25 mm thick made of a covering plastic foil containing a filling material (silica, polyurethane, etc.) are evacuated in order to achieve pressures of ca. 0.1–1 mbar. These panels typically have a K-factor of 6–10 mW/mK. They are glued inside the cabinets and doors (on the plastic or on the metal liner). Polyurethane foam is then poured the same way as for conventional foaming. With VIPs the overall K-factor can be reduced down to the level of 100% CFC-11 foams. VIPs are used by several OEMs. Their cost is very high, i.e., 30–35 €/m² or ca. 50–75 € for a refrigerator with 60% VIP coverage. This implies a doubling of the cost contribution for insulation. On the other hand, VIPs allow for energy consumption reductions as high as 20%, provided their reliability over the lifetime of a refrigerator is guaranteed.

7.3.1.7 Markets

The production of cold domestic appliances reached ca. 80 million units in 2002, requiring more than 500,000 MT of polyurethane foam as filling and insulation material. In appliances, the cost to produce a cabinet varies between 100 and 250 € as a function of the size and degree of sophistication (this number is for the most common models; top end models can be two to three times more costly). The cost of polyurethane foam raw materials for the filling of a cabinet is ca. 3–7% of total cost. However, the role of the foam is essential not only as insulation material but also to insure the structural integrity of the refrigerator.

7.3.2 Construction

7.3.2.1 Introduction

Rigid polyurethane foam is widely applied for thermal insulation purposes in the building and construction industry where it is available as foam board, sandwich panels, sprays, aerosol cans, and shaped and molded foams.^{1,3,9,10} For their manufacture, polyisocyanurate (PIR) technology is frequently applied, in addition to polyurethane types of technology, similar to those described in Section 7.3.1 for appliance foams. PIR technology is particularly significant in North America where it dominates the construction foams market. It is characterized by the use of an excess polymeric MDI (pMDI), with an isocyanate index ranging from 2 to 5, usually in combination with a polyester polyol as described in Section 7.2.2. Together with suitable catalysts, high isocyanate indices facilitate the formation of isocyanate trimers, as described in Section 7.4.3, from which PIR foams derive their excellent flammability characteristics.

Both PIR and polyurethane construction foams are characterized by their excellent thermal conductivity with K-factors between 20 and 30 mW/mK, low densities ranging from 30 to 100 kg/m³ at high mechanical strengths of 100–1000 kPa. They are used over a temperature range from –80 to +100°C and are especially efficient when one or more of these strengths are combined with their adhesive bonding, easy mold-filling, and flexible processing capabilities. The very low thermal conductivity enables application of thinner panels when space filling is an issue. Adhesive bonding in combination with high strength is exploited successfully in steel-faced sandwich panels. These panels derive their excellent mechanical strength at low weight from a unique, foam-based composite structure which explains why the steel sandwich market is dominated by the use of polyurethane foam as insulation material.¹⁹ Mold filling latitude is utilized when foaming articles with a complex shape, such as liquid natural gas (LNG) tank housings, by means of “pour in place” techniques or spray foams. On-site insulation of cavities around doors, windows, and beams using commercially available one-component spray cans is another well-known example of the processing flexibility of rigid polyurethane foams. Spray foams combine thermal insulation, filling, mechanical strength, and adhesion in a very cost-effective way.

Construction foams are manufactured by high efficiency mixing of pMDI with formulated polyol blends containing catalysts, surfactants, and, optionally, flame retardants, as defined by processing and application requirements. Polyols usually contain relatively high amounts of reactive functional groups per molecule (functionality) and relative short molecular chains (chain-length) compared to polyols in flexible foams in order to achieve the desired high crosslink density, which is key to end-product performance. Examples of frequently used polyols are described in [Section 7.2.2](#) and comprise sorbitol, glycerine, and sucrose/glycerine co-initiated polyols, blended with polyester polyols and polyether polyols based on initiators containing aromatic groups. Reactivity is tuned for a particular manufacturing process by varying the catalyst package which usually contains amines to balance foam rise and gelation reactions. Salt complexes are important toward the end of the foaming process as they have the ability to accelerate curing, particularly via trimer formation; see [Section 7.2.4.1](#). Together with CO₂ from the H₂O-isocyanate reaction, pentane isomers and HCFC-141b are blowing agents of choice for construction foams, albeit the latter is being phased out.¹³ Occasionally, HFCs as described in [Section 7.2.3](#) are used as well, especially in North America, when very low thermal conductivity and severe flammability requirements must be satisfied.

Flame retardants are important additives for building and construction applications.²⁰ Their role is to reduce heat and smoke emission by slowing down polymer combustion and degradation with the aim to increase escape time in case of fire. Flame retardants can be divided in reactive and non-reactive components. Commonly used non-reactive flame retardants include, in decreasing order of importance, organophosphorous compounds, with or without halogen substitution; melamine; and alumina trihydrate. Bromine and phosphorous containing polyols are the main representatives of reactive flame retardants. Flame retardancy is further enhanced by the use of polyester and aromatic polyether polyols. Together with polyisocyanurate trimer formation at high pMDI indices, these polyols contribute to good flammability test performance by virtue of their higher thermal stability.

7.3.2.2 Continuous Production

Foam panels of up to 20 cm thickness are commonly produced by means of a continuous production unit which is known as a double band laminator (DBL). Depending on the type of facer on the panel, a further distinction can be made into flexible-faced (DBL-FF) and rigid-faced (DBL-RF) foam panels. A typical layout of a DBL-FF unit is given by [Figure 7.9](#). This process consists of a multi-component dosing unit; a high-pressure impingement mixing head; a laydown section where, immediately after mixing, the foaming mass is evenly distributed over the full width of the band; and a heated conveyor to transport and cure the foaming mass followed by a panel cutting unit where the panels are cut at the desired length. Before cooling down, insulation boards are typically stacked to finalize the curing (bundle cure). This technique is often applied in North America where insulation boards are

DOUBLE BAND LAMINATOR

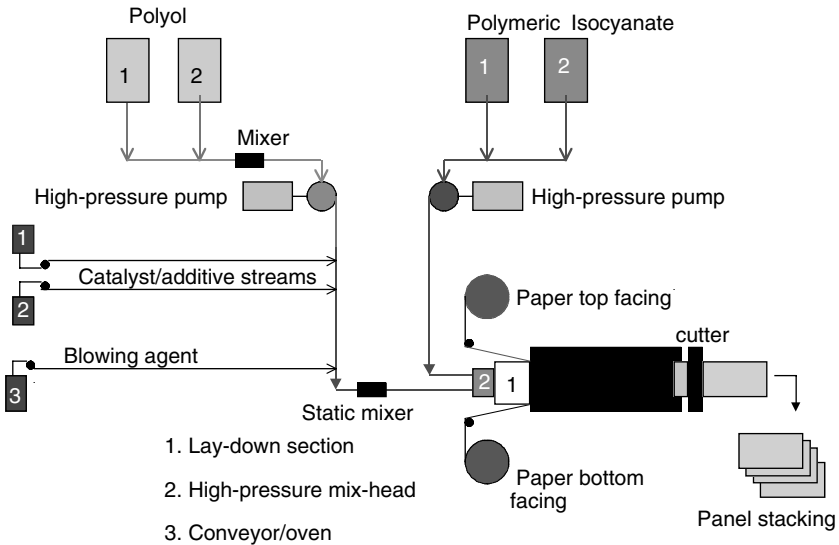


FIGURE 7.9

Layout of double band laminator for the continuous production of flexible faced insulation panels.

frequently produced via PIR technology where sufficient heat is stored in the panels to boost curing and adhesion to the facer. After cooling down, the panels are ready for transport. Examples of flexible facings include paper, aluminum foil, bonded fibers, bitumen, or combinations thereof. DBL-FF lines may achieve running speeds up to 60 m/min when producing polyisocyanurate boards.

For DBL-RF with steel sandwich panels, the rolls with flexible facings are replaced by steel coils and the unit is extended with steel profiling and pre-heating sections to pre-shape and prepare the steel for the foaming operation, which is otherwise identical to that of DBL-FF production. State of the art machinery including additional equipment can be as long as 150 m for steel sandwich panel production. The maximum length of steel-faced panels can be up to 22 m. DBL-RF line speed varies from 4 to 15 m/min, depending on panel thickness.

Rigid bunstock or block foam is sometimes produced in a continuous fashion using foam lines that require less investment than typical DBL lines. Mixing is carried out by a low pressure mix head, which enables continuous dosing of up to 10 components, including solids and pastes. The foaming mass is poured on a moving belt conveyor which is open on the top side, except, in many cases, at the very end of the belt where a moving lid is used to impose a square shape on the otherwise freely expanding foam in order to minimize waste. Blocks produced on a continuous line are typically cut in sizes of 1–2 m width, 2–4 m length, and up to 1 m height, depending on

the foam density. After cutting, the blocks need to be cured for 1–2 weeks before being sold as such or being cut in the desired final shape, typically panels, shaped shells, or cubes.

7.3.2.3 Discontinuous Production

Discontinuous production of panels is carried out using molds with well-defined shapes and sizes, ranging from 3 to 12 m in length, 1 to 2 m in width, and 5 to 20 cm in thickness. In this technology, a reacting polyol-pMDI mixture is injected through a hole in the side of the panel and the injection hole is closed immediately afterwards. Alternative technologies include multiple shot injection, filling tube process, and mix head withdrawal process. In the latter, the entire mix head is inserted into the mold and withdrawn during pouring. After injection, the foaming mass fills the mold, whereby the air in the mold is released through small venting holes. The foam is left in the mold for 10 to 60 min depending on the thickness of the panel. Demolding takes place when the stiffness of the foam is sufficient for the panel to keep its desired shape. Discontinuous panel manufacturing is characterized by its great flexibility to produce almost any desired panel shape with any kind of facer, which leads to a higher cost per square meter. Continuous panel manufacturing is less flexible but has a much lower cost per square meter.

7.3.2.4 Products and Applications

In residential building operations, polyurethane foams are being applied throughout the entire building, in roofing, walls, and flooring. Roof insulation is either applied onto a roof deck followed by a moisture barrier, between the roof cover and the tiles, or between the beams on the inside of the roof. Insulation thickness for roofs varies from 2 to 20 cm depending on the needs and local building regulations. Wall insulation can be divided into three areas: cavity filling, and insulation on the outside or the inside of the wall. External insulation foam, which can be PIR board or sprayed foam, is later covered, for example, with plaster to provide a waterproof layer or a siding material such as brick or wood. Insulation panels at the inside wall of a building are usually applied to upgrade its energy efficiency. Polyurethane or polyisocyanurate foam is ideally suited to this purpose as it requires the smallest thicknesses of all available insulation materials to achieve a desired thermal insulation performance.

Steel sandwich panels are by far the largest application of polyurethane insulation foams in the commercial building market in Europe, while DBL-FF is the largest application in North America. In this application, the specific strengths of polyurethane foam are combined as in no other product to provide thermal insulation, mechanical strength and building efficiency. Steel sandwich panels are directly mounted to the steel structure of the building and doors and windows can be cut out of panels on the building site. An example is given in [Figure 7.10](#). Sandwich building technology

www.iran-mavad.com



FIGURE 7.10

Construction of industrial building using steel faced panels. (Reprinted with permission from Koschade, R., *Die Sandwichbauweise (How to Build a Steel Sandwich)*, Ernst & Sohn, Berlin, 2000.)

provides full freedom to architects and builders to design the entire building using different profiles and colors. Despite their continuous production, there is a huge variety of colors and profiles available at thicknesses ranging from 2 to 20 cm. The steel facings are giving an extra positive contribution to the fire rating of steel sandwich elements. This was demonstrated by a series of tests conducted according to a new European publication on fire testing of building products.^{10,21}

Garage and entry doors are another example of a smaller but fast-growing market where aluminum or steel sandwich panels provide a combination of high energy efficiency, comfort, and appearance. Both polyurethane and PIR technologies are used in these applications. The thickness of these doors is on average 35 to 55 mm.

Another typical polyurethane application in the commercial building market is heating and ventilation. Specially shaped panels and shells are cut out of rigid polyurethane foam blocks, produced either continuously on bun-stock lines or on discontinuous molding facilities.

Spray foam is one of the oldest applications within the construction market. It provides a simple, direct, and efficient way of applying thermal insulation. In contrast to the above-discussed applications, the polyurethane chemicals for spray foam production are brought to the building site and subsequently foamed on-site using mobile equipment. Spray foam is particularly useful for the insulation of cavities at the outside of storage tanks, under roofs,

underneath floors in cellars, etc. In North America, the predominant spray foam application is roofing, where it is applied externally to the roof deck.

Industrial applications can be split into pipe and tank on one side and district heating on the other side. Tanks are usually insulated via spray foam, as discussed above under commercial applications, but can also be poured in place; cavities are filled by discontinuous foaming, which is then applied in ships for cryogenic storage of gases such as LNG. Pipes are mainly insulated via pre-shaped pipe shells.

District heating serves the thermal insulation of underground pipes for transportation of warm water and steam from power plants to residential areas and transportation of liquids over long distances. The diameters of these pipes may vary from 0.15 to 1.5 m. Pipes for district heating are pre-assembled in factories whereby the cavity between a steel inner pipe and a high density polyethylene (HDPE) outer pipe is filled with polyurethane foam via discontinuous or continuous operations. Applied foam densities are 70 to 80 kg/m³. The foams provide very good thermal insulation and excellent mechanical strength, which guarantee the 30-year lifetimes required by governmental certification procedures.

7.3.2.5 Markets

The total consumption of rigid polyurethane foam in the construction industry on a global basis was ca. 3500 kT in 2000 and is expected to grow to ca. 4400 kT by 2005. The overview per geography and application, given by Table 7.3, shows Europe to be the biggest consumer, followed by the U.S.,

TABLE 7.3

Market Data Rigid Construction Foam Per Application in kT, Year 2000

Global	DBL-FF	DBL-RF + DCP	Block	Spray	PIP
Polyol	215	168	78	96	75
pMDI	356	168	78	96	49
Total	571	440	201	256	124
North America					
Polyol	118	20	25	33	22
pMDI	199	33	42	57	34
Total	317	53	67	90	56
Europe					
Polyol	64	110	25	32	18
pMDI	106	180	40	53	27
Total	170	290	65	85	45
Latin America					
Polyol	7.5	1.2	3.8	2.4	1.1
pMDI	11.5	1.8	5.2	3.7	1.8
Total	19.0	3.0	9.0	6.1	2.9
Pacific					
Polyol	26	37	24	29	8
pMDI	39	57	24	29	8
Total	65	94	60	75	20

the Pacific region, and Latin America, in that order. It is furthermore clear that the largest segment by far is formed by DBL, followed by block and spray foam. The U.S. and Europe are the largest consumers. The DBL-FF market is larger than DBL-RF in the U.S., whereas in Europe this trend is reversed. This is undoubtedly a reflection of differences in building practice between the two regions.

7.4 Foaming Process

7.4.1 Mixing

By far the most common route to the manufacture of rigid polyurethane foams comprises the mixing of pMDI with a formulated polyol containing blowing agent(s) and additives. In practice, high-velocity jet impingement mixing at pressures ranging from 50 to 200 bars is the preferred technique used to create sufficient fluid motion for both components to form a fine dispersion that allows molecular diffusion of reactants to be faster than their rate of reaction.⁴⁷ The initial mixture resulting from the turbulence of jet impingement has been described as composed of “striations” of about 10–100 μm thickness.^{48,49} It is generally believed that this degree of mixing intimacy is sufficient for thermodynamically and kinetically driven interfacial mixing phenomena to be rapid enough to establish kinetic control of reactivity rather than diffusion control.

The impingement mixing process itself has hitherto been studied in some detail for RIM formulations^{47–54} using, for example, visual inspection of flow patterns,^{47–50} adiabatic temperature rise,^{47,48,50,51,55} emulsion testing,⁵⁰ physical properties of molded parts^{48,49,51–55} or tracers⁴⁸ as indicators of mixing quality. Characterizing the intensity of mixing by Re_{nzl} , the nozzle Reynolds number of the component of highest viscosity (usually the polyol), these studies conclude that the extent of mixing increases sharply with increasing Re_{nzl} until a critical value Re_{cr} is reached. Beyond Re mixing efficiency remains flat for so-called I-heads, whereas for “self-cleaning” L-heads it still increases further, albeit at a much lower rate.^{50,55} This is attributed to turbulence enhancement due to the 90° bend that has to be passed by the mixture before exiting the L-head,⁵⁵ as shown by Figure 7.11. Some disagreement exists with regard to the magnitude of Re_{cr} which ranges from 200^{47,53} to 380⁵⁵ whereas physical property enhancement flattens only beyond $Re = 500$ ⁵⁵ when the incremental effect beyond Re_{cr} of the L-head design is taken into account.

The relevance of these results for rigid polyurethane systems is not immediately obvious due to the presence of significant amounts of blowing agents and, eventually, flame retardants that are known to reinforce or counteract interfacial mixing phenomena observed for linear⁵⁵ and crosslinked^{55–58} RIM systems. For example, chlorofluorocarbon based blowing agents such as

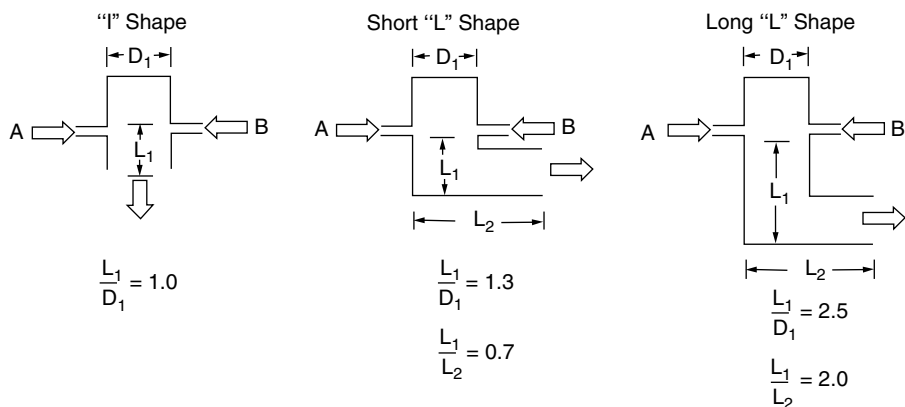


FIGURE 7.11

Schematic diagram of mix heads for high-pressure impingement mixing. (Reprinted with permission from Molnar, J.A., Jr. and Lee, L.J., *J. Appl. Polym. Sci.*, 37, 2295, 1989.)

CFC-11, HCFC-141b, HFC-134a, and HFC-245fa are considered to be compatible with rigid polyol formulations,^{59–63} whereas pentane isomers are reported to form emulsions with certain aromatic polyester polyols.⁶⁴ Apart from reducing polyol viscosity, it is very likely that the solvency of these additives exerts a significant influence on polyol-pMDI compatibility and thereby on interfacial mixing as well. Similar arguments hold for surfactants.⁶⁵ Undoubtedly, there are effects from water which is usually present at rather high concentrations in the formulated polyol since the polyols in these blends are necessarily more polar than typical flexible polyols due to their high OH content for crosslinking.⁶⁶ For example, a typical pentane blown polyol may contain around 2% (w/w) water which translates into 46 mol% for a 750 molecular weight polyol. It is very likely that these highly mobile molecules react early during foam rise,⁶⁷ thereby enhancing polyol-pMDI compatibility at the interface due to the concomitant formation of urea-based oligomers; see [Section 7.4.5](#).

7.4.2 Nucleation

Nucleation is the next noticeable event to occur immediately after mixing polyol and pMDI. This phenomenon is of great practical interest due to its impact on the ultimate cell size—and thereby on the insulation performance—of a fully cured foam; see [Section 7.5.1.1](#). From a macroscopic point of view, foam nucleation is evident from a change in color of the reacting mixture which adopts a creamy appearance due to the evolution of gas bubbles, becoming big enough in size to scatter light. This change occurs at a characteristic time, usually about 5–20 sec after the mixing started, which is known as the cream time. At that stage, nucleation has occurred already and the entrapped gas is in metastable equilibrium with its surroundings which implies that, to a good approximation, its free energy is changing

linearly with time. By using this assumption, it has been shown that r_c , the critical radius of a gas-bubble or liquid droplet dispersed in a polyol, can be expressed as:⁶⁸⁻⁷⁰

$$r_c = \frac{2\sigma v}{v(p^b - p^a) + RT(\ln x^* - \ln x^s)} \quad (7.1)$$

where $p^b - p^a$ represents the pressure difference between the interior of a dispersed bubble (or droplet) and its ambient surroundings, and σ represents the interfacial tension of the polyol-gas/liquid blend. Molar volume, loading level, and ambient pressure solubility of the blowing agent in the polyol are indicated by v , x^* , and x^s , respectively. The stationary state described by Equation 7.1 should not be confused with the preceding nucleation phase which is essentially an unstable, transient stage. Qualitative information about the actual nucleation phenomena may nevertheless be derived when it is assumed (1) that each bubble or droplet is produced by one nucleus and (2) that polyol and pMDI are not yet mixed on a molecular scale when nuclei are formed. Under these premises, nucleation can be considered to take place either in the polyol phase or in the pMDI phase of the reacting polyol/pMDI mixture, and Equation 7.1 can be assumed to represent critical radii before any chemical reaction has actually changed their phase behavior. Equation 7.1 thus provides indirect information about the preceding nucleation stage, such that, for a given system, smaller values of r_c hint towards more efficient nucleation and vice versa.⁷⁰ For simplicity, and for the practical reason that blowing agents are usually dissolved only in the polyol, the discussion below will focus on the polyol phase.

Literature reports two classical, limiting forms of Equation 7.1: one in which the solubility term vanishes because $x^s = x^*$ and one in which the pressure term vanishes because $p^b = p^a$. These limiting forms are known as the Laplace and Kelvin equations,⁷¹ respectively. The Laplace equation is valid for one-component systems and for two-component gas-liquid systems where the gas is essentially insoluble in the liquid phase, such as N_2 in most polyols. In these systems, $x^s \approx x^*$, and r_c is accordingly determined by surface tension and by the intrinsic kinetic energy of the dispersed gas. For gases above their critical point, such as N_2 , p^b can take much higher values than p^a and hence r_c will be small which explains the well-known suitability of N_2 as a nucleating gas in rigid foam manufacture.

The Kelvin equation is valid for incompressible liquid-liquid and solid-liquid systems where $p^a = p^b$ and r_c is consequently determined by the ratio of x^* over x^s alone. An illustrative example for rigid foams is the nucleating effect of essentially insoluble perfluorinated liquids⁷² which are therefore characterized by very high x^*/x^s ratios,⁷⁰ while $p^a = p^b$ in this case. Together with their very small surface tension, this explains why highly significant cell size reductions, presumably caused by very small r_c values, have been found upon addition of even small amounts of perfluorocarbons.⁷² The opposite is also true: highly soluble blowing agents with vapor pressures close to

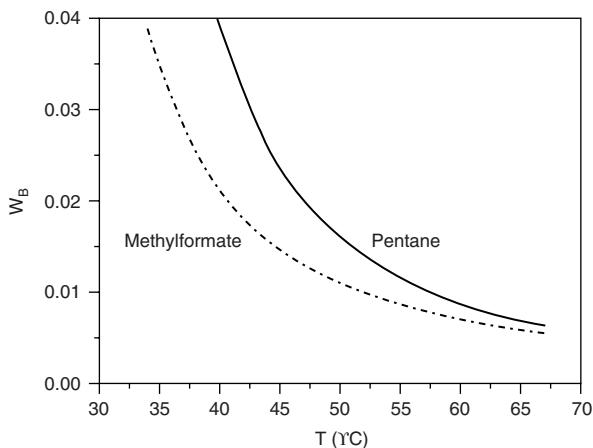


FIGURE 7.12

Construction of industrial building using steel faced panels. (Reprinted with permission from Koschade, R., *Die Sandwichbauweise (How to Build a Steel Sandwich)*, Ernst & Sohn, Berlin, 2000.)

ambient are poor nucleators. In this case, $p^a \approx p^b$ and $x^*/x^s \leq 1$ due to very strong attractive intermolecular interactions between the blowing agent and polyol. The vapor pressure of the blowing agent is accordingly reduced in the presence of polyol which is reflected by a significant boiling point elevation in polyol-blowing agent mixtures, especially at lower loadings.^{59-61,73} An example is given by Figure 7.12, where elevations up to 30°C are observed for pentane and methyl formate, blowing agents that are known to be relatively poorly soluble. Similar data for highly soluble blowing agents such as CFC-11 show even stronger effects.^{59,62}

As a result, nucleation with either liquid or gaseous CFC-11 is not likely to occur until, in real life foam formation, temperature rises sufficiently to force CFC-11 into the vapor phase. This is nicely illustrated by a study⁷⁴ of CFC-11 nucleation in the absence of air, which revealed a 1000-fold decrease in number density of bubbles and a corresponding 10-fold increase in final cell size versus air nucleated foams.

The situation is more complex when low-boiling blowing agents (LBBA) such as HCFC-22, HFC-134a, propane, and butane are considered. In these cases, both terms of Equation 7.1 are operational and nucleation efficiency will depend on the steepness of the slope of the LBBA solubility versus pressure profile.^{70,75} For example, the solubility of butane is expected to increase fourfold upon increasing its partial pressure from 1 to 2 bars.⁷⁰ A polyol-butane blend loaded with up to several bars of butane in a typical storage tank will thus be heavily supersaturated with butane once the mixture has been laid down under ambient pressure after leaving the mix head nozzle. Rigid foams (partially) expanded with LBBAs such as butane and HFC-134a are therefore expected⁷⁰ and actually observed^{69,76,77} to have reduced cell sizes.

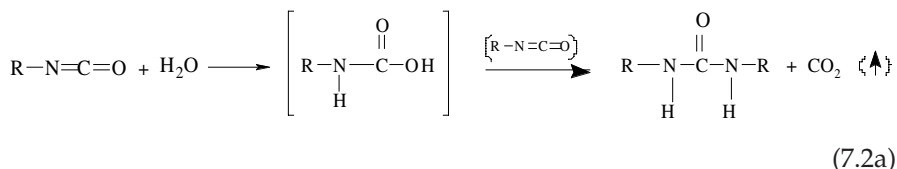
The success of Equation 7.1 in describing nucleation phenomena in a qualitative sense should not conceal that current understanding of nucleation in quantitative terms is rather poor. This is due to the complexity of real life foaming where phase mixing, emulsification, and fast temperature rise due to chemical reactions all occur simultaneously. It is, for example, unclear whether nucleation in rigid foams should be characterized as homogeneous, i.e., by forming nuclei as described above, or as heterogeneous by formation of new gaseous phases at the interface of insoluble gases, liquids, or solids such as, respectively, N_2 or liquid or solid perfluorinated particles.⁷⁸ The fact that very fine, open-celled foam can be obtained via nucleation with polytetrafluoroethylene (PTFE) particles^{79–81} at least suggests that heterogeneous nucleation is overriding in this particular case. Similar uncertainties exist with respect to the importance of coalescence of freshly formed nuclei and with respect to nucleation by CO_2 formed (possibly at the polyol-pMDI interface) from the H_2O -pMDI reaction, which is also known to occur during early stages of the foam rise process;⁶⁷ see [Section 7.4.5](#). In all, the conclusion seems warranted that much more experimental and theoretical research work needs to be carried out in order to create the next level of understanding in this field.

7.4.3 Expansion

Rigid polyurethane foams are applied at densities ranging from about 20 to 50 kg/m³. Starting from initial raw material densities around 1 kg/l or 1000 kg/m³, this implies that a 20- to 50-fold volumetric expansion is taking place during the foaming process which is complete within 1 min, and frequently even faster. During that relatively short time frame, excessive bubble growth as well as bubble collapse and coalescence of bubbles should be minimized in order to produce foams with uniform small cells that are desired for various commercial applications. In practice, these requirements are fulfilled by adding 1–2% (w/w) of a branched polydimethylsiloxane-(co)polyether surfactant to the formulated polyol. These compounds are thought to provide the necessary lowering of surface tension and sufficient surface elasticity (or “dynamic” surface tension) to counteract the thinning tendency, due to Gibbs-Marangoni drainage in expanding liquid films; see also [Section 7.2.4.2](#).

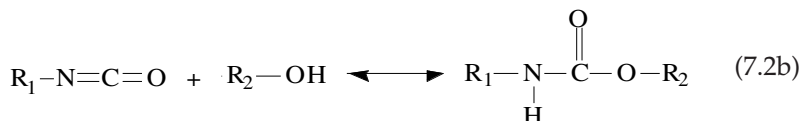
From a mechanistic point of view, foam expansion is driven by the evaporation of the blowing agent and the liberation of CO_2 gas, which is usually generated via the H_2O -pMDI reaction, albeit other reactions have been exploited for that purpose as well.^{1–3} In chemical terms, this reaction is an example of the reaction of -NCO groups with “active” hydrogens attached to atoms of higher electronegativity than carbon. First discovered by Wurtz⁸³ and Hoffman, this chemistry has later been extended by Bayer⁸⁴ who discovered the poly-addition polymerization reaction of di-isocyanates with glycols which forms the basis of today's polymeric urethane products. The reaction of pMDI with H_2O proceeds via the formation of carbamic acid, an unstable

intermediate which dissociates into CO₂ and amine. The latter reacts relatively quickly with pMDI to form urea. The overall reaction sequence is given by:



where R represents the pMDI backbone. The overall reaction is exothermic with a total heat release of about 45 kcal/mol of H₂O.⁸⁵⁻⁸⁷ This mechanism is commonly referred to by using the somewhat misleading term “water blowing.”

The polymer backbone further comprises urethane linkages resulting from the reaction of polyol with pMDI:⁸⁸⁻⁹¹



This reaction is also exothermic with a reaction heat of 24 kcal/mol urethane. The reaction rate is strongly influenced by the structure of the polyol and isocyanate compound. The fact that current formulations frequently contain H₂O up to a CO₂ mole fraction of 0.5 thus immediately leads to the conclusion that most rigid foam polymers are more appropriately termed copoly(urethane-urea) polymers rather than polyurethanes. This is most readily detected by on-line FTIR techniques. Figure 7.13 gives an example showing the kinetic development of urethane and urea linkages in a typical “water-blown” foam as compared to a CFC-11 blown counterpart.^{4,67} The broad absorbance centered at 1730 cm⁻¹ is assigned to urethane groups⁹³ while the absorbance of urea groups tends to shift to lower wavenumbers, depending on their solvation state.⁹² In the very early stages of copolymerization, the reaction mixture comprises polyurea, copoly(urethane), isocyanate terminated polyether, monomers/oligomers, and non-reacted water (if used as a co-blowing agent). Reaction between the monomers and oligomers results in both a molecular weight increase and a concomitant change in the values of the interaction parameters. It is apparent that urethane absorbance (1730 cm⁻¹), urea absorbance (1715 cm⁻¹), and dissolved hydrogen-bonded urea (1661 cm⁻¹) are developing as the copolymerization proceeds. It is also worth noting that solidification via chemical gelation and/or vitrification occurs very quickly (time < 60 sec, at isocyanate conversion, p_{NCO} < 0.60) in these non-linear, highly branched systems.⁶⁷

A wide variety of reactions with isocyanates have been described⁸⁸⁻⁹¹ in addition to urea and urethane formation, but their importance in the context

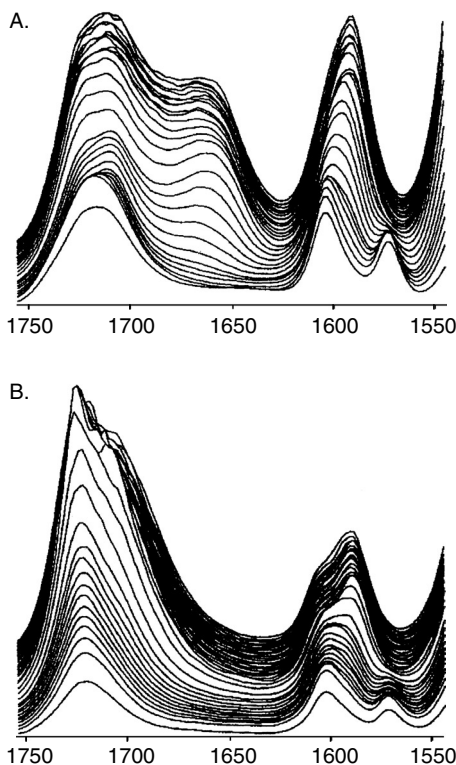
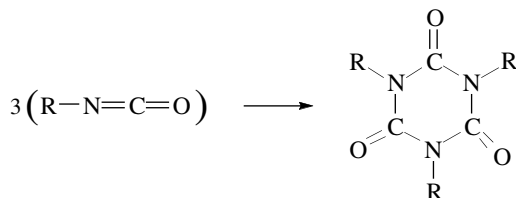


FIGURE 7.13

Time-resolved, exploded view of the carbonyl region of the mid-infrared spectrum for a H₂O blown foam (A) and a CFC-11 blown foam (B) using identical polyol compositions and isocyanate index. (Reprinted with permission from Grünbauer, H.J.M., Rigid polyurethane foams, in *Polymeric Materials Encyclopedia*, vol. 10, ed. J.C. Salamone, CRC Press, Boca Raton, FL, 1996, 7504–7512.)

of rigid foam formation is rather limited. An exception to this rule is the trimerization of isocyanate (Structure 7.7) which is, especially in the U.S., of technical and commercial significance, as described in [Section 7.3.2](#):



(Structure 7.7)

This reaction is again exothermic. The heat generated by urea, urethane, and trimer formation is responsible for the evaporation of the blowing agent, the second driving force of the expansion process next to the formation of CO₂. Heat balance models correlating these exotherms to foam expansion via

simplified kinetic equations and heats of evaporation are relatively successful in predicting actual foam rise profiles,^{59–62,73} provided that the boiling point elevation effects shown by Figure 7.12 are taken into account.

Measurement of foam expansion has been attempted using many techniques. These include floats riding the foam surface⁹³ and recording foam height using simple rulers⁹⁴ and optical^{95,96} or ultrasonic⁹⁷ sensors. By far the most elegant method is based on the buoyant force exerted by air on the expanding foam.⁹⁸ At 200 g of formulated material this force leads to an apparent weight loss of ≈ 5 g for foams of about 30 kg/m^3 free rise density, which is accurately measurable by pouring the foaming mass in a $20 \times 20 \times 20 \text{ cm}^3$ cardboard box positioned on a standard laboratory balance. Fitted with a computer interface, this type of experimental setup is capable of fully characterizing dynamic foaming profiles by simultaneous recording of multiple signals. An example is given by Figure 7.14, where typical foam volume expansion and exotherm development are plotted against time for a formulation blown with CO_2 via Reaction 7.2a. The rise rate profile in this figure is calculated by differentiating the volume expansion profile and smoothing. This profile, in turn, follows directly from the apparent weight loss and the density of air.⁹⁸ The on/off signal of the stirrer indicates both the stirring time and the “gel” or “string” time, here 57 sec after start of stirring. This characteristic time is commonly defined as the time at which strings of solid material can be pulled from a rising foam using a wooden spatula. It is interesting to note that, at this time, volume expansion is nearly complete whereas the temperature in the foam core has only reached about 90°C , almost 50°C below the final value of more than 160°C . This implies that resin formation is far from complete when the foam is fully risen and it also suggests that polymer strength is being built up afterwards, despite the early start of reaction kinetics immediately after mixing polyol and pMDI.

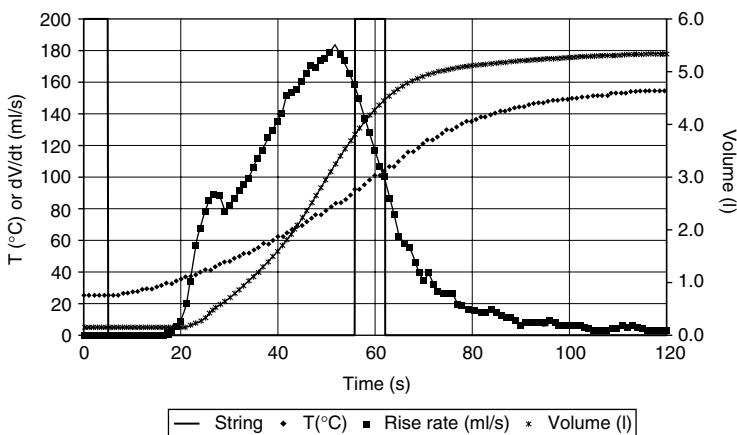


FIGURE 7.14

Rise rate, volume expansion, and reaction exotherm of a water-blown rigid foam.

7.4.4 Rheology

The balance between foam expansion and polymer resin formation is of great practical importance, as commercial foamers always strive for smooth expansion profiles, or high “flowability,” in combination with fast curing to reduce cycle time in molding applications or to increase line speed in laminated foam manufacture. It is therefore not surprising to find several literature references reporting measurement of important rheological parameters during foam rise. This is experimentally rather difficult due to the combination of high volumetric expansion rates with fast exothermic chemical reactions.⁹⁹ Experimental approaches that have met with some success include foam modulus measurement by means of a pulse rheometer setup^{100,101} or a flooded parallel plate fixture in a rheometer,^{99,102–104} as well as the use of on-line recording instruments, such as measurement of drag forces on immersed spheres,^{105,106} vibrating needles,^{107,108} spheres,^{109,110} rods, or collets,^{111,112} and a vane rheometer.¹¹³

Figure 7.15 shows a typical rigid foam profile obtained by means of a Nametre vibrating collet.¹¹¹ This instrument operates by emitting a flat shear wave of 1–20 μm amplitude into the surrounding medium, which leaves the growing foam cells intact. Provided proper precautions are taken to ensure constant immersion depth by using an overflow device, the rheology profile of a rising foam can thus be recorded starting from a few seconds after mixing onward. It has been shown^{111,114} that, mathematically, the system is equivalent to an electrical AC circuit in resonance, whereby elastic and viscous components of the viscous drag forces caused by the surrounding medium act as “mechanical” capacitance X_m and resistance R_m forces, respectively. The resistance against the shear force exerted by the vibrating rod, R_m , is given by Equation 7.3:

$$R_m = \sqrt{\pi f_M \eta_n \rho} \quad (7.3)$$

where f_M represents the resonance frequency of the rod in the medium and η_n and ρ its nominal viscosity¹¹¹ and density, respectively. By simultaneous on-line recording of foam expansion and viscosity rise, the density term can be eliminated to yield the actual polymer viscosity build-up during foam rise. The expansion, η_n , and R_m profiles of Figure 7.15 are exemplary. Taken together, these profiles nicely illustrate that R_m , the actual mechanical resistance against shear forces, remains at an almost constant low level during the first 60 sec of the foaming process, despite the continuously increasing polymer viscosity. The reason is the concomitant volume expansion which compensates for the increasing viscosity term in Equation 7.3 via its connection with the density term. In other words, the flowability of a rising foam is primarily dependent on its volumetric expansion rate, albeit resin formation needs to be in balance, such that premature gelation due to too high polymerization rates has to be avoided.

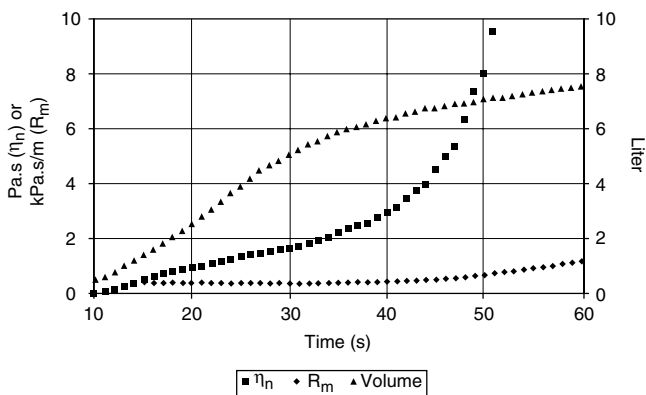


FIGURE 7.15

Volume expansion, nominal viscosity rise, and mechanical resistance profile of a typical rigid foam.

Throughout the initial stages, the resonance frequency f_M remains virtually constant, until appreciable elastic forces start to develop, which are noticeable as a shift in f_M . By using proper calibration constants, it is possible¹¹¹ to extract the mechanical capacity term X_m and to convert the profile into more common rheological parameters, such as dynamic viscosity and modulus η' and G' , respectively. The resulting profile of Figure 7.16 clearly shows the expected features of a steep increase of η' upon gelation, followed by a much slower build-up of G' during the subsequent curing phase.¹⁰²

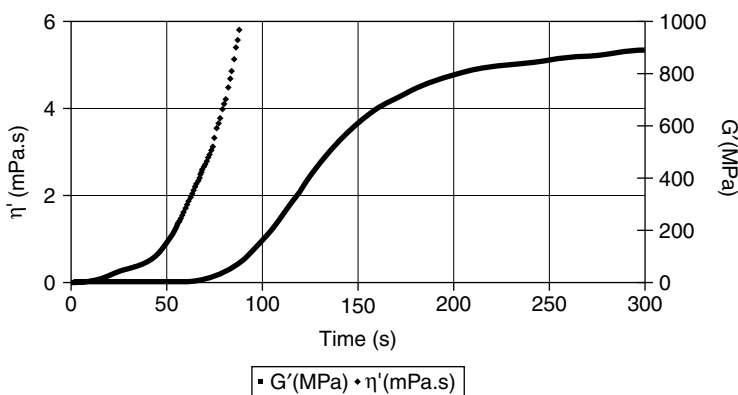


FIGURE 7.16

Buildup of dynamic viscosity η' and dynamic modulus of G' of a rigid foam polymer during foam rise.

7.4.5 Polymer Morphology

The development of the polymer microstructure and morphology during rigid foam formation can be divided into four processes: first, the urea-urethane co-polymerization itself as well as the subsequent development of the polymer architecture and microstructure;^{67,115–119} second, the competition between the co-polymerization and the polyurea macrophase separation;^{4,67,119–128} third, the solidification processes of vitrification and chemical gelation and how these impact the development of macroscopic properties;^{4,120–121} and, finally, the build-up of the prevailing polymer morphology of the foam, several hours to days after the reaction is complete, as the result of a slow curing process.

The role of water—about 2 to 4% w/w of polyol in, respectively, 50 and 100% CO₂ blown foams—is important not only for the foam expansion process, but for the polyurea that is formed as a result, and has a significant impact on the evolution of the morphology and on the ultimate mechanical properties of the polymer. This is nicely illustrated by Figure 7.17, which compares the loss tangent, $\tan \delta$, obtained by dynamic mechanical spectroscopy (DMS) as a function of temperature for CFC-11 and H₂O blown foams over a wide range of isocyanate indices. The once commercial CFC-11 blown polyol system comprised a fine-tuned optimized blend, while the water-blown polyol system incorporated a high functionality base polyol and a high equivalent weight, viscosity cutting polyol.⁶⁷ The contrast in behavior is immediately apparent from inspection of Figure 7.17. A smooth $\tan \delta$ shift with increasing index is observed for the CFC-11 foams, which is typical for a gradual increase in crosslink density.¹³⁵ In contrast, the water-blown foam shows a sharp transition at -40°C , which gradually disappears at higher isocyanate indices.

Meanwhile, a broad transition emerges at higher temperatures. At an index of approximately 1, there is a maximum in the loss peak at approximately 200°C , accompanied by a broad shoulder between 100 and 200°C . As the index is further increased, the transition narrows, which was ascribed to isocyanurate formation. Combining the DMS profiles from Figure 7.17 with additional information from DSC, TEM, and solvent extraction studies, the conclusion seems warranted^{67,118–121} that, in the water-blown case, polymer strength build-up is dominated by the high functionality, base polyol component, and concomitant precipitation of urea. The latter is particularly evident from TEM images revealing the presence of irregularly spaced dark spots with a length scale of 50–300 nm. The number of these “spots” (tentatively ascribed to urea-urethane precipitates) was observed to increase with increasing isocyanate index, while above an isocyanate index of 0.7, the “spots” could no longer be discerned.¹²⁰ Figure 7.18 presents an example recorded at an isocyanate index of 0.5.

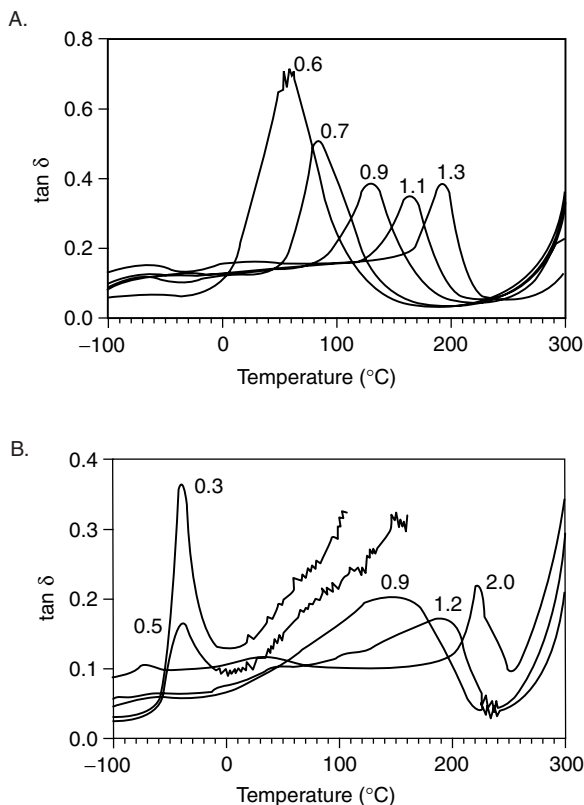


FIGURE 7.17

DMS spectra of CFC-11 blown foam **(A)** and water-blown foam **(B)** at varying isocyanate indices, as indicated by the curve labels. (Reprinted with permission from Grünbauer, H.J.M., Rigid polyurethane foams, in *Polymeric Materials Encyclopedia*, vol. 10, ed. J.C. Salamone, CRC Press, Boca Raton, FL, 1996, 7504–7512.)

In this view, the low temperature transition at -40°C is due to non-reacted, high equivalent weight, low viscosity polyol component. This confirms the practical notion of its “viscosity cutting” action in polyol formulations: it acts as a reactive diluent for reacting/precipitating species during the early stages of the foaming process, thereby replacing the solvency effect of liquid blowing agents that are absent in this case.⁶⁷

Probing the polymer morphology of (partially) water-blown foams on the nanometer scale by means of SAXS^{119–121} revealed a rather complex architecture which is best interpreted by using fractal concepts.^{130–133} To illustrate, Figure 7.19 shows Lorentz corrected scattered intensity, $I(q) \cdot q^2$ versus q , plotted for five different water-blown model foams made with single-polyol formulations of increasing propylene oxide per OH (PO/OH) chain length.¹²¹ The shoulder in the scattering curve of the foam derived from the 30 PO/OH polyol is readily discernible. In this particular foam, the polyether chain is of a sufficient length that when reaction between the hydroxyl group of

this chain and the isocyanate group from a polyurea sequence length takes place, a block copolymer is evolved. At shorter chain lengths, this tendency is apparently hampered due to a lack of mobility of the polymer chain segments involved. The result in SAXS is a steadily decaying scattering intensity $I(q)$ that becomes linear when plotted as $\ln I(q)$ vs. $\ln q$. This behavior has been interpreted in terms of a fractal concept^{120,131} such that the fractal dimension calculated from the slope of the $\ln I(q)$ vs. $\ln q$ curve indicates whether an open, lung type structure with a characteristic high surface to volume ratio or a more densely connected structure is involved.^{120,121}

Figure 7.20 presents a plot of the mass fractal dimension, F_m , as a function of the equivalent weight of the polyol for the above mentioned series of model copoly(urethane-urea) foams.¹²¹ In general, as the equivalent weight of the polyol increased (a greater number of propylene-oxide segments and thus chain length), a concomitant decrease in the mass fractal dimension, F_m , was observed. In other words, the shorter the chain length, the more dense and rigid the structure. Furthermore, the higher the functionality of the isocyanate that was employed, the higher the observed mass fractal dimension, F_m , and therefore the greater the propensity for branching, and the more dense and connected was the structure that was evolved. These results are of great practical interest due to their immediate connection with effective diffusion coefficients of CO_2 and blowing agents as defined in Section 7.5.2.1. It has been observed¹²¹ that foams exhibiting a rigid

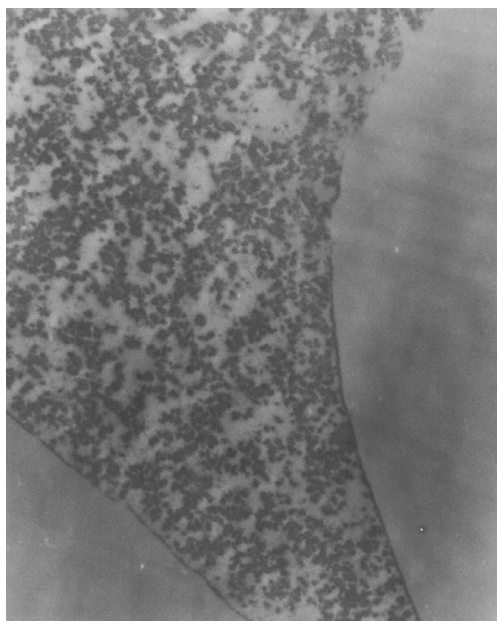


FIGURE 7.18

TEM image of the fully water-blown foam of Figure 7.17 at an isocyanate index of 0.5. (Reprinted with permission from Grünbauer, H.J.M. and Folmer, J.C.W., *J. Appl. Polym. Sci.*, 54, 935, 1994.)

www.iran-mavad.com

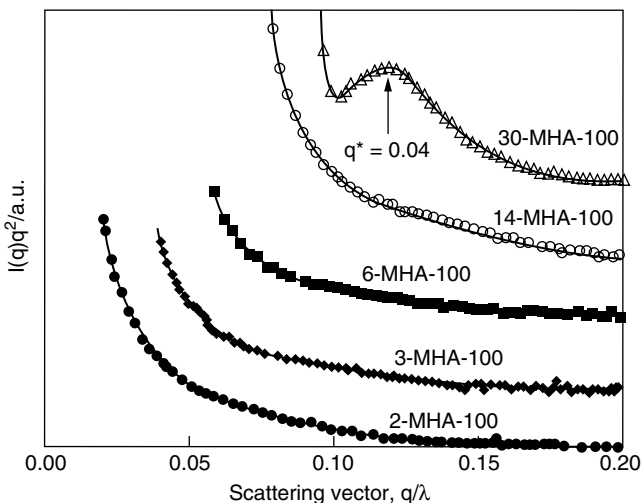


FIGURE 7.19

Lorentz corrected scattering profiles of water-blown mode foams from single polyol formulations at nominal PO/OH chain lengths of 2, 3, 6, 14, and 30. (Reprinted with permission from Megat-Yusoff, P.S., Ph.D. thesis, Victoria University of Manchester, 1996.)

interconnected structure with a characteristic high value of the mass fractal dimension, F_m , also displayed a low value of effective diffusion coefficient, D_{eff} .¹²¹ Moreover, when the equivalent weight of the polyol component in the formulation was increased resulting in a concomitant decrease in the crosslink density and mass fractal dimension, the effective diffusion coefficient was observed to increase.¹²¹ This was explained in terms of the “looseness” or “openness” of the polymer network. The more open and loose the network structure, the higher was the propensity for diffusion of the gaseous blowing agent through the foam structure.

The overall picture of polymer microstructure and morphology development emerging from these studies is that of a reactive co-polymerization process, more specifically a reaction-induced phase separation process. For the case in which water is employed as a co-blowing agent, upon mixing and molecular contact between the components the di- or polyisocyanate-water reaction proceeds, generating polyurea and carbon dioxide. The polyurea formed undergoes macrophase separation almost instantaneously, and will subsequently aggregate. The formation of urethane from the di- or polyisocyanate-hydroxyl reaction (derived from the high functionality base polyols), reacts after and/or in competition with the water. Thus, there exists a kinetic competition between the polyurea polymerization, the macrophase separation, and the subsequent association of the polyurea so formed, and the incipient crosslinking reaction to form the covalent polymer network.

The kinetic competition between multiple processes results in a “frustration” on the system with respect to the structure development process. The extremely high crosslink density that results from the short chains (low equivalent weight) on the high functionality base polyol, generates a very

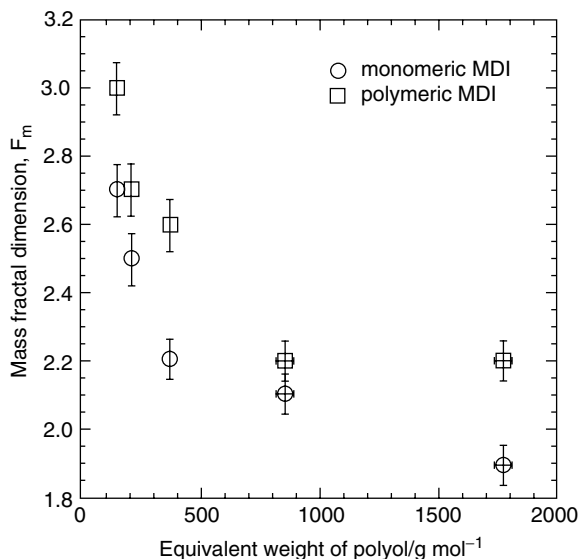


FIGURE 7.20

Mass fractal dimension F_m as a function of equivalent weight for water-blown-made foam from single polyol formulations at nominal PO/OH chain lengths of 2, 3, 6, 14, and 30. (Reprinted with permission from Megat-Yusoff, P.S., Ph.D. thesis, Victoria University of Manchester, 1996.)

rigid and tight polymer network structure (similar to a fine-mesh fishing net). This in turn prevents the formation of molecular associations (hydrogen bonds) between segregated polyurea aggregates, beyond a certain size and length scale; hence, the lack of appreciable concentrations of hydrogen-bonded urea in comparison to that observed in a flexible copoly(urethane-urea) foam. In a very short time frame (30–60 sec depending on the formulation) chemical gelation of the polymer network and vitrification of the polyurea kinetically “trap” the evolving morphology and freeze it in place. The result is a very irregular, phase-separated morphology that exhibits fractal symmetry.

7.5 Physical Properties

7.5.1 Thermal Conductivity

7.5.1.1 K-factor Contributions

It is generally accepted that thermal insulation performance of rigid polyurethane foam arises from three heat transfer controlling phenomena: polymer conduction, gas conduction, and radiation. The overall thermal conductivity, indicated as λ or K-factor, is determined by the sum of these contributions, as well as by the density of the foam and the material distribution over struts

and windows.^{5,136-139} The example¹³⁶ in Figure 7.21 shows that, typically, the K-factor versus density profile exhibits a minimum at about 30–50 kg/m³, which can be explained as the result of a balance between radiation and polymer conduction. At constant cell size, radiation is particularly important at very low densities where the number of radiation scattering cell windows per unit volume is smallest. An increase in density results in an increasing number of cell windows per unit volume, hence the radiation contribution decreases as does the K-factor. At higher densities, this effect is counteracted by an obvious increase in polymer conduction, which explains the upswing of the K-factor profile. Similarly, at constant density and cell gas composition, the radiation transfer contribution to thermal conductivity decreases with decreasing cell size,^{139,140} down to values below 1 mW/mK for cells smaller than 100 μm .¹⁴¹

Figure 7.21 also suggests that, at 30 kg/m³ density, the radiation heat transfer contributes about 20% to the K-factor. This number should be compared with quotes of several older studies which range from 15 to 20%¹³⁷ to 30%^{139,140} for CFC-11 foams, whereas estimates of 10–20% and 6% have been made in more recent work for 141B¹⁴² and air-filled open celled foams,¹⁴³ respectively. Values reported for the contribution of polymer conduction also range between 17 and 30%.^{136, 139,140, 142,143} Table 7.4 gives a summary of preferred mean values. This table clearly shows that, by far, the most important K-factor contribution arises from gas conduction, i.e., roughly 50–70%, depending on the type of foam. Optimization of blowing agents is thus an obvious choice to improve product performance, and it is not surprising that significant efforts have been undertaken in recent years to develop the CFC-11 alterna-

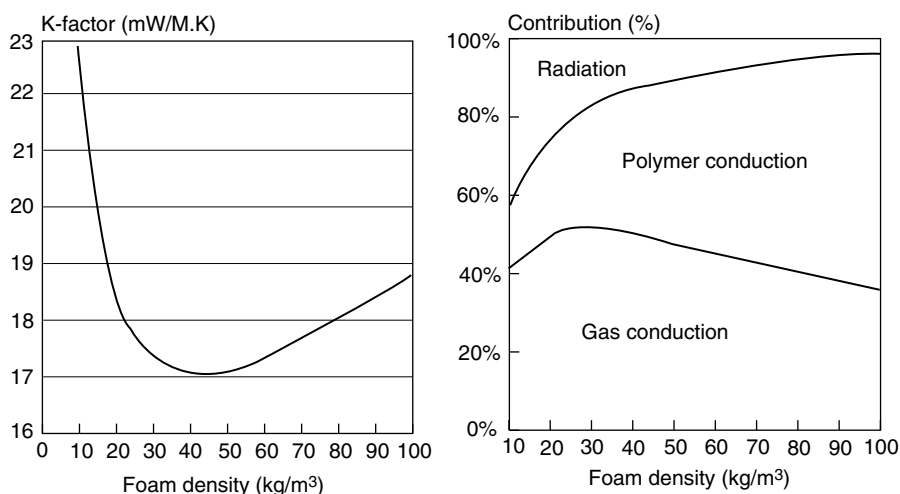


FIGURE 7.21

Contributions to foam K-factor as a function of foam density. (Reprinted with permission from Grünbauer, H.J.M., Rigid polyurethane foams, in *Polymeric Materials Encyclopedia*, vol. 10, ed. J.C. Salamone, CRC Press, Boca Raton, FL, 1996, 7504–7512.)

TABLE 7.4

Contributions to Rigid Polyurethane Foam K-factor

Parameter	Influencing Factor	Weight (%)
Radiative heat transfer—Radiation through the foam	Opacity of the foam—Cell structure	13
Solid heat transfer—Conduction through the polymer matrix	Thermal conductivity of the polymer	20
Gaseous heat transfer through gas mixture contained in cells	Gas K-factor of the blowing agent mixture (conductive)	67

tives of Table 7.1. Once the blowing agent (combination) is fixed, further K-factor improvements could be made by reduction of either the polymer conduction or the radiative heat transfer component.

Heat transfer from conduction through the solid matrix is determined by the chemical structure of the polymer, by the density of the foam and the distribution of mass between the struts and windows at the cellular level of the foam.^{136,139,140} The minimum foam density permitted is limited by the long-term dimensional stability of the foam; see Section 7.5.2.2. For this reason, reduction of radiative heat transfer is the most attractive option for K-factor improvement. In polymeric foam, the radiative contribution to heat transfer is influenced by the ability of the polymer to absorb radiative energy.^{139,140} Polyurethane foams can be thought of as an aggregate of opaque struts and thin transparent windows. Reducing the cell size is equivalent to increasing the number of opaque barriers.^{139,140} An alternative approach to reduce the radiative thermal conductivity is to increase the ability of the polymeric material to interact with the radiative energy modification of the polymeric structure or by addition of additive that would absorb, reflect, or scatter the radiative energy.¹⁴⁴

7.5.1.2 Condensation

Inspection of Table 7.2 shows that several currently used blowing agents are in the liquid state at ambient conditions, with boiling points ranging from 15°C for HFC-245 fa to 50°C for cyclopentane. Accordingly, their vapor pressures are below 1 bar under ambient conditions with a minimum value for cyclopentane of 0.34 bar at 20°C. Classical thermodynamics dictates that condensation of a vapor always occurs at pressures equal to or higher than its vapor pressure at a given temperature.^{71,136} This implies that, at 20°C, condensation of, for example, cyclopentane will occur when the gas phase of a closed celled foam contains cyclopentane at a mole fraction of 0.34 or higher.^{145,146} A similar reasoning holds for other blowing agents, such as CFC-11¹³⁶ and HCFC-141b.¹⁴⁷ Condensation will also take place at lower mole fractions when the temperature is decreased until all blowing agent is eventually condensed. This

phenomenon is of significant practical importance for two main reasons. First of all, the thermal conductivity of the foam is usually affected appreciably as a result of several partially balanced effects. Liquified blowing agent no longer contributes to gas phase thermal conductivity as the gas phase will be enriched in gases with higher thermal conductivity, such as N_2 , O_2 from ingressed air, and (residual) CO_2 . A second reinforcing effect could be due to the thermal conductivity contribution of liquified blowing agent which is higher than that of gaseous blowing agent. Third, the overall reduction of cell gas pressure may have an opposite influence which is, however, small at the cell gas pressures considered. As a result, overall thermal conductivity of the foam is usually increased significantly.

Reduction of total cell gas pressure is also at the origin of the second practical impact of blowing agent condensation. Due to the high porosity of 95–97% of rigid polyurethane foams, their dimensional stability can be characterized as a subtle balance between polymer strength and cell gas pressure.^{136,145,146} Partial loss of cell gas pressure may hence cause significant problems, especially at low service temperatures in freezers and refrigerators or when construction foams are exposed to cold climates. Both effects are nicely illustrated by Figure 7.22, which shows gas thermal conductivity and cell gas pressure of a free-rise foam containing 0.09 mol of total blowing agent per 100 g of formulation.¹⁴⁶ The total cell gas pressure is about 0.7 bar due to the cooldown of the foam from its maximum exotherm to ambient temperature.^{136,146} At 20°C, this pressure is maintained at cyclopentane mole fractions below 0.5. Above this limiting concentration, cyclopentane starts to condense and the total cell gas pressure decreases with increasing cyclopentane content until, at 100% cyclopentane, the vapor pressure (0.34 bar) of cyclopentane at 20°C is reached.

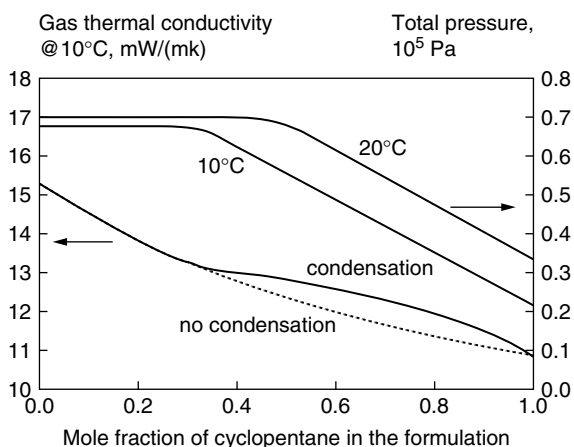


FIGURE 7.22

Gas thermal conductivity and cell gas pressure as a function of blowing agent composition in a CO_2 /cyclopentane blown free-rise foam. (Reprinted with permission of Sage Publications Ltd., from Fleurent, H. and Thijs, S., *J. Cell. Plast.*, 31, 580, 1995.)

www.iran-mavad.com

Figure 7.22 also shows this effect at 10°C, together with the concomitant increase in K-factor. At this lower temperature, condensation starts earlier due to the lower value (0.22 bar) of the vapor pressure of cyclopentane. Needless to say, the strength of the polymer matrix should be designed to counteract this pressure drop in order to maintain dimensional stability, especially in refrigerators and freezers. Alternatively, low boiling blowing agents are frequently considered in these cases as they allow for the use of more cost-effective lower foam densities while maintaining K-factor performance due to the absence of condensation effects. Not surprisingly, Table 7.1 shows several examples, which are currently in use.

Foam dimensional stability is further affected by penetration of blowing agent into the foam polymer matrix, especially in the longer term as well as by the exchange of cell gases with external gases which takes place during the foam aging process, which is discussed below. The matrix “solubility” effect has been extensively investigated^{148–150} for cyclopentane, pentane isomers, HCFC-141b, and CFC-11. In all cases, matrix loadings up to 10% by weight have been found, particularly in foams that have been in use for a prolonged period of time, i.e., for 10 years or longer.¹⁴⁹

7.5.2 Aging

7.5.2.1 Gas Diffusion

The most important aging phenomenon observed with rigid foams is undoubtedly the loss of thermal insulation performance, and sometimes dimensional stability, due to the exchange of blowing agent and atmospheric gases between the foam core and its environment. The thermodynamic force driving this exchange is the difference in concentration across the foam boundary of the gases involved. This process can be approximated as a classical sorption/desorption process that can be quantified in terms of effective diffusion coefficients, indicated by D_{eff} , by applying Fick’s law, once the concentrations of the various gases in the foam are known as a function of time.¹⁵¹ In practice, concentrations are obtained, for example, via internal gas pressure recording,¹⁵² weight loss measurement,^{153,154} and GC analysis of gases evolved from vacuum exposed foam surfaces^{155–157} or from crushed cylinders, sampled on various location of a foam slab.^{158–163}

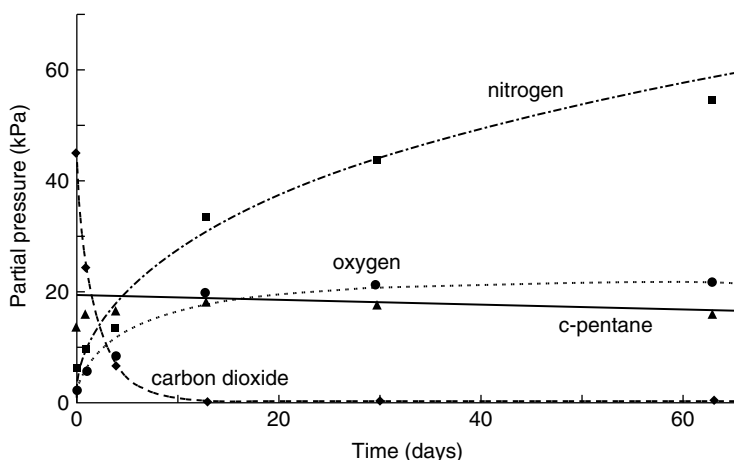
Essential in this treatment is that a foam slab is considered as a continuum. This approach has the advantage that details of the foam structure, such as open cell content and material distribution, need not be known. Also, D_{eff} data from relatively fast aging thin foam slices can be scaled up to predict long-term aging performance of real live slabs of greater thickness,¹⁵¹ an approach which is frequently referred to as the “slicing method.”^{162,164} Its major disadvantage is its dependence on local material properties at the sampling point of forthcoming D_{eff} values. This needs to be taken into account when computing predictions of actual long-term aging behavior.¹⁶³ In addition, variations among D_{eff} data derived from different foam types may be expected due to their dependence on the actual foam sample considered.

TABLE 7.5

Effective Diffusion Coefficients of Various Blowing Agents and Atmospheric Gases

Blowing Agent or Gas	$D_{\text{eff}} \times 10^{13} \text{ (m}^2/\text{s)}$	Ref.
CFC-11	2.7	80, 81, 84, 87
HCFC-141b	1.5	84, 87
HCFC 22	32	79, 87
Isomeric pentanes	2.5	86
N ₂	57	80, 81, 83, 86, 87
O ₂	647	80, 81, 83, 86, 87
CO ₂	1540	79, 83, 84, 86, 87, 90

Although not negligible, these variations are nevertheless smaller than those between blowing agents, so that meaningful conclusions can be drawn about diffusivity trends for various atmospheric gases and blowing agents from the D_{eff} compilation given by Table 7.5. This table gives average D_{eff} values obtained under ambient conditions by various authors. Despite the spread in the original data, the conclusion seems warranted that D_{eff} values of physical blowing agents are of the order of $10^{-13} \text{ m}^2/\text{s}$, except perhaps for HCFC-22, which is however gaseous at ambient conditions. D_{eff} of air, 80% N₂ + 20% O₂, is of the order of $10^{-11} \text{ m}^2/\text{s}$, whereas D_{eff} of CO₂ ranks highest with an average D_{eff} value of the order of $10^{-10} \text{ m}^2/\text{s}$. The relative ranking of Table 7.5 is clearly manifest in aging studies of unfaced foam slabs where CO₂ diffusion is completed within days, air exchange takes from several months to years, and full exchange of the blowing agent itself is difficult to measure during the service life of the foam.^{165,166} This is illustrated in Figure 7.23 which shows the time dependence of partial pressures of N₂, O₂, CO₂ and cyclopentane in unfaced aging foam.

**FIGURE 7.23**

Time dependence of partial pressures for a cyclopentane blown polyurethane foam (30 mm slab = 45 kg m⁻³). (Reprinted with permission from Svanström, M. et al., *Cell. Polym.*, 16, 182, 1997.)

The outward diffusion of blowing agent being very slow, several approaches to predict aging from so-called accelerated aging tests have been proposed. One approach, the slicing method, has been mentioned already. It has the advantage of simplicity, speed, and ease of scaling,¹⁶² but it is disadvantaged by the need to cut thin slices. This introduces a layer of damaged cells at the surface, which is difficult to quantify. An alternative approach is the so-called ACERMI method,^{167,168} which comprises acceleration of gas exchange by increasing the temperature of the foam. Despite its wide acceptance, this method has its shortcomings as well. Detailed examination of the temperature dependence of the diffusion of various gases and blowing agents has clearly demonstrated significant variations among thermally induced acceleration factors of various gases and blowing agents.^{169,170} As a result, the balance between the different diffusion processes is shifted and predicted aged properties may be, and are actually found to be,¹⁷¹ in error.

7.5.2.2 *Dimensional Stability*

Dimensional stability is almost as important as K-factor performance to the success or failure of a given foam formulation. It is frequently measured by the compressive strength at 10% compression. This is a reliable means of assessing dimensional stability because it is related to the pressure inside the foam cells and its evolution with time and temperature, as well as the strength of cell walls of the foam. It is influenced by several factors, such as:

1. The polymer formulation, which can give higher or lower strength, and the foam density.
2. The boiling point of the blowing agent. A blowing agent with a lower boiling point will give a higher initial cell pressure and therefore a higher compressive strength and will also tend to condense less at lower temperatures (which occur during the operation of a refrigerator or in a cold climate) than a product with higher boiling point.
3. The flow properties of the foam. A foam with good flowability will have a better density and compressive strength distribution throughout the cabinet and a more homogeneous cell structure, i.e., fewer elongated cells.
4. The ratio between the rate of outward CO₂ diffusion and inward air diffusion.
5. The penetration of physical blowing agent into cell walls.

Except for the first, all factors are mediated by the choice of the blowing agent and the exchange of gas and blowing agent between the foam interior and the outside world. It follows that it is hardly possible to overemphasize the importance of these phenomena for the performance of polyurethane insulation foams in industrial practice. Assuming typical lifetimes of 20 to 50 years for construction materials and 15 years for refrigerators, it is thus

of obvious importance to assess the impact of diffusion processes on long-term thermal conductivity and stability after the short-term depletion of CO₂ has been completed. In that respect, real life studies over periods of 30 years for CFC-11 and up to 9 years for HCFC-141b and pentane are rather reassuring.¹⁷² In full agreement with expectations based on D_{eff} of the type displayed by Table 7.5, K-factor aging profiles of these foams show a tendency to flatten after an initial upswing with plateau values ranging from 25 to 30 mW/mK, depending on the blowing agent, sample thickness, and presence or absence of a facer material.¹⁷²

The position of CO₂ as a blowing agent deserves some special attention in this context. In principle, CO₂ comprises a very attractive option for expansion of insulation foams due to its moderate gas K-factor, its low global warming potential versus physical blowing agents, and the convenience of the reactive route given by Equation 7.2a or one of its counterparts. Apart from the relatively high cost of generating CO₂, ultimately via phosgenation of amines, its high diffusivity is the only drawback preventing its widespread use as a blowing agent. Several attempts have been reported in the literature to counteract or circumvent this unfortunate feature. The most obvious route is to increase the foam density in order to balance the pressure drop that occurs within weeks after a fully CO₂ blown foam is manufactured.¹³⁶ In that case, the plateau K-factor will be around 32 mW/mK,¹⁷³ i.e., the value for air. Lower plateau values can be attained by applying suitable diffusion barriers,¹⁷⁴ which are capable of retaining a significant portion of the initial CO₂ concentration over a prolonged period of time (or forever in the case of metal facings). Other alternatives that have been considered are reduction of CO₂ diffusion by means of optimizing the urethane-urea copolymer morphology,^{120,121} polyurethane polymer structure,¹⁷⁵ via relief of the density requirement by using open cells^{80,81,176} or via improved crosslinking of the polyurethane resin involved.^{177–179}

7.6 Conclusions

Inherent to the very nature of rigid polyurethane foam formation is the requirement of a proper balance between properties and actions of all ingredients present in the starting formulation. This review has clearly shown that several years of intense research have greatly enhanced our understanding of the fundamentally complex science of foam formation and physical property development. As a result, today's polyurethane industry is much better positioned to implement product improvements required by customers and/or regulatory bodies than 15 years ago when the first attempts to replace CFC-11 technology were necessarily guided by "Edisonian" trial and error approaches. In hindsight, one can only admire the historical development of CFC-11-based polyurethane insulation foams and their early non-CFC-based counterparts "from scratch!"

Meanwhile, rigid polyurethane foam technology has now matured to an environmentally responsible position.

Contrasting with the implied optimism of this statement however is the general feeling that responding to ever more stringent upcoming environmental regulations on, e.g., flammability and energy consumption remains a challenge to the industry unless dramatic performance improvements can be realized. It is, for example, unlikely that current developments in blowing agent technology will give rise to quantum-leap improvements of, say, 30% or more in thermal conductivity. To achieve these levels of performance, entirely new product and processing concepts need to be invented and implemented. A good example in this context is the use of open-celled foam⁷⁹⁻⁸¹ in combination with vacuum insulation¹⁷⁹ for refrigerators. It is from this type of innovative thinking that new concepts will emerge to serve tomorrow's customer and environmental needs. Rigid polyurethane foam technology is sufficiently broad and versatile to face this challenge as positively as it is currently responding to the challenge of implementing zero ODP, low GWP technology on a global basis.

Acknowledgments

The authors would like to thank the following colleagues: Professor Anthony J. Ryan, University of Sheffield, U.K., and Dr. Puteri S. Megat Yusoff, University of Technology, Kuala Lumpur, Malaysia. They are also grateful to The Dow Chemical Company for granting permission to publish this chapter.

References

1. Oertel, G., ed., *Polyurethanes Handbook*, 1st ed., Carl Hanser Verlag, Munich, 1985.
2. Woods, G., *The ICI Polyurethanes Book*, John Wiley & Sons, New York, 1987.
3. Gum, W.F., Riese, W. and Ulrich, H. eds., *Reaction Polymers Chemistry: Technology, Applications, Markets*, 1st ed., Carl Hanser Verlag, Munich, 1992.
4. Grünbauer, H.J.M., Rigid polyurethane foams, in *Polymeric Materials Encyclopaedia*, vol. 10, ed. J.C. Salamone, CRC Press, Boca Raton, FL, 1996, 7504-7512.
5. Smits, G.F. and Thoen, J.A., *J. Therm. Insul.*, 14, 81, 1990.
6. Lewis, K.M., Kijak, I. and Reuter, K.B., *J. Cell. Plast.*, 32, 235, 1996.
7. Britton, D.J., *Cell. Polym.*, 8, 125, 1989.
8. Dämmstoffe im Hochbau (Insulation Materials in Buildings), Information for Builders, Architects and Engineers, Wirtschaftsministerium Baden-Württemberg, Stuttgart, 1999.
9. Steildachdämmung mit Polyurethan-Hartschaumstoff (Pitched Roof Insulation with Rigid Polyurethane Foam), IVPU, Stuttgart, 1995.
10. European Thermal Insulation Markets: The Current and Future Prospects for Polyurethane, UTECH 2000 (Urethanes Technology), Crain Communications Ltd, London, 2000.

11. Rowland, F.S., *Annu. Rev. Phys. Chem.*, 42, 731, 1991.
12. Tominaga, T., *Pure Appl. Chem.*, 64, 529, 1992.
13. Graber, M., Mutisya, G., and Mulumba, M.A., eds., *Production and Consumption of Ozone Depleting Substances under the Montreal Protocol 1986–2000*, UNEP, Nairobi, 2002.
14. Skochdopole, R.E., *Chem. Eng. Prog.*, 57, 55, 1961.
15. Collishaw, P.G. and Evans J.R.G., *J. Mat. Sci.*, 29, 486, 1994.
16. Glicksman, L.R. and Torpey, M., Polyurethanes 87, Proceedings of the SPI, 30th Annual Conference, 80, 1987.
17. King, J.A., Latham, D.D., and Martin, C.A., Polyurethane Expo 2001, Proceedings of the Alliance for the Polyurethane Industry, 473, 2001.
18. Barton, A.F.M., *Handbook of Solubility Parameters and Other Cohesion Parameters*, CRC Press, Boca Raton, FL, 1983.
19. Koschade, R., *Die Sandwichbauweise (How to Build a Steel Sandwich)*, Ernst & Sohn, Berlin, 2000.
20. Troitzsch, J., *International Plastics Flammability Handbook*, 2nd ed., Hanser Verlag, Munich, 1990.
21. SPE 13823 (en): Reaction to fire tests for building products - Building products excluding floorings exposed to the thermal attack by a single burning item, ICS 13.220.50, Nederlands Normalisatie Instituut (NEN), Delft, 2000.
22. Ward, E.R., *Chem. Britain*, 15, 297, 1979.
23. Ingold, C.K., *Structure and Mechanism in Organic Chemistry*, 2nd ed., Cornell University Press, Ithaca, NY, 1969.
24. Haber, F., *Z. Elektrochem.*, 22, 506, 1898.
25. Janssen, H.J., Kruithof, A.J., Steghuis, G.J., and Westerterp, K.R., *Ind. Eng. Chem. Res.*, 29, 754, 1990.
26. Wagner, E.C., *J. Org. Chem.*, 19, 1862, 1954.
27. Richter, R.H. and Priester, Jr., R.D., Isocyanates, organic, in *Kirk-Othmer Encyclopedia of Chemical Technology*, vol. 14, 4th ed., Wiley-Interscience, New York, 1995, 902-934.
28. Iben, H., Kattaneq, S., Backhauss, L., Welschinger, B., Gansera, B., Loeschau, S., and Meyer, A., French Patent 2,325,637, 1997.
29. Zaby, G., Judat, H., Boonstra, R., De Vos, S., Eckermann, R.W., and Humburger, S., German Patent 3,744,001, 1998.
30. Zaby, G., Judat, H., Humburger, S., De Vos, S., and Eckermann, R.W., German Patent 3,736,988, 1989.
31. Ohlinger, R., Schnez, H., Pfannenstiehl, L., Blumberg, B., and Raabe, H.J., U.S. Patent 4,581,174, 1986.
32. Richter, R. and Ulrich, H., *Tetrahedron Lett.*, 22, 1875, 1974.
33. Thiele, L. and Becker, R., *Adv. Urethane Sci. Technol.*, 12, 59, 1993.
34. Kanner, B. and Decker, T.G., *J. Cell. Plast.*, 5, 32, 1969.
35. Vincent, B., in *Surfactants*, ed. T.F. Tadros, Academic Press, London, 1984.
36. Grüning, B. and Koerner, G., *Tenside Surf. Det.*, 26, 313, 1989.
37. Hostettler, F., German patent 1,091,324, 1960.
38. Sandridge, R.L., Morecroft, A.S., Hardy, E.E., and Saunders, J.H., *J. Chem. Eng. Data*, 5, 495, 1960.
39. Hill, R.M., ed., *Silicone Surfactants, Surfactant Science Series*, vol. 86, Marcel Dekker, New York, 1999.
40. Owen, M.J., in *Surfactants in Solution*, vol. 6, ed. K.L. Mittal and P. Bothorel, Plenum Press, New York, 1986.

41. Owen, M.J. and Kendrick, T.C., *Macromolecules*, 3, 458, 1970.
42. Kendrick, T.C. et al., *J. Colloid Interface Sci.*, 24, 135, 1967.
43. Kendrick, T.C. and Owen, M.J., *Chem. Phys. Appl. Praat. Surface* (Spain) 5th ed., 2, 57, 1968.
44. Schmidt, G., *Tenside Surf. Det.*, 27, 324, 1990.
45. Haluska, L.A., U.S. patent 2,868,824, 1956.
46. Boudreau, R.J., *Mod. Plast.*, 44, 133, 1967.
47. Lee, L.J., Ottino, J.M., Ranz, W.E., and Macosko, C.W., *Polym. Eng. Sci.*, 20, 868, 1980.
48. Kolodziej, P., Macosko, C.W., and Ranz, W.E., *Polym. Eng. Sci.*, 22, 388, 1982.
49. Kolodziej, P., Yang, W.P., Macosko, C.W., and Welinghoff, S.T., *J. Polymer Sci. Part B: Polym. Phys.*, 24, 2359, 1986.
50. Molnar, J.A. Jr. and Lee, L.J., *J. Appl. Polym. Sci.*, 37, 2295, 1989.
51. Nelson, M. and Lee, L.J., *J. Appl. Polym. Sci.*, 37, 251, 1989.
52. Manas-Zloczower, I. and Macosko, C.W., *Polym. Eng. Sci.*, 28, 1219, 1988.
53. Richter, E.B. and Macosko, C.W., *Polym. Eng. Sci.*, 18, 1012, 1978.
54. Tucker, C.L. and Suh, N.P., *Polym. Eng. Sci.*, 20, 875, 1980.
55. Baser, S.A., Shetty, D.G., and Khakhar, D.V., *Polym. Eng. Sci.*, 33, 1611, 1993.
56. Fields, S.D., Thomas, E.L., and Ottino, J.M., *Polymer*, 27, 1423, 1986.
57. Wickert, P.D., Macosko, C.W., and Ranz, W.E., *Polymer*, 28, 1105, 1987.
58. Machuga, S.C., Midje, H.L., Peanasky, J.S., Macosko, C.W., and Ranz, W.E., *AIChE. J.*, 34, 1057, 1988.
59. Rojas, A.J., Marciano, J.H., and Williams, R.J., *Polym. Eng. Sci.*, 22, 840, 1982.
60. Baser, S.A. and Khakhar, D.V., *Polym. Eng. Sci.*, 34, 632, 1994.
61. Baser, S.A. and Khakhar, D.V., *Polym. Eng. Sci.*, 34, 642, 1994.
62. Basile, G., Musso, E., Tesser, R., and Di Serio, M., *Cell. Polym.*, 13, 98, 1994.
63. Williams, D.J., Bogdan, M.C., Parker, R.C., and Knopeck, G.M., *J. Cell. Plast.*, 33, 238, 1997.
64. Singh, S.N., Burns, S.B., and Costa, J.S., *Cell. Polym.*, 16, 444, 1997.
65. Biesmans, G., Colman, L., and Vandensande, R., *J. Coll. Int. Sci.*, 140, 199, 1998.
66. Hager, S.L., Craig, T.A., Jorgenson, M.W., Artevia, L.D., and Macosko, C.W., *J. Cell. Plast.*, 30, 44, 1994.
67. Grünbauer, H.J.M., Thoen, J.A., Folmer, J.C.W., and van Lieshout, H.C., *J. Cell. Plast.*, 28, 36, 1992.
68. Han, J.H. and Han, C.D., *J. Polym. Sci.*, 28, 743, 1990.
69. Grünbauer, H.J.M., Broos, J.A.F., Thoen, J.A., Smits, G.F., Lehnert, A.B., and Hoenke, M.S., Polyurethanes 92, Proceedings of SPI 34th Annual Conference, 1990, 36, 1992.
70. Grünbauer, H.J.M., *Cell. Polym.*, 14, 366, 1995.
71. Pitzer, K.S. and Brewer, L., *Thermodynamics*, McGraw-Hill, New York, 1961.
72. Volkert, O., Polyurethanes 91, Proceedings of SPI/ISOPA World Congress, 1991, 740, 1991.
73. Modesti, M., Adriani, V., and Simioni, F., *Polym. Eng. Sci.*, 40, 2046, 2000.
74. Vaze, N. and Khakhar, D.V., in *Macromolecules: Current Trends*, vol.2, ed. S. Venkatachalam, Allied Publishers, New Delhi, 1995; Niyogi, D., Kumar, R., and Gandhi, K.S., *AIChE J.*, 38, 1170, 1992; Niyogi, D., Kumar, R., and Gandhi, K.S., *Polym. Eng. Sci.*, 39, 199, 1999.
75. Latham, D.D., *J. Cell. Plast.*, 34, 124, 1998.
76. Smits, G.F. and Grünbauer, H.J.M., U.S. Patent 4,945,119, 1990.
77. Grünbauer, H.J.M. and Smits, G.F., U.S. Patent 4,972,003, 1990.

78. van Stralen, S. and Cole, R., *Boiling Phenomena*, vol. 1, McGraw-Hill, New York, 1979.
79. Smits, G.F., Proceedings of UTECH 1994 Conference, The Hague, paper 19, 1994.
80. Smits, G.F. and Thoen, J.A., U.S. Patent 5,250,579, 1993.
81. Smits, G.F., Cini, G., Grünbauer, H.J.M., and Broos, J.A.F., U.S. Patent 5,721,284, 1998.
82. Owen, M.J., Kendrick, T.C., Kingston, B.M., and Lloyd, N.C., *J. Coll. Int. Sci.*, 24, 141, 1967.
83. Wurtz, A., *C.R. Hebd. Seances Acad. SCI*, 27, 241, 1848.
84. Bayer, O., *Angew. Chemie*, A59, 257, 1947.
85. Van Gheluwe, P. and Leroux, J., *J. Appl. Polym. Sci.*, 28, 2053, 1983.
86. Hébrard, M.J. and Laroux, J., *Anal. Instrum.*, 15, 201, 1986.
87. Lovering, E.G. and Laidler, K.J., *Can. J. Chem.*, 40, 26, 1962.
88. Pinner, S.H., *Plastics (London)*, 11, 206, 215, 1947.
89. Cooper, W., Pearson, R.W., and Darke, S., *Ind. Chem.*, 3, 121, 1960.
90. Sayigh, A.A.R., Ulrich, H., and Farissey, W.J., Diisocyanates, in *Condensation Monomers*, ed. J.K. Stille and T.W. Campbell, Wiley-Interscience, New York, 1972.
91. Richter, R. and Ulrich, H., Synthesis and preparative applications of isocyanates, in *The Chemistry of Cyanates and Their Thio Derivatives*, Part 2, ed. S. Patai, John Wiley & Sons, New York, 1977.
92. Dillon, J.G., *Infrared Spectroscopic Atlas of Polyurethanes*, Technomic, Lancaster, PA, 1989.
93. Jennings, R., *J. Cell. Plast.*, 5, 159, 1969.
94. Rowton, R.L., *J. Cell. Plast.*, 16, 287, 1980.
95. van Thuyne, A. and Zeegers, B., *J. Cell. Plast.*, 14, 150, 1978.
96. Jianqiu, Y., Jianyuan, Z., Dening, W., Chunpu, H., Shengkang, Y., Yiou, C., Yufu, C., Ziqian, X., Jin, S., and Yin, W.J., *J. Cell. Plast.*, 26, 39, 1990.
97. Artevia, L.D., Macosko, C.W., Priester, R.D., Jr., Schrock, A.K., and Turner, R.B., Proceedings of SPI/ISOPA World Congress 1991, 509, 1991.
98. Baser, S.A. and Khakhar, D.V., *J. Cell. Plast.*, 29, 280, 1993.
99. Mora, E., Artavia, L.D., and Macosko, C.W., *J. Rheol.*, 35, 921, 1991.
100. Carrierre, C.J., Bank, D.H., and Christenson, C.P., *Polym. Eng. Sci.*, 32, 426, 1992.
101. Carrierre, C.J., Bank, D.H., and Christenson, C.P., *Mater. Eng.*, 9, 743, 1995.
102. Lipshitz, S.D. and Macosko, C.W., *Polym. Eng. Sci.*, 16, 803, 1976.
103. Besette, M.D. and Sundstrom, D.W., *Polym. Process Eng.*, 3, 25, 1985.
104. Nabata, Y., Mamada, A., and Yamasaki, H., *J. Appl. Polym. Sci.*, 35, 155, 1988.
105. Kostrzewski, W., *J. Cell. Plast.*, 21, 424, 1985.
106. Kostrzewski, W. and Lindt, J.T., *J. Polym. Eng.*, 16, 187, 1986.
107. Corfield, M., UTECH Asia '99 Conference Book of Papers, science and testing paper1/11, 1999.
108. Jones, S.A., Scott, K.W., Willoughby, B.G., and Sheard, E.A., *J. Cell. Plast.*, 38, 285, 2002.
109. Webb, D.D., Proceedings of SPI 28th Annual Conference, 2, 1984.
110. Matusik, F.J. and Nelson, D.W., U.S. patent 4,488,427, 1984.
111. Fitzgerald, J.V., Matusik, F.J., Nelson, D.W., and Schrag, J.L., U.S. Patent 4,754,640, 1988.
112. McClusky, J.V., O'Neill, R.E., Priester, R.D., Jr., and Ramsey, W.A., *J. Cell. Plast.*, 30, 224, 1994.

113. Zhang, X.D., Giles, D.W., Barocas, V.H., Yasunaga, K., and Macosko, C.W., *J. Rheol.*, 42, 871, 1998.
114. Ferry, J.D., *Viscoelastic Properties of Polymers*, John Wiley & Sons, New York, 1980.
115. Marciano, J.H., Rojas, A., and Williams, R.J.J., *Polymer*, 23, 1489, 1982.
116. McClusky, J.V., Priester, R.D., Jr., O'Neill, R.E., Turner, R., Harthcock, M.A., and Davis, B.L., *J. Cell. Plast.*, 26, 346, 1990.
117. Peng, S., Jackson, P., Sendijarevic, V., Frisch, K.C., Prentice, G.A., and Fuchs, A., *J. Appl. Polym. Sci.*, 77, 374, 2000.
118. Grünbauer, H.J.M. and Thoen, J.A., Proceedings of SPI 33rd Annual Technical and Marketing Conference, 318, 1990.
119. Grünbauer, H.J.M., Folmer, J.C.W., van Lieshout, H.C., Lidy, W., and Thoen, J.A. *Polym. Prep.*, 32, 517, 1991.
120. Grünbauer, H.J.M. and Folmer, J.C.W., *J. Appl. Polym. Sci.*, 54, 935, 1994.
121. Megat-Yusoff, P.S., Ph.D. thesis, Victoria University of Manchester, 1996.
122. Turner, R.B., Spell, H.L., and Wilkes, G.L., Proceedings of SPI 28th Annual Technical and Marketing Conference, 244, 1988.
123. Armistead, J. P., Turner, R.B., and Wilkes, G.L., *J. Appl. Polym. Sci.*, 35, 601, 1988.
124. Creswick, M.L., Lee, K.D., Turner, R.B., and Huber, L.M., Proceedings of SPI 28th Annual Technical and Marketing Conference, 11, 1985.
125. Artavia, L.D., Ph.D. thesis, University of Minnesota, 1991.
126. Mora, E., M.Sc. dissertation, University of Minnesota, 1991.
127. Elwell, M.J.A., Ph.D. thesis, Victoria University of Manchester, 1993.
128. Neff, R., Ph.D. thesis, University of Minnesota, 1995.
129. Li, W., Ph.D. thesis, University of Sheffield, 2002.
130. Wilkes, G.L., Abouzhar, S., and Radovich, D., *J. Cell. Plast.*, 19, 248, 1983.
131. Avnir, D., ed., *The Fractal Approach to Heterogeneous Chemistry*, John Wiley & Sons, New York, 1989.
132. Schaefer, D.W., Bunker, B.C., and Wilcoxon, J.P., *Proc. R. Soc. Lond. A.*, 423, 35, 1989.
133. Feder, J., *Fractals*, Plenum Press, New York, 1989.
134. Harrison, A., *Fractals in Chemistry*, Oxford Science Publications, Oxford, 1995.
135. Kaiser, T., *Polym. Sci.*, 373, 14, 1989.
136. Smits, G.F. and Thoen, J.A., *J. Cell. Plast.*, 29, 57, 1993.
137. Buist, J.M., Doherty, D.J., and Hurd, R., Urethane rigid foams: factors affecting their behaviour as thermal insulants, in *Progress in Refrigerator Science and Technology*, Pergamon Press, Oxford, 1963.
138. Schuetz, M.A. and Glicksman, L.R., *J. Cell. Plast.*, 20, 114, 1984.
139. Glicksman, L.R., *Cell. Polym.*, 10, 276, 1991.
140. Cunningham, A., Jeffs, G.M.F., Rosbotham, I.D., and Sparrow, D.J., *Cell. Polym.*, 7, 1, 1988.
141. Eeckhaut, G. and Cunningham, A., *J. Cell. Plast.*, 32, 528, 1996.
142. Chung-jen Tseng, Yamaguchi, M., and Ohmori, T., *Cryogenics*, 37, 305, 1997.
143. Jhy-Wen Wu, Wen-Fa Sung, and Hsin-Sen Chu, *Int. J. Heat Mass Transfer*, 42, 2211, 1999.
144. Gluck, D.G., Soukup, T.G., and Moore, W.J., U.S. patent 4,795,763, 1989.
145. Fleurent, H., *Cell. Polym.*, 13, 419, 1994.
146. Fleurent, H. and Thijs, S., *J. Cell. Plast.*, 31, 580, 1995.
147. Yourd, R.A., *J. Cell. Plast.*, 32, 601, 1996.
148. Daems, D., Rosbotham, D., Singh, S.N., and Franco, M.V., *J. Cell. Plast.*, 32, 485, 1996.

149. Svanström, M. and Ramnäs, O., *J. Cell. Plast.*, 32, 159, 1996.
150. Singh, S.N., Biesmans, G., Karramans, M., and Randall, D., *J. Cell. Plast.*, 34, 75, 1998.
151. Crank, J., *The Mathematics of Diffusion*, 2nd ed., Oxford University Press, Oxford, 1993.
152. Cuddihy, E.F., *J. Cell. Plast.*, 12, 114, 1976.
153. Cuddihy, E.F. and Moacanin, J., *J. Cell. Plast.*, 3, 73, 1967.
154. Bhattacharjee, D. and Booth, J.R., *J. Cell. Plast.*, 31, 244, 1995.
155. Norton, F.J., *J. Cell. Plast.*, 3, 23, 1967.
156. Brandreth, D.A. and Ingersoll, H.G., *J. Cell. Plast.*, 16, 134, 1980.
157. Page, M.C. and Glicksman, L.R., *J. Cell. Plast.*, 28, 268, 1992.
158. du Cauze de Nazelle, G.M.R., Ph.D. thesis, Delft University of Technology, the Netherlands, 1995.
159. Cunningham, A., Rosbotham, I.D., and Sparrow, D.J., *Cell. Polym.*, 9, 367, 1990.
160. Svanström, M. and Ramnäs, O., *J. Cell. Plast.*, 31, 375, 1995.
161. Svanström, M., Ramnäs, O., Olsson, M., and Jarfelt, U., *Cell. Polym.*, 16, 182, 1997.
162. Bart, G.C.J. and du Cauze de Nazelle, G.M.R., *J. Cell. Plast.*, 29, 29, 1993.
163. Boscoletto, A.B. and Cellarosi, B., *Cell. Polym.*, 10, 263, 1991.
164. Isberg, J., Ph.D. thesis, Chalmers University of Technology, Göteborg, Sweden, 1988.
165. Ball, G.W., Healy, W.G., and Partington, J.B., *Eur. J. Cell. Plast.*, 1, 50, 1978.
166. Ball, G.W., *Cell. Polym.*, 13, 434, 1994.
167. Roux, G., Trambly, G., and Venuti, G., *Cell. Polym.*, 9, 278, 1990.
168. Ball, G.W., *Cell. Polym.*, 16, 110, 1997.
169. Biesmans, G., De Vos, R., and Rosbotham, I.D., *Cell. Polym.*, 13, 292, 1994.
170. Biesmans, G., Karremans, M., Randall, D., and Singh, S.N., *J. Cell. Plast.*, 34, 349, 1998.
171. Albrecht, W. and Zehendner, H., *Cell. Polym.*, 16, 35, 1997.
172. Albrecht, W., *Cell. Polym.*, 19, 319, 2000.
173. IVPJ Joint Project, *Cell. Polym.*, 10, 470, 1991.
174. Grünbauer, H.J.M., Cikut, L., Haworth, G.J., and Beerwart, A., *J. Cell. Plast.*, 33, 140, 1997.
175. Kaplan, W.A. and Tabor, R.L., *J. Cell. Plast.*, 30, 243, 1994.
176. Christman, D.L. and Reichel, C.J., *J. Cell. Plast.*, 32, 82, 1996.
177. Moore, S.E., *J. Cell. Plast.*, 30, 494, 1994.
178. Nichols, J.B., Bhattacharjee, D., Moreno, O., and Mirasol, S., *J. Cell. Plast.*, 32, 139, 1996.
179. Kucukpinar, E. Proceedings of UTECH 2003 Conference, The Hague, 2003.